1450

BNL—NCS-36272
DOE/NDC-36/U
NEANDC(US)-221/U
INDC(USA)-96U
INFORMAL REPORT
LIMITED DISTRIBUTION

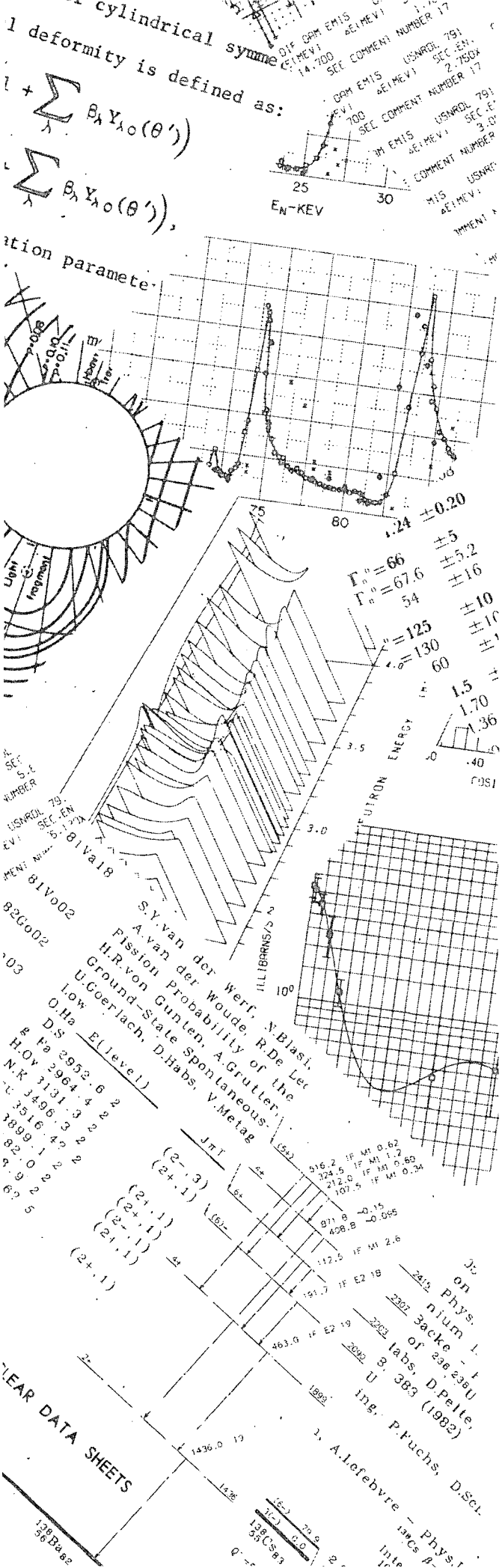

REPORTS TO THE DOE NUCLEAR DATA COMMITTEE

Compiled by
NATIONAL NUCLEAR DATA CENTER
for the
U.S. Department of Energy
Nuclear Data Committee

May 1985

BROOKHAVEN NATIONAL LABORATORY
ASSOCIATED UNIVERSITIES, INC.
UPTON, LONG ISLAND, NEW YORK 11973

national
nuclear
data
center

BNL-NCS-36272
DOE/NDC-36/U
NEANDC(US)-221/U
INDC(USA)-96/L
Informal Report
Limited Distribution

REPORTS TO

THE DOE NUCLEAR DATA COMMITTEE

MAY 1985

Compiled by the

NATIONAL NUCLEAR DATA CENTER
BROOKHAVEN NATIONAL LABORATORY
ASSOCIATED UNIVERSITIES, INC.

UNDER CONTRACT NO. DE-AC02-76CH00016 WITH THE
UNITED STATES DEPARTMENT OF ENERGY

Printed in the United States of America
Available from
National Technical Information Service
U.S. Department of Commerce
5285 Port Royal Road
Springfield, VA 22161

NTIS price codes:
Printed Copy: A09; Microfiche Copy: A01

PREFACE

The reports in this document were submitted to the Department of Energy, Nuclear Data Committee (DOE-NDC) in April, 1985. The reporting laboratories are those with a substantial program for the measurement of neutron and nuclear cross sections of relevance to the U.S. applied nuclear energy program.

The authors of the Status Report contributions are responsible for collecting and editing individual contributions from their laboratory and are not necessarily the sole authors of the contributions. The scientists responsible for the work described in each individual contributions are listed at the beginning of the contribution.

The material contained in these reports is to be regarded as comprised of informal statements of recent developments and preliminary data. Persons wishing to make use of these data should contact the individual experimenter for further details. The data which appear in this document should be quoted only by permission of the contributor and should be referenced as private communication, and not by this document number. Appropriate subjects are listed as follows:

1. Microscopic neutron cross sections relevant to the nuclear energy program, including shielding. Inverse reactions where pertinent are included.

2. Charged-particle cross sections, where they are relevant to (1.) above, and where relevant to developing and testing nuclear models.

3. Gamma ray production, radioactive decay, and theoretical developments in nuclear structure which are applicable to nuclear energy programs.

4. Proton and alpha-particle cross sections, at energies of up to 1 GeV, which are of interest to the space program.

These reports cannot be regarded as a complete summary of the nuclear research efforts in the U.S. A number of laboratories whose research is less programmatically oriented do not submit reports; neither do the submitted reports reflect all the work related to nuclear data in progress at the submitting laboratory.

This compilation has been produced almost completely from master copies prepared by the individual contributors listed in the Table of Contents, and reports are reproduced without change from these master copies.

The CINDA-type index which follows the Table of Contents was prepared by Norman E. Holden of the National Nuclear Data Center, Brookhaven National Laboratory, Upton, Long Island, New York.

TABLE OF CONTENTS

TABLE OF CONTENTS (cont.)

NEUTRON DATA REFERENCES

Element	Quantity	Energy (eV) Min	Max	Type	Documentation Ref	Page	Date	Lab	Comments
^{1}H	$\sigma_{el}(\theta)$	5.0+7	6.5+7	Expt	DOE-NDC-36	33	Apr85	DAV	Drummond+ 2 ENS. 180/90 DEG. NDG.
^{6}Li	$\sigma_{el}(\theta)$	4.0+6		Theo	DOE-NDC-36	151	Apr85	OHO	Knox+ NDG. R-MATRIX ANAL.
^{6}Li	$\sigma_{dif.inl}$	4.0+6		Theo	DOE-NDC-36	151	Apr85	OHO	Knox+ NDG. R-MATRIX ANAL.
^{6}Li	$\sigma_{n,t}$	. +0	+2	Expt	DOE-NDC-36	120	Apr85	NBS	Carlson. NDG. $^{10}B(N,A)/^{6}LI(N,T)$TBD.
^{6}Li	$\sigma_{n,t}$	1.5+7		Expt	DOE-NDC-36	69	Apr85	LRL	Goldberg+ CS(14.92MEV)=32+-4MB.
^{7}Li	$\sigma_{el}(\theta)$	4.0+6		Theo	DOE-NDC-36	151	Apr85	OHO	Knox+ NDG. R-MATRIX ANAL.
^{7}Li	$\sigma_{dif.inl}$	4.0+6		Theo	DOE-NDC-36	151	Apr85	OHO	Knox+ NDG. R-MATRIX ANAL.
^{7}Li	$\sigma_{n,X\gamma}$	2.0+5	4.0+7	Expt	DOE-NDC-36	130	Apr85	ORL	Larson. NDG. 85SANTA FE CONF.
^{7}Li	$\sigma_{n,t}$	1.5+7		Expt	DOE-NDC-36	69	Apr85	LRL	Goldberg+ CS(14.94MEV)=302+-15MB.
^{7}Li	$\sigma_{n,nt}$	1.5+7		Expt	DOE-NDC-36	2	Apr85	ANL	Smith+ REL $^{238}U(N,F)$.SEE ANL-NDM-87.
^{9}Be	$\sigma_{el}(\theta)$	4.0+6	1.0+7	Expt	DOE-NDC-36	7	Apr85	ANL	Smith+ NDG. TBC.
^{9}Be	$\sigma_{el}(\theta)$	1.1+7	1.7+7	Expt	DOE-NDC-36	161	Apr85	TNL	Dave+ GRPH. ANGDIST CFD OTHR EXPT.
^{9}Be	$\sigma_{dif.inl}$	4.0+6	1.0+7	Expt	DOE-NDC-36	7	Apr85	ANL	Smith+ NDG. TBC.
^{9}Be	$\sigma_{dif.inl}$	1.1+7	1.7+7	Expt	DOE-NDC-36	161	Apr85	TNL	Dave+ GRPH. ANGDIST CFD OTHR EXPT.
^{9}Be	$\sigma_{n,2n}$	NDG		Eval	DOE-NDC-36	87	Apr85	LRL	Perkins+ NDG.
^{10}B	$\sigma_{el}(\theta)$	3.0+6	5.0+6	Expt	DOE-NDC-36	144	Apr85	OHO	Sadowski+ NDG. ANGDIST. ANAL TBC.
^{10}B	$\sigma_{dif.inl}$	3.0+6	5.0+6	Expt	DOE-NDC-36	144	Apr85	OHO	Sadowski+ NDG. ANGDIST. ANAL TBC.
^{10}B	$\sigma_{n,\alpha}$	. +0	. +2	Expt	DOE-NDC-36	120	Apr85	NBS	Carlson. NDG. $^{10}B(N,A)/^{6}LI(N,T)$TBD.
^{11}B	Evaluation		2.0+7	Eval	DOE-NDC-36	96	Apr85	LAS	Young. NDG. TBC.
^{11}B	σ_{tot}	NDG		Eval	DOE-NDC-36	96	Apr85	LAS	Young. NDG. TBD.
^{11}B	$\sigma_{el}(\theta)$	NDG		Eval	DOE-NDC-36	96	Apr85	LAS	Young. NDG. TBD.
^{11}B	$\sigma_{el}(\theta)$	1.5+7	1.7+7	Expt	DOE-NDC-36	163	Apr85	TNL	Dave+ NDG. SIG, ANAL POWER.
^{11}B	$\sigma_{dif.inl}$	NDG		Eval	DOE-NDC-36	96	Apr85	LAS	Young. NDG. TBD.
^{11}B	$\sigma_{dif.inl}$	1.5+7	1.7+7	Expt	DOE-NDC-36	163	Apr85	TNL	Dave+ NDG. SIG, ANAL POWER.
^{11}B	$\sigma_{n,\gamma}$	NDG		Expt	DOE-NDC-36	55	Apr85	KTY	Kovash+ NDG. TBD.
^{11}B	$\sigma_{n,X\gamma}$	1.5+7		Eval	DOE-NDC-36	96	Apr85	LAS	Young. GRPH CFD EXPT.
^{12}C	σ_{tot}	3.0+5	4.0+6	Expt	DOE-NDC-36	48	Apr85	KTY	Hicks+ NDG. AGREES EVALUATIONS.
^{12}C	$\sigma_{el}(\theta)$	4.0+6	1.0+7	Expt	DOE-NDC-36	7	Apr85	ANL	Smith+ NDG. TBC.
^{12}C	$\sigma_{el}(\theta)$	9.0+6	1.2+7	Theo	DOE-NDC-36	163	Apr85	TNL	Dave+ NDG. PHASE SHIFT ANAL TBP.
^{12}C	$\sigma_{el}(\theta)$	2.0+7	2.6+7	Theo	DOE-NDC-36	144	Apr85	OHO	Meigooni+ NDG. CC ANALYSIS.
^{12}C	$\sigma_{el}(\theta)$	2.0+7	6.0+7	Theo	DOE-NDC-36	151	Apr85	OHO	Petler+ NDG. OM ANALYSIS.
^{12}C	$\sigma_{dif.inl}$	4.0+6	1.0+7	Expt	DOE-NDC-36	7	Apr85	ANL	Smith+ NDG. TBC.
^{12}C	$\sigma_{dif.inl}$	2.0+7	2.6+7	Theo	DOE-NDC-36	144	Apr85	OHO	Meigooni+ NDG. CC ANALYSIS.

NEUTRON DATA REFERENCES

Element	Quantity	Energy (eV) Min	Max	Type	Documentation Ref	Page	Date	Lab	Comments
^{12}C	$\sigma_{n,n'\gamma}$	NDG		Expt	DOE-NDC-36	90	Apr85	LAS	Wender+ NDG.
^{12}C	$\sigma_{n,p}$	6.5+7		Expt	DOE-NDC-36	33	Apr85	DAV	Ford+ P SPECT. 0 DEG. NDG.
^{12}C	$\sigma_{n,n\alpha}$	2.0+7	2.6+7	Expt	DOE-NDC-36	144	Apr85	OHO	Finlay. NDG. MEAS FOR KERMA FACTOR.
^{13}C	$\sigma_{el}(\theta)$	2.0+7	6.0+7	Theo	DOE-NDC-36	151	Apr85	OHO	Petler+ NDG. OM ANALYSIS.
^{13}C	$\sigma_{n,p}$	6.5+7		Expt	DOE-NDC-36	33	Apr85	DAV	Ford+ P SPECT. 0 DEG. NDG.
^{14}N	$\sigma_{el}(\theta)$	1.1+7	1.7+7	Expt	DOE-NDC-36	161	Apr85	TNL	Dave+ GRPH. ANGDIST CFD OTHR EXPT.
^{16}O	σ_{tot}		7.0+7	Exth	DOE-NDC-36	145	Apr85	OHO	Islam+ NDG. CC FIT.
^{16}O	$\sigma_{el}(\theta)$	1.8+7	2.6+7	Exth	DOE-NDC-36	145	Apr85	OHO	Islam+ NDG. MEAS+CC FIT.
^{16}O	$\sigma_{dif.inl}$	1.8+7	2.6+7	Exth	DOE-NDC-36	145	Apr85	OHO	Islam+ NDG. MEAS+CC FIT.
^{27}Al	$\sigma_{el}(\theta)$	1.1+7	1.7+7	Expt	DOE-NDC-36	164	Apr85	TNL	Dave+ GRPHS. PR/C 30, 1435.
^{27}Al	$\sigma_{dif.inl}$	1.1+7	1.7+7	Expt	DOE-NDC-36	164	Apr85	TNL	Dave+ GRPHS. PR/C 30, 1435.
^{27}Al	$\sigma_{n,p}$	1.4+7	1.5+7	Eval	DOE-NDC-36	6	Apr85	ANL	Evain+ NDG. TBP ANL-NDM-89.
^{27}Al	$\sigma_{n,p}$	1.5+7		Expt	DOE-NDC-36	2	Apr85	ANL	Meadows+ EN=14.7MEV. REL $^{238}U(N,F)$.
^{27}Al	$\sigma_{n,\alpha}$	1.5+7		Expt	DOE-NDC-36	2	Apr85	ANL	Meadows+ EN=14.7MEV. REL $^{238}U(N,F)$.
^{28}Si	$\sigma_{el}(\theta)$	8.0+6	1.7+7	Expt	DOE-NDC-36	166	Apr85	TNL	Dave+ NDG. HOWELL THESIS.
^{28}Si	$\sigma_{dif.inl}$	8.0+6	1.7+7	Expt	DOE-NDC-36	166	Apr85	TNL	Dave+ NDG. HOWELL THESIS.
^{28}Si	$\sigma_{n,p}$	1.4+7	1.5+7	Eval	DOE-NDC-36	6	Apr85	ANL	Evain+ NDG. TBP ANL-NDM-89.
^{28}Si	$\sigma_{n,p}$	1.5+7		Expt	DOE-NDC-36	2	Apr85	ANL	Meadows+ EN=14.7MEV. REL $^{238}U(N,F)$.
^{29}Si	$\sigma_{n,np}$	1.4+7	1.5+7	Eval	DOE-NDC-36	6	Apr85	ANL	Evain+ NDG. TBP ANL-NDM-89.
^{29}Si	$\sigma_{n,np}$	1.5+7		Expt	DOE-NDC-36	2	Apr85	ANL	Meadows+ EN=14.7MEV. REL $^{238}U(N,F)$.
^{32}S	$\sigma_{el}(\theta)$	8.0+6	1.7+7	Expt	DOE-NDC-36	166	Apr85	TNL	Dave+ NDG. HOWELL THESIS.
^{32}S	$\sigma_{el}(\theta)$	8.0+6	4.0+7	Theo	DOE-NDC-36	166	Apr85	TNL	Dave+ GRPH. CC CALC. CFD OTHR EXPTS.
^{32}S	$\sigma_{dif.inl}$	8.0+6	1.7+7	Expt	DOE-NDC-36	166	Apr85	TNL	Dave+ NDG. HOWELL THESIS.
^{32}S	$\sigma_{dif.inl}$	8.0+6	4.0+7	Theo	DOE-NDC-36	166	Apr85	TNL	Dave+ GRPH. CC CALC. CFD OTHR EXPTS.
^{33}S	σ_{tot}	1.0+4	4.0+5	Expt	DOE-NDC-36	127	Apr85	ORL	Coddens+ NDG. MEAS+R-MATRIX ANALYS.
^{33}S	Res.Params.	NDG		Expt	DOE-NDC-36	127	Apr85	ORL	Coddens+ NDG. WN, WG, WA ANALYSIS.
^{33}S	$\langle\Gamma\rangle/D$	NDG		Expt	DOE-NDC-36	127	Apr85	ORL	Coddens+ NDG.
^{34}S	$\sigma_{el}(\theta)$	2.2+7		Expt	DOE-NDC-36	146	Apr85	OHO	Alarcon+ EN=21.7MEV. NDG. CC ANAL.
^{34}S	$\sigma_{dif.inl}$	2.2+7		Expt	DOE-NDC-36	146	Apr85	OHO	Alarcon+ EN=21.7MEV. NDG. CC ANAL.
^{39}K	$\sigma_{n,\gamma}$	NDG		Expt	DOE-NDC-36	128	Apr85	ORL	Macklin. SEE NSE 88,129.
^{39}K	Res.Params.	NDG		Expt	DOE-NDC-36	128	Apr85	ORL	Macklin. SEE NSE 88, 129.
^{41}K	$\sigma_{n,\gamma}$	NDG		Expt	DOE-NDC-36	128	Apr85	ORL	Macklin. SEE NSE 88, 129.
^{41}K	Res.Params.	NDG		Expt	DOE-NDC-36	128	Apr85	ORL	Macklin. SEE NSE 88, 129.

NEUTRON DATA REFERENCES

Element	Quantity	Energy (eV) Min	Max	Type	Documentation Ref	Page	Date	Lab	Comments
^{40}Ca	$\sigma_{el}(\theta)$	2.2+7		Expt	DOE-NDC-36	146	Apr85	OHO	Alarcon+ EN=21.7MEV. NDG. CC ANAL.
^{40}Ca	$\sigma_{el}(\theta)$	1.9+7	2.6+7	Expt	DOE-NDC-36	146	Apr85	OHO	Alarcon+ NDG.ANALYS NEUT+PROTON DATA.
^{40}Ca	$\sigma_{el}(\theta)$	1.4+7	1.7+7	Expt	DOE-NDC-36	167	Apr85	TNL	Dave+ NDG. SIG, ANAL POWER.
^{40}Ca	$\sigma_{dif.inl}(\theta)$	1.4+7	1.7+7	Expt	DOE-NDC-36	167	Apr85	TNL	Dave+ NDG. SIG, ANAL POWER.
^{40}Ca	$\sigma_{dif.inl}$	2.2+7		Expt	DOE-NDC-36	146	Apr85	OHO	Alarcon+ EN=21.7MEV. NDG. CC ANAL.
^{40}Ca	$\sigma_{n,\gamma}$	NDG		Expt	DOE-NDC-36	90	Apr85	LAS	Wender+ NDG.
^{40}Ca	$\sigma_{n,p}$	6.5+7		Expt	DOE-NDC-36	33	Apr85	DAV	Castaneda+ P SPECT. 6-70 DEG. NDG.
^{40}Ca	$\sigma_{n,p}$	6.6+7		Expt	DOE-NDC-36	34	Apr85	DAV	Castaneda+ ANG DIST. NDG.
^{48}Ca	σ_{tot}	1.0+4	4.0+6	Expt	DOE-NDC-36	126	Apr85	ORL	Carlton+ NDG. 84KNOXVILLE CONF.
^{48}Ca	σ_{tot}		4.0+6	Expt	DOE-NDC-36	127	Apr85	ORL	Harvey+ NDG. 84OHIO CONF.
^{48}Ca	$\sigma_{n,\gamma}$	1.0+1	5.0+5	Expt	DOE-NDC-36	126	Apr85	ORL	Carlton+ NDG. 84KNOXVILLE CONF.
^{48}Ca	Res.Params.	1.9+4	1.1+5	Expt	DOE-NDC-36	126	Apr85	ORL	Carlton+ 2 CAPT.RES, 19.3, 106.9KEV.
^{46}Ti	$\sigma_{n,p}$	1.4+7	1.5+7	Eval	DOE-NDC-36	6	Apr85	ANL	Evain+ NDG. TBP ANL-NDM-89.
^{46}Ti	$\sigma_{n,p}$	1.5+7		Expt	DOE-NDC-36	2	Apr85	ANL	Meadows+ EN=14.7MEV. REL ^{238}U(N,F).
^{47}Ti	$\sigma_{n,p}$	1.4+7	1.5+7	Eval	DOE-NDC-36	6	Apr85	ANL	Evain+ NDG. TBP ANL-NDM-89.
^{47}Ti	$\sigma_{n,p}$	1.5+7		Expt	DOE-NDC-36	2	Apr85	ANL	Meadows+ EN=14.7MEV. REL ^{238}U(N,F).
^{47}Ti	$\sigma_{n,np}$	1.4+7	1.5+7	Eval	DOE-NDC-36	6	Apr85	ANL	Evain+ NDG. TBP ANL-NDM-89.
^{47}Ti	$\sigma_{n,np}$	1.5+7		Expt	DOE-NDC-36	2	Apr85	ANL	Meadows+ EN=14.7MEV. REL ^{238}U(N,F).
^{48}Ti	$\sigma_{n,p}$	1.4+7	1.5+7	Eval	DOE-NDC-36	6	Apr85	ANL	Evain+ NDG. TBP ANL-NDM-89.
^{48}Ti	$\sigma_{n,p}$	1.5+7		Expt	DOE-NDC-36	2	Apr85	ANL	Meadows+ EN=14.7MEV. REL ^{238}U(N,F).
^{48}Ti	$\sigma_{n,np}$	1.4+7	1.5+7	Eval	DOE-NDC-36	6	Apr85	ANL	Evain+ NDG. TBP ANL-NDM-89.
^{48}Ti	$\sigma_{n,np}$	1.5+7		Expt	DOE-NDC-36	2	Apr85	ANL	Meadows+ EN=14.7MEV. REL ^{238}U(N,F).
^{49}Ti	$\sigma_{n,np}$	1.4+7	1.5+7	Eval	DOE-NDC-36	6	Apr85	ANL	Evain+ NDG. TBP ANL-NDM-89.
^{49}Ti	$\sigma_{n,np}$	1.5+7		Expt	DOE-NDC-36	2	Apr85	ANL	Meadows+ EN=14.7MEV. REL ^{238}U(N,F).
^{51}V	$\sigma_{n,p}$	1.4+7	1.5+7	Eval	DOE-NDC-36	6	Apr85	ANL	Evain+ NDG. TBP ANL-NDM-89.
^{51}V	$\sigma_{n,p}$	1.5+7		Expt	DOE-NDC-36	2	Apr85	ANL	Meadows+ EN=14.7MEV. REL ^{238}U(N,F).
^{51}V	$\sigma_{n,\alpha}$	5.5+6	9.6+6	Expt	DOE-NDC-36	1	Apr85	ANL	Kanno+ CFD ENDF/B-V. SEE ANL-NDM-86.
^{51}V	$\sigma_{n,\alpha}$	1.5+7		Expt	DOE-NDC-36	2	Apr85	ANL	Meadows+ EN=14.7MEV. REL ^{238}U(N,F).
Cr	$\sigma_{el}(\theta)$	4.0+6	1.0+7	Expt	DOE-NDC-36	7	Apr85	ANL	Smith+ NDG. TBC.
Cr	$\sigma_{dif.inl}$	4.0+6	1.0+7	Expt	DOE-NDC-36	7	Apr85	ANL	Smith+ NDG. TBC.
Cr	$\sigma_{n,X\gamma}$	2.0+5	4.0+7	Expt	DOE-NDC-36	130	Apr85	ORL	Larson. NDG. 85SANTA FE CONF.
^{52}Cr	$\sigma_{n,p}$	1.4+7	1.5+7	Eval	DOE-NDC-36	6	Apr85	ANL	Evain+ NDG. TBP ANL-NDM-89.
^{52}Cr	$\sigma_{n,p}$	1.5+7		Expt	DOE-NDC-36	2	Apr85	ANL	Meadows+ EN=14.7MEV. REL ^{238}U(N,F).

NEUTRON DATA REFERENCES

Element	Quantity	Energy (eV) Min	Max	Type	Documentation Ref	Page	Date	Lab	Comments
^{53}Cr	$\sigma_{n,X\gamma}$	2.0+5	4.0+7	Expt	DOE-NDC-36	130	Apr85	ORL	Larson. NDG. 85SANTA FE CONF.
^{53}Cr	$\sigma_{n,np}$	1.4+7	1.5+7	Eval	DOE-NDC-36	6	Apr85	ANL	Evain+ NDG. TBP ANL-NDM-89.
^{53}Cr	$\sigma_{n,np}$	1.5+7		Expt	DOE-NDC-36	2	Apr85	ANL	Meadows+ EN=14.7MEV. REL ^{238}U(N,F).
^{55}Mn	$\sigma_{n,2n}$	1.4+7	1.5+7	Eval	DOE-NDC-36	6	Apr85	ANL	Evain+ NDG. TBP ANL-NDM-89.
^{55}Mn	$\sigma_{n,2n}$	1.5+7		Expt	DOE-NDC-36	2	Apr85	ANL	Meadows+ EN=14.7MEV. REL ^{238}U(N,F).
^{55}Mn	$\sigma_{n,\alpha}$	1.4+7	1.5+7	Eval	DOE-NDC-36	6	Apr85	ANL	Evain+ NDG. TBP ANL-NDM-89.
^{55}Mn	$\sigma_{n,\alpha}$	1.5+7		Expt	DOE-NDC-36	2	Apr85	ANL	Meadows+ EN=14.7MEV. REL ^{238}U(N,F).
^{55}Mn	Res.Params.	3.4+2	2.3+3	Expt	DOE-NDC-36	129	Apr85	ORL	Macklin. 4 RES. EO, WG, GWT GIVEN.
Fe	$\sigma_{el}(\theta)$	4.0+6	1.0+7	Expt	DOE-NDC-36	7	Apr85	ANL	Smith+ NDG. TBC.
Fe	$\sigma_{dif.inl}$	4.0+6	1.0+7	Expt	DOE-NDC-36	7	Apr85	ANL	Smith+ NDG. TBC.
Fe	$\sigma_{n,emis}$	6.5+7		Expt	DOE-NDC-36	34	Apr85	DAV	Hamilton+ NDG. 4-32 DEGS.
^{54}Fe	$\sigma_{n,2n}$	1.4+7	1.5+7	Expt	DOE-NDC-36	3	Apr85	ANL	Smither+ GRPH.
^{54}Fe	$\sigma_{n,p}$	1.4+7	1.5+7	Eval	DOE-NDC-36	6	Apr85	ANL	Evain+ NDG. TBP ANL-NDM-89.
^{54}Fe	$\sigma_{n,p}$	1.5+7		Expt	DOE-NDC-36	2	Apr85	ANL	Meadows+ EN=14.7MEV. REL ^{238}U(N,F).
^{54}Fe	$\sigma_{n,\alpha}$	1.4+7	1.5+7	Eval	DOE-NDC-36	6	Apr85	ANL	Evain+ NDG. TBP ANL-NDM-89.
^{54}Fe	$\sigma_{n,\alpha}$	1.5+7		Expt	DOE-NDC-36	2	Apr85	ANL	Meadows+ EN=14.7MEV. REL ^{238}U(N,F).
^{56}Fe	$\sigma_{n,X\gamma}$	2.0+5	4.0+7	Expt	DOE-NDC-36	130	Apr85	ORL	Larson. NDG. 85SANTA FE CONF.
^{56}Fe	$\sigma_{n,p}$	1.5+7		Expt	DOE-NDC-36	2	Apr85	ANL	Meadows+ EN=14.7MEV. REL ^{238}U(N,F).
^{56}Fe	Res.Params.	1.2+3	2.3+4	Expt	DOE-NDC-36	130	Apr85	ORL	Weston+ CAPT AREA RATIO. 2 RES.
^{56}Fe	Res.Params.	1.2+3		Eval	DOE-NDC-36	142	Apr85	ORL	Perey. 85SANTA FE CONF.
^{57}Fe	$\sigma_{n,X\gamma}$	2.0+5	4.0+7	Expt	DOE-NDC-36	130	Apr85	ORL	Larson. NDG. 85SANTA FE CONF.
^{cmp}Fe	$\sigma_{\alpha,emis}$	9.4+6	1.1+7	Expt	DOE-NDC-36	147	Apr85	OHO	Ahmad+ STAINLESS STEEL. NDG.CFD CALC.
^{cmp}Fe	$\sigma_{p,emis}$	9.4+6	1.1+7	Expt	DOE-NDC-36	147	Apr85	OHO	Ahmad+ STAINLESS STEEL. NDG.CFD CALC.
^{59}Co	$\sigma_{el}(\theta)$	4.0+6	1.0+7	Expt	DOE-NDC-36	7	Apr85	ANL	Smith+ NDG. TBC.
^{59}Co	$\sigma_{dif.inl}$	4.0+6	1.0+7	Expt	DOE-NDC-36	7	Apr85	ANL	Smith+ NDG. TBC.
^{59}Co	γ Spectra	2.0+3		Expt	DOE-NDC-36	20	Apr85	BNL	NDG. AVG RES CAPT SPECT.
^{59}Co	$\sigma_{n,2n}$	1.4+7	1.5+7	Eval	DOE-NDC-36	6	Apr85	ANL	Evain+ NDG. TBP ANL-NDM-89.
^{59}Co	$\sigma_{n,2n}$	1.5+7		Expt	DOE-NDC-36	2	Apr85	ANL	Meadows+ EN=14.7MEV. REL ^{238}U(N,F).
^{59}Co	$\sigma_{n,p}$	1.4+7	1.5+7	Eval	DOE-NDC-36	6	Apr85	ANL	Evain+ NDG. TBP ANL-NDM-89.
^{59}Co	$\sigma_{n,p}$	1.5+7		Expt	DOE-NDC-36	2	Apr85	ANL	Meadows+ EN=14.7MEV. REL ^{238}U(N,F).
^{59}Co	$\sigma_{n,\alpha}$	1.5+7		Expt	DOE-NDC-36	114	Apr85	MHG	Agrawal+ EN=14.62. REL ^{56}FE(N,P).
^{59}Co	$\sigma_{n,\alpha}$	1.4+7	1.5+7	Eval	DOE-NDC-36	6	Apr85	ANL	Evain+ NDG. TBP ANL-NDM-89.
^{59}Co	$\sigma_{n,\alpha}$	1.5+7		Expt	DOE-NDC-36	2	Apr85	ANL	Meadows+ EN=14.7MEV. REL ^{238}U(N,F).

NEUTRON DATA REFERENCES

Element	Quantity	Energy (eV) Min	Max	Type	Documentation Ref	Page	Date	Lab	Comments
Ni	$\sigma_{n,X\gamma}$	2.0+5	4.0+7	Expt	DOE-NDC-36	130	Apr85	ORL	Larson. NDG. 85SANTA FE CONF.
^{58}Ni	Evaluation	1.0+6	2.0+7	Eval	DOE-NDC-36	141	Apr85	ORL	Hetrick+ 85SANTA FE CONF.
^{58}Ni	σ_{tot}	. +0	. +6	Expt	DOE-NDC-36	143	Apr85	ORL	Perey+ 85SANTA FE CONF.
^{58}Ni	$\sigma_{el}(\theta)$	4.0+6	1.0+7	Expt	DOE-NDC-36	7	Apr85	ANL	Smith+ NDG. TBC.
^{58}Ni	$\sigma_{el}(\theta)$	8.0+6	1.7+7	Expt	DOE-NDC-36	169	Apr85	TNL	Dave+ NDG. TBP NP/A.
^{58}Ni	$\sigma_{el}(\theta)$	. +0	. +6	Expt	DOE-NDC-36	143	Apr85	ORL	Perey+ 85SANTA FE CONF.
^{58}Ni	$\sigma_{dif.inl}$	4.0+6	1.0+7	Expt	DOE-NDC-36	7	Apr85	ANL	Smith+ NDG. TBC.
^{58}Ni	$\sigma_{dif.inl}$	8.0+6	1.7+7	Expt	DOE-NDC-36	169	Apr85	TNL	Dave+ NDG. TBP NP/A.
^{58}Ni	$\sigma_{n,\gamma}$	. +0	. +6	Expt	DOE-NDC-36	143	Apr85	ORL	Perey+ 85SANTA FE CONF.
^{58}Ni	$\sigma_{n,X\gamma}$	2.0+5	4.0+7	Expt	DOE-NDC-36	130	Apr85	ORL	Larson. NDG. 85SANTA FE CONF.
^{58}Ni	$\sigma_{n,2n}$	1.5+7		Expt	DOE-NDC-36	2	Apr85	ANL	Meadows+ EN=14.7MEV. REL ^{238}U(N,F).
^{58}Ni	$\sigma_{n,p}$	1.5+7		Expt	DOE-NDC-36	2	Apr85	ANL	Meadows+ EN=14.7MEV. REL ^{238}U(N,F).
^{58}Ni	Res.Params.		6.5+5	Expt	DOE-NDC-36	143	Apr85	ORL	Perey+ 85SANTA FE CONF.
^{58}Ni	$\langle\Gamma\rangle/D$		6.5+5	Expt	DOE-NDC-36	143	Apr85	ORL	Perey+ 85SANTA FE CONF.
^{58}Ni	$\sigma_{\alpha,emis}$	8.0+6	9.4+6	Expt	DOE-NDC-36	147	Apr85	OHO	Graham+ NDG. SIG,E SPECT CFD HF CALC.
^{58}Ni	$\sigma_{p,emis}$	8.0+6	9.4+6	Expt	DOE-NDC-36	147	Apr85	OHO	Graham+ NDG. SIG,E SPECT CFD HF CALC.
^{60}Ni	Evaluation	1.0+6	2.0+7	Eval	DOE-NDC-36	141	Apr85	ORL	Hetrick+ 85SANTA FE CONF.
^{60}Ni	$\sigma_{el}(\theta)$	8.0+6	1.7+7	Expt	DOE-NDC-36	169	Apr85	TNL	Dave+ NDG. TBP NP/A.
^{60}Ni	$\sigma_{dif.inl}$	8.0+6	1.7+7	Expt	DOE-NDC-36	169	Apr85	TNL	Dave+ NDG. TBP NP/A.
^{60}Ni	$\sigma_{\alpha,emis}$	8.0+6	9.4+6	Expt	DOE-NDC-36	147	Apr85	OHO	Graham+ NDG. SIG,E SPECT CFD HF CALC.
^{60}Ni	$\sigma_{p,emis}$	8.0+6	9.4+6	Expt	DOE-NDC-36	147	Apr85	OHO	Graham+ NDG. SIG,E SPECT CFD HF CALC.
Cu	σ_{tot}	. +5	4.0+6	Expt	DOE-NDC-36	1	Apr85	ANL	Guenther+ NDG. TBP NP/A.
Cu	$\sigma_{el}(\theta)$	. +5	4.0+6	Expt	DOE-NDC-36	1	Apr85	ANL	Guenther+ NDG. TBP NP/A.
Cu	$\sigma_{dif.inl}$	. +5	4.0+6	Expt	DOE-NDC-36	1	Apr85	ANL	Guenther+ NDG. TBP NP/A.
Cu	$\sigma_{n,n'\gamma}$	. +5	4.0+6	Expt	DOE-NDC-36	1	Apr85	ANL	Guenther+ NDG. TBP NP/A.
^{63}Cu	Evaluation	1.0+6	2.0+7	Eval	DOE-NDC-36	141	Apr85	ORL	Hetrick+ 85SANTA FE CONF.
^{63}Cu	$\sigma_{n,p}$	9.0+6		Expt	DOE-NDC-36	147	Apr85	OHO	Ahmad+ NDG. CFD HF CALC.
^{63}Cu	$\sigma_{n,\alpha}$	9.0+6		Expt	DOE-NDC-36	147	Apr85	OHO	Ahmad+ NDG. CFD HF CALC.
^{65}Cu	Evaluation	1.0+6	2.0+7	Eval	DOE-NDC-36	141	Apr85	ORL	Hetrick+ 85SANTA FE CONF.
^{65}Cu	$\sigma_{n,2n}$	1.5+7		Expt	DOE-NDC-36	2	Apr85	ANL	Meadows+ EN=14.7MEV. REL ^{238}U(N,F).
^{65}Cu	$\sigma_{n,p}$	1.4+7	1.5+7	Eval	DOE-NDC-36	6	Apr85	ANL	Evain+ NDG. TBP ANL-NDM-89.
^{65}Cu	$\sigma_{n,p}$	1.5+7		Expt	DOE-NDC-36	2	Apr85	ANL	Meadows+ EN=14.7MEV. REL ^{238}U(N,F).
^{65}Cu	$\sigma_{n,p}$	9.0+6		Expt	DOE-NDC-36	147	Apr85	OHO	Ahmad+ NDG. CFD HF CALC.

NEUTRON DATA REFERENCES

Element	Quantity	Energy (eV) Min	Max	Type	Documentation Ref	Page	Date	Lab	Comments
^{65}Cu	$\sigma_{n,\alpha}$	9.0+6		Expt	DOE-NDC-36	147	Apr85	OHO	Ahmad+ NDG. CFD HF CALC.
^{64}Zn	$\sigma_{n,2n}$	1.4+7	1.5+7	Eval	DOE-NDC-36	6	Apr85	ANL	Evain+ NDG. TBP ANL-NDM-89.
^{64}Zn	$\sigma_{n,2n}$	1.5+7		Expt	DOE-NDC-36	2	Apr85	ANL	Meadows+ EN=14.7MEV. REL ^{238}U(N,F).
^{64}Zn	$\sigma_{n,p}$	1.4+7	1.5+7	Eval	DOE-NDC-36	6	Apr85	ANL	Evain+ NDG. TBP ANL-NDM-89.
^{64}Zn	$\sigma_{n,p}$	1.5+7		Expt	DOE-NDC-36	2	Apr85	ANL	Meadows+ EN=14.7MEV. REL ^{238}U(N,F).
^{78}Kr	$\sigma_{n,\gamma}$	2.0-2	2.0+7	Eval	DOE-NDC-36	37	Apr85	HED	Schenter+ GRPH. CFD ENDF/B-4.
^{86}Kr	σ_{tot}		8.0+5	Expt	DOE-NDC-36	126	Apr85	ORL	Carlton+ NDG. MEAS+R-MATRIX ANALYS.
^{95}Rb	Res.Params.	1.4+4	2.7+4	Expt	DOE-NDC-36	26	Apr85	BNL	.2 ES. E0, WT.
^{86}Sr	$\sigma_{n,\gamma}$	1.0+2	1.0+6	Expt	DOE-NDC-36	71	Apr85	LRL	Bauer+ TBL. MAXW CS.
^{87}Sr	$\sigma_{n,\gamma}$	1.0+2	1.0+6	Expt	DOE-NDC-36	71	Apr85	LRL	Bauer+ TBL. MAXW CS.
^{90}Zr	$\sigma_{n,p}$	6.5+7		Expt	DOE-NDC-36	33	Apr85	DAV	Ford+ P SPECT. 0 DEG. NDG.
^{91}Zr	Res.Params.	2.9+2		Expt	DOE-NDC-36	129	Apr85	ORL	Salah. E0, J/P1, WN, WG.
^{93}Zr	Res.Int.Abs.		2.2+4	Expt	DOE-NDC-36	129	Apr85	ORL	Macklin. (RES INT-1/V)=15.0B.
^{93}Zr	$\sigma_{n,\gamma}$		3.0+5	Expt	DOE-NDC-36	129	Apr85	ORL	Macklin. NDG. CFD ENDF/B-V.
^{93}Zr	Res.Params.	NDG		Expt	DOE-NDC-36	129	Apr85	ORL	Macklin. NDG. 138 RES.
^{96}Zr	Res.Params.	3.0+2		Expt	DOE-NDC-36	129	Apr85	ORL	Salah. E0, J/P1, WN, WG.
^{93}Nb	Evaluation		2.0+7	Expt	DOE-NDC-36	6	Apr85	ANL	Smith+ NDG. TBP ANL-NDM-88.
^{93}Nb	$\sigma_{el}(\theta)$	4.0+6	1.0+7	Expt	DOE-NDC-36	7	Apr85	ANL	Smith+ NDG. TBC.
^{93}Nb	$\sigma_{dif.inl}$	NDG		Expt	DOE-NDC-36	6	Apr85	ANL	Smith+ NDG. TBP ANL-NDM-88.
^{107}Pd	Res.Int.Abs.	NDG		Expt	DOE-NDC-36	128	Apr85	ORL	Macklin. SEE NSE 89, 79.
^{107}Pd	$\sigma_{n,\gamma}$	3.0+3	6.0+6	Expt	DOE-NDC-36	128	Apr85	ORL	Macklin. SEE NSE 89, 79.
^{107}Pd	Res.Params.	NDG		Expt	DOE-NDC-36	128	Apr85	ORL	Macklin. SEE NSE 89, 79.
^{113}In	$\sigma_{dif.inl}$	1.4+7	1.5+7	Eval	DOE-NDC-36	6	Apr85	ANL	Evain+ NDG. TBP ANL-NDM-89.
^{113}In	$\sigma_{dif.inl}$	1.5+7		Expt	DOE-NDC-36	2	Apr85	ANL	Meadows+ EN=14.7MEV. REL ^{238}U(N,F).
^{115}In	$\sigma_{dif.inl}$	1.4+7	1.5+7	Eval	DOE-NDC-36	6	Apr85	ANL	Evain+ NDG. TBP ANL-NDM-89.
^{115}In	$\sigma_{dif.inl}$	1.5+7		Expt	DOE-NDC-36	2	Apr85	ANL	Meadows+ EN=14.7MEV. REL ^{238}U(N,F).
^{116}Sn	$\sigma_{el}(\theta)$	4.0+6		Expt	DOE-NDC-36	50	Apr85	KTY	Zhou+ NDG. CC ANAL. TBD.
^{116}Sn	$\sigma_{dif.inl}$	4.0+6		Expt	DOE-NDC-36	50	Apr85	KTY	Zhou+ NDG. CC ANAL. TBD.
^{116}Sn	$\sigma_{n,n'\gamma}$	2.5+6	4.5+6	Expt	DOE-NDC-36	53	Apr85	KTY	Gasci+ NDG. ANAL TBC.
^{116}Sn	$\sigma_{\alpha,emis}$	1.5+7		Expt	DOE-NDC-36	158	Apr85	AI	Kneff+ TBL. EN=14.8MEV.
^{117}Sn	$\sigma_{\alpha,emis}$	1.5+7		Expt	DOE-NDC-36	158	Apr85	AI	Kneff+ TBL. EN=14.8MEV.
^{118}Sn	$\sigma_{el}(\theta)$	4.0+6		Expt	DOE-NDC-36	50	Apr85	KTY	Zhou+ NDG. CC ANAL. TBD.
^{118}Sn	$\sigma_{dif.inl}$	4.0+6		Expt	DOE-NDC-36	50	Apr85	KTY	Zhou+ NDG. CC ANAL. TBD.

NEUTRON DATA REFERENCES

Element	Quantity	Energy (eV) Min	Max	Type	Documentation Ref	Page	Date	Lab	Comments
^{118}Sn	$\sigma_{n,p}$	6.5+7		Expt	DOE-NDC-36	33	Apr85	DAV	Castaneda+ P SPECT. 6-70 DEG. NDG.
^{118}Sn	$\sigma_{\alpha,emis}$	1.5+7		Expt	DOE-NDC-36	158	Apr85	AI	Kneff+ TBL. EN=14.8MEV.
^{119}Sn	$\sigma_{\alpha,emis}$	1.5+7		Expt	DOE-NDC-36	158	Apr85	AI	Kneff+ TBL. EN=14.8MEV.
^{120}Sn	$\sigma_{el}(\theta)$	4.0+6		Expt	DOE-NDC-36	50	Apr85	KTY	Zhou+ NDG. CC ANAL. TBD.
^{120}Sn	$\sigma_{dif.inl}$	4.0+6		Expt	DOE-NDC-36	50	Apr85	KTY	Zhou+ NDG. CC ANAL. TBD.
^{120}Sn	$\sigma_{n,n'\gamma}$	NDG		Expt	DOE-NDC-36	53	Apr85	KTY	Gasci+ NDG. ANAL TBC.
^{120}Sn	$\sigma_{\alpha,emis}$	1.5+7		Expt	DOE-NDC-36	158	Apr85	AI	Kneff+ TBL. EN=14.8MEV.
^{122}Sn	$\sigma_{el}(\theta)$	4.0+6		Expt	DOE-NDC-36	50	Apr85	KTY	Zhou+ NDG. CC ANAL. TBD.
^{122}Sn	$\sigma_{dif.inl}$	4.0+6		Expt	DOE-NDC-36	50	Apr85	KTY	Zhou+ NDG. CC ANAL. TBD.
^{122}Sn	$\sigma_{\alpha,emis}$	1.5+7		Expt	DOE-NDC-36	158	Apr85	AI	Kneff+ TBL. EN=14.8MEV.
^{124}Sn	$\sigma_{el}(\theta)$	4.0+6		Expt	DOE-NDC-36	50	Apr85	KTY	Zhou+ NDG. CC ANAL. TBD.
^{124}Sn	$\sigma_{dif.inl}$	4.0+6		Expt	DOE-NDC-36	50	Apr85	KTY	Zhou+ NDG. CC ANAL. TBD.
^{124}Sn	$\sigma_{\alpha,emis}$	1.5+7		Expt	DOE-NDC-36	158	Apr85	AI	Kneff+ TBL. EN=14.8MEV.
^{136}Xe	σ_{tot}		5.0+5	Expt	DOE-NDC-36	127	Apr85	ORL	Fogelberg+ NDG. 84KNOXVILLE CONF.
^{136}Xe	Res.Params.	NDG		Expt	DOE-NDC-36	127	Apr85	ORL	Fogelberg+ NDG. 84KNOXVILLE CONF.
^{136}Xe	$\langle\Gamma\rangle/D$	NDG		Expt	DOE-NDC-36	127	Apr85	ORL	Fogelberg+ NDG. 84KNOXVILLE CONF.
^{160}Dy	$\sigma_{n,\gamma}$	NDG		Expt	DOE-NDC-36	125	Apr85	ORL	Beer+ NDG. PR/C 30, 464.
^{161}Dy	$\sigma_{n,\gamma}$	NDG		Expt	DOE-NDC-36	125	Apr85	ORL	Beer+ NDG. PR/C 30, 464.
^{170}Yb	$\sigma_{n,\gamma}$	NDG		Expt	DOE-NDC-36	125	Apr85	ORL	Beer+ NDG. PR/C 30, 464.
^{171}Yb	$\sigma_{n,\gamma}$	NDG		Expt	DOE-NDC-36	125	Apr85	ORL	Beer+ NDG. PR/C 30, 464.
^{173}Yb	γ Spectra	NDG		Expt	DOE-NDC-36	20	Apr85	BNL	.NDG. TBD. AVG RES CAPT SPECT.
^{175}Lu	$\sigma_{n,\gamma}$	NDG		Expt	DOE-NDC-36	125	Apr85	ORL	Beer+ NDG. PR/C 30, 464.
^{175}Lu	$\sigma_{n,\gamma}$	NDG		Theo	DOE-NDC-36	76	Apr85	LRL	Gardner+ NDG.
^{175}Lu	$\sigma_{n,2n}$	NDG		Theo	DOE-NDC-36	76	Apr85	LRL	Gardner+ NDG.
^{176}Lu	$\sigma_{n,\gamma}$	NDG		Expt	DOE-NDC-36	125	Apr85	ORL	Beer+ NDG. PR/C 30, 464.
^{176}Hf	$\sigma_{n,\gamma}$	NDG		Expt	DOE-NDC-36	125	Apr85	ORL	Beer+ NDG. PR/C 30, 464.
^{177}Hf	$\sigma_{n,\gamma}$	NDG		Expt	DOE-NDC-36	125	Apr85	ORL	Beer+ NDG. PR/C 30, 464.
^{182}W	$\sigma_{el}(\theta)$	4.9+6	6.0+6	Expt	DOE-NDC-36	148	Apr85	OHO	Annand+ NDG. CFD CC CALC.
^{182}W	$\sigma_{dif.inl}$	4.9+6	6.0+6	Expt	DOE-NDC-36	148	Apr85	OHO	Annand+ NDG. CFD CC CALC.
^{184}W	$\sigma_{el}(\theta)$	4.9+6	6.0+6	Expt	DOE-NDC-36	148	Apr85	OHO	Annand+ NDG. CFD CC CALC.
^{184}W	$\sigma_{dif.inl}$	4.9+6	6.0+6	Expt	DOE-NDC-36	148	Apr85	OHO	Annand+ NDG. CFD CC CALC.
^{190}Os	σ_{tot}	3.0+5	4.0+6	Expt	DOE-NDC-36	48	Apr85	KTY	Hicks+ NDG. 1 PCT ACCURACY.
^{192}Os	σ_{tot}	3.0+5	4.0+6	Expt	DOE-NDC-36	48	Apr85	KTY	Hicks+ NDG. 1 PCT ACCURACY.

NEUTRON DATA REFERENCES

Element	Quantity	Energy (eV) Min	Max	Type	Documentation Ref	Page	Date	Lab	Comments
^{190}Pt	$\sigma_{el}(\theta)$	5.0+6		Expt	DOE-NDC-36	48	Apr85	KTY	Hicks+ NDG. TBD.
^{190}Pt	$\sigma_{dif.inl}$	5.0+6		Expt	DOE-NDC-36	48	Apr85	KTY	Hicks+ NDG. TBD.
^{192}Pt	$\sigma_{el}(\theta)$	5.0+6		Expt	DOE-NDC-36	48	Apr85	KTY	Hicks+ NDG. TBD.
^{192}Pt	$\sigma_{dif.inl}$	5.0+6		Expt	DOE-NDC-36	48	Apr85	KTY	Hicks+ NDG. TBD.
^{194}Pt	σ_{tot}	3.0+5	4.0+6	Expt	DOE-NDC-36	48	Apr85	KTY	Hicks+ NDG. 1 PCT ACCURACY.
^{194}Pt	$\sigma_{el}(\theta)$	5.0+6		Expt	DOE-NDC-36	48	Apr85	KTY	Hicks+ NDG. TBD.
^{194}Pt	$\sigma_{dif.inl}$	5.0+6		Expt	DOE-NDC-36	48	Apr85	KTY	Hicks+ NDG. TBD.
^{196}Pt	σ_{tot}	3.0+5	4.0+6	Expt	DOE-NDC-36	48	Apr85	KTY	Hicks+ NDG. 1 PCT ACCURACY.
^{196}Pt	$\sigma_{el}(\theta)$	2.5+6		Expt	DOE-NDC-36	48	Apr85	KTY	Hicks+ NDG. TBD.
^{196}Pt	$\sigma_{dif.inl}$	2.5+6		Expt	DOE-NDC-36	48	Apr85	KTY	Hicks+ NDG. TBD.
^{198}Hg	$\sigma_{n,\gamma}$	2.6+3	5.0+5	Expt	DOE-NDC-36	125	Apr85	ORL	Beer+ NDG. TBP PR/C.
^{198}Hg	Res.Params.	NDG		Expt	DOE-NDC-36	125	Apr85	ORL	Beer+ NDG. TBP PR/C.
^{198}Hg	$\langle\Gamma\rangle/D$	NDG		Expt	DOE-NDC-36	125	Apr85	ORL	Beer+ NDG. TBP PR/C.
^{199}Hg	$\sigma_{n,\gamma}$	2.6+3	5.0+5	Expt	DOE-NDC-36	125	Apr85	ORL	Beer+ NDG. TBP PR/C.
^{199}Hg	Res.Params.	NDG		Expt	DOE-NDC-36	125	Apr85	ORL	Beer+ NDG. TBP PR/C.
^{199}Hg	$\langle\Gamma\rangle/D$	NDG		Expt	DOE-NDC-36	125	Apr85	ORL	Beer+ NDG. TBP PR/C.
^{200}Hg	$\sigma_{n,\gamma}$	2.6+3	5.0+5	Expt	DOE-NDC-36	125	Apr85	ORL	Beer+ NDG. TBP PR/C.
^{200}Hg	Res.Params.	NDG		Expt	DOE-NDC-36	125	Apr85	ORL	Beer+ NDG. TBP PR/C.
^{200}Hg	$\langle\Gamma\rangle/D$	NDG		Expt	DOE-NDC-36	125	Apr85	ORL	Beer+ NDG. TBP PR/C.
^{201}Hg	$\sigma_{n,\gamma}$	2.6+3	5.0+5	Expt	DOE-NDC-36	125	Apr85	ORL	Beer+ NDG. TBP PR/C.
^{201}Hg	Res.Params.	NDG		Expt	DOE-NDC-36	125	Apr85	ORL	Beer+ NDG. TBP PR/C.
^{201}Hg	$\langle\Gamma\rangle/D$	NDG		Expt	DOE-NDC-36	125	Apr85	ORL	Beer+ NDG. TBP PR/C.
^{202}Hg	$\sigma_{n,\gamma}$	2.6+3	5.0+5	Expt	DOE-NDC-36	125	Apr85	ORL	Beer+ NDG. TBP PR/C.
^{202}Hg	$\sigma_{n,n'\gamma}$	NDG		Expt	DOE-NDC-36	51	Apr85	KTY	Kleppinger+ NDG. EXC FCN,ANGDIST. TBD.
^{202}Hg	Res.Params.	NDG		Expt	DOE-NDC-36	125	Apr85	ORL	Beer+ NDG. TBP PR/C.
^{202}Hg	$\langle\Gamma\rangle/D$	NDG		Expt	DOE-NDC-36	125	Apr85	ORL	Beer+ NDG. TBP PR/C.
^{204}Hg	$\sigma_{n,\gamma}$	2.6+3	5.0+5	Expt	DOE-NDC-36	125	Apr85	ORL	Beer+ NDG. TBP PR/C.
^{204}Hg	$\sigma_{n,n'\gamma}$	NDG		Expt	DOE-NDC-36	51	Apr85	KTY	Kleppinger+ NDG. EXC FCN,ANGDIST. TBD.
^{204}Hg	Res.Params.	NDG		Expt	DOE-NDC-36	125	Apr85	ORL	Beer+ NDG. TBP PR/C.
^{204}Hg	$\langle\Gamma\rangle/D$	NDG		Expt	DOE-NDC-36	125	Apr85	ORL	Beer+ NDG. TBP PR/C.
Pb	σ_{tot}	3.0+5	4.0+6	Expt	DOE-NDC-36	48	Apr85	KTY	Hicks+ NDG. AGREES OTHER MEAS.
^{204}Pb	σ_{tot}	3.0+5	4.0+6	Expt	DOE-NDC-36	49	Apr85	KTY	Hanly+ NDG. TBC.
^{204}Pb	$\sigma_{el}(\theta)$	2.5+6	7.0+6	Expt	DOE-NDC-36	49	Apr85	KTY	Hanly+ NDG. TBD.

NEUTRON DATA REFERENCES

Element	Quantity	Energy (eV) Min	Max	Type	Documentation Ref	Page	Date	Lab	Comments
^{204}Pb	$\sigma_{dif.inl}$	2.5+6	7.0+6	Expt	DOE-NDC-36	49	Apr85	KTY	Hanly+ NDG. TBD.
^{204}Pb	$\sigma_{n,n'\gamma}$	NDG		Expt	DOE-NDC-36	51	Apr85	KTY	Kleppinger+ NDG. EXC FCN,ANGDIST. TBD.
^{204}Pb	$\sigma_{\alpha,emis}$	1.5+7		Expt	DOE-NDC-36	158	Apr85	AI	Kneff+ TBL. EN=14.8MEV.
^{206}Pb	σ_{tot}	3.0+5	4.0+6	Expt	DOE-NDC-36	49	Apr85	KTY	Hanly+ NDG. TBC.
^{206}Pb	$\sigma_{el}(\theta)$	2.5+6	7.0+6	Expt	DOE-NDC-36	49	Apr85	KTY	Hanly+ NDG. TBD.
^{206}Pb	$\sigma_{dif.inl}$	2.5+6	7.0+6	Expt	DOE-NDC-36	49	Apr85	KTY	Hanly+ NDG. TBD.
^{206}Pb	$\sigma_{\alpha,emis}$	1.5+7		Expt	DOE-NDC-36	158	Apr85	AI	Kneff+ TBL. EN=14.8MEV.
^{207}Pb	$\sigma_{\alpha,emis}$	1.5+7		Expt	DOE-NDC-36	158	Apr85	AI	Kneff+ TBL. EN=14.8MEV.
^{208}Pb	$\sigma_{el}(\theta)$	4.0+6	7.0+6	Expt	DOE-NDC-36	148	Apr85	OHO	Annand+ NDG. CFD STAT MDL CALC.
^{208}Pb	$\sigma_{el}(\theta)$	7.0+6	5.0+7	Theo	DOE-NDC-36	150	Apr85	OHO	Finlay+ NDG. PHENOMENOLOGICAL OM ANAL.
^{208}Pb	$\sigma_{dif.inl}$	4.0+6	7.0+6	Expt	DOE-NDC-36	148	Apr85	OHO	Annand+ NDG. CFD STAT MDL CALC.
^{208}Pb	$\sigma_{\alpha,emis}$	1.5+7		Expt	DOE-NDC-36	158	Apr85	AI	Kneff+ TBL. EN=14.8MEV.
^{209}Bi	$\sigma_{el}(\theta)$	4.0+6	7.0+6	Expt	DOE-NDC-36	148	Apr85	OHO	Annand+ NDG. CFD STAT MDL CALC.
^{209}Bi	$\sigma_{dif.inl}$	4.0+6	7.0+6	Expt	DOE-NDC-36	148	Apr85	OHO	Annand+ NDG. CFD STAT MDL CALC.
^{209}Bi	$\sigma_{n,p}$	6.5+7		Expt	DOE-NDC-36	33	Apr85	DAV	Castaneda+ P SPECT. 6-70 DEG. NDG.
^{209}Bi	$\sigma_{n,p}$	6.5+7		Expt	DOE-NDC-36	33	Apr85	DAV	Ford+ P SPECT. 0 DEG. NDG.
^{232}Th	$\sigma_{el}(\theta)$	5.5+5		Expt	DOE-NDC-36	102	Apr85	LTI	Beghian+ NDG.
^{232}Th	$\sigma_{dif.inl}$	5.5+5		Expt	DOE-NDC-36	102	Apr85	LTI	Beghian+ GRPH. ANG DIST.
^{232}Th	$\sigma_{dif.inl}$		3.4+6	Theo	DOE-NDC-36	105	Apr85	LTI	Beghian+ NDG.
^{232}Th	$\sigma_{n,\gamma}$	1.4+5	9.6+5	Expt	DOE-NDC-36	112	Apr85	MHG	Wilderman+ NDG.
^{232}Th	Frag Spectra	7.0+5	1.0+7	Expt	DOE-NDC-36	84	Apr85	LRL	Becker+ GRPH K-DISTRIBUTION.
^{232}U	ν_d	NDG		Expt	DOE-NDC-36	107	Apr85	LTI	Beghian+ TBD.
^{233}U	$\sigma_{n,f}$	1.5+7		Expt	DOE-NDC-36	113	Apr85	MHG	Zasadny+ EN=14.62. REL ^{56}FE(N,P).
^{233}U	ν_p	5.0-3	1.0+1	Expt	DOE-NDC-36	132	Apr85	ORL	Gwin+ 85SANTA FE CONF+NSE 87, 381.
^{233}U	Fiss.Yield	NDG		Expt	DOE-NDC-36	123	Apr85	SAC	Trochon+ NDG. ANAL TBD.
^{235}U	$\sigma_{el}(\theta)$	1.0+5	5.0+5	Expt	DOE-NDC-36	102	Apr85	LTI	Beghian+ NDG. AGREES ENDF/B-V.
^{235}U	$\sigma_{el}(\theta)$	5.5+5		Expt	DOE-NDC-36	102	Apr85	LTI	Beghian+ GRPH. ANG DIST.
^{235}U	$\sigma_{dif.inl}$	1.0+5	5.0+5	Expt	DOE-NDC-36	102	Apr85	LTI	Beghian+ NDG. AGREES ENDF/B-V.
^{235}U	$\sigma_{dif.inl}$	5.5+5		Expt	DOE-NDC-36	102	Apr85	LTI	Beghian+ GRPH. ANG DIST.
^{235}U	$\sigma_{n,n'\gamma}$	1.0+5	5.0+5	Expt	DOE-NDC-36	102	Apr85	LTI	Beghian+ NDG. TBC.
^{235}U	$\sigma_{n,f}$	3.0+5	1.2+6	Expt	DOE-NDC-36	116	Apr85	NBS	Carlson+ GRPH CFD EXPT, ENDF.
^{235}U	$\sigma_{n,f}$	2.0+6	6.0+6	Expt	DOE-NDC-36	118	Apr85	NBS	Dias+ NDG. PREL DATA, GEEL MTG.
^{235}U	$\sigma_{n,f}$	2.5+6		Expt	DOE-NDC-36	118	Apr85	NBS	Duvall+ NDG. TBD. ASSOC.PART.TECHN.

NEUTRON DATA REFERENCES

Element	Quantity	Energy (eV) Min	Max	Type	Documentation Ref	Page	Date	Lab	Comments
^{235}U	$\sigma_{n,f}$	2.5+2	1.0+3	Expt	DOE-NDC-36	118	Apr85	NBS	Schrack. NDG. REL $^{10}B(N,A)$.
^{235}U	$\sigma_{n,f}$	1.4+7		Expt	DOE-NDC-36	119	Apr85	NBS	Wasson+ REANALYSE DATA. NO CHANGE.
^{235}U	ν_p	5.0-3	1.0+1	Expt	DOE-NDC-36	132	Apr85	ORL	Gwin+ 85SANTA FE CONF+NSE 87, 381.
^{235}U	ν_d	2.5-2		Expt	DOE-NDC-36	107	Apr85	LTI	Beghian+ GRPHS. SPECTRA.
^{235}U	Fiss.Yield	2.5-2		Expt	DOE-NDC-36	123	Apr85	ILL	Goennewein+ NDG. MASS,E DISTR. ANAL T
^{235}U	Fiss.Yield	FISS		Expt	DOE-NDC-36	69	Apr85	LRL	Nethaway+TBL.^{85}KR,$^{155,156}EU$,^{161}TB.
^{235}U	Fiss.Yield	NDG		Expt	DOE-NDC-36	123	Apr85	SAC	Trochon+ NDG. ANAL TBD.
^{235}U	Fiss.Yield	2.5-2		Expt	DOE-NDC-36	154	Apr85	BNW	Reeder+ IND.ISOM.YIELD. 90-RB,138-CS
^{235}U	Frag Spectra	2.5-2		Expt	DOE-NDC-36	123	Apr85	ILL	Goennewein+NDG.MASS,E DISTR.ANAL TBD
^{238}U	σ_{tot}	NDG		Eval	DOE-NDC-36	141	Apr85	ORL	Olsen. NDG. TRANS.MEAS.ANALY.
^{238}U	$\sigma_{el}(\theta)$	5.5+5		Expt	DOE-NDC-36	102	Apr85	LTI	Beghian+ NDG.
^{238}U	$\sigma_{dif.inl}$	.. +5	3.0+6	Theo	DOE-NDC-36	94	Apr85	LAS	Arthur. GRPH CFD EXPTS.
^{238}U	$\sigma_{dif.inl}$	5.5+5		Expt	DOE-NDC-36	102	Apr85	LTI	Beghian+ GRPH. ANG DIST.
^{238}U	$\sigma_{dif.inl}$		3.1+6	Theo	DOE-NDC-36	105	Apr85	LTI	Beghian+ NDG.
^{238}U	$\sigma_{n,\gamma}$	1.4+5	9.6+5	Expt	DOE-NDC-36	112	Apr85	MHG	Wilderman+ NDG.
^{238}U	Fiss.Yield	NDG		Eval	DOE-NDC-36	99	Apr85	LAS	England+ NDG.ODD-EVEN PAIRNG TOO LGI
^{238}U	Fiss.Yield	FISS		Expt	DOE-NDC-36	69	Apr85	LRL	Nethaway+TBL.^{85}KR,$^{155,156}EU$,^{161}TB.
^{238}U	Res.Params.	NDG		Eval	DOE-NDC-36	141	Apr85	ORL	Olsen. NDG. TRANS.MEAS.ANALY.
^{237}Np	$\sigma_{n,2n}$	7.0+6	1.6+7	Theo	DOE-NDC-36	76	Apr85	LRL	Gardner+ GRPH (G/M).
^{237}Np	$\sigma_{n,f}$	1.5+7		Expt	DOE-NDC-36	113	Apr85	MHG	Zasadny+ EN=14.62. REL 56FE(N,P).
^{238}Pu	$\sigma_{n,f}$	1.0-1	8.0+4	Expt	DOE-NDC-36	157	Apr85	RPI	Alam+ NDG. TBD.
^{239}Pu	σ_{tot}		3.0+1	Theo	DOE-NDC-36	138	Apr85	ORL	DeSaussure+ 85SANTA FE CONF.
^{239}Pu	$\sigma_{n,\gamma}$		3.0+1	Theo	DOE-NDC-36	138	Apr85	ORL	DeSaussure+ 85SANTA FE CONF.
^{239}Pu	$\sigma_{n,f}$		6.0+2	Theo	DOE-NDC-36	138	Apr85	ORL	DeSaussure+ 85SANTA FE CONF.
^{239}Pu	α		3.0+1	Theo	DOE-NDC-36	138	Apr85	ORL	DeSaussure+ 85SANTA FE CONF.
^{239}Pu	ν_p	5.0-3	1.0+1	Expt	DOE-NDC-36	132	Apr85	ORL	Gwin+ 85SANTA FE CONF+NSE 87, 381.
^{239}Pu	ν_d	NDG		Expt	DOE-NDC-36	107	Apr85	LTI	Beghian+ TBD.
^{239}Pu	Fiss.Yield	FISS		Expt	DOE-NDC-36	69	Apr85	LRL	Nethaway+TBL.^{85}KR,$^{155,156}EU$,^{161}TB.
^{240}Pu	σ_{tot}	3.0-3	6.0+0	Expt	DOE-NDC-36	133	Apr85	ORL	Spencer+ 85SANTA FE CONF.
^{240}Pu	$\sigma_{dif.inl}$		2.5+6	Theo	DOE-NDC-36	105	Apr85	LTI	Beghian+ NDG. TBP JP/G.
^{240}Pu	Res.Params.	1.1+0		Expt	DOE-NDC-36	133	Apr85	ORL	Spencer+ 85SANTA FE CONF.
^{241}Pu	ν_p	5.0-3	1.0+1	Expt	DOE-NDC-36	132	Apr85	ORL	Gwin+ 85SANTA FE CONF+NSE 87, 381.
^{242}Pu	$\sigma_{dif.inl}$		2.5+6	Theo	DOE-NDC-36	105	Apr85	LTI	Beghian+ NDG. TBP JP/G.

NEUTRON DATA REFERENCES

Element	Quantity	Energy (eV) Min	Max	Type	Documentation Ref	Page	Date	Lab	Comments
^{244}Pu	$\sigma_{dif.inl}$		2.5+6	Theo	DOE-NDC-36	105	Apr85	LTI	Beghian+ NDG. TBP JP/G.
^{241}Am	$\sigma_{n,\gamma}$		1.0+7	Theo	DOE-NDC-36	76	Apr85	LRL	Gardner+ GRPH (G/M).
^{243}Am	$\sigma_{n,\gamma}$		1.0+7	Theo	DOE-NDC-36	76	Apr85	LRL	Gardner+ GRPH (G/M).
^{242}Cm	$\sigma_{n,f}$	1.0-1	8.0+4	Expt	DOE-NDC-36	157	Apr85	RPI	Alam+ NDG. TBD.
^{244}Cm	$\sigma_{n,f}$	NDG		Expt	DOE-NDC-36	157	Apr85	RPI	Block+ NDG. TBP NSE.
^{246}Cm	$\sigma_{n,f}$	NDG		Expt	DOE-NDC-36	157	Apr85	RPI	Block+ NDG. TBP NSE.
^{248}Cm	$\sigma_{n,f}$	NDG		Expt	DOE-NDC-36	157	Apr85	RPI	Block+ NDG. TBP NSE.
^{249}Cf	$\sigma_{n,f}$	5.0-3	2.0+7	Expt	DOE-NDC-36	131	Apr85	ORL	Dabbs+ CS(.025EV)=1555B. TBP NSE.
^{249}Cf	Res.Int.Fiss	NDG		Expt	DOE-NDC-36	131	Apr85	ORL	Dabbs+ RI=2380+-85B. TBP NSE.
^{252}Cf	Spect.fiss n	SPON		Theo	DOE-NDC-36	100	Apr85	LAS	Madland+ GRPH CFD EXPT.

ARGONNE NATIONAL LABORATORY

A. CROSS SECTION MEASUREMENTS

1. Fast-Neutron Scattering from Indium

(A. Smith, P. Guenther, J. Whalen and I. van Heerden[a])

A manuscript describing this work has been recently published in J. Phys. G11 125 (1985).

---

[a] University of Western Cape, South Africa.

2. Neutron Total, Scattering and Inelastic-Gamma-Ray Cross Sections of Yttrium at Few-MeV Energies,

(C. Budtz-Jørgensen[a], P. Guenther, A. Smith, J. Whalen, W. McMurray[b], M. Renan[c] and I. van Heerden[c])

This work, noted in the past report, has now been formally published in Z. Phys. A319 47 (1984).

---

[a] Visiting scientist from the Central Bureau for Nuclear Measurements, Geel, Belgium.
[b] National Accelerator Center, Faure, South Africa.
[c] University of Western Cape, South Africa.

3. Total, Scattering and Gamma-Ray-Production Cross Sections of Elemental Copper

(P. Guenther, D. Smith, A. Smith and J. Whalen)

This experimental effort is now completed, covering the incident energy range from a few-hundred-keV to 4 MeV. A manuscript describing the work has been submitted to Nucl. Phys.

4. Energy-differential Cross Section Measurement for the $^{51}V(n,\alpha)^{48}Sc$ Reaction

(I. Kanno[a], J. W. Meadows and D. L. Smith)

The activation method was used to measure cross sections for the $^{51}V(n,\alpha)^{48}Sc$ reaction in the threshold region, from 5.515 MeV up to 9.567

MeV. Twenty approximately-monoenergetic cross section values were obtained in this experiment. These data points span the energy region at roughly equal intervals. The experimental resolutions were in the range 0.153 to 0.233 MeV (FWHM). The present differential data cover ~ 50% of the total integral response of this reaction for the standard ^{235}U thermal-neutron-induced-fission neutron spectrum, and ~ 44% of the corresponding response for the standard ^{252}Cf spontaneous-fission neutron spectrum. Over the range 7.6 to 9.5 MeV the present experimental cross sections are noticeably larger (e.g. by ~ 50% at ~ 8.6 MeV) than the corresponding values from the ENDF/B-V evaluation. From ~ 6.7-7.5 MeV, the present values are somewhat below those of ENDF/B-V. At still lower energies the agreement is reasonably good considering the uncertainties introduced by energy scale definition very near the effective threshold where the cross section varies rapidly with neutron energy. Calculated integral cross sections based in part on the present work agree reasonably well within errors with reported integral results, provided that the reported data are renormalized to conform with recently-accepted values for appropriate standard reactions. This work has been published.[1]

[a]Visiting exchange associate, Kyoto Univ., Japan.
[1]I. Kanno et al., ANL/NDM-86, Argonne National Laboratory (1984).

5. Cross-section Measurement for the $^{7}Li(n,n't)^{4}He$ Reaction at 14.74 MeV

(D. L. Smith, J. W. Meadows, M. M. Bretscher and S. A. Cox)

The cross section for the $^{7}Li(n,n't)^{4}He$ reaction was measured at an average neutron energy of 14.74 MeV, with a resolution of 0.324 MeV, relative to the ^{238}U neutron-fission cross section. Tritium activities for the irradiated lithium-metal samples (enriched to 99.95% in ^{7}Li) were deduced using a liquid-scintillation counting method which relies upon the tritiated-water standard from the U.S. National Bureau of Standards. The measured cross section ratio of $^{7}Li(n,n't)^{4}He$ to ^{238}U neutron fission is 0.2523 (± 2.2%). The derived $^{7}Li(n,n't)^{4}He$ reaction cross section is 0.301 (± 5.3%) barn, based on the ENDF/B-V value of 1.193 (± 4.8%) barn for the ^{238}U neutron-fission cross section. The results of this work have been published.[1]

[1] D. L. Smith et al., ANL/NDM-87, Argonne National Laboratory (1984).

6. Neutron Activation Cross Section Measurements at 14.7 MeV

(J. W. Meadows, D. L. Smith and S. A. Cox)

Neutron activation cross section measurements have been performed at 14.7 MeV for the following reactions:

$^{27}A\ell(n,\alpha)^{24}Na$	$^{27}A\ell(n,p)^{27}Mg$
$Si(n,X)^{28}A\ell$	$Ti(n,X)^{46}Sc$
$Ti(n,X)^{47}Sc$	$Ti(n,X)^{48}Sc$
$^{51}V(n,\alpha)^{48}Sc$	$^{51}V(n,p)^{51}Ti$
$Cr(n,X)^{52}V$	$^{55}Mn(n,\alpha)^{52}V$
$^{55}Mn(n,2n)^{54}Mn$	$Fe(n,X)^{54}Mn$
$^{54}Fe(n,\alpha)^{51}Cr$	$^{56}Fe(n,p)^{56}Mn$
$^{59}Co(n,\alpha)^{56}Mn$	$^{59}Co(n,p)^{59}Fe$
$^{59}Co(n,2n)^{58}Co$	$^{58}Ni(n,p)^{58}Co$
$^{58}Ni(n,2n)^{57}Ni$	$^{65}Cu(n,p)^{65}Ni$
$^{65}Cu(n,2n)^{64}Cu$	$^{64}Zn(n,2n)^{63}Zn$
$Zn(n,X)^{64}Cu$	$^{113}In(n,n')^{113m}In$
$^{115}In(n,n')^{115m}In$	

The objective of these measurements is to provide a comprehensive and internally consistant data set, which should shed some light on several persistant problems, and also to provide an experimental test of a recent evaluation of 14 MeV activation data (see item No. B.2).

All measurements were made relative to the ^{238}U fission cross section, and activities were determined by gamma-ray counting with Ge(Li) detectors. Detector calibration was based on comparison with standard sources and on coincidence counting (see item D.3). Preliminary results are now available for 14 reactions. A comparison with the evaluation shows an average of 1.054 for the ratio of the evaluated cross sections to the results of these measurements. However the distribution is fairly broad with a standard deviation of 0.139.

7. Measurement of the $^{54}Fe(n,2n)^{53}Fe$ Reaction
(R. K. Smither and L. R. Greenwood)

Measurements of the $^{54}Fe(n,2n)^{53}Fe$ reaction cross section were completed in collaboration with the dosimetry group of the TFTR fusion reactor at Princeton Plasma Physics Laboratory.[1] This reaction was found to be far more useful than the $^{27}Al(n,2n)^{26}Al$ reaction reported previously in measuring the plasma ion temperature in d-t fusion reactors. The principal advantages of the $^{54}Fe(n,2n)$ reaction are the longer half-life of ^{53}Fe (8.5m), a more distinctive gamma ray (378 keV), and slightly lower threshold energy. In the ^{26}Al case, the ground state is very long-lived (T 1/2=7.3 × 10^5y), and we must excite the isomeric state (T 1/2=6s) which decays with 511-keV gamma emission from positron annihilation. The measurements are shown in Figure A-1. Typical neutron energy spectra are also shown for fusion reactors operating at temperatures of 1 and 9 keV. The steep energy dependence of the iron reaction is easily seen when compared to other reactions.

The $^{54}Fe(n,2n)$ reaction is also of interest to fusion reactor waste-handling assessments since ^{53}Fe decays to the long-lived isotope ^{53}Mn (T 1/2=3.7 × 10^6y). The present data represent the principal production

reaction for ^{53}Mn in fusion reactors; however, ^{53}Mn can also be made weakly from the (n,d) and (n,np) reactions of ^{54}Fe. Measurements of other long-lived reaction products are now in progress, primarily by 14-MeV neutron irradiations at RTNS-II followed by gamma or beta-counting, or the relatively new technique of accelerator mass spectrometry. Isotopes now being studied include ^{55}Fe, ^{59}Ni, ^{63}Ni, ^{93}Zr, ^{92}Nb, ^{94}Nb and ^{93}Mo.

---

[1] R. K. Smither and L. R. Greenwood, Damage Analysis and Fundamental Studies Quarterly Progress Report, DOE/ER-0046/17, pp. 11-13, May 1984.

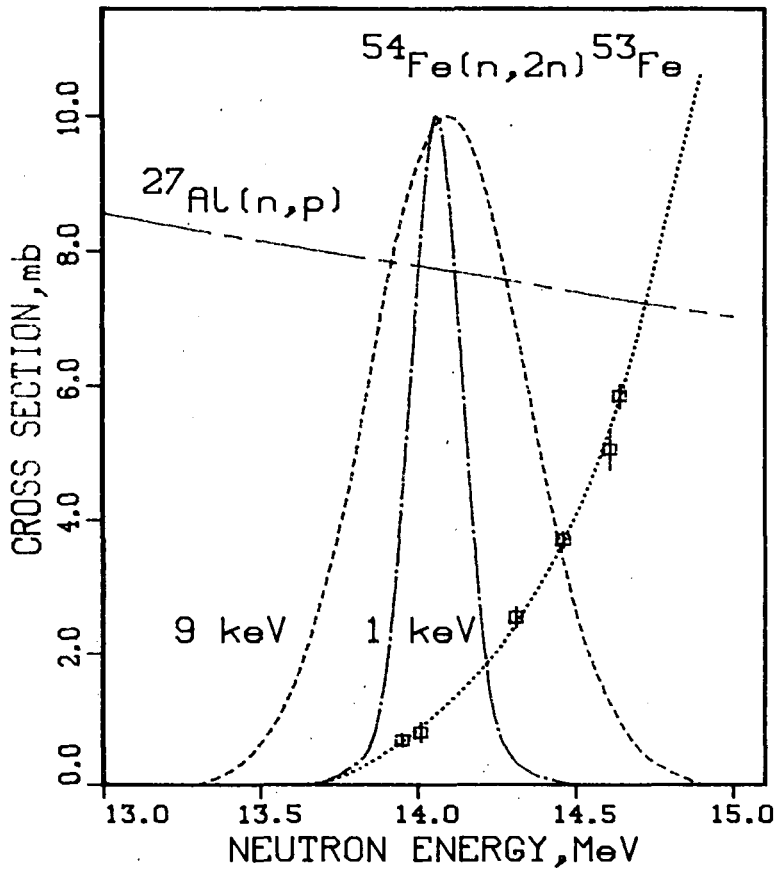

Fig. A-1. Cross section measurements are shown for the $^{54}Fe(n,2n)^{53}Fe$ reaction. Neutron energy distributions are also shown for fusion plasmas with ion temperatures of 1 and 9 keV. The sharp energy dependence of the ^{54}Fe reaction is quite evident when compared to that for the $^{27}Al(n,p)$ reaction.

8. Measurement of Cu Spallation Cross Sections from 40-450 MeV
(L. R. Greenwood and R. K. Smither)

Spallation cross sections have been measured for 20 different radioisotopes produced by proton irradiation of copper at energies between 40 and 450 MeV.[1] Copper foils were placed directly in the proton beam of the Intense Pulsed Neutron Source (IPNS) at Argonne. Some of the cross sections are illustrated in Figure A-2. The sharply different thresholds and energy dependencies for each isotope makes these data highly useful for neutron or proton flux spectral adjustments. This technique has been tested and found to work quite well both at the IPNS and at the Los Alamos Meson Physics Facility (LAMPF).[2] Further measurements are planned to extend our data to 800 MeV at LAMPF.

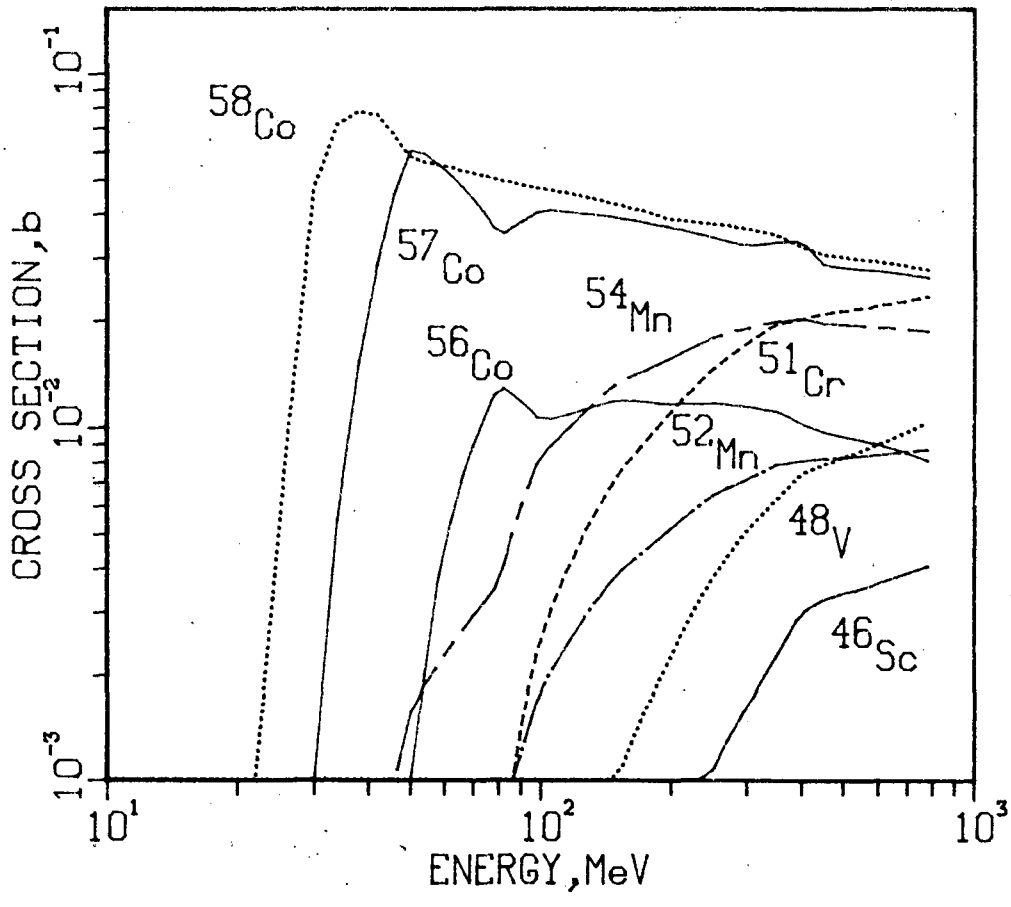

Fig. A-2. Spallation cross sections are shown for several isotopes produced by proton irradiation of copper targets. The sharply different thresholds and energy dependencies can be used to measure the high energy neutron spectrum at spallation neutron sources.

[1] L. R. Greenwood and R. K. Smither, Damage Analysis and Fundamental Studies Quarterly Progress Report, DOE/ER-0046/18, pp. 11-17, August 1984.
[2] D. R. Davidson, L. R. Greenwood. R. C. Reedy, and W. F. Sommer, Measured Radiation Environment at the LAMPF Irradiation Facility, Proceedings of the 12th International Symposium on Effects of Radiation in Materials. Williamsburg, VA, June 1984.

B. CROSS SECTION EVALUATIONS

1. Evaluated Nuclear-Data File for Niobium
(A. B. Smith, D. L. Smith and R. J. Howerton[a])

A comprehensive evaluated nuclear-data file for elemental niobium has been completed. This file, in the ENDF format and extending over the energy range 0-20 MeV, is suitable for comprehensive neutronic calculations, particularly those dealing with fusion-energy systems. It also provides a dosimetry file for the important ^{93}Nb(n,n')^{93m}Nb activity. Particular attention is given to the internal consistency of the file, energy balance, and the quantitative specification of uncertainties. The file is compared with previous evaluations, and areas of both agreement and disagreement are noted. The file is now undergoing integral testing, and upon its completion, will be submitted for ENDF/B-VI. Documentation of this file will be published as ANL/NDM-88.

[a] Lawrence Livermore National Laboratory.

2. Compilation and Evaluation of 14-MeV Neutron Activation Cross Sections for Nuclear Tehnology Applications: Set I
(B. P. Evain[a], D. L. Smith and P. Lucchese[b])

Available 14-MeV experimental neutron activation cross sections are compiled and evaluated for the following reactions of interest for nuclear technology applications: ^{27}Aℓ(n,p)^{27}Mg, Si(n,x)^{28}Aℓ, Ti(n,x)^{46}Sc, Ti(n,x)^{47}Sc, Ti(n,x)^{48}Sc, ^{51}V(n,p)^{51}Ti, ^{51}V(n,α)^{48}Sc, Cr(n,x)^{52}V, ^{55}Mn(n,α)^{52}V, ^{55}Mn(n,2n)^{54}Mn, Fe(n,x)^{54}Mn, ^{54}Fe(n,α)^{51}Cr, ^{59}Co(n,p)^{59}Fe, ^{59}Co(n,α)^{56}Mn, ^{59}Co(n,2n)^{58}Co, ^{65}Cu(n,p)^{65}Ni, Zn(n,x)^{64}Cu, ^{64}Zn(n,2n)^{63}Zn, ^{113}In(n,n')^{113m}In and ^{115}In(n,n')^{115m}In. The compiled values are listed and plotted for reference without adjustments. From these collected results those values for which adequate supplementary information on nuclear constants, standards and experimental errors is provided are selected for use in reaction-by-reaction evaluations. These data are adjusted as needed to account for recent revisions in the nuclear constants and cross section standards. The adjusted results are subsequently transformed to equivalent cross sections at 14.7 MeV for the evaluation process. The evaluations are

performed utilizing a least-squares method which considers correlations between the experimental data. This work will be published as ANL/NDM-89.

---

[a] Visiting exchange associate, Ecole Normale Superior, France.
[b] Visiting exchange associate, FRAMATOME, France.

C. DEVELOPING MEASUREMENT PROGRAMS

1. Direct Neutron Scattering Processes in the 4-10 MeV Region (A. B. Smith and P. T. Guenther)

The neutron-scattering measurement program, first carried out to 1.5 MeV, then extended to 4.0 MeV, is now extended to 10 MeV with the same degree of detail previously reported at the lower energies. In the initial phases of the work, the focus is on the direct processes; i.e., elastic scattering and the direct excitation of low-lying collective states. The interpretation gives particular attention to the energy-dependence of the interpretative models and to a correlation with basic nuclear structure concepts formulated in the context of the shell model. Measurements are made at least at every 500 keV from 4-10 MeV and at scattering angles distributed between approximately 20-160 degrees. Considerable attention is given to resolutions and to the differential cross section accuracies. The work now in progress includes:

(1) Beryllium, elastic- and inelastic-scattering and breakup process. The results are correlated with independently measured total cross sections to obtain the (n,2n) cross sections, and will be interpreted using the R-matrix formalism.

(2) Carbon, elastic- and inelastic-scattering. These measurements are used to confirm the measurement accuracies but will also contribute to basic and applied understanding.

(3) Chromium, elastic- and inelastic-scattering. The first vibrational levels are resolved.

(4) Iron, elastic- and inelastic-scattering. The collective low-lying states are resolved.

(5) Nickel (primarily ^{58}Ni), together with the above iron and chromium results, a good understanding of the major constituents of stainless steel is being obtained.

(6) Cobalt, elastic- and inelastic-scattering. The observed structure is being correlated with shell-model prediction.

(7) Niobium, elastic-scattering. Confirmation of the energy dependence of the effective mass (ref. Mahaux and Ngo, Nucl. Phys. A378 205 (1982)) is sought.

2. Neutron-Emission-Spectrum Measurements
(P. Guenther and A. Smith)

A program of neutron-emission-spectrum measurements has been undertaken. The initial emphasis is on incident energies up to the onset of significant (n,2n) contributions and the mass region near A=100 (e.g. Nb). The objective is the determination of direct, precompound and compound components before the observables are distorted by significant (n,2n) contributions. The measurements compliment the on-going studies of elastic and discrete-inelastic scattering and the correlated evaluation program. The measurements are made relative to the ^{252}Cf spontaneous fission neutron spectrum, which, at the energies of interest, is a very well known standard. This method has been successfully used by this group in other contexts[1] for a number of years and avoids uncertainties associated with independent detector calibrations.

---

[1] A. Smith, P. Guenther and R. Sjoblom, Nucl. Instruments and Methods 140 397 (1976).

3. Neutron Activation Cross Section Measurements in the E_d=7 MeV ^{9}Be(d,n)^{10}B Thick-Target Neutron Spectrum
(D. L. Smith, J. W. Meadows and L. R. Greenwood)

A number of irradiations of aluminum, titanium, iron, cobalt, nickel, copper, zinc, niobium and indium samples have been performed in the intense neutron source formed by 7-MeV deuteron bombardment of a thick beryllium target. Integral data for several well-known reactions will be used to test the consistency of integral-differential comparison in this spectrum. In addition, integral cross sections will be sought for a variety of lesser-known, low-yield reactions. Continuation of the data analysis effort is awaiting completion of the characterization of the ^{9}Be(d,n)^{10}B neutron spectrum at this deuteron energy (see item No. D.1).

D. TECHNIQUES AND FACILITIES

1. Investigation of Thick-Target Neutron Emission from ^{9}Be(d,n)^{10}B at E_d=7 MeV for Angles Other Than Zero Degrees
(D. L. Smith, J. W. Meadows and P. T. Guenther)

The ^{9}Be(d,n)^{10}B thick-target neutron spectrum has been demonstrated

to be very useful in the integral testing of neutron activation cross section data.[1] The neutron production is intense and measurements have been performed by the time-of-flight method in order to characterize the spectrum for various deuteron energies (e.g., Refs. 2 and 3). However, the available data on neutron emission at angles other than zero degrees is sparse. There are indications of considerable anisotropy, even at relatively low energies (e.g., Ref. 3). This anisotropic emission can have a considerable impact on integral measurements for certain geometeries. Thus, a detailed set of measurements have been performed on the spectrum formed by 7-MeV deuterons on a beryllium wafer. These data are being analyzed, and the results will be used in the processing of data acquired from the irradiation of a number of sample materials in this neutron field (see item No. C.3).

---

[1] H. Liskien, D. L. Smith and R. Widera, Proc. of the Antwerp Conf., p. 409 (1982).
[2] A. Crametz, H.-H. Knitter and D. L. Smith, Proc. of the Antwerp Conf., p. 902 (1982).
[3] K. A. Weaver et al., Nucl. Sci. Eng. 52, 35 (1973).

2. Gamma-Ray Detector Calibration Methods for the Activation Cross Section Measurement Program

(J. W. Meadows and D. L. Smith)

Gamma-ray detector calibration methods utilized in a program of activation measurements at the ANL Fast Neutron Generator were reviewed and tested. The activities of two ^{60}Co sources and a ^{48}Sc source were measured by coincidence counting and also by comparison with the following three standard sources: (1) A National Bureau of Standards ^{60}Co Source. (2) A National Bureau of Standards Mixed Source (^{125}Sb, ^{154}Eu and ^{155}Eu). (2) A Laboratoire de Metrologie des Rayonnements Ionisants ^{152}Eu Source. The results were in good agreement. Details of the calibration procedures and the results of these measurements are available in a report.[1]

---

[1] J. W. Meadows and D. L. Smith, ANL/NDM-60, Argonne National Laboratory (1984).

3. Intense Ion-Source Development

(J. F. Whalen, J. W. Meadows, A. F. Engfer and A. B. Smith)

The large PIG tandem ion source, under development for some time, has passed bench tests and is being installed at the Tandem Dynamitron. The bench tests promise pulsed-hydrogen-beam source-intensity increases of × 5-10, i.e. peak nanosecond pulsed intensities of 50-100 mA. The installation will be slow as building modifications are required.

E. NUCLEAR MODEL ANALYSES

1. Tests of Optical-Model, Compound-Nucleus and Coupled-Channels Codes

(R. D. Lawson and A. B. Smith)

As a result of the tragic death of Peter Moldauer in January 1984, it has been necessary to review the performance of a collection of computer codes used for the interpretation and evaluation of neutron-induced processes. The two primary ANL codes are: ABAREX (a spherical optical-statistical code)[1] and ANLECIS (a coupled-channels-statistical code).[2] A third code is the heavy-ion coupled-channels code PTHOLEMY.[3] Detailed comparisons were made between these three codes and with results obtained with other codes both here and abroad. The comparisons included not only cross sections, but also S-matrix elements, transmission coefficients, etc. All three ANL codes are in very good agreement. Comparisons with results obtained elsewhere varied from good agreement to large discrepancies. The latter have been traced to mechanical code errors elsewhere and these have been rectified. Some more modest discrepancies in, for example, transmission coefficients remain and are being examined. The ANL comparisons have been extended to various fitting algorithms, and the results of fitting experimental data are converging in a well-understood manner. It seems evident from this exercise that significant discrepancies persist between various codes used about the world. Caution is advised in the interpretation of results from various institutions, particularly where data "fitting" is involved.

---

[1] P. Moldauer, private communication (1983).
[2] Developed from the ECIS of J. Raynal by P. Moldauer (1983).
[3] S. Pieper, private communication (1985).

1. BROOKHAVEN NATIONAL LABORATORY

The reactor-based neutron-nuclear physics research at BNL is composed of three categories: the study of nuclear structure with the (n,γ) reaction, the (n,γ) reaction mechanism and its application to pure and applied physics, and the spectroscopy of neutron-rich, fission product nuclides. These programs use the H-1 and H-2 beam ports of the HFBR. The tailored beam facility produces beams of thermal, 2- and 24-keV neutrons. A monochromator is used for resonance neutron studies. The TRISTAN on-line mass separator is used with a U-235 target to produce fission product nuclei. These facilities are operated in collaboration with a wide variety of collaborators from national laboratories and universities. In the following sections the complete program is outlined, and those sections of relevance to nuclear energy and other applications are described in detail.

A. NUCLEAR STRUCTURE WITH THE (n,γ) REACTION

The H-1 beam tube at the HFBR provides two beams used almost entirely for neutron capture γ-ray studies. These include the tailored beam facility, which provides beams of thermal, 2 and 24 keV neutrons, and the neutron monochromator, which provides thermal and energy-selected beams up to about 25 eV. These wide ranging beams provide a unique method of nuclear structure investigation due to the primarily nonselective character of the (n,γ) reaction. Indeed, in appropriate cases, all levels of a given spin-parity range in the final nucleus may be about equally populated without regard to the structure of the final state wave functions. This is primarily achieved with the use of the tailored beams, which provide resonance averaging of the primary transitions, and which are absolutely indispensable in the construction of level schemes. The primary transitions unambiguously disclose level positions, which can only be done indirectly from secondary transitions by the inferential application of the Ritz Combination Principle. The secondary transitions, however, are themselves of crucial importance for the information they provide on the electromagnetic matrix elements connecting low lying levels and, thereby, on the applicability of different nuclear models.

1. Studies of Even-even Nuclei

1.1 Tests and Refinements of the Interacting Boson Approximation (IBA)

In the last several years a major advance in nuclear structure studies has been the development and testing of the IBA. Briefly, the basic problem of nuclear structure in heavy nuclei is the practical intractability of the shell model in the face of large numbers of valence nucleons. The familiar geometrical models attempt to overcome this

difficulty by the macroscopic strategem of assuming an overall nuclear shape. The IBA offers an alternate scheme, at once more abstract and more general: it assumes an enormous truncation of the possible shell model configurations such that low lying excitations can be treated, in effect, in terms of bosons which represent pairs of fermions that are coupled to angular momentum 0 (s bosons) or 2 (d bosons). The complex Hamiltonian of the shell model is replaced by an extraordinarily simple one consisting of elementary interactions between bosons. A particularly attractive feature is that three natural limiting symmetries, denoted group theoretically as SU(5), SU(3), and O(6), arise when one or another term in this Hamiltonian dominates. These symmetries correspond crudely to the familiar vibrator, rotor, and asymmetric rotor of the geometrical models but contain features unique to the IBA which have been empirically verified. Since intermediate situations are easily handled by adjusting the relative sizes of the various terms in the Hamiltonian, the IBA offers the very attractive possibility of treating vastly different nuclei within a single scheme. Many of the most crucial and detailed tests to date have been carried out at BNL using data from the (n,γ) reaction which, due to its inherent non-selectivity and general applicability, is ideally suited to testing a model that itself attempts to generate complete sets of low-lying, collective excitations over broad regions of nuclei. Thus the experimental program has generated a symbiotic theoretical effort to better understand the IBA itself, and its relationship to other models.

a. Identification of a New Region of O(6) Symmetry

Ever since the discovery that the O(6) limit is manifested empirically in ^{196}Pt and neighboring Pt isotopes, there has been high interest in searching for additional examples of this new symmetry. Following the recent acquisition by the Koln group of extensive data in the A=130 region from $(\alpha,n\gamma)$ and $(^{13}C,x,n\gamma)$ reactions it has been possible to identify an extensive set of nuclei which display the characteristics of O(6). The region spans the nuclei ^{120}Xe-^{128}Xe and ^{128}Ba-^{134}Ba and in all cases, the nuclei are equivalent or better representatives of the symmetry than is ^{196}Pt. Moreover, the discrepancies which exist are of a similar nature in all cases, and can be largely accounted for by the introduction of a small degree of triaxiality into the Hamiltonian. In fact the similarity between this region and the Pt nuclei extends to the level of the parameters in the Hamiltonian, which differ only by a constant scaling factor. (BNL/Koln)

b. The Role of the n-p Interaction in Transitional Regions

Nuclear transition regions have long been considered the most stringent testing ground for nuclear models. Two examples of the data characterizing the most important structural changes in such regions are the energy of the first 2^+ state and the ratio E_{4+1}/E_{2+1}. The latter has a limiting value of 2 for vibrational, 2.5 for γ soft, and 3.33 for axially symmetric rotational nuclei while the former is expected to drop

continuously from near closed shell values of >1 MeV to ≈100 keV in well deformed regions. When such quantities are plotted against N (or Z), while they clearly show the trends mentioned above, it is equally evident that there is a strong Z (or N) dependence, i.e., each element passes through the transition region differently. However, the importance of the neutron-proton interaction as the driving force towards deformation and hence collective structure is well established. A crude, but plausible, measure of the strength of that interaction can be taken as the product of the number of valence neutrons and protons or, in the language of the IBA, $N_\pi \cdot N_\nu$. Plotting the above data against this quantity yields a dramatic simplification. Instead of numerous separate curves, there is now a simple and smooth empirical dependence on this single quantity which describes, for example, Ba, Ce, Nd, and Xe nuclei from N=64 to 80. The same is true, to an even greater extent, for the A≈100 and A≈150 spherical deformed transition regions. The only discrepancies occur in the neighborhood of a subshell closure, such as at Z=64 or Z=38, and, in fact point to the need to account for, in terms of N_π, the existence and eventual dissipation of these shell gaps as a function of neutron number. This feature is also apparent from a TRISTAN study of g factors, and is dealt with in more detail later. Finally, the above observations suggest an extremely simplified parameterization of the IBA Hamiltonian, in which the parameter characterizing the transition between two symmetry structures is varied linearly with $N_\pi \cdot N_\nu$. The results of such an approach show excellent agreement with the data. (BNL/Koln)

c. An Underlying SU(3) Symmetry Near Neutron Number N=104

While the O(6) limit of the IBA is undoubtedly the best empirically established symmetry, it is equally important to find examples of SU(3) symmetry. This symmetry corresponds to a special case of deformed nuclei in which the most important characteristics are a) the β and γ bands are degenerate (for states of equal spin), b) γ→g and β→g B(E2) values are forbidden since the β and γ bands occur in the same excited representation of SU(3) while the ground band is in another, c) a vanishing value of Z_γ, the γ-g bandmixing parameter, d) when the symmetry is broken in the E2 operator, a specific ratio of (β→g)/(γ→g) transitions emerges, equal to 1/6. The bulk of deformed nuclei are certainly not SU(3) because β and γ bands are seldom close in energy and γ→g B(E2) values are nearly always collective. Recent data, however, are suggestive that a better SU(3) region may indeed exist. Detailed studies of γ→g transitions in ^{178}Hf with the (n,γ) reaction have shown that the E2 branching ratios are much closer than is typical to the Alaga rules. Existing data on absolute γ→g B(E2) values simultaneously show relatively small values. Inspired by this, a detailed survey of the N≈104 region is being undertaken. The results so far suggest an underlying structure which, although strongly modulated by mixing with quasi-particle degrees of freedom, may nevertheless be closer to SU(3) than previously thought. (BNL/Koln)

d. M1 Transitions in Collective Nuclei

In lowest order in the IBA, the collective M1 operator does not yield transitions since it is simply proportional to the total angular momentum. In IBA-2, however, this constraint is lifted, since the operator is specified in terms of the neutron and proton degrees of freedom separately. Transitions can then occur in cases where the wave functions of the states involved contain components which are not fully symmetric with respect to interchange of neutrons and protons. In general, the IBA-2 Hamiltonian gives rise to a set of low lying states which are n-p symmetric, and a set of higher lying states which are antisymmetric. The mixing between the two depends on the parameterization of the Hamiltonian, and can thus to some extent be measured via the M1 transition strengths among the lower lying states. Moreover, predictions for these can be made in specific cases and work is currently in progress on two examples, the case of deformed nuclei, and the case of the triaxial limit of IBA-2, which is referred to as $SU^*(3)$. In the former, the lowest antisymmetric mode is a $K^\pi = 1^+$ band, which was recently identified for the first time in ^{156}Gd via (e,e') measurements at Darmstadt. Its characteristic signature is an enhanced B(M1) value to the ground state ($\approx 2\mu^2_N$). For the low lying states, an expression results which is similar in form to that derived in a collective framework, where the origin of M1 transitions has also been attributed to mixing with $K^\pi = 1^+$ modes, albeit of unknown origin and location. In the case of the triaxial limit, the predicted low lying M1 strengths are abnormally large, and throw serious doubt on the validity of the $SU^*(3)$ description. (Groningen/BNL)

1.2 Related Experimental Studies

a. ARC Studies in the A=100 Region

The nuclei near A=100 are of considerable interest because of the strikingly rapid onset of deformation which takes place in this region. In addition, the presence of the Z=40 subshell gives rise to collective intruder bands at low excitation. An extensive study of a number of nuclei has therefore been started via ARC measurements at BNL. The nuclei involved so far include ^{96,98}Mo, ^{102}Ru, and ^{106}Pd. In the case of the Mo nuclei, Coulomb excitation experiments have been performed at the Daresbury and Oxford tandems, and preliminary comparisons have already been made with an IBA-2 calculation which includes mixing with intruder configurations. The ^{102}Ru study has been complemented with curved crystal spectrometer measurements at the ILL, Grenoble, and a detailed level scheme is being constructed. In this case, contrary to prior expectations, it seem possible to describe all the states below 2 MeV within a simple IBA-1 framework. The results for the ^{106}Pd study are currently being analyzed. (BNL/SUNY/Beijing/Studsvik/Manchester)

b. High Precision Spectroscopy in Well Deformed Nuclei: $^{162,164}Dy$

As mentioned earlier, the combination of ARC studies at BNL with the high precision γ and β spectrometers at the ILL, Grenoble, provide data of unrivaled quality and extent, with the added bonus of a guarantee that all states within certain spin and excitation ranges will be populated. The best example to date of the application of these techniques was the case of ^{168}Er, which raised a host of new questions concerning the structure of deformed nuclei, as well as illuminating many aspects of the IBA. Two further studies of comparable scope have therefore been launched for $^{162,164}Dy$. The ARC data is already published for both, while the ILL β and γ spectrometer measurements have been completed and are currently being analyzed at BNL and ILL. The analysis of these data represents a formidable task, but the resulting level schemes should allow many of the questions raised by the ^{168}Er study to be pursued, and provide further detailed tests of our understanding of the structure of well deformed nuclei. (BNL/Manchester/ILL)

c. Studies of Heavier Deformed Nuclei: ^{178}Hf, ^{184}W

Nuclei situated near the end of the rare-earth deformed region may be expected to show properties which reflect the onset of asymmetric structure and/or the influence of hexadecapole deformation, which is known to maximize in that region. Moreover, as discussed earlier, there is now some suggestion that this region may represent one in which the characteristics of the SU(3) symmetry are best evidenced. Two studies are therefore under way. Average resonance capture data at neutron energies of 2 and 24 keV have been taken and analyzed for both ^{178}Hf and ^{184}W, and γ and β spectrometer data has also been obtained at the ILL in each case. The analysis of these latter results, and the subsequent construction of the level schemes, is in progress. (Koln/ILL/BNL)

d. Studies of O(6)/Vibrational Nuclei: ^{136}Ba, $^{124,126}Te$

In this region, the underlying single particle structure consists of neutron holes and proton particles. In general in the IBA-2 framework, such a situation should give rise to an O(6)-like structure, and these nuclei should therefore exhibit an influence of this nature, in competition with the tendency of the nearby closed shell to induce spherical structure. The $^{135}Ba(n,\gamma)^{136}Ba$ reaction has been studied at the ILL, Grenoble, using the spectrometers GAMS and BILL and at BNL via ARC measurements, and also measurements of low energy and primary γ rays following thermal neutron capture. This study has also been extended by performing coincidence and angular correlation measurements with a thermal neutron beam at Grenoble. The results of all measurements have been combined to produce a detailed level scheme ranging up to 2.3 MeV in excitation energy,

and the interpretation of this scheme is currently in progress. ARC measurements of ^{124}Te and ^{126}Te are planned for FY 1985. (Manchester/BNL/ILL)

e. M1 Transitions in Collective Nuclei: ^{168}Er, ^{196}Pt

As mentioned earlier, a theoretical study of the IBA-2 predictions for M1 transitions between low lying states in deformed and triaxial nuclei is in progress. In parallel with this, a number of experimental studies are being undertaken. In ^{168}Er, a number of E2/M1 mixing ratios for $\gamma \rightarrow g$ transitions have been extracted from ratios of L subshell conversion electron intensities, measured at the BILL β spectrometer at the ILL, Grenoble. The extreme sensitivity of this instrument results in a determination of these quantities which is more precise than could be obtained via angular correlation measurements. The results now reveal discrepancies in an earlier IBA-1 treatment of M1 transitions, and can be used to test the IBA-2 formulation being developed. In addition, mixing ratios for ^{196}Pt have been obtained at BNL using the newly installed angular correlation facility on the neutron monochromator beam. These results reveal a "normal" strength for the M1 transitions ($\approx 10^{-4}\mu^2_N$) and hence pose a severe problem to the $SU^*(3)$ description of this region, which yields far larger values. (Manchester/ILL/BNL)

2. Studies of Odd-A Nuclei

2.1 The IBFA, Boson-Fermion Symmetries and Supersymmetries

The concept of symmetry in the IBA description of even-even nuclei has proved to be one of the model's crucial ingredients, both because of the recognition of the existence of the symmetries themselves, and because they provide benchmarks in the formulation of a unified description of a broad range of nuclei. The importance of the recently proposed symmetries in odd-even systems can thus be viewed in the same light, and their role in pointing to a simple prescription for the changing collective structure in odd A nuclei throughout a major shell is likely to prove even more essential, given the much greater complexity of the general IBFA Hamiltonian. The group structure of a boson-fermion system is described by $U^B(6) \times U^F(m)$ where m specifies the number of states available to the odd fermion, and thus depends on the single particle space assumed. Of the structures studied in detail to date, the case of m=12 is the one with the broadest potential. The fermion is allowed to occupy orbits with j = 1/2, 3/2, and 5/2, so that the assumed single particle space corresponds to the negative parity states available to an odd neutron at the end of the N = 82-126 shell, namely, $p_{1/2}$, $p_{3/2}$ and $f_{5/2}$. The region of interest thus spans the W-Pt nuclei, and since one prerequisite for an odd-A symmetry is the existence of that same symmetry in the neighboring even-even core nucleus, the odd Pt nuclei around A = 196 offer the obvious testing ground for the O(6) limit of U(6/12). The heavier even-

even W nuclei, on the other hand, have the characteristics of an axial rotor, and hence the neighboring odd W isotopes offer the possibility to study the validity of the SU(3) limit. Finally, given a definition and understanding of these two limits, the construction of a simple description of the transitional odd A Os nuclei can be considered. An extensive program, both experimental and theoretical, is therefore underway to explore and develop these possibilities. In addition, if a particular symmetry exists in neighboring even-even and odd-even nuclei, it is possible to ask whether the two schemes stem from a common parent supersymmetric group structure of the type U(6/m). The concept of supersymmetry is currently of high interest in high energy physics, gravity theories, astrophysics, and condensed matter physics. However, it is only in nuclear physics that actual empirical evidence for the validity of this type of idea has so far been obtained.

a. The SU(3) Limit of U(6/12) and the Nilsson Model

While various O(6) and SU(5) group chains applicable to odd A nuclei have by now received considerable attention, the properties of the SU(3) limit of U(6/12) have not yet been studied in great detail. Since the requisite SU(3) core symmetry implies an axial rotor, the Nilsson model offers an obvious framework in which to investigate the structure of the corresponding odd-even symmetry. Moreover, the establishment of a connection between the Nilsson model and the U(6/12) SU(3) symmetry provides a unique physical insight into the structure of the symmetry itself and the role of the various operators in the corresponding IBFM (Interacting Boson-Fermion Model) Hamiltonian. During the past year, it was possible to establish a link between the two models via a comparison of the single particle structure in the two frameworks, and a clear correspondence between bands in the U(6/12) SU(3) symmetry scheme and the Nilsson orbits stemming from the $p_{1/2}$, $p_{3/2}$, and $f_{5/2}$ shell model states was obtained. Moreover, it was found that the specific single particle structure and coupling of rotational bands implicit in the boson fermion symmetry appears to be realized empirically in the low lying structure of ^{185}W. The adoption of the symmetry scheme also leads naturally to the known fragmentation of single particle strength from the higher lying Nilsson orbits in this region. The SU(3) Hamiltonian incorporates a specific Coriolis interaction which manifests itself in both the distinctive single particle structure and in the predicted B(E2) values. (BNL/Manchester)

b. A CQF in Odd-A Nuclei

The Consistent Q Formalism (CQF) has proved to be a particularly attractive starting point in the description of the collective structure of a broad range of even-even nuclei, with the framework of the IBM. The method is predicated on maintaining a consistent form for the IBM boson quadrupole operator in both the Hamiltonian and in the description of E2 transitions, and leads to a number of essentially parameter-free

predictions for relative energies and B(E2) values across a wide region of nuclei. In order to formulate an equivalent approach for the boson-fermion Hamiltonian, it was necessary to develop a compatible parameterization for the fermion degrees of freedom. This was achieved by recognizing that the pseudo-orbital angular momentum decomposition inherent in the various U(6/12) group chains allows the fermion generators to be split into components involving $(\ell,\ell') = (0,2)$ and $(2,2)$, analogous to the s,d boson space. Thus the structure of the fermion quadrupole operator can be defined by the same parameter χ as used in the boson case, and then the wave functions and E2 operators are uniquely determined. It is then possible to predict the changes in relative energies, B(E2) values and single particle structure factors across the region from SU(3) (^{185}W) to O(6) (^{195}Pt) simply by varying χ between the values which generate these two symmetries. The results so far are extremely encouraging and appear already to account for a number of empirical features in the transitional odd Os nuclei which hitherto had no satisfactory quantitative interpretation. It is indeed worth noting here that this region of odd A nuclei is one for which there is no well established applicable nuclear model, since it involves single particle orbits in a potential which is intermediate between deformed and γ unstable. Work on this study will continue and an extensive set of related experimental studies are also in progress (see below). (BNL/Gent/Manchester)

c. Microscopic Interpretation of Boson-Fermion Symmetries

It was suggested in an earlier paragraph that the establishment of a link between the Nilsson model and the structure of the SU(3) limit of U(6/12) should help in providing physical insight into the otherwise purely algebraic origins of the latter approach. In fact, one such understanding has already emerged with respect to the Casimir operator of the group $U^{BF}(6)$. This group was introduced into the symmetry chains purely on an algebraic basis, as an alternative coupling scheme which is necessary to obtain the correct energy spectra in both the Pt and W regions. The question remained, however, as to the underlying physical reason for the evident empirical necessity of this choice of chain decomposition. The link with the Nilsson scheme allowed a qualitative interpretation, which has now been put on a firm quantitative basis. The role of the $U^{BF}(6)$ term was seen to be related to the position of the Fermi surface in the corresponding Nilsson scheme. It was also possible to show that the $U^{BF}(6)$ Casimir operator contributes <u>exchange</u> terms to the Hamiltonian, not only of the d-d boson type normally included, but also of an s-d form, hitherto ignored. It has been recognized for some time that the competition between the quadrupole and exchange terms in the general IBFM Hamiltonian controls the position of the effective Fermi level in the deformed potential. These results in turn led to a study by groups at Groningen and MSU of the microscopic conditions (i.e., quasi-particle energies, occupation amplitudes, etc.) necessary to generate a supersymmetric structure. It is hoped to pursue these ideas during the coming year and to obtain an understanding of the microscopy underlying the newly proposed CQF approach in this region. (MSU/U. of Penn./BNL)

2.2 Related Experimental Studies

a. The SU(3)-O(6) Transition in the Odd-N W-Pt Nuclei: $^{185,187}W$, $^{187,189,191}Os$, $^{193,197}Pt$

Following the development of the CQF approach in the IBFM framework to describe the W-Pt region, an extensive set of (n,γ) studies are in progress on the odd-N, W, Os, and Pt nuclei. For the latter two elements in particular, data available prior to these studies were sparse and incomplete. ARC measurements at neutron energies of 2 and 24 keV have been completed for $^{185,187}W$, ^{189}Os, and ^{197}Pt, and similar measurements are planned for $^{187,191}Os$ and ^{195}Pt in the coming year. In the case of ^{187}Os and ^{193}Pt, the feasibility of these measurements will depend critically on the availability of the target material. The rarity of these isotopes has previously precluded their study by the ARC technique, but the recent upgrading of the three crystal pair spectrometer may now permit such measurements. For ^{187}W, BILL and GAMS data from the ILL have also been obtained and an extensive level scheme has been constructed, which it should now be possible to interpret in some detail. A series of Ge singles, coincidence,and angular correlation studies are in progress on ^{189}Os and ^{197}Pt, using the neutron monochromator beam, and an additional (n,n'γ) study of ^{189}Os is planned at the University of Kentucky during FY 1985. (BNL/Manchester/Kentucky/ILL)

b. Search for Symmetry/Supersymmetry in the Odd-N Ba Nuclei: $^{131,133,135}Ba$

The odd mass Ba nuclei represent another region where the underlying core structure may be close to the O(6) limit, and may therefore give evidence of a supersymmetry in the odd mass system. The nuclei ^{131}Ba and ^{133}Ba have been studied at BNL, following thermal neutron capture on the neutron monochromator facility, and at ILL with the GAMS spectrometers. The data analysis and level scheme construction are still in progress. In the case of ^{135}Ba, ARC data at 2 and 24 keV have been taken in order to identify the complete set of low spin states. The theoretical interpretation of the results will clearly be coupled to the understanding and insights gleaned from the studies in the W-Pt region. (BNL/Yale/ILL)

3. Other Studies

3.1 Modelling of Odd-odd Nuclei: ^{176}Lu and ^{238}Np

The structure of odd-odd nuclei has long been a challenge for nuclear models. Generally, attempts to predict the levels of such nuclei, at least in heavy deformed regions, have been qualitatively based on the level schemes of the neighboring odd Z and odd N nuclei. Recently, however, Hoff has developed a more sophisticated model that incorporates

such empirical results in a quantitative way including, for example, most of the effects of Coriolis mixing, as well as some of the effects of the neutron-proton interaction in the odd-odd nucleus. The model yields level predictions up to well over 1 MeV. In order to test these ideas a very careful ARC study of ^{176}Lu was carried out with the 2 and 24 keV filtered beams at BNL. The ^{175}Lu target spin of $7/2^+$ permitted the observation of the complete set of 2^--5^- levels in ^{176}Lu below about 1100 keV. However, special problems arise in an odd-odd deformed nucleus since the high level densities imply that some of the primary transitions may not be resolved. Therefore, a careful spectral analysis of multiplet structures and an interval calculation of the likelihood of missed levels were carried out. The empirical results were compared with the model predictions in terms of histograms of the cumulative number of levels of different spins vs excitation energy. The comparison involves a total of 40 predicted rotational bands, and the overall agreement is remarkably good. An additional study of ^{238}Np is planned. (LLL/BNL)

3.2 Level Schemes of ^{191,193}Ir

Following extensive spectroscopic studies with γ-ray spectrometers at the ILL, Grenoble, and earlier single resonance measurements on the neutron monochromator facility, an ARC study of ^{191,193}Ir is being considered for the coming year on the filtered beam facility at BNL. (Munich/Fribourg/BNL)

3.3 The ^{59}Co(n,γ)^{60}Co Reaction at En = 2 keV

A natural Co target was used to study the average resonance capture spectrum at a neutron energy of 2 keV. At this energy there are in fact no actual resonances encompassed by the energy spread of the neutron beam, so that the observed primary intensities must result from capture in the tails of the known nearby resonances. An attempt will therefore be made to interpret the results in terms of the detailed structure of these resonances. (Petten/BNL)

3.4 Non-statistical Effects in ARC: ^{174}Yb

The average resonance capture method is predicated on the statistical nature of the (n,γ) reaction. An experiment is planned for FY 1985 to test this hypothesis in more detail for the case of ^{174}Yb. Measurements on the filtered beam will be made in the normal manner, and also using the ^{173}Yb target material itself as an additional filter in the beam. Nonstatistical effects should then be apparent from the differences in the two spectra of primary γ rays. (Prague/Petten/BNL)

B. NUCLEAR SPECTROSCOPY OF FISSION PRODUCT NUCLEI

The on-line isotope separator, TRISTAN, at the HFBR is a facility, unique in this country, for the study of neutron-rich nuclei far off stability, produced by thermal neutron induced fission of uranium. The reactor provides an intense external neutron beam, making excellent shielding possible. This combination of high beam intensity, long running time, and low background makes it possible to do experiments at TRISTAN which cannot be done elsewhere. As a user facility, most experiments are of a collaborative BNL/USER nature. The fruitful collaboration with a large group of outside users (including an expanding group of foreign scientists) permits a wide variety of approaches to nuclear structure studies. TRISTAN is also proving to be an excellent resource for training the next generation of nuclear chemists and physicists. At present eleven graduate students are performing their experimental doctoral studies at TRISTAN.

A high interest is associated with the study of nuclei far off stability for a number of reasons. The neutron-proton force is sensitive to the spatial overlaps of neutron and proton orbits, and, therefore, its effects vary with both neutron and proton number. By providing combinations of these not available elsewhere, neutron-rich nuclei provide the opportunity to study not just an extension of familiar phenomena but the possibility of observing entirely new effects. Particularly important areas of study center on the investigation of a wide variety of collective phenomena, of phase transitions, of deformation regions, of symmetries and, possibly, supersymmetries. The latter two phenomena are especially relevant for odd nuclei where the predicted symmetries require specific combinations of single particle and core structure, some of which may not be available near stability. Besides the work on collective phenomena, TRISTAN provides access to nuclear regions that are expected to be magic in nature. One goal of current TRISTAN studies is the study of nuclei near new doubly closed shell nuclei such as ^{132}Sn, and in the region of ^{78}Ni. Finally, the access to unstable nuclei with level sufficiently large decay energies leads to the possibility of observing radioactivity in the form of β-delayed neutron emission and, in a few cases, of double delayed neutron radioactivity. Such studies are of both applied and structure importance, since they give information on the emission of decay heat from fission products and because they represent the inverse of neutron capture experiments on unstable targets, so that they can provide information on cross sections of neutron-rich nuclides, which is of particular interest for astrophysics and nuclear theory.

1. Perturbed Angular Correlation Studies

In the perturbed angular correlation (PAC) technique, a radioactive source is placed in a strong external magnetic field. Shifts in the normal angular correlation patterns of coincident gamma rays are induced and measured and the magnetic moments of intermediate states can be extracted. The delivery, installation, and successful testing of the superconducting

magnet facility midway through 1984 has greatly enhanced the number of nuclei accessible by this technique, by virtue of the increase in applied magnetic field. For nuclei near closed shells, the magnetic moment is highly sensitive to the specific nucleon orbits involved in a given state, and small admixtures of certain configurations may considerably change its value. For collective nuclei, it is an effective measure of the number of valence protons taking part in the collective motion, and as shown by earlier interpretations of TRISTAN data, represents a sensitive probe to disclose the presence and structural effects of proton subshell closures.

1.1 Transitional Nuclei near N=88-90; Effective g Factors and Proton-boson Numbers near Proton Subshells

An earlier TRISTAN study, interpreted within the framework of the neutron-proton version of the Interacting Boson Approximation (IBA-2), showed that the empirical behavior of the g factors of the lowest 2^+ states in even-even nuclei can be reproduced over broad ranges of nuclei if only the valence protons are considered to be taking part in the collective motion. Not surprisingly, however, this study also showed that the generally smooth and gradual variation in g factor values is interrupted in the region of proton subshell closures, such as those occurring around Z=64, N=82-90 and Z=40, N=50-60. From a microscopic point of view, it is natural to assume that the g factors appropriate to neutron and proton bosons, g_π and g_ν, should each vary as a function of the respective boson numbers, N_π and N_ν. However, it has recently been found that constant effective values of g_π and g_ν can describe a broad range of nuclei in the Ba-Dy region. The anomalous values of $g(2^+_1)$ that occur in the region of the Z=64 subshell closure can then be used to extract the effective number of proton bosons which take part in the collective motion. The justification for this latter step lies in the recognition that, around N=90, the filling of the $h_{9/2}$ neutron orbit allows a strong attractive n-p interaction with the $h_{11/2}$ proton orbit, making it energetically favorable for protons to enter this orbit, and resulting in the gradual eradication of the subshell effects. During 1984, $g(2^+_1)$ values for ^{142}Ba and ^{146,148}Ce have been measured. Data analysis is still in progress, and more statistics are required in the cases of ^{142}Ba and ^{148}Ce. Nevertheless, these new results, as well as existing data for Ba, Nd, Sm, Gd, and Dy isotopes, confirm the validity of the above approach. Moreover, this treatment can be extended to the A=100 nuclei to provide a tentative prediction for the behavior of g factors in the region of the Z=40 subshell, and it is hoped to test some of these predictions by further PAC measurements in the coming year. (Negev/BNL)

1.2 g Factors of Nuclei near the ^{132}Sn Closed Shell

The versatile array of ion sources now available at TRISTAN, coupled with the new superconducting magnet facility, constitute a uniquely powerful combination to study g factors in the vicinity of the doubly magic

shell closure at ^{132}Sn. Measurements have already been made using the time dependent PAC technique on the 6^+_1 state in ^{132}Te and the 5^-_1 state in ^{124}Sn, and the data are currently being analyzed. In addition, results from TRISTAN studies for the g factors of the 4^+_1 states in N=82 isotones, ^{136}Xe and ^{138}Ba, along with existing value for $g(4^+_1)$ in ^{140}Ce and $g(6^+_1)$ in ^{134}Te and ^{138}Ba, have been successfully described in terms of configuration-mixed shell-model wave functions. One set of effective orbital and spin proton g factors was obtained from the known ground state g factors of ^{139}La($7/2^+$) and ^{141}Pr($5/2^+$) and this set appears to adequately reproduce the core polarization effects for all four nuclei. (Negev/Weizmann/Studsvik/ISU/BNL/Clark)

1.3 g Factor of the $7/2^+$ 427.1 keV Level in ^{119}Cd

The time-integral PAC technique has been used in the measurement of the g factor of the $7/2^+$ 427.1 keV state in ^{119}Cd populated in the decay of ^{119}Ag. The results will provide an insight into the neutron orbital configurations contributing to that level. The results are currently being analyzed. (BNL)

2. Structure of Highly Deformed Nuclei in the A=100 Region

2.1 Rotational Bands Near A=100

In a previous TRISTAN study, six rotational bands were found in ^{99}Y, ^{101}Y, ^{99}Sr, and ^{101}Zr. All the bands had small and similar values of $h^2/2I$ that indicated deformations of $\beta \approx 0.3$-0.4 and imply that these nuclei are among the most deformed known, with I = 0.8 I-rigid. The extension of studies in this region relies on the successful performance of the high efficiency thermal ion source. Experiments have been performed during 1984 on the decays of ^{101}Sr, ^{99}Y, ^{100}Rb, ^{100}Y, ^{102}Sr, and ^{103}Sr and further measurements are planned in parallel with continuing ion source development. Preliminary results of the more recent measurements indicate the identification of a new excited 0^+ state in ^{100}Zr and the discovery of a new isotope (^{103}Sr). The half life of ^{103}Sr was measured as approximately 35 ms, making it the shortest-lived β-decaying fission product known. (Oklahoma/ISU/BNL)

2.2 Search for Intruder States in ^{96}Zr

The high degree of deformation and the suddenness of the onset of deformation in the A=100 region is primarily due to the existence of a strong subshell closure at Z=40. The driving force of the onset of deformation arises from the promotion of protons to the $g_{9/2}$ orbit, induced by neutron occupation of the spin-orbit partner $g_{7/2}$ orbit which occurs around N=58. Thus, ^{96}Zr, with Z=40, N=56, while spherical in its ground state, may be expected to exhibit coexisting deformed character in its excited state. Studies proposed at TRISTAN will search for these

rotation-like intruder bands in the coming year. The initial search will concentrate on identifying excited 0^+ bands and determining their decay characteristics. The intruder bands are expected to have significantly different B(E2) and B(E0) values than the normal vibrational states. γ-γ angular correlations and conversion electron measurements will therefore be necessary to identify and characterize the states. (Kentucky/LLL/BNL)

3. Structure Studies in Near Closed Shell Nuclei

Further development of the thermal and high temperature plasma ion sources makes it possible to produce a wealth of data on nuclei near or at new semi- or doubly-magic regions. Such studies can provide sensitive tests, in a systematic fashion of the changing single particle structure as one moves further from stability, and of the predictive power of the shell model.

3.1 Nuclei Near ^{132}Sn

The total β-decay energies of the three isomers of ^{130}In were studied at TRISTAN in 1984. A mass excess of -70.05 ± 0.20 MeV was determined for ^{130}In. The relative excitation energies of the three β-decaying isomers have been obtained, resulting in the first level information for the $\pi^{-1}\nu^{-1}$ nucleus neighboring ^{132}Sn. Results from β-γ coincidence measurements successfully determined the spins of the three isomers at 0, $\approx$200, and $\approx$600 keV as 1^-, 10^-, and 5^+, respectively. This ordering confirms the predictions of previous calculations which indicate that the 1^- and 10^- states should have the lowest energies in the $(\pi g^{-1}_{9/2}, \nu h^{-1}_{11/2})$ multiplet.

Experiments on the decay of ^{135}Te to ^{135}I have identified three excited states below 1.7 MeV. The ^{135}I nucleus comprises three protons outside the ^{132}Sn core, and two of the levels, at 603 and 870 keV, can be interpreted as $(g_{7/2})^2_0(d_{5/2})$ and $(g_{7/2})^3_{5/2}$ states, respectively, while the third at 1184 keV probably corresponds to a state primarily of the type $(g_{7/2})^3_{9/2}$, which is calculated to occur at 1216 keV. More detailed shell model calculations will be attempted during 1985.

Detailed angular correlation experiments on levels in ^{130}Sb have made it possible to determine a number of spins and parities. The data will continue to be analyzed in 1985 and g factor measurements will be performed if suitable levels for study can be identified. Similar investigations of ^{132}Sb and ^{131}Sb have begun and will continue, and a study of ^{136}Sb is planned. Studies for levels in ^{130}Sn are also being considered as part of a broader program to study the evolution of single particle structure of the heavier Sn isotopes. (Studsvik/ISU/Maryland/Georgia/BNL)

3.2 Studies of Odd-A Nuclei Near N=82

These experiments should allow a study of the evolution of odd A single particle structure from the N=82 closed shell. While extensive studies of heavier, and therefore largely collective, nuclei in this region have already been completed, the nuclei with N=84,85 may evince an interesting interplay between single particle and collective degrees of freedom, the exact character of which will probably depend strongly on the proton number. Four-detector angular correlation data have been taken for the decay of ^{139}Xe to levels in ^{139}Cs, and the analysis of this data is in progress. In addition, the Xe isobar of ^{139}Cs is also being studied via the decay of ^{139}I. This represents the first experiment using the negative surface ionization source. Since this source is still in a development stage, great detail on ^{139}Xe levels is not yet available. Nevertheless, current data suggest the discovery of a low lying triplet of states in ^{139}Xe. Another program is in progress to study the level structure of ^{141}La and the data collected so far are yielding an extremely complex level structure. Further experiments with the conversion electron detector and with higher energy resolution are planned. (Maryland/BNL)

3.3 Decay of ^{83}Ge to Levels in ^{83}As

The level structure of the N=50 nucleus ^{83}As will be investigated by the decay of ^{83}Ge. Experiments began early in 1984, and ^{83}Ge was directly observed for the first time. A preliminary half life of 1.8 sec was measured and four γ rays were observed in a coincidence experiment. More detailed data from the thermal or high temperature plasma ion source will be necessary to complete the study of this nucleus. This study represents the beginning of what will undoubtedly become an extensive series of investigations into nuclei in the second new doubly magic region accessible by TRISTAN, centered on ^{78}Ni. (ISU/BNL).

4. Nuclear Structure in the Heavy Cd Isotopes

4.1 The Role of the SU(5) Symmetry in ^{119}Cd

Following the recent recognition that the intruder states in ^{118,120}Cd are substantially higher than the two phonon vibrational levels, the lower lying levels (<1500 keV) of these isotopes closely mirror the vibrational structure predicted by the SU(5) symmetry of the IBA. Consequently, a search can be made for the analogous symmetry in the odd-even nucleus of ^{119}Cd. Given the odd neutron single particle states, the relevant group structure would be U(6/20). Consequently, an extensive study of the decay of ^{119}Ag to ^{119}Cd has been undertaken yielding a fairly complete set of levels up to ≈1500 keV in excitation with spin and parity assignments made to a large number of levels via angular correlation measurements. The results are being analyzed first in the framework of the general weak coupling limit of the IBFM where it is hoped that the overall

structural changes across a broad region of odd-A Cd nuclei can be accounted for simply by the changes in single quasi-particle energies and occupation amplitudes. The results of these calculations can then in turn be compared to the very specific wave functions of the SU(5) symmetry to check the validity of the latter approach in this region. (BNL)

4.2 The Decay of the 18 sec Isomer of ^{115}Ag to ^{115}Cd

The decay scheme of the 18 sec isomer of ^{115}Ag into ^{115}Cd was investigated for the first time via singles and γ-γ coincidence measurements. The results would complete the chain of decay schemes of the odd $^{109-119}$Cd isotopes which will be analyzed using the weak coupling limit of the IBFM. (BNL)

4.3 Q_β Measurements for the Decay of ^{120}Ag with the Superconducting Magnet

During 1984, it became possible to measure Q values using a hyperpure Ge detector located inside the superconducting magnet. The end point energy of ^{120}Ag was determined to be ≈7.5 MeV in the first experiment with this system. This value is about 2 MeV higher than values previously reported in the literature. (Lafayette/Clark/BNL)

5. Delayed Neutron Emission

5.1 Direct Measurement of Natural Line Widths in Delayed Neutron Emission

The time-of-flight apparatus developed at TRISTAN is being used to develop systematics of neutron resonances in the 1-100 keV range in neutron-rich nuclides as a unique experimental basis for testing theoretical extrapolations of level parameters and neutron cross sections from stable to very unstable nuclides. The time-of-flight spectrometer yields more than 10 resolved peaks between 3 and 100 keV in ^{95}Rb and in ^{97}Rb. Natural widths have been deduced for two ^{95}Rb peaks: 414 ± 33 eV for the 14.44 ± 0.04 keV resonance and 670 ± 270 eV for the 26.70 ± 0.11 keV resonance. (Cornell/BNL)

5.2 New Activities Identified by Delayed Neutron Emission

By using the FEBIAD and high temperature plasma ion sources, and a large, high efficiency neutron counter, several new isomers and isotopes have been identified in 1984. Simultaneous neutron and β multi-scaling experiments were used to measure half lives and Pn values. The observation of ^{75}Cu was confirmed and a half life of 1.3 ± 0.1s was measured as well as a Pn value of 3.6%. This is the heaviest known isotope of Cu and the lightest known delayed neutron precursor produced in fission.

Previous TRISTAN measurements of the half life of ^{124}Ag via delayed neutron emission were in conflict with measurements via γ-ray multiscaling also done at TRISTAN. The experiments were repeated using the high temperature plasma source, yielding β-decaying components with half lives of 0.17s and 0.54s. Therefore, the earlier γ-ray experiments did not observe the longer-lived isomer, and the shorter-lived isomer does not appear to be a delayed neutron precursor. In the same series of experiments, a new isotope of Ag, ^{125}Ag, was tentatively identified and a half life of 0.16 ± 0.04s was measured. At mass 128 a neutron emitting precursor from an isomer of ^{128}In was observed with a half life of 19 ± 3s. Some initial experiments were performed on the two-neutron emitter ^{98}Rb in an attempt to determine if the neutron emission is sequential or if the neutrons are emitted simultaneously. The differing mechanisms (if both exist) are expected to have different angular distributions. Much higher counting statistics will be necessary to be able to make any conclusions regarding this mechanism. (PNW/BNL)

6. Hyperfine Interaction Studies

Hyperfine interaction studies are being investigated by two experimental techniques: dye laser spectroscopy and electronic field perturbation by ion implantation. In the former method, the frequency of a laser beam is tuned to coincide with that of an optical transition in the isotope of interest, and resonance fluorescence is observed. By measuring the fluorescent intensity as a function of the laser frequency, the isotope shift, the isomer shift, and the hyperfine splitting can be determined. The nuclear spins, magnetic dipole moments, and electric quadrupole moments can be deduced from the measured hyperfine splitting. In the latter method, the ions are implanted in a suitable host which provides an electric field gradient causing a precession of the nuclear spin, which is measured via β-γ angular correlations.

6.1 Laser Spectroscopy

Initial test experiments using the Dye Laser Facility developed by the Texas A&M TRISTAN Users Group were performed during 1984. These tests used the colinear fast beam technique, in which the ion beam from TRISTAN and the laser beam intersect in an interaction region about 10 cm long. The laser is tuned to near resonance frequency, and the ion energy is then varied slightly to effect an equivalent laser frequency scan. The fluorescent light is collected by a parabolic mirror and focussed onto a photomultiplier. In the experiment, the magnetic moment of the $3/2^+$ ground state of ^{131}Xe was measured and found to be in good agreement with accepted values. The experiment indicated a few areas which need to be improved before experiments on lower intensity radioactive beams can be performed. The ion optics need to be improved to obtain better beam transmission and focus in the interaction region. The design of the beam line components made changes and realignment very difficult. Apertures and lens diameters

were, in general, too small for typical ion beams. There was also a need for more sensitive ion detection equipment if radioactive beam experiments are to be possible. All of these changes are being incorporated, and the revised apparatus will be tested in 1985. (Texas A&M/BNL)

6.2 Quadrupole Moment Measurements via Doubly Charged Ion Implantation

Earlier attempts at TRISTAN to measure the quadrupole moments by ion implantation into a single crystal were unsuccessful largely due to the inability of 60 keV ions to penetrate deeper than the amorphous oxide layer which instantly forms on the crystal with exposure to even trace amounts of oxygen. In 1985 a study of doubly charged ion beams, with energy up to 120 keV, will be conducted. If beams of sufficient intensity can be provided, measurements of quadrupole moments will be undertaken using the γ-γ and β-γ PAC techniques. A modified experimental apparatus will be used which incorporates a new thin-walled experimental chamber. This will offer a great simplification and increase in flexibility by allowing the β detector to be placed in air. Furthermore, due to the small dimensions of the new chamber, detectors can be positioned closer to the target, thus providing a significant gain in efficiency. (BNL/ISU)

C. RESEARCH AND DEVELOPMENT IN SUPPORT OF FACILITIES

1. TRISTAN Ion Source Development

Following several years of research and development, successful and reliable designs have been arrived at for the positive surface ionization and FEBIAD (Forced Electron Beam Induced Arc Discharge) sources. These can now be constructed on a regular basis, as the need arises, and in each case they exhibit typical lifetimes of 1500 hours or more. Further development will therefore be concentrated on improving the lifetimes and efficiencies of the thermal, high temperature plasma, and negative surface ionization sources.

During 1984, the lifetime of the thermal ion source was extended to about fourteen days. One important improvement to this source consists of supporting the Ta filament by thin W wires, instead of Ta. This prevents the filament from fusing to the support wire, which causes bending, and ultimately short circuits, during thermal expansion. The source also used a W target container to withstand higher temperatures. However, W vapor tended to collect on the filament, forming a Ta-W alloy which is extremely brittle. The filament easily broke during thermal expansion while the current was being changed. An additional modification was the use of Ta for the ionizer rather than Re. This gave enhanced yields, about 2-5 times greater, even at lower temperatures. During 1985, other combinations of target container/filament materials will be tested in hopes of extending

the lifetime and reliability of this ion source. Improvements to the filament support design as described for the thermal ion source have also extended the reliability and lifetime of the high temperature plasma source to about ten days. Further tests will be performed to investigate the operating mechanism of the source. In the case of the negative surface ionization source, much higher efficiency operation with a yield as high as 10^8 atoms/sec was obtained by using LaB_6, an electron deflection magnet/collector system and efficient heat shields. Initial tests suffered from long holdup times due to too large a target. A smaller graphite cloth target gave much improved yields for shorter lived fission products. However, the source exhibited long-term beam instabilities and further tests are necessary to fully understand their origins.

2. Ion Source Handling and Containment Facilities

The considerable increase in the number of ion sources in use at TRISTAN, and in their lifetimes and efficiencies, has created a need to develop improved facilities for handling and storing these sources once they have been irradiated. Consequently, a considerable effort has been expended to develop remote handling tools for the removal and repair of sources, and also to improve and expand existing storage facilities. A long manipulator to remove the clamps that hold the source to the housing and also the ion source itself has been designed and tested off line. All of the ion sources are being modified to provide a fixture to allow the use of this tool. Similarly, the ion source housing is being modified to allow remote removal of the Faraday cage and electrical connectors. The electrical connectors have been standardized and can now be rapidly inserted and removed. Several surplus lead storage pigs have been obtained and are being modified to accommodate TRISTAN ion sources. In 1985 a lead storage vault will be built to serve as an additional holding area for ion sources.

3. TRISTAN Beam Line Modifications

A general purpose electrostatic quadrupole triplet lens was designed and fabricated and will now be tested. If the design proves satisfactory, several more lenses will be constructed, as it is expected that for ideal operation two will be required on the 0° line and another on each of the 45° lines to provide additional flexibility in designing and installing equipment. The designs for electrostatic switch yards used at two other on-line isotope separators (ISOLDE and GSI) have been obtained and studied in preparation for the design of a second mass line facility at TRISTAN. The GSI design is more usable at TRISTAN than the ISOLDE type. As time is available, modifications necessary to implement the switch yard will be considered.

4. TRISTAN Experiment Facility Development

4.1 Superconducting Magnet for Perturbed Angular Correlations and Q_β Measurements

The superconducting magnet facility was delivered in 1984 and successfully installed on the 45° beam line. It is now fully operational and is intended principally for the measurement of g-factors via the perturbed angular correlation technique. The facility consists of a split pole Nb-Ti superconducting magnet housed in a ^{4}He cryostat, which also contains a λ-point refrigeration unit. The maximum field available is 6.25 Tesla when the system is operated at 4.2°K, and 6.75T if the λ point refrigerator is used to cool the magnet to 2.2°K. Field homogeneity is such that the magnetic field changes by <1% over an area of 1 cm^2 at the target position. The activity is transported from one of two possible collection points to the measuring position via a moving tape system running in a room temperature horizontal bore tube through the center of the magnet. A maximum of four Ge detectors can be positioned in the plane perpendicular to the field direction, at a minimum distance of 8.5 cm from the source. The design of the cryostat and magnet coils is such that the absorbing material between source and detector is minimal and an additional feature allows the system to be used in an alternative configuration as a solenoid magnet for electron measurements, such as Q_β studies. By removing the lower iron pole piece from the magnet, a hyperpure Ge detector may be inserted on the vertical axis and connected to a feed-through connector in the outer vacuum shield. The magnetic field can then be used to focus electrons on the face of the detector, thus greatly enhancing the solid angle for electron detection, relative to that for γ rays. In on-line measurements, an enhancement factor of 15 was observed. Attempts to use the HpGe detector to observe conversion electrons were successful only for intense lines due to the large β continuum. It should be possible to suppress the β continuum by installing another solid state β-gating detector in place of the upper pole piece of the magnet. This possibility will be explored further and some improvements in the moving tape collector and detector positioning apparatus are also planned. A larger sprocket wheel will be installed, making it possible to move the tape into the magnet in less than half of the time it now takes.

4.2 Solid State Conversion Electron Detector

In early 1984 the Si(Li) conversion electron detector was installed on the 0° switch magnet port. The detector is mounted in a cryostat attached to a vacuum chamber and moving tape collector system. Tests were performed and modifications made to minimize mechanical vibrations and electrical noise experienced by the detector. The on-line tests determined a detector resolution of 2.5 keV FWHM at 400 keV and 2.9 keV at 1 MeV. However, repeated temperature cycling and contamination of the

detector surface made replacement necessary. It was also found necessary to improve the ion optics. A new quadrupole triplet has been built and incorporated into the beam line. A new 2π β detector will be constructed at the University of Oklahoma that will replace the currently used $(4/3)\pi$ detector, thus improving the overall efficiency of the β-e^- gating system. Further improvement is planned for 1985 when the experimental chamber will be modified to facilitate a "parent port" mode of operation. This will enable the measurement of conversion electrons for nuclei with half lives shorter than the present limit of 0.5 sec.

5. New Three-Crystal Pair Spectrometer at the ARC Facility

In considering the overall range of targets which can be studied with the ARC technique, the most crucial limitations are the level density at the binding energy, and the amount of target material available. While nothing can be done about the former, the latter limitation can be alleviated by improving the efficiency of the three-crystal pair spectrometer. The critical factors which determine this efficiency are the size and shape of the Ge crystal, the distance between it and the target, and the effective solid angle for 511 keV radiation detected by the NaI crystals. The current system employs NaI crystals which are far larger than necessary, with the result that the source-to-detector distance has been increased unnecessarily. A new design has therefore been developed, which employs a pair of NaI crystals of smaller diameter, and places the Ge crystal forward of center in order to optimize these two conflicting factors. The expected increase in efficiency from this modification is a factor of ≈ 3. The new NaI spectrometer has been delivered, and its installation should be completed early in 1985, making it possible to undertake a number of measurements which were hitherto considered impractical because of lack of sufficient target material. In many other cases, the quality of data should be considerably enhanced by the improved statistics obtainable.

6. Other Uses of Filtered Beams

Studies at TRISTAN utilizing proton recoil detectors and delayed neutron spectrometers require an energy dependent efficiency calibration in order to measure the intensity of particular neutron resonances at low energies. The thermal, 2, and 24 keV filtered beams at the HFBR provide appropriate standard neutron intensities that are routinely used for such calibrations by the Idaho group. A similar use of these beams is being made by a group from Caltech, involved in a search for monopoles, and the thermal beam is used on a regular basis for biomedical studies.

D. NATIONAL NUCLEAR DATA CENTER

1. Cross Section Evaluation Working Group (CSEWG) Activities

The annual CSEWG meeting was held at BNL in May, 1984. The formats for all but the data covariance file were fixed at this meeting. The "standards" evaluation will be completed by July 1985.

The ENDF utility codes were upgraded to handle the new ENDF-VI formats which have been adopted. ANSI standard Fortran-77 has been used to make the programs machine independent and more efficient.

2. BNL-325 Volume 1 Part B

The evaluations of the thermal cross sections, resonance parameters, and average resonance properties for the isotopes in the mass range A=61-100 has been completed. The introduction for this part deals with (1) the systematics of the s-, p- and d-wave strength functions, average radioactive widths, and potential scattering radii, (2) alpha widths of resonances, and (3) subthreshold fission.

The volume has been published by Academic press.

3. Nuclear Data Sheets

The NNDC has been producing the Nuclear Data Sheets at the rate of about an issue a month. Of these, nine issues a year are devoted to the nuclear structure evaluation and the remaining three to the publication of Recent References.

The NNDC evaluated A=58, 150, 48, 53, 57, 141, 142 and 47 and submitted them for publication.

The U.S. is part of an international network of evaluators contributing recommended values of nuclear structure information to the Evaluated Nuclear Structure Data File (ENSDF). Publication of the Nuclear Data Sheets proceeds directly from this computerized file. In addition to the U.S., evaluations have been received or are anticipated from Germany, United Kingdom, USSR, France, Japan, Belgium, Kuwait, Sweden, the People's Republic of China and Canada.

A new edition of the Nuclear Wallet Cards (last published in 1979) incorporating the new Wapstra mass evaluation has been produced. Since this publication represents a subset of data extracted from the computerized ENSDF file, it is consistent and current with the Nuclear Data Sheets.

CROCKER NUCLEAR LABORATORY AND DEPARTMENT OF PHYSICS
UNIVERSITY OF CALIFORNIA, DAVIS

A. MEASUREMENTS

1. A Measurement of the n-p 180/90 Degree Cross Section Ratio at 65 and 50 MeV*, (J.R. Drummond, F.P. Brady, J.L. Romero, T.D. Ford,** C.M. Castaneda, B. McEachern, and M.A. Hamilton)

A measurement of the 180 to 90 degree cross section ratio is of interest because recent data from Louvain[1] in the range 45 to 65 MeV showed a larger ratio than earlier data from Harwell[2] and Crocker Nuclear Lab.[3] Large area scintillation detectors were used to cover the range 5 to 30 degrees (lab), and 40 to 46 degrees. A delta energy - delta energy telescope covered the 0 degree range. Position sensitive wire chambers covered all three ranges allowing all three cross sections to be measured at the same time, permitting cancellation of systematic errors in the ratio to a higher of degree accuracy than the absolute measurements.

2. Continuum Protons from (n,p) Reaction on ^{40}Ca, ^{118}Sm, and ^{209}Bi at 65 MeV*. (C.M. Castaneda, F.P. Brady, J.R. Drummond, T.D. Ford,** B. McEachern, and J.L. Romero)

We have measured the proton spectra produced by 65 MeV neutrons on ^{40}Ca, ^{118}Sn, ^{209}Bi from 6 to 70 degrees. Angle integrated spectra are compared to precompound models and the effect of the neutron excess is explored in that context.

3. The (n,p) Reaction at Zero Degrees from ^{12}C, ^{13}C, ^{90}Zr, and ^{209}Bi at 65 MeV*. (T.D. Ford,** F.P. Brady, C.M. Castaneda, J.L. Romero, J.R. Drummond, B. McEachern, M.L. Webb, N.S.P. King,# J. Martoff,$ and K. Wang$)

The first spectra from the UC Davis cyclotron's zero degree facility for (n,p) scattering have been obtained from ^{12}C, ^{13}C, ^{90}Zr, and ^{209}Bi at an incident neutron energy of 65 MeV. Cross sections for the

---

* Supported by NSF grant PHY 81-21003

** Supported by AWU

Los Alamos National Laboratory, Los Alamos, NM 87545

$ Stanford University, Palo Alto, CA 94305

(1) A. Bol et al., Phys. Rev. C (June 1984).

(2) J.P. Scanlon et al., Nucl. Phys. 41:403 (1963).

(3) T.C. Montgomery et al., Phys. Rev. C16:499 (1977).

ground state, the ∿4.4 MeV and the GDR are extracted for the carbon isotopes. Two broad resonances in ^{209}Bi at ∿7.5 MeV and ∿15 MeV and a broad resonance in ^{90}Zr at ∿22 MeV are compared with previous work done at Davis away from zero degrees.

4. The Analog of the ^{40}Ca G.D.R. through the (n,p) Reaction at 65.5 MeV*. (C.M. Castaneda, J.L. Romero, F.P. Brady, J.R. Drummond, T.D. Ford,** and B. McEachern)

The charge exchange reaction $^{40}Ca(n,p)^{40}K$ has been measured at 65.5 MeV. A strong enhancement is observed at energies corresponding to the analog of the ^{40}Ca G.D.R. The angular distribution is partially consistent with a $\Delta L = 1$ transfer, but at forward angles deviates from it. Comparison with the (^3He,t) and (p,n) reaction have been made.

5. Natural Fe (n,n'x) Elastic and Inelastic Spectra at 65 MeV*. (M.A. Hamilton, T.D. Ford,** J.L. Romero, F.P. Brady, C.M. Castaneda, and J.R. Drummond)

The detection of Giant Resonances due to collision interaction of different particles at various energies has been of particular interest in recent years. The unique combination of a monoenergetic neutron beam and the Multiwire Chamber Neutron Detection System at Crocker Nuclear Lab has made possible, for the first time, the measurement of Giant Resonances due to (n,n'x). Measurements of ^{nat}Fe (n,n'x) for 65 MeV incident neutrons were made at angles between 4 and 32 degrees. Analyses of the (n,n'x) spectra and an extraction of giant dipole and quadrupole resonance cross sections are being accomplished so that a comparison with (p,p'x) at 62 MeV can be made.[1] The ratio of neutron to proton matrix elements can then be obtained and compared to theoretical predictions.

B. FACILITIES AND DETECTORS

1. Development of a Facility for Measurements of (n,px) Scattering Cross Sections Down to Zero Degrees at 65 MeV Incident Energy* (T.D. Ford,** F.P. Brady, C.M. Castaneda, J.L. Romero, J.R. Drummond, and B. McEachern)

In July 1983 the University of California at Davis, Crocker Nuclear Laboratory prototype zero degree facility collected its first spectra. Zero degree cross sections were measured for ^{12}C, ^{13}C, ^{90}Zr, and

---

* Supported by NSF grant PHY 81-21003

** Supported by AWU

(1) F.E. Bertrand and R.W. Peelle, Phys. Rev. C8:1045 (1973).

^{209}Bi. Now, a second generation zero degree facility is under development. The detection system which allows (n,px) measurements over a wide range of angle (0-60° lab) and outgoing proton energy (20-65 MeV), is shown in Fig. B.1.

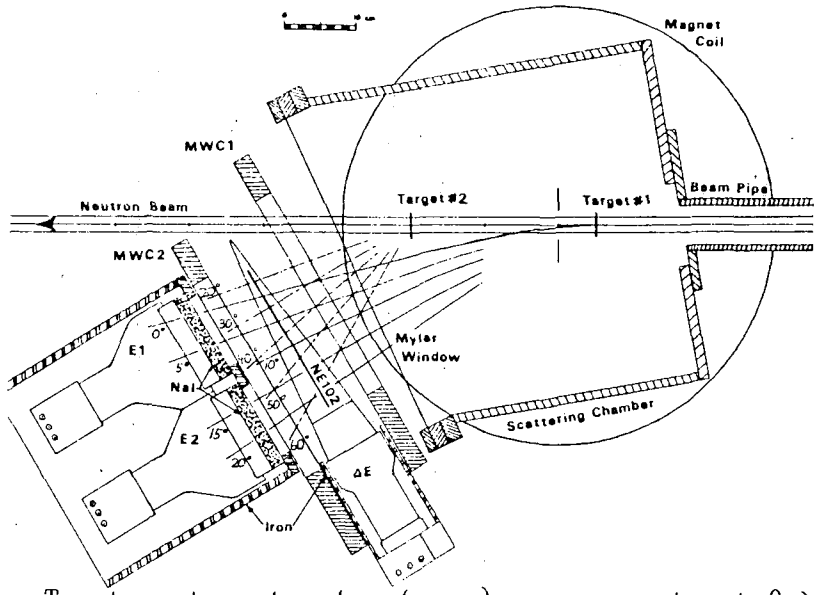

Fig. B.1. Two target system for (n,px) measurements at $\theta \geq 0°$.

Charged particles, say protons, from target #1 pass through and are bent by the magnetic field. This allows measurements at and around 0°. Particles from target #2 do not pass through appreciable field and so are not bent. Trajectory analysis allows spectra from the two targets to be unambiguously separated. This system has been constructed and is being installed. An intrinsic Ge detector of relatively large area (55 mm) which can stop 70 MeV protons is being mounted for testing in the facility.

2. Mapping of Large Scintillators to Improve Resolution for the Crocker Nuclear Laboratory Zero Degree Scattering Facility.*
(J.R. Drummond, F.P. Brady, J.L. Romero, T.D. Ford,** C.M. Castaneda, B. McEachern, and M.A. Hamilton)

Relatively large NaI and NE102 scintillation detectors are used in the CNL scattering facility, where the energy resolution varies significantly across the detector. Using position sensitive wire chambers, and mapping the detector using N-P scattering to cover the entire detector face saves time, is less ambiguous than using a radioactive source, is significantly faster than direct mapping with the cyclotron beam, and eliminates PMT and amplifier drift effects. A correction in the mapping is made for the kinetic shift and the peak fitted. A comparison of maps made using radioactive sources, and ones made using a tightly collimated proton beam, and using this method shows good agreement. Since the proton peak is easier to fit than the Compton edge of the source the analysis is easier to apply. The intrinsic resolution of the detector from center to edge is also determined.

HANFORD ENGINEERING DEVELOPMENT LABORATORY

A. NUCLEAR DATA EVALUATIONS

1. Low Activation Cross Sections for Fusion Application (F. M. Mann)

Based upon the importance of long-term waste management for the fusion material programs, a program to develop needed nuclear data is continuing. As part of a GA-LLNL-HEDL-U.Wisc. collaboration, activation rates for a conceptual fusion reactor were calculated and then compared to the results of the other participants. For the major reactions producing short halflife isotopes, the calculations are in relatively good agreement. However, for the isotopes important in long term waste management, the agreement is often poor. Exceptions to this poor agreement usually result from the use of a common data source, rather than implying little scatter in the data.

A neutron-induced reaction cross section library was recently completed based on long-term waste management needs. The library contains 343 isotopes with at least 14 reactions per isotope, resulting in a total of about 6000 reactions. Over 90% of the stable isotopes and all the unstable nuclei with a halflife greater than 5 years and a mass less than 220 amu are included. The systematics code THRESH was used to calculate reactions other than (n,gamma) for En to 40 MeV. These cross sections were modified whenever possible by the ENDF/B-V and ACTL-84 cross sections libraries. Special evaluations by LANL and HEDL were also used. For (n,gamma) cross sections not available in other libraries, estimates were based on neighboring nuclei. This continuous energy library has now been processed into a 63 multigroup format.

To supplement the cross section library, a decay data library is being developed. The library contains over 1200 isotopes (all isotopes reached by the reactions in the cross section library being included). The library contains halflife and decay branching information and will soon contain dose and photon spectral information as well.

2. ENDF/B-VI Fission Product, Actinide, Fission Yields, Delayed Neutron, Activation and Dosimetry Evaluations (F. M. Mann, R. E. Schenter, F. Schmittroth, T. R. England* and C. W. Reich**)

Due to recent funding reductions in this area, work has been severely limited on the "four-year" plan for ENDF/B-VI presented in the previous Nuclear Data Committee Report. A summary of the fission product and actinide data contained in the ENDF/B-V files has been published.[1]

---

* Los Alamos National Laboratory

** Idaho National Engineering Laboratory

[1] T. R. England, et al., Summary of ENDF/B-V Data for Fission Products and Actinides, EPRI NP-3787, LA-UR 83-1285, ENDF-322, Final Report, (December 1984).

B. DELAYED NEUTRON DATA

1. Spectra Evaluations (F. M. Mann, R. E. Schenter, T. R. England* and W. B. Wilson*)

   See LANL contribution .

2. Pn Evaluations (F. M. Mann, M. Schreiber, R. E. Schenter and T. R. England*)

Evaluations of 77 precursors, and studies of effects on fission yields and Pn systematics have been published.[2]

C. FISSION YIELDS

1. ENDF/B Evaluations (T. R. England,* G. K. Schenter** and R. E. Schenter)

   See LANL contribution .

D. FFTF EXPERIMENTS

1. Noble Gas Cross Sections (R. E. Schenter, J. A. Rawlins, D. W. Wootan, F. Schmittroth and R. L. Simons)

The Fast Flux Test Facility (FFTF) structural materials irradiation vehicle, MOTA, was designed to provide in-reactor creep rupture behavior results for structural materials.[3] In order to identify precisely times when specimens rupture, "tag gases" of specific isotopic enrichments in Kr and Xe are put into the test capsules. Upon release of tag gas from a specimen rupture mass, spectrometric measurements are made to determine precisely amounts of all the stable Kr and Xe isotopes. Significant changes occur in the concentration of several of these isotopes due to neutron capture providing a very good integral cross section measurement for fast neutrons (1 eV < E < 1 MeV). Figure A-1 shows typical results for using this data along with recent differential data for Kr78.

---

* Los Alamos National Laboratory
** Cornell University

[2] F. M. Mann, et al., "Evaluation of Delayed-Neutron Emission Probabilities," Nucl. Sci. and Eng., 87 418 (1984).

[3] R. J. Puigh and R. E. Schenter, "The In-Reactor Creep Rupture Experiment in MOTA," to be presented at the Twelfth International Symposium on Effects of Radiation on Materials," Williamsburg, VA (June 1984).

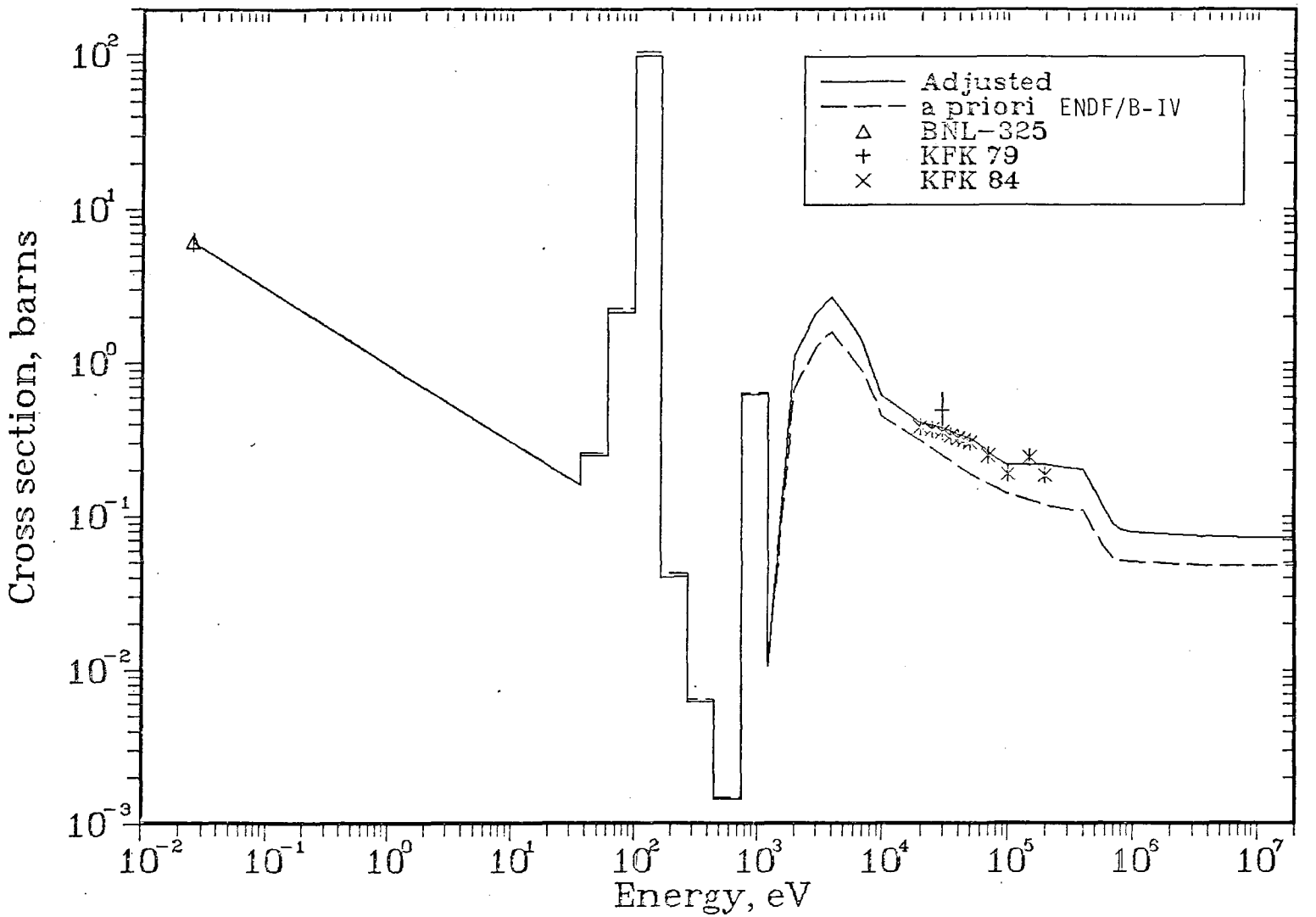

Figure A-1. Kr-78 Capture Cross Section Results. The "apriori" curve is from ENDF/B-IV. Recent differential data (KFK 84) is included.

A. NUCLEAR DATA MEASUREMENT

1. Precise Gamma-Ray Emission-Probability Measurements for Selected Actinide Nuclides

As a part of our laboratory involvement in the work of an International Atomic Energy Agency Coordinated Research Program to measure and evaluate required nuclear decay data for selected transactinium nuclides, we are making precise (overall accuracy $\lesssim$1%) measurements of the emission probabilities (absolute intensities) of the prominent gamma-ray transitions from a number of such nuclides of particular importance for fission-reactor technology. Nuclides whose gamma-ray emission probabilities are being measured in this activity include: ^{238,239,240}Pu, ^{241}Pu (+^{237}U), ^{232}U (and members of its decay chain), ^{233,235}U, ^{233}Pa and ^{229}Th (and members of its decay chain). Thus far, papers presenting the results of our measurements on ^{238,239,240}Pu, ^{232,233,235}U and ^{233}Pa have already appeared in the literature. Papers describing our work on the ^{241}Pu (+^{237}U) decay, carried out in collaboration with individuals from the University of Idaho, have been accepted for publication; and the measurements on ^{229}Th and its daughter nuclides have recently been completed.

Briefly summarized below is the status of our measurement activity for those nuclides for which our data have not yet appeared in the literature.

^{229}Th (plus daughters) (R. G. Helmer, M. A. Lee, C. W. Reich and I. Ahmad*)

To aid in the quantitative assay of ^{229}Th by means of gamma-ray spectrometry, we have made precise measurements of the emission probabilities of several gamma rays in the energy region from 40 keV to 809 keV from the decay of ^{229}Th and members of its decay chain. The decay-rate calibration of an isotope-separated sample of ^{229}Th, produced at Argonne National Laboratory, was obtained by measuring the total alpha particle emission rate utilizing a low-geometry Si(Au) surface-barrier detector gated in such a way that only the alpha-particles from ^{229}Th decay were recorded. The overall uncertainty in the decay-rate calibration determined in this manner was ~1.1%. The percentage uncertainties in the measured gamma-ray emission probabilities ranged from 1.3% to 4.0% over this energy region.

* Argonne National Laboratory

Table A-1 Emission-probability (P_γ) values for selected gamma rays from ^{229}Th and members of its decay chain. The daughters are in secular equilibrium. Gamma rays arising from the decay of a nuclide other than ^{229}Th are labelled (in parentheses) by the parent nuclide.

E_γ(keV)[a]	P_γ (Photons/100 ^{229}Th decays)
31.10 31.50 31.57	{ 2.33 ± 0.05
40.10(^{225}Ra)	28.5 ± 0.7
42.25 42.76	{ 0.189 ± 0.006
43.99	0.724 ± 0.017
56.52	0.297 ± 0.007
94.73[b]	0.443 ± 0.008
107.11	0.769 ± 0.013
110.33	0.122 ± 0.003
123.19[b]	0.187 ± 0.003
124.55 124.65	{ 1.378 ± 0.020
131.93	0.311 ± 0.005
136.99	1.113 ± 0.016
142.96	0.381 ± 0.006
147.63 148.09	{ 1.037 ± 0.015
150.0(^{225}Ac)	0.757 ± 0.011
154.34[b]	0.877 ± 0.013
156.41	1.176 ± 0.018
179.76	0.204 ± 0.004
193.51	4.20 ± 0.06
204.69	0.566 ± 0.009
210.13 210.85	{ 3.02 ± 0.04
218.1(^{221}Fr)[c]	11.01 ± 0.16
292.8(^{213}Bi)	0.408 ± 0.007
440.46(^{213}Bi)	24.8 ± 0.3
465.4(^{209}Tl)	1.923 ± 0.027
808.9(^{213}Bi)	0.278 ± 0.011

a) Nominal values only.

b) Gamma-ray peak contains a contribution from radiation emitted by a member of the ^{229}Th decay chain.

c) Gamma-ray peak contains a small contribution from ^{229}Th decay.

Our measured emission-probability data for selected gamma-ray transitions from ^{229}Th and members of its decay chain are summarized in Table A-1.

In two fairly recent publications [1,2], emission-probability data for the gamma radiation from ^{229}Th and its daughters are presented. However, as noted in Ref. (3), these two sets of data are in strong disagreement with each other, both in their overall normalization and in the intensity ratios of a number of the gamma rays. Our data favor neither of the earlier measurements, but tend to lie in between those two sets of results.

^{241}Pu (+^{237}U) (R. G. Helmer and C. W. Reich)

The abstract of a paper which has been accepted for publication in International Journal of Applied Radiation and Isotopes follows:

"As an aid in the quantitative assay of ^{241}Pu by means of γ-ray spectrometry, we have measured the emission probabilities of four prominent γ rays from the decay of ^{241}Pu and three from the decay of its ^{237}U daughter in the energy range from 77 to 267 keV. The decay-rate calibration of chemically purified source material was determined by comparison of the number of nuclei present with previously calibrated solutions of ^{239}Pu and ^{240}Pu using isotope-dilution mass spectrometry. The percentage uncertainties in the measured γ-emission probabilities range from 0.9% for three of the transitions to 2.4% for the 77-keV transition."

^{241}Pu (+^{237}U) (H. Willmes*, T. Ando** and R. J. Gehrke)

"The decay rate of chemically purified ^{241}Pu source material was determined by observation of the grow-in of the 59.5-keV γ ray from the decay of the ^{241}Am daughter over a period of 154 days. From the resulting source calibration and measurements of γ intensities, emission

[1] J. K. Dickens and J. W. McConnell, Radiochem. Radioanal. Letters 47, 331 (1981).

[2] S. S. Rattan, A. V. R. Reddy, V. S. Mallapurkar, R. J. Singh, Satya Prakash and M. V. Ramaniah, Phys. Rev. C 27, 327 (1983).

[3] J. K. Dickens, Phys. Rev. C 28, 1404 (1983).

* University of Idaho

** Graduate Student at the University of Idaho

probabilities were determined for four γ rays from the decay of ^{241}Pu and for eight γ rays from the decay of its ^{237}U daughter. The uncertainties in the emission probabilities were less than 1% for the 148-keV γ ray from ^{241}Pu and for the 65-, 165-, 208-, and 268-keV γrays from ^{237}U. Uncertainties for the remaining γ rays were between 1.0 and 4.2%. The applicability of the various transitions to the quantitative assay of ^{241}Pu is discussed."

2. K X-Ray Emission Probability of ^{93m}Nb (R. J. Gehrke, J W Rogers, J. D. Baker)

The use of the $^{93}Nb(n,n')^{93m}Nb$ reaction to monitor fast neutron fluence is currently being applied at several laboratories around the world. The niobium dosimeter appears to have the desirable properties of providing a neutron fluence measure that corresponds to the changes in the mechanical properties of ferritic materials used in structural components of nuclear reactors and a reaction product with a suitably long half-life [$T_{1/2}$ = (16.13 $\pm$ 0.15) y].

In order to fully utilize the $^{93}Nb(n,n')^{93m}Nb$ reaction to monitor fast neutron fluence it would be useful to be able to count dried aliquots of dissolved niobium wire with either low energy Si(Li) or Ge x-ray spectrometers. However, in order to determine the ^{93m}Nb activity it is necessary to know the K x-ray emission probability. Because of the inconsistency of previously measured values, we have undertaken to determine the K x-ray emission probability of ^{93m}Nb using a hyperpure planar Ge detector.

The K x-ray efficiency of the Ge detector was measured with standardized sources of high specific or carrier-free activity. The radionuclides used to measure the efficiency were ^{85}Sr, ^{88}Y, ^{92m}Nb, ^{99m}Tc and ^{109}Cd. A solution of high specific activity ^{93m}Nb, which was standardized at the Central Bureau for Nuclear Measurements by liquid scintillation, was used for the activity standard. Thin sources were prepared by drying a known aliquot of the standard solution onto analytical paper which was then contained between a layer of plastic and polyester tape. The K_α & K_β peaks were added and a background subtracted. From the ratio of the K x-ray emission rate to the disintegration rate, the ^{93m}Nb K x-ray emission probability was determined to be:

(11.04 $\pm$ 0.28) K x-rays per 100 decays.

---

1. R. J. Gehrke, J W Rogers and J. D. Baker, "Niobium Neutron Fluence Dosimeter Measurements", to be published in the proceedings of the 5th ASTM-EURATOM Symposium on Reactor Dosimetry held Sept. 24-28, 1984 in Geesthacht, West Germany.

For some time now, an international intercomparison effort has been underway to determine the degree of consistency among a number of laboratories in their measurement of the K x-ray emission rate of samples of ^{93m}Nb. The results reported here represent our contribution to this intercomparison. It is anticipated that a full report of the results of this intercomparison will be published when it is completed.

3. Delayed-Neutron Spectral Measurements (R. C. Greenwood, A. J. Caffrey)

The following is the abstract of a paper submitted for publication in Nuclear Science and Engineering:

"Measurements of the energy spectra of delayed neutrons for the isotope-separated, fission-product precursors $^{93-97}Rb$ and $^{143-145}Cs$, over the energy region from ~10 keV to ~1300 keV, are reported. These data were obtained at the TRISTAN ISOL facility using gas-filled proton-recoil proportional counters. The data for each of the Rb and Cs isotopes show good qualitative agreement with the existing ^{3}He ionization chamber data at energies above ~200 keV. In addition, they provide definitive spectral information down to ~10 keV. Of particular note is the observation of line structure below ~200 keV with energy resolution much better than that obtained using ^{3}He ionization chambers."

B. NUCLEAR DATA EVALUATION

1. Mass-Chain Evaluation for the Nuclear Data Sheets (M. A. Lee, R. G. Helmer, C. W. Reich)

As a part of our involvement in the work of the International Nuclear Structure and Decay Data Evaluation Network, which carries out the evaluation of basic nuclear-physics data for publication in the Nuclear Data Sheets, we have the evaluation responsibility for the ten mass chains in the region $153 \leq A \leq 162$. Prior to 1984, evaluations for A=154, 159, 158, 153 and 157 have been published in Nuclear Data Sheets.

During 1984, the A=161 mass-chain evaluation has been published in this journal. The evaluations for A=160 and 162 have been completed and are in the prepublication review process. Work on A=155 and 156 is currently in progress and is scheduled to be completed before the end of this fiscal year.

DECAY STUDIES OF FISSION PRODUCTS WITH TRISTAN AT THE HFBR AT BNL

The TRISTAN on-line mass separator facility at the High Flux Beam Reactor at Brookhaven National Laboratory is used to study the decays of mass-separated neutron-rich nuclides produced in thermal neutron fission of ^{235}U. A number of different elements can be ionized and separated using a variety of ion sources including the newly developed high-temperature thermal and high-temperature plasma ion sources. Measurements made at TRISTAN are discussed below. Members of the Ames Laboratory group (John C. Hill, F. K. Wohn, J. A. Winger, and M. E. Nieland) have collaborated with other users from BNL, K. Sistemich (KFA Jülich, Germany), A. Wolf and Z. Berant (Nuclear Research Centre, Beer Sheva, Israel) and R. F. Petry (U. of Oklahoma). Experiments involved decay scheme studies via γ-ray spectroscopy, γγ angular correlations, and perturbed angular correlations.

1. Decay of ^{83}Ge to Levels in the N=50 Isotone ^{83}As (Winger *et al.*)

The decay of ^{83}Ge to levels in the N=50 isotone ^{83}As was investigated by γ singles, multispectral scaling, and γγ coincidence techniques. The structure of ^{83}As is of interest since it can be pictured as 5 protons outside of a doubly-magic ^{78}Ni core. No information on ^{83}Ge decay is available other than its half-life and no information on excited states in ^{83}As exists in the literature. We have measured the half-life to be 1.85±0.07 s. A total of 18 γ rays have been assigned to ^{83}Ge decay. A preliminary level scheme for ^{83}As includes excited states at 306, 711, 1256, 1329, 1434, and 3733 keV. Data analysis is still in progress. Using a large space shell-model code which is now running on the Ames Laboratory VAX computer, calculations are in progress on the level structure of ^{83}As and other N=50 isotones.

2. Decay of ^{99}Sr to Highly Deformed ^{99}Y (Petry *et al.*, Wohn *et al.*)

This decay scheme was completed and published.[1] 71 γ transitions were placed in a decay scheme with 26 levels, for which β feedings and logft values were deduced. Five rotational bands were identified, with Nilsson orbitals (bandhead energies in keV in parentheses) 5/2[422] (0), 5/2[303]

---

[1] Petry, Dejbakhsh, Hill, Wohn, Shmid, and Gill, Phys. Rev. C 31, 621 (1985).

(487), 3/2[301] (536), 1/2[431] (1011), and 3/2[431] (1119). A detailed particle-rotor model calculation, which included Coriolis coupling via matrix diagonalization, of the 5 bands in ^{99}Y was published.[2] Excellent agreement was obtained for the level energies, intraband M1+E2 and interband E1 or M1+E2 transitions.

3. Decay of the Low-Spin Isomer of ^{100}Y (Hill *et al.*)

The decay scheme of the low-spin isomer of ^{100}Y to the even-even N=60 isotone ^{100}Zr is completed and will soon be submitted for publication. 67 γ rays have been placed in 21 levels with energies up to 4288 keV. β feedings and logft values were also determined. The β feeding to the ground-state of ^{100}Zr is consistent with a value of zero. Analysis of the low-lying levels (2_1^+ at 213 keV, 0_2^+ at 331 keV, 4_1^+ at 564 keV, 0_3^+ at 830 keV, and 2_2^+ at 879 keV) show that the characteristics of these levels are reasonably well reproduced by assuming mixing of coexisting deformed and spherical states, with the 0_2^+ and 2_2^+ states dominantly spherical and the yrast band dominantly rotational. The 0_3^+ state is more difficult to characterize but its position is compatible with that of a β vibration of the rotational shape.

4. Decays of ^{101}Sr and ^{101}Y to the Deformed Nuclei ^{101}Y and ^{101}Zr (Wohn, *et al.*)

Neither of these decay schemes have been completed. Preliminary results for the decay of ^{101}Sr have resulted in the identification of 4 rotational bands, corresponding to the Nilsson orbitals (with bandhead energies in keV in parentheses) 5/2[422] (0), 3/2[301] (510), 5/2[303] (666), and 3/2[431] (996). The 1/2[431] band that was identified in ^{99}Y has not been identified in ^{101}Y. The band structure of ^{101}Y is very similar to that of ^{99}Y. In the decay scheme for ^{101}Y to ^{101}Zr only the two bands 3/2[411] (0) and 3/2[541] (216 keV) have been identified so far. Upon completion of these two decay schemes, detailed particle-rotor model calculations (see Ref. 2) will be made.

5. Characterization of the New Nuclide ^{102}Sr (Hill *et al.*)

Last year we reported the observation of the new nuclide ^{101}Sr. This year with the development of the high-temperature thermal ion source it was possible to mass-separate and study the new nuclide ^{102}Sr. From γ multispectral scaling data the half-life for ^{102}Sr was measured to be 68±8 ms. On the basis of γ singles and γγ coincidence measurements a total of 22 γ rays were assigned to ^{102}Sr decay. No information is available in

---

[2] Wohn, Hill, and Petry, Phys. Rev. C 31, 634 (1985).

the literature on excited states in ^{102}Y. A preliminary level scheme for ^{102}Y has been constructed consisting of excited states at 94, 208, 244, 312, 498, 899, 1348, and 1690 keV. An equilibrium γ ray measurement was carried out for the A=102 mass chain in order to determine the ground state β feeding. Final construction of a ^{102}Y level scheme is still in progress. A study of levels in the odd-odd nucleus ^{100}Y populated in ^{100}Sr decay is also in progress.

6. Magnetic Moments for 4_1^+ States in the N=82 Isotones ^{136}Xe and ^{138}Ba (Berant *et al.*)

Beta decaying sources of ^{136}I and ^{138}Cs were used to populate the 4_1^+ states in ^{136}Xe and ^{138}Ba. The magnetic moments of the above states were measured using the technique of integral perturbed angular correlations. g factors of 0.80±0.15 and 0.80±0.14 were measured for ^{136}Xe and ^{138}Ba respectively. The above results[3] along with those for the g factors in the 4_1^+ state in ^{140}Ce and the 6_1^+ states in ^{134}Te and ^{138}Ba are well described by a shell-model calculation employing configuration-mixed wave functions and a single set of effective-proton g factors ($g_\ell' = 1.12$, $g_s' = 4.12$) that account in an empirical fashion for core polarization effects.

7. Magnetic Moments for 2_1^+ States in ^{146}Ce and ^{148}Ce (Wolf *et al.*)

Sources of ^{146}La and ^{148}La were used to populate the 2_1^+ states in ^{146}Ce and ^{148}Ce. The magnetic moments of the 2_1^+ states were measured using the technique of integral perturbed angular correlations. In order to obtain a larger effect a superconducting magnet was used to produce a magnetic field at the sample of about 6.5T. Analysis of the data is in progress.

---

[3]Berant, Wolf, Hill, Wohn, Gill, Mach, Rafailovich, Kruse, Wildenthal, Peaslee, Aprahamian, Goulden, and Chung, Phys. Rev. C 31, 570 (1985).

A. INTRODUCTION

During the past year we have continued studies of low energy neutron scattering from deformable and spherical nuclei to determine the extent to which collective excitations of different character affect elastic scattering, as well as the better known effects on inelastic scattering. We have learned that non-axial quadrupole excitations, or γ-band excitations, albeit a factor of five weaker than ground band excitations, still alter elastic scattering cross sections in a significant way at quite low energies. Thus these low energy cross sections may be an effective probe of collective nuclear dynamics at low excitation energies. This question is addressed in two papers which are in process of being published.[1,2] Other important questions, about the validity of optical potential approaches to scattering and the strengths of absorptive potentials, are also being addressed.

A second thrust of our neutron induced reaction program is the study of the collective excitations of deformed and shape transitional nuclei themselves, through the study of the $(n,n'\gamma)$ reactions and other reaction studies pursued with triton beams at the Los Alamos tandem accelerator facility. These studies deal with the symmetries of collective excitations, primarily through application of the IBA symmetries for even-A nuclei and boson-fermion models which employ supersymmetry concepts to classify excitations in odd-A nuclei. Both collective and non-collective excitations in the spherical Sn isotopes are also being studied through the $(n,n'\gamma)$ reaction. These studies are important in connecting nuclear structures in different mass ranges to each other, and also extend and complement the scattering studies mentioned in the paragraph above.

A third area in which work has been done this year is in our new neutron and proton capture program. The pulsed-beam 180° radiative capture facility has been completely designed and partially fabricated. The principal element in this system is a dipole magnet which has been designed to permit gamma-ray detection at both 0° and 180° through innovative use of multiple beam lines and a special magnet design.

An alpha-capture study on ^{12}C to levels in ^{16}O has been completed,[3] and is being published. Briefly, the goal was to search for the special 2^+ level

---

[1] M.T. McEllistrem, Proc. Int'l. Conf. Neutron-Nucleus Collisions, A Probe of Nuclear Structure, AIP Conf. Proc. No. 124 (ed. by J. Rapaport, R.W. Finlay, S.M. Grimes, and F.S. Dietrich, (1985)), p. 208.

[2] M.C. Mirzaa, J.P. Delaroche, J.L. Weil, J. Hanly, and M.T. McEllistrem, to be published in Physical Review C.

[3] M.A. Kovash, R.W. Lourie, W. Pugh, C.E. Hyde-Wright, D.G. Marchlenski, H.R. Suiter, J.C. Brown, and R.G. Seyler, to appear in Physical Review C.

near 10 MeV excitation energy in the final nucleus which would have signalled the presence of tetrahedral symmetry.

The fourth area in which work has been partially completed, and is still in progress, is in the study of very low energy neutron scattering in ^{189}Os. This problem is fascinating for several reasons, but the primary choice of this particular target had to do with strengthening the nuclear physics underlying the Re/Os nucleochronology.

B. NEUTRON SCATTERING SECTION

1. Shape-transitional Nuclei. (Hicks, Hanly, McEllistrem)

Our ongoing scattering studies from several Os and Pt nuclei[1,2] entail differential cross section measurements for elastic and inelastic scattering at low incident energies here and some 8 MeV measurements at Bruyeres-le-Chatel (BRC). Confident analysis and interpretation of these scattering studies in terms of the dynamics of their structures requires confident knowledge of the scattering potential, which is designed to reflect accurately the particular nucleus being studied. For this purpose the most important data are precise and accurate total cross sections measured from quite low energies to at least several MeV. We have measured total cross sections from 300 keV to 4 MeV with an accuracy of about one percent for separated isotope samples of ^{194,196}Pt and for ^{190,192}Os. To test our measurements for accuracy and reproducibility, we remeasured cross sections for ^{196}Pt with two slightly different sample configurations, and measured values also for natural Pb and C samples. Our measurements for C agreed with evaluations for that nucleus to within an average deviation of about 0.7%. Good agreement was also obtained with previous measurements for Pb.

These data will be combined with our previous differential elastic and inelastic scattering cross sections[1,2] to test for sensitivity to the collective excitations of these Os and Pt nuclei. At Kentucky we had measured differential cross sections at 1.6 MeV and at 2.5 MeV incident energies for some of the isotopes. We now have also measured differential scattering cross sections with 8 MeV neutrons at BRC. What is immediately striking about the raw data for scattering from ^{194}Pt and ^{190,192}Os isotopes is that the second 2^+ level is very weakly excited in ^{194}Pt, but strongly excited in the two Os isotopes. This explains beautifully why our low energy measurements[2] for that level were almost isotropic, showing no evidence of direct excitation at all. The 8 MeV data confirm that indeed, little or no direct excitation occurs. For reasons too complicated to discuss here, this means that multi-step excitation amplitudes in scattering at this neutron energy are quite unimportant; only single step direct excitation contributes noticeably to these 2^+ levels. The 8 MeV data are now being reduced to yields, and corrected for sample size effects and other experimental properties both at BRC and at the University of Kentucky. The independent data reduction at the two centers will give confidence in the cross sections finally reported (and analyzed) when the data reduction and analyses are complete.

In the coming year differential cross sectiins will be measured for scattering by ^{196}Pt at 2.5 MeV, to complement similar data already obtained for ^{194}Pt and $^{190,192}Os$ isotopes. Measurements for these three nuclei will also be made near neutron energy of 5 MeV, where the cross sections for the low-lying collective levels will be almost pure direct components; the compound system components are negligible at these energies, except for very highly excited levels. These data will complement the 8 MeV data already taken at BRC, and allow separation of inelastic levels not separable in the higher energy experiment.

All of the differential scattering cross sections will be combined with the total cross sections already measured in an analysis which will determine the expected large role of different types of collective excitations in neutron scattering. These studies should enable definite statements about the character of the non-axial quadrupole excitations of some or all of these nuclei. They will also enable us to explore the differences and similarities between excitation of collective modes by neutrons, and by protons and heavy ions.

2. Pb Isotope Study. (Hanly, McEllistrem)

Dan Horen, Cleland Johnson, and Alan MacKellar of Kentucky have discovered[4] some interesting structures in neutron scattering from ^{208}Pb and ^{206}Pb. These structures may be interpreted as requiring explicit intermediate resonances in scattering by these nuclei; the usual optical model approach would be misleading, since effects of such unusually large resonances would have to be artificially incorporated into the scattering potentials to fit the scattering data. This effect is probably much less pronounced in ^{206}Pb than in ^{208}Pb, since in the former two valence nucleon excitations exist to distribute resonance strengths. But in ^{204}Pb the effects of such anomalous resonances are completely distributed into the sea of compound levels at the excitation energy of the compound nucleus in the scattering experiment.[5] Thus ^{204}Pb would be the first nucleus in this mass region which would present a statistical distribution of excitations, properly describable by a standard scattering potential approach. We have begun a careful comparison of scattering from ^{204}Pb and ^{206}Pb, to ascertain the roles of structure properties in altering the scattering from expectations of a simple spherical potential model; presumably the spherical optical model is most appropriate for scattering from ^{204}Pb. Total cross sections have been measured for neutrons incident on separated isotope samples of ^{206}Pb and of ^{204}Pb for incident energies from 300 keV to 4 MeV. Because of the large resonance spacings in these nuclei even at incident energies near several MeV, sample self-shielding corrections are quite important. These and other corrections are now being made to these data.

---

[4]Private communication.

[5]D.J. Horen, R.L. Macklin, J.A. Harvey, and N.W. Hill, Phys. Rev. C29, 2126 (1984).

We expect to make the important differential scattering cross section comparisons for these nuclei in the near future. Some initial measurements have been made for ^{206}Pb at an incident energy of 7 MeV, but it will be important to make measurements at somewhat lower energies as well, where elastic scattering is quite sensitive[1] to nuclear structure differences for different isotopes. First, careful measurements will be made for an incident energy near 2.5 to 3 MeV, to have accurate measurements near the energies where data exist for the shape-transitional Os and Pt nuclei. The most important new measurements will be those for ^{204}Pb, to test by comparison to ^{206}Pb cross sections the effects of the two extra valence particle excitations in ^{204}Pb. We will also make differential cross section measurements near 5 MeV, where once again compound system cross sections will be small enough that direct components will be evident.

The Pb scattering experiment, for both isotopes, provides a study in which quadrupole collective effects are expected to be quite weak. Thus these nuclei provide baseline scattering potentials not perturbed by strong collective coupling; this is an excellent way to provide a baseline for the analysis of strong coupling in the shape-transitional Os and Pt isotopes.

3. Neutron Scattering from Sn Isotopes. (Zhou, Harper, Weil)

Some of the most accurate and precise differential scattering cross sections for complex nuclei have been published,[6] for neutrons of energy 1.00 and 1.63 MeV incident on separated isotope samples of the five even-A Sn isotopes with A = 116 to 124. Total cross sections had been published in an earlier paper for the same isotopes.[7] The combined, spherical potential model for these rigid nuclei described the elastic scattering cross sections well, and showed the effects of the changing numbers of valence neutron excitations on the absorptive potential. The potentials vary in a reasonable way from isotope to isotope, and the cross sections show a smooth, systematic dependence on neutron excess.[6] In spite of this, the differential inelastic scattering cross sections to the first excited 2^+ levels are substantially smaller than expected on the basis of the reasonable potential models for the scattering. At this time, this is an unresolved problem, except for the suggestion that this is precisely what would occur if the absorptive potential were explicitly parity or orbital angular momentum dependent. Such orbital angular momentum dependencies have recently been claimed by Carlton et al.[8] based on very low energy neutron scattering from light, even-A nuclei.

---

[6]R.W. Harper, J.L. Weil, and J.D. Brandenberger, Phys. Rev. C30, 1454 (1984).

[7]R.W. Harper, T.W. Godfrey, and J.L. Weil, Phys. Rev. C26, 1432 (1982).

[8]R.F. Carlton, J.A. Harvey, and C.H. Johnson, Phys. Rev. C29, 1988 (1984) and references cited therein; C.H. Johnson, Proc. Int'l. Conf. Neutron-Nucleus Collisions, A Probe of Nuclear Structure, AIP Conf. Rep. 124 (ed. by J. Rapaport, R.W. Finlay, S.M. Grimes, and F.S. Dietrich (1985), p. 446.

Elastic and inelastic scattering measurements have also been completed here for 4 MeV neutrons incident on these Sn isotopes, and the four data sets are now being combined into a common analysis. It is already clear that a spherical potential model cannot be constructed which will have the expected energy dependence and describe all the data. At the same time, the differential scattering cross sections to the first excited 2^+ levels show evidence for some weak, direct excitation. Thus a coupled channels model which incorporates the vibrational excitations of the first 2^+ levels explicitly is now being attempted to see whether that would provide a consistent description of the four data sets, differential scattering cross section data at 1.00, 1.63, and 4.00 MeV as well as total cross sections from about 300 keV to 5 MeV.

Resonance self-shielding corrections for the above mentioned total cross sections are being calculated. They amount to several percent at the lowest energies, and thus may affect the determination of optical model parameters to be used in the coupled-channel fits to the complete data set.

As noted earlier, the differential scattering cross sections for the Sn isotopes are among the most precise and accurate cross sections measured. They provide an excellent data set to use for tests of modified statistical models. These cross sections measured for many levels at an incident neutron energy of 4 MeV are the right data to test the ability of the compound system reactions model of Weidenmuller and collaborators. This model has been developed most recently by Tepel, Hofman, and Herman[9] (THH) to represent the cross sections accurately. It is expected that in the case of many open channels and in a spherical nucleus, that model should be accurate to about 10 or 15%. An extensive test of this model is possible in the Sn study, spanning excitations in five even-A nuclei.

C. NUCLEAR STRUCTURE STUDIES

1. Shape Transitional Nuclei. (Kleppinger, Khan, Yates)

The ongoing study of collective excitations in the even-A Os, Pt, and Hg nuclei as well as their odd-A neighbors encompassed also the study of ^{200}Hg, and the results have now been published.[10] An earlier study[11] in this laboratory had shown that the isotone ^{198}Pt had a level scheme and transition rates which did not allow that nucleus to be inserted into the collective

---

[9] J.W. Tepel, H.M. Hofman, and M. Herman, Proc. Int'l. Conf. Nuclear Cross Sections for Technology, NBS Spec. Pub. 594, 762 (1980).

[10] A. Khan and S.W. Yates, Phys. Rev. C29, 1081 (1984).

[11] S.W. Yates, A. Khan, A.J. Filo, M.C. Mirzaa, J.L. Weil, and M.T. McEllistrem, Nucl. Phys. A446, 519 (1983).

excitation systematics which seem to prevail in this mass region. Earlier studies of ^{200}Hg also seemed to suggest that the usual collective models would not describe that nucleus, and suggested that some of the difficulties found for description of ^{198}Pt were present also in ^{200}Hg. For example, the first excited 0^+ level does not fit into any of the collective schemes. The presently published ^{200}Hg study confirms that there are indeed many similarities between the characters of these two isotones, with very similar departures from expectations of collective excitation models.

Next year excitation functions and gamma-ray angular distributions for the (n,n'γ) reactions in the ^{202}Hg and ^{204}Hg nuclei will be measured, to develop full level and decay schemes for these nuclei. The comparison of these schemes to those for their Pb isotones with A = 204 and 206 will help separate the different roles played by neutron and proton holes in this mass region. If the neutron scattering studies, discussed in the section above, reveal different direct coupling strengths for proton and neutron scattering in the Pb isotopes, the knowledge of the separate roles played by neutron and proton excitations in the target will be important for interpreting scattering differences. Extending our nuclear structure characterizations beyond the presently completed study[10] of ^{200}Hg and toward the closed shells of ^{208}Pb is also important.

Excitation functions and angular distributions will be measured for (n,n'γ) reactions on ^{204}Pb, to complete the very sparse knowledge of excitations in that nucleus. These level schemes are needed not only to complement the neutron scattering experiments, but also for comparison with the information being developed from the study of Hg isotopes, discussed above. We will also be looking for evidence that, with four valence nucleon excitations, ^{204}Pb will begin to show some evidence of developing quadrupole collective strengths in this experiment as well as in the neutron scattering study.

2. ^{96}Zr Study. (Molnar, Yates)

The nucleus ^{90}Zr has long been known as an especially stable, spherical nucleus occasioned by shell and subshell closure at Z = 40 and N = 50. Experiments at Kentucky and Debrecen on the ^{96}Zr(p,n)^{96}Nb reactions, as well as experiments at other centers, provide evidence that the double subshell closure makes ^{96}Zr also a stable, spherical nucleus. There was reason to expect that, as in other spherical, stable nuclei p-h excitations across the pairing gap would lead to collective levels and a collective band. These levels would have little overlap with the levels from excitations without crossing the pairing gap. An experiment at Kentucky this last year newly identified a 2^+ level which decays strongly to the second 0^+ level, but very little to the ground state. This immediately suggests that the second 0^+ level may be the head of such a collective band, with the newly discovered 2^+ level as the second member. Deformed structures qualitatively similar to this are well known in ^{40}Ca, and other magic or stable spherical nuclei. A

paper detailing this suggestion and the data from several experiments which support it is now being prepared.[12]

The one week data taking period completed in the Fall of 1984 was quite fruitful, but hardly a complete study of the levels of this nucleus. To investigate the presence of coexisting collective or deformed states in this nucleus it will be important to identify some higher spin members of bands and establish their collectivity. The experiments will be aimed at characterizing all states below approximately 3.5 MeV excitation in ^{96}Zr. Besides the gamma-ray work to be done at Kentucky and in Budapest, the ^{94}Zr(t,p) reactions will be studied with the triton beam of the LANL tandem. When all of this work is completed, fairly complete characterization of the parentage and behavior of nearly all levels should be obtained. In a final phase, shell model calculations may be performed in collaboration with Dr. J. A. Becker of LLNL. Dr. Becker has made extensive shell model calculations in this mass region with realistic two-body interactions.

3. Level Schemes in the Sn Isotopes. (Gacsi, Shi, Weil)

Earlier work on ^{124}Sn in this laboratory[13] had tentatively identified sets of levels above the pairing gap which, from their energies and decays, are strong candidates for two-and three-phonon vibrational multiplets. These are co-existent levels, whose collective character has not been diffused into the many non-collective levels nearby. They would be similar to the well known coexistent deformed bands in spherical nuclei, except that they would not be deformed. While deformed structures co-exist with spherical neighbors, it might be more surprising to find vibrational structures maintaining their separate character, without strong mixing with the many nearby levels.

Presently work is proceeding on the study of ^{116}Sn levels, and many new levels have been found, and are being characterized. Angular distributions have been measured for 25 gamma-rays for an incident neutron energy of 3.05, and for many more at 3.75 and 4.50 MeV. A decay scheme has been constructed that combines information from our (n,n'γ) excitation function for E_n = 2.5 to 4.5 MeV, and ^{115}Sn(n,γ) results of S. Raman of the ORELA facility at ORNL. The decay scheme contains 190 γ-rays and many new levels, including 60 levels between 3.5 MeV and 9.5 MeV excitation energy. Our analysis is not yet complete enough to identify levels in this nucleus which correspond to collective structures not associated with the structure of the ground state. Gamma-ray angular distributions and excitation functions have also been measured for many transitions in ^{120}Sn, to attempt to ascertain collective excitations above the pairing gap in this nucleus. Such collective structures, if they are confirmed by further work in these isotopes, may

---

[12] G. Molnar, S.W. Yates, and R.A. Meyer, to be submitted to the Physical Review C.

[13] J.L. Weil and J. Sa, Bull. Am. Phys. Soc. 28, 702 (1983).

have important effects on scattering cross sections. Thus the present work complements the Sn scattering studies reported in the previous section.

D. PULSED-BEAM 180° RADIATIVE CAPTURE FACILITY

1. Target Room Developments. (Trice, Kovash)

During the past year we have begun a development program aimed at studying radiative capture reactions of charged particles and neutrons at angles from 0° to 180°. Special beam handling is required to reach these extreme angles. Work is now proceeding on schedule on all four of the major components of this effort.

A new target chamber/pivot-post-assembly has been constructed and installed along with the three moveable carriages for supporting the massive γ-ray detectors and magnets. A new beam line to this target chamber has been installed and is operational, and the kicker magnet and its vacuum chamber which are used to transport the beam into the 180° scattering system have been constructed and installed. The kicker magnet injects beam into one of three lines, separated from each other by 7°. It is this multiple line system which allows us to handle detection at both 0° and 180°, as well as other angles. The second magnet of the 180° scattering system, a 45° bend C-shaped dipole, has been designed using the computer code POISSON. The low-carbon steel for this magnet is currently on order.

2. High Efficiency Gamma-Ray Detection. (Kovash, Trice)

Two 4" ϕ x 3" bismuth germanate (BGO) detectors have been ordered. Testing on the first crystal to arrive has shown it to be of superb energy resolution. For 10.8 MeV γ-rays from the $^{27}Al(p,\gamma)^{28}Si$ reaction, the measured resolution is 4.5% --comparable to a large NaI crystal at this energy! In February 1985 we will use this detector to begin our study of the $^{11}B(n,\gamma)^{12}B$ reaction at $E_n \simeq 20$ MeV, to search for 1 $\hbar\omega$ gamma-ray transitions to the $d_{5/2}-p_{3/2}^{-1}$ final states of $J^\pi = 4^-$, 3^-, and 2^- in ^{12}B.

A large NaI spectrometer has been designed and ordered from the Bicron Corporation. The central crystal is 8" ϕ x 10", and is surrounded by a segmented annulus of 6 NaI sectors, each of 1-3/4" thickness. This spectrometer will be the primary detector for our high resolution radiative capture studies.

3. Data Acquisition System. (Riley, Trice, Kovash)

A new DEC LSI 11/23 microcomputer with 1-1/2 MB memory has been purchased for data acquisition. Along with it we have obtained a CAMAC crate, controller, graphics terminal and printer, charge-and voltage-sensitive ADCs, and scalers. Presently the data acquisition software is being developed for this equipment.

4. Radiative Capture Measurements . (Kovash, Trice)

Work will soon begin on the $^{11}B(n,\gamma)^{12}B$ capture reaction to search for the analogues of the second harmonic resonances which were discovered in intermediate energy proton scattering experiments. For the initial stages of this search, we will use the BGO detection system. Its low sensitivity to neutrons may improve performance for capture experiments in a neutron environment.

5. The $^{81}Br(p,n)$ and (p,n) Cross Sections. (Fisher, Hershberger, and Gabbard).

The $^{81}Br(p,n)^{81}Kr$ cross sectons to low-spin, odd parity levels of ^{81}Kr can reveal the separate Gamow-Teller (GT-M1) strengths of the transitions which would be important if ^{81}Br were to be used to detect solar neutrinos. A large solar neutrino detector based on neutrino capture in that nucleus is being actively proposed by G.S. Hurst, Ray Davis, Bruce Cleveland, and others. To interpret the capture rates properly, it is quite useful to have separate determinations of GT-M1 strengths for each excited level of interest. Separating these levels in a (p,n) detection experiment would determine those rates, if the M1 portion of the (p,n) reaction amplitude can be isolated.

To interpret the (p,n) strengths properly, it is quite important to have proton and neutron scattering potentials which are well adapted to the particular nuclei of this reaction. Low energy measurements of proton scattering from ^{81}Br and (p,n) cross sections can provide useful constraints on the scattering potentials used at low and intermediate energies. Such measurements are planned in our laboratory.

A second problem is the development of targets of Br stable under beam for protracted bombardment periods. This is a difficult target technology problem now being investigated. Finally, extensive DWBA calculations are being done to test the ability to extract GT-M1 strengths through (p,n) measurements at several different proton energies.

A. NUCLEAR DATA - MEASUREMENTS

1. Beta-delayed Two-proton Decay of ^{22}Al and ^{26}P [1]

M.D. Cable,[a] J. Honkanen,[b] E.C. Schloemer,[c] M. Ahmed,[d] J.E. Reiff, Z.Y. Zhou,[e] and Joseph Cerny

Following the discovery[2,3] of beta-delayed two-proton emission, we have attempted to establish the mechanism(s) for this decay mode in the decays of both ^{22}Al and ^{26}P. These nuclides were produced at the 88-Inch Cyclotron via the (^{3}He,p4n) reaction at 110 MeV on targets of ^{24}Mg and ^{28}Si, respectively. Proton-proton coincidence experiments have been performed in high geometry configurations at small angles (~0-70°) and at large angles (70-170°). Monte Carlo simulations of the expected proton-proton coincidence data were made for decay by sequential emission, by (transient) ^{2}He emission, or by simultaneous, uncorrelated emission.

The experimental results show that the dominant two-proton emission mechanism is a sequential process for both ^{22}Al and ^{26}P. Fig. 1 presents the decay scheme for ^{22}Al most consistent with our overall results. A decay scheme for ^{26}P appears in ref. 3. Some puzzling features of the large-angle two-proton measurements for ^{22}Al have been observed and suggest further investigation.

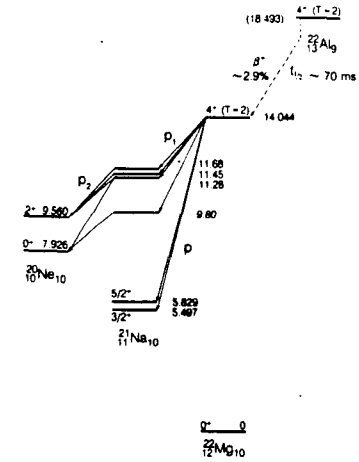

Fig. 1. Proposed new partial decay scheme for ^{22}Al. XBL 842-9422

---

[1] Condensed from LBL-17983, Phys. Rev. C30, 1276 (1984)

[2] M.D. Cable, J. Honkanen, R.F. Parry, S.H. Zhou, Z.Y. Zhou and J. Cerny, Phys. Rev. Lett. 50, 404 (1983).

[3] J. Honkanen, M.D. Cable, R.F. Parry, S.H. Zhou, Z.Y. Zhou and J. Cerny, Phys. Lett. 133B, 146 (1983).

2. Additional Beta-delayed Protons from the $T_z = -3/2$ Nuclei ^{21}Mg, ^{25}Si, ^{29}S, and ^{41}Ti [4]

Z.Y. Zhou,[e] E.C. Schloemer,[c] M.D. Cable,[a] M. Ahmed,[d] J.E. Reiff and Joseph Cerny

Beta-delayed proton emission has proven to be a useful tool for understanding nuclei far from stability. Most of the beta decay strength is concentrated at and below the isobaric analog state (IAS) of the parent nucleus (precursor) ground state. Identification of beta strength to states above the IAS is important not only because it provides additional tests of nuclear models of beta decay, but also because proton emission from such beta daughter nuclei frequently constitutes an important component of the background in searches for more exotic nuclei. Therefore we have re-measured the beta-delayed proton spectra of four $T_z = -3/2$ nuclei: ^{21}Mg, ^{25}Si, ^{29}S and ^{41}Ti. Fourteen previously unreported proton groups were observed and beta decay branching ratios were derived for each.

In all these studies, beam energies and/or measurement conditions were selected to produce the isotope of interest with little or no contamination from other beta-delayed particle emitters. ^{21}Mg was produced from ^{20}Ne at a beam energy of 41.5 MeV while ^{25}Si, ^{29}S and ^{41}Ti were produced from Mg, Si and Ca targets, respectively, at ~32 MeV.

Present Addresses:
a) Lawrence Livermore National Laboratory.
b) Department of Physics, University of Jyvaskyla, Finland.
c) A.T.&T. Bell Laboratories, Holmdel, NJ.
d) Bell Communications Research Inc., Red Bank, NJ.
e) Department of Physics, Nanjing University, Nanjing, China.

3. Discovery of Radioactive Decay of ^{222}Ra and ^{224}Ra by ^{14}C Emission [5]

P.B. Price,[a] J.D. Stevenson,[b] S.W. Barwick and H.L. Ravn[c]

Rose and Jones[6] recently reported the discovery of a new mode of radioactive decay in which a ^{223}Ra nucleus emits a 29.9 MeV ^{14}C nucleus with a branching ratio relative to alpha decay of $(8.5 \pm 2.5) \times 10^{-10}$. Using the ISOLDE on-line isotope separator at CERN to produce sources of ^{221}Fr, ^{221}Ra, ^{222}Ra, ^{223}Ra, and ^{224}Ra, and using polycarbonate track-recording films

[4] Condensed from IBL-18853

[5] Condensed from a paper submitted to Phys. Rev. Lett.

[6] H.J. Rose and G.A. Jones, Nature 307, 245 (1984).

sensitive to energetic carbon nuclei but not to alpha particles, we have confirmed the Rose and Jones discovery and have discovered two new cases of the rare ^{14}C decay mode - in ^{222}Ra and ^{224}Ra. We have also set a stringent upper limit on the $^{14}C/\alpha$ branching ratio for ^{221}Fr and ^{221}Ra. Searches for modes of decay in which heavier particles such as ^{24}Ne are emitted are in progress.

Present Addresses:
a) Also at Space Sciences Laboratory.
b) Physics Department, Michigan State University, East Lansing, MI 48824.
c) EP Division, CERN, 1211 Geneve, Switzerland.

4. Radioactive Decay of ^{223}Ra by ^{14}C Emission

S. Yashita, K. Gregorich and A. Ghiorso

Recently H.J. Rose and G.A. Jones at the University of Oxford reported[6] the very difficult observation of an exotic radioactive decay mode in ^{223}Ra, its spontaneous disintegration by the emission of ^{14}C particles. We felt that it was important to try and confirm their somewhat surprising discovery by an independent method. Using an ^{227}Ac source in a specially converted magnetic system, we suppressed the alpha radiation by a factor > 10^4, extending the life of the detector system indefinitely. During 25 days of exposure we observed a group of 21 events in the 29 MeV range and with a magnetic rigidity of ~4.9 Kgm. The ^{14}C to α branching ratio in ^{223}Ra was found to be $6 \pm 1 \times 10^{-10}$ assuming a 65% abundance in C^{6+}. Due to the very low alpha counting rate, chiefly due to the small amount of ^{219}Rn that escaped from the source and decayed in the vicinity of the detector, there was no quadruple pileup problem to provide a background. Within our present experimental accuracy the magnetic rigidity, energy and branching ratio support the assignment of ^{14}C emission from ^{223}Ra as proposed by the Oxford experiment.

5. The Decay of ^{248}Es

Wen Xin Li, K.E. Gregorich, R.B. Welch, W. Kot, D. Lee, and G.T. Seaborg

We have studied the electron capture and alpha decays of ^{248}Es. In these experiments about 40 gamma rays which are due to the decay of ^{248}Es were seen. The strongest of these gamma rays has the same energy as the only known gamma ray accompanying the β decay of 23h ^{248}Bk which feeds the same levels in ^{248}Cf. The apparent half lives of these gamma rays vary from about 22 minutes to about 45 minutes suggesting the existence of two isomers of ^{248}Es. This is further supported by the data arising from the measurement of the ~0.25% alpha decay branch. The existence of two isomers is not surprising because similar behavior is seen in ^{250}Es. In ^{248}Es one expects

to see coupling of the 7/2[624] neutron state with the 7/2[633] or 3/2[521] proton state leaving open the possibility for coupling into high spin and low spin states. Further experiments and the analysis of gamma-gamma coincidence data from a similar experiment will be necessary for further understanding of the decay of ^{248}Es.

6. The Decay of ^{250}Fm

W.P. Kwan, K.E. Gregorich, Wen Xin Li, D. Lee, R.B. Welch, W. Kot and G.T. Seaborg

We have studied the alpha and electron capture decays of ^{250}Fm. Previous experiments have left open the possibility of a large (>10%) electron capture branch in ^{250}Fm,[7] which would present a unique opportunity to study the level structure of ^{250}Es. While no electron capture branch was found in the present experiment, we have remeasured the ^{250}Fm half life (28.8 ± 0.3 min.) by monitoring the 7.43 MeV alpha decay and have determined that the electron capture branching ratio is less than 4%. The ^{250}Fm was produced at the 88-Inch Cyclotron by the ^{249}Cf (^{3}He, 2n) ^{250}Fm reaction. In this experiment no evidence for the electron capture decay of ^{250}Fm was found. No statistically significant short component in the Es KX-rays was seen above the 5.3 hour component due to ^{251}Fm produced by the ^{249}Cf (^{3}He, n) ^{251}Fm reaction. In addition, no unrecognized gamma rays with about a 30 minute half life were found, nor were the gamma rays accompanying the electron capture decay of the ^{250}Es daughter seen. The alpha decay of the ^{250}Fm was easily followed by monitoring the 7.43 MeV alpha group. By fitting the decay of this 7.43 MeV alpha group with an error weighted least squares procedure, we have found the half life of ^{250}Fm to be 28.8 ± 0.3 minutes. By comparing the initial activity of the ^{250}Fm alphas with the minimum 28.8 minute component which would have been detectable in the Es KX-rays and correcting for detection efficiencies and X-ray production rates, we have determined that the upper limit for the electron capture branch in ^{250}Fm is 4%.

7. Actinide Production in the ^{136}Xe + ^{249}Cf Reaction

K.E. Gregorich, R.B. Welch, W. Kot, D. Lee, K.J. Moody and G.T. Seaborg

As part of our ongoing systematic study of the deep-inelastic reaction mechanism in the actinide region, we have been studying actinide production in the ^{136}Xe + ^{249}Cf reaction. The choice of this relatively neutron deficient target in the actinide region allows us to study what effect

[7] S. Amiel et al., Phys. Rev. 106, 553 (1957).

the position of the target with respect to beta stability has on the deep-inelastic production cross sections for target-like nuclides. A Cf target was bombarded at the IBL SuperHILAC with ^{136}Xe ions at energies of 1.00, 1.08 and 1.16 times the nominal Coulomb barrier. The production cross sections for the highest energy bombardments are presented as a contour plot in Fig. 1. While it can be seen that the largest yields lie along the line of beta stability, the width of the distribution allows significant yields away from beta stability. The yields of the neutron-rich below-target nuclides are of primary interest and suggest that more neutron-rich targets will produce new neutron-rich below-target nuclides in quantities sufficient to allow their identification when fast chemical separations are developed. Also of interest are the neutron-deficient above-target yields, which drop off much more rapidly than did the yields for products from analogous transfers in the ^{136}Xe + ^{248}Cm reaction.[8] The yields of these products may be lowered either because they feel the steep rise in energy from the neutron-deficient side of the valley of beta stability or because the fission barriers for the neutron-deficient isotopes of Md and heavier elements are lower than for isotopes closer to beta stability, causing a lower fission survival rate for the former.

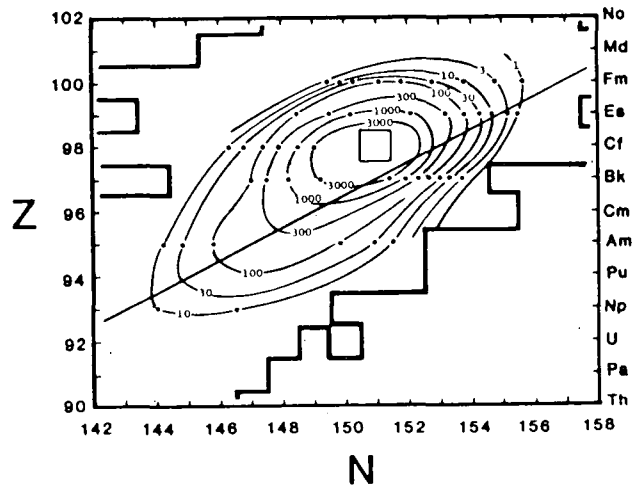

Fig. 1. A contour plot of the production cross sections from ^{136}Xe + ^{249}Cf at 1.16 times the Coulomb barrier. The contours are labeled in μb. The heavy line shows the limit of known nuclides, and the diagonal line shows the position of beta stability. XBL 8410-4161

[8] K.J. Moody, IBL-16249 (1983).

8. First Observation of the Neutron-Rich Isotope ^{19}B [9]

J.A. Musser[a] and J.D. Stevenson[b]

The most neutron-rich boron isotope previously observed to be particle stable is ^{17}B.[10] In the same experiment ^{16}B was shown to be unstable to prompt neutron emission. Current nuclear mass models predict that this even-odd gap structure should continue through ^{18}B and ^{19}B, and that ^{19}B is the most neutron-rich particle-stable boron isotope. In our experiment we produced projectile fragments by interactions of an intense 670 MeV/nucleon ^{56}Fe beam in a 7.9 g/cm^2 Be target. The charges and masses of the projectile fragments were obtained using the 0° spectrometer facility at the Bevalac in conjunction with a detector telescope[11] in the focal plane of the spectrometer. Fig. 1 is a scatter plot of our data for the heaviest boron isotopes in the Čerenkov plane. Our data indicate for the first time that ^{19}B is particle-stable, whereas ^{18}B is unstable to prompt neutron emission. With a longer run and minor modifications, it appears possible with our detector system to extend the known limits of particle stability of light, neutron-rich nuclei to the predicted position of the neutron drip line.

Present Addresses:
a) Department of Physics, Randall Laboratory, University of Michigan, Ann Arbor, MI 48109.
b) National Superconducting Cyclotron Laboratory, Michigan State University, East Lansing, MI 48824.

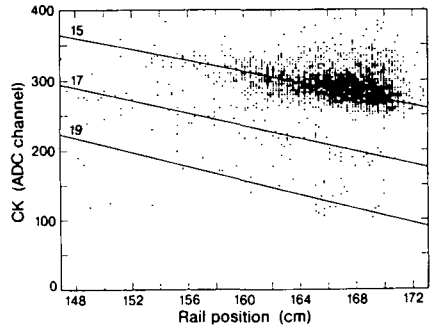

Fig. 1. Data for heaviest boron isotopes. Expected locations of ^{15}B, ^{17}B, and ^{19}B are shown.[12]

XBL 8410-4289

---

[9] Condensed from a paper submitted to Physical Review Letters.

[10] J.D. Bowman, A.M. Poskanzer, R.G. Korteling and G.W. Butler, Phys. Rev. C9, 836 (1974).

[11] J.D. Stevenson and J.A. Musser, Nucl. Instr. & Meth. 213, 285 (1983).

9. Measurements of Interaction Cross Sections and Radii of He Isotopes

I. Tanihata,[a] O. Yamakawa,[a] H. Hamagaki,[a] O. Hashimoto,[a] S. Nagamiya, Y. Shida, N. Yoshikawa, K. Sugimoto,[b] T. Kobayashi, D. Greiner, N. Takahashi,[c] and Y. Nojiri[c]

We have made the first measurements of the interaction cross sections of all known He isotopes (^{3}He, ^{4}He, ^{6}He, and ^{8}He) using secondary beams of He on Be, C, and Al targets and from these have deduced their radii. The interaction cross section (σ_I), defined as the total cross section for the nucleon (proton and/or neutron) removal from the incident nucleus, was measured by a transmission-type experiment and calculated by the equation

$$\sigma_I = \frac{1}{N_t} \log(R_0/R) \quad ,$$

where R_0 is the ratio of the number of outgoing nuclei to the number of incoming nuclei for an empty-target run, and R is the same ratio for a target-in run. Since the interaction cross section σ_I between stable nuclei is known to be essentially independent of the beam energy above 200 MeV/nucleon[12] and is at its saturated value at the present beam energy, we assumed that σ_I reflects a well defined nuclear size and then operationally defined a nuclear radius by the equation

$$\sigma_I = \pi \, (R(p) + R(t))^2 \quad .$$

The nuclear radii calculated by this formula using the known data of σ_I between stable isotopes are systematically larger by 0.2 fm than the half-density radii determined by the electron scattering in the whole mass range,[13] indicating that the presently defined radius corresponds to the sampling of a density point lower than the half density.

Permanent Addresses:
a) also Institute for Nuclear Study, University of Tokyo Tanashi, Tokyo 188, Japan.
b) Faculty of Science, Osaka University.
c) also, Laboratory for Nuclear Studies, Osaka University, Toyonaka, Osaka 560, Japan.

---

[12] A.S. Goldhaber and H.H. Heckman, Ann. Rev. Nucl. Part. Sci. 28, 161 (1978).

[13] I. Tanihata, Proceedings of the Workshop on Prospects for Research with Radioactive Beams from Heavy Ion Accelerators, April, 1984 Washington, DC, LBL-18187, UC-34A, p. 162.

10. Recent Experimental Results from OASIS

P.A. Willmarth, J.M. Nitschke, P.K. Iemmertz and R.B. Firestone

Our on-going study of the decay properties of very neutron-deficient lanthanides has resulted in the identification of several new isotopes (See Table I). These new isotopes were produced at the SuperHILAC's on-line isotope separator OASIS and decay studies were carried out in the new spectroscopy laboratory.[14] The isotope of interest is passed through a slit in the focal plane of the mass separator and transported ionoptically to a fast cycling tape which is periodically positioned between an array of detectors. On an event-by-event basis, all possible decay modes are measured and the information written on computer tape for subsequent replay and analysis. Two general classes of decays are of interest: (1) direct or β-delayed particle emission along with any coincident gamma rays, x-rays, or positrons, and (2) gamma rays in coincidence with positrons or x-rays from electron capture and conversion processes.

Table I.

Reaction	E_{lab} MeV	Isotope	Decay Mode	$T_{1/2}$ s
$^{92}Mo(^{40}Ca,3pn)$	170	^{128}Pr	β+, EC	3.0±0.1
$^{92}Mo(^{40}Ca,2pn)$	170	^{129}Nd	βp, β+, EC	4.9±0.2
$^{92}Mo(^{40}Ca,pn)$	170	^{130}Pm	βp, β+, EC	2.2±0.5
$^{92}Mo(^{54}Fe,3p2n)$	275	^{141}Tb	β+, EC	2.7±1.0
$^{92}Mo(^{54}Fe,4pn)$	275	^{141}Gd	βp, β+, EC	13.3±1.2
$^{92}Mo(^{56}Fe,3p2n)$	275	^{143}Tb	β+, EC	11.8±0.5
$^{92}Mo(^{56}Fe,p3n)$	257			
$^{92}Mo(^{58}Ni,3p3n)$	325	^{144}Ho	βp, β+, EC	0.7±0.1
$^{92}Mo(^{56}Fe,3p2n)$	257			
$^{92}Mo(^{58}Ni,4p2n)$	325	^{144}Dy	βp?, β+, EC	?
$^{92}Mo(^{56}Fe,3pn)$	257			
$^{92}Mo(^{58}Ni,5pn)$	325	$^{144}Tb^{m}$	βp?, β+, EC	4.5±0.5

[14] J.M. Nitschke, Nucl. Instr. Meth. 206, 341 (1983).

B. Nuclear Data - Theory

1. Theoretical Estimates of the Rates of Radioactive Decay of Radium Isotopes by ^{14}C Emission [15]

Y.-J. Shi and W.J. Świątecki

The recently discovered[16] radioactive decay of $^{222,223,224}Ra$ by the emission of ^{14}C and, in particular, the branching ratios of these decays to alpha emission, can be accounted for with reasonable accuracy by a barrier penetrability calculation, provided a realistic potential-energy barrier is used. We took a Coulomb barrier modified by the canonical nuclear proximity attraction[17,18] and obtained branching ratios within a factor of 10 of the observed values without the adjustment of any parameters. (This implies an accuracy in the penetrability integrals of about 3%.)

2. Estimates of Radioactive Decay by the Emission of Nuclei Heavier than Alpha Particles [19]

Y.-J. Shi and W.J. Świątecki

The barrier penetrability calculations, developed to account for the recently discovered radioactive decay of Ra isotopes by ^{14}C emission, have been applied to a systematic search for other exotic decays. The potential energy barrier consists of a sum of electrostatic and proximity potentials, supplemented by a power law interpolation from the contact configuration to the configuration of the parent nucleus. Some three dozen candidate decays are listed, with nominal branching ratios of the exotic to alpha decays greater than 10^{-12}. Some of these decays might be detected experimentally in the near future.

---

[15] Condensed from IBI-18366 and Phys. Rev. Lett. 54, 300 (1984)

[16] H.J. Rose and C.A. Jones, Nature 307, 245 (1984); P.B. Price et al., submitted to Phys. Rev. Lett. (1984).

[17] J. Blocki et al., Ann. Phys. 105, 427 (1977).

[18] J. Blocki and W.J. Świątecki, Ann. Phys. 132, 53 (1981).

[19] Condensed from IBI-18349, to appear in Nucl. Phys.

C. Nuclear Data - Evaluation

1. Isotopes Project

E. Browne, J.M. Dairiki, R.B. Firestone, C.M. Iederer, V.S. Shirley

The Isotopes Project compiles and evaluates nuclear structure and decay data and disseminates these data to the scientific community. The group coordinates its nuclear data evaluation efforts with those of other data centers via national and international nuclear data networks. The group is currently rèsponsible for the evaluation of mass chains A = 167-194. All evaluated data are entered into the international Evaluated Nuclear Structure Data File (ENSDF) and published in Nuclear Data Sheets. In addition to the evaluation effort, the Isotopes Project is responsible for production of the Radioactivity Handbook.

Most of the group's effort during the past year was directed toward production of the Radioactivity Handbook, scheduled for publication in 1985. The primary purpose of the Handbook is to provide applied scientists with a source of recommended decay data. Recommended decay data are taken from the current version of ENSDF and analyzed to provide adopted values (e.g., radiation energies and intensities) for presentation in the Handbook. Additional calculations and evaluation provide recommended data for x-rays, conversion electrons, and continuous radiations (β^-,β^+ and internal Bremsstrahlung). For each mass chain, relationships between the isobars are given on a "skeleton" mass scheme.

The ENSDF file and the handbook data were organized into a numerical database using DATATRIEVE, a DEC database management system, to facilitate the manipulation of the large amounts of data which were processed. An interactive menu of DEC-DCL, DATATRIEVE, and Fortran programs and procedures was developed to efficiently analyze the data and prepare the final tables. Computer codes for scientific checking and statistical analysis of the handbook data were developed to guarantee the highest possible quality and uniformity in the final product. The UNIX text processing system is used to prepare the tables and to lay out the final pages.

The database that was developed for production of the Radioactivity Handbook has been made available to remote users by on-line retrieval. This database includes the ENSDF numerical data, adopted decay data from the Radioactivity Handbook, Wapstra's 1984 mass evaluation, and an interactive menu of utility programs and procedures to automatically retrieve, analyze, or make tables from the database. With the completion of the Radioactivity Handbook, the database will contain information for A=1-266. On-line access to the database is available by telephone and via DECNET, MILNET and TYMNET.

During the past year evaluations of nuclear structure data for all nuclides with A=192 and A=174 were published in Nuclear Data Sheets. Evaluations of A=171 and A=181 have been submitted and accepted for

publication. Beginning in 1985, the Isotopes Project will implement an integrated database evaluation system. Many of the codes and procedures developed for production of the Radioactivity Handbook will be adapted as tools to increase the efficiency and uniformity of the evaluation process. For example, the code SPINOZA is a valuable physics analysis and checking program; it is especially useful in deriving spin/parity assignments for complicated level schemes. The code GAMUT presents the evaluation network with a uniform, statistical process for deriving alpha-particle and gamma-ray energies and intensities.

Additionally, the Isotopes Project answers specific data requests, maintains recent references (filed by individual isotope) and encourages general use of its extensive library, which contains comprehensive data files and major nuclear physics journals.

A. NUCLEAR DATA APPLICATIONS-MEASUREMENTS

1. Measurements and Calculations of the Leakage Multiplication from Hollow Beryllium Spheres (Wong, Plechaty, Bauer, Haight, Hansen, Howerton, Komoto, Lee, Perkins, and Pohl)

Proposed fusion reactors utilize Be in the surrounding blanket to multiply the fusion neutrons for use in breeding tritium and in some cases also fissile material. To have confidence that the breeding is calculated correctly, it is essential to validate the Be cross sections via integral experiments. Recent measurements of the leakage multiplication from Be[1] and BeO[2] were 20 to 30% lower than calculations. The leakage multiplication is defined as the number of neutrons leaking out of the Be per 14-MeV source neutron introduced at its center. In view of the large discrepancies observed we have undertaken a program to calculate and measure the leakage multiplication from spherical Be shells as a function of thickness.

The method utilized is that of "Pulsed Spheres".[3] The Be spherical shells are pulsed at their centers with 14-MeV neutrons. These neutrons propagate outward through the spherical shells and are measured by time-of-flight techniques with NE213, Stilbene, and ^{6}Li glass scintillators positioned at 7.28 meters. We have measured the leakage spectra of high energy neutrons (> 1 MeV) with NE213 and Stilbene from spherical shells of Be of thicknesses 4.5, 14.2 and 19.9 cms. In all cases, the inner void radius was 8 cm. These Be thicknesses correspond to 0.8, 2.5, and 3.5 MFP (mean-free-path) for 14 MeV neutrons. Comparison with calculations employing ENDL-84[4] shows that excellent agreement is obtained for the leakage spectra above 1-MeV neutron energy. Table A-1 presents the measured and calculated integrals of the leakage spectra for the 3.5 MFP Be shell. The agreement using ENDL-84 cross sections is within the estimated accuracy of the measurements, typically ± 5%. Similar agreement is observed for the smaller spherical shells.

---

1 T. K. Basu et al., Nucl. Sci. & Eng., 70, 309 (1979).
2 V. R. Nargundkar et al., Fusion Technology, 6, 93 (1984).
3 C. Wong et al., UCRL-51144, Rev.I, Lawrence Livermore National Laboratory (1972).
4 S. T. Perkins et al., UCRL-91276, Lawrence Livermore National Laboratory (1984).

TABLE A-1. Measured and Calculated Integrals (using ENDL-84) for 3.5 MFP Be (in terms of the ratio of detector counts with shell in divided by detector counts with shell out).

	Stilbene		NE213	
	Calc.	Meas.	Calc.	Meas.
$1.0 \leq E_n \leq 15$ (MeV)	0.600	0.574	0.658	0.653
$3.75 \leq E_n \leq 15$ (MeV)	0.351	0.349	0.371	0.369

Monte-Carlo calculations showed that, for the thickest Be shell, up to 40% of the leakage neutrons were below 1 eV. For the low energy measurements with ^{6}Li glass, helium bags were inserted in the flight path to reduce the attenuation of thermal and epithermal neutrons. The pulse repetition rate was decreased to 100 Hertz because the flight time of a thermal neutron is 3 ms. Figure A-1 shows the measured and calculated time-of-arrival spectra for the 3.5 MFP Be shell. Measurements extended out to 9 ms and the burst width was 10 μs. Calculations employed ENDL-84 Be cross sections. Figure A-1 confirms the predicted copious emission of epithermal and thermal neutrons from the large Be shell. A comparison of the calculated and measured integrals of the spectra in Fig. A-1 shows that ENDL-84 overestimates the total measured counts by 15% between thermal and ∿2 MeV. The corresponding value for the 2.5 MFP Be shell is 5%. Folding in the results of the comparisons above 1 MeV, and estimating the accuracy of the detector efficiencies, we tentatively conclude that ENDL-84 overestimates the leakage multiplication by 13% for the 3.5 MFP Be, and by 5% for the 2.5 MFP Be.

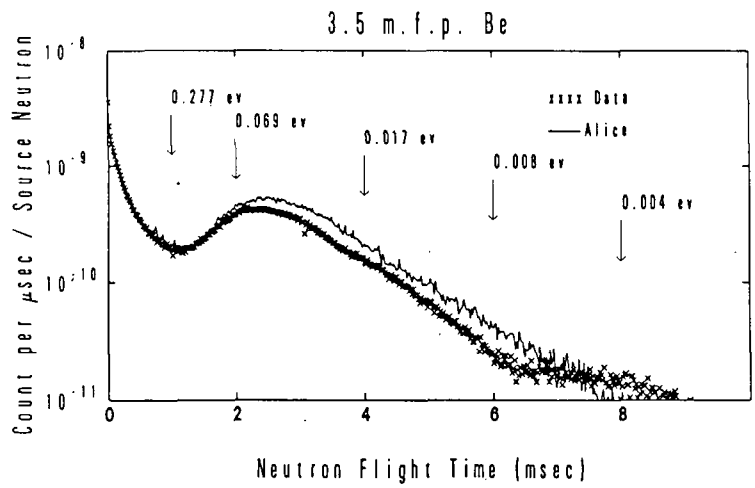

Fig. A-1. Measured and calculated time-of-arrival spectra for the 3.5 MFP Be shell.

2. Measurements of ^{6}Li and ^{7}Li Neutron-Induced Tritium Production Cross Sections at 15 MeV (Goldberg, Barber, Barry, Bonner, Fontanilla, Griffith, Haight, Nethaway, and Hudson)

Tritium production cross sections have been inferred from direct measurements of tritium generated in wafers of ^{6}LiH and ^{7}LiH under bombardment by 15 MeV neutrons produced at the Lawrence Livermore National Laboratory's RTNS-I facility. Sealed in a thin-walled Pb container, each hydride wafer was immersed in boiling Hg which first amalgamated the Pb and then dissociated the LiH. The hydrogen, acting as a carrier, was directed to an electronic counter and mixed carefully with methane. The counting procedure provided an accurate measure of tritium originally generated in each wafer. The TART Monte Carlo code was employed in the analysis of the data. The tritium production cross section for ^{6}Li exposed to 14.92 MeV neutrons is 32 ± 4 mb and that for ^{7}Li exposed to 14.94 MeV neutrons is 302 ± 15 mb.

3. Measurement of Fast Neutron Fission Yields (Nethaway, Momyer)

We irradiated ^{235}U, ^{238}U, and ^{239}Pu metal targets with fast neutrons from the FLATTOP Critical Assembly at the Los Alamos National Laboratory. FLATTOP is a natural-uranium-reflected ^{235}U or ^{239}Pu critical assembly which provides a neutron energy distribution in the central irradiation position which is slightly degraded from a pure fission-spectrum distribution. The uranium targets were irradiated in an oralloy core in FLATTOP, and the plutonium target in a plutonium core. The isotopic compositions of targets and cores were: ^{235}U (1.0% ^{234}U, 93.2% ^{235}U, 0.6% ^{236}U, and 5.2% ^{238}U), ^{238}U (0.18% ^{235}U and 99.82% ^{238}U), and ^{239}Pu (93.6% ^{239}Pu, 5.8% ^{240}Pu, and 0.6% ^{241}Pu). The targets weighed about four grams each, and were irradiated for four hours.

After the irradiations the target materials, which remained sealed in aluminum cans, were dissolved in closed systems so that the gaseous fission products could be collected for krypton and xenon analysis. Aliquots of the target solutions were taken for direct gamma-ray assay and for various chemical separations (rare-earths, cadmium, and antimony). The fission yields were measured relative to the yields of several well-known fission products (^{95}Zr, ^{99}Mo, ^{140}Ba, ^{144}Ce, and ^{147}Md).[5,6] Some of the measured fission yields are given in Table A-2. The yields have not been corrected for the isotopic impurities in the ^{235}U and ^{239}Pu targets.

---

5 B. F. Rider, General Electric Co. Report, NEDO-12154-3(C), October (1981).

6 D. R. Nethaway and G. W. Barton, Lawrence Livermore National Laboratory, UCRL-51458 (1973).

TABLE A-2. Fission yields measured for fast-neutron fission of ^{235}U, ^{238}U, and ^{239}Pu. The errors given do not include an uncertainty of about 3% in the number of fissions, or the uncertainty in the decay scheme.

Nuclide	Fission Yield (atoms/fission)		
	^{235}U	^{238}U	^{239}Pu
^{85}Kr	$(3.19 \pm 0.03) \times 10^{-3}$	$(1.66 \pm 0.04) \times 10^{-3}$	$(1.48 \pm 0.02) \times 10^{-3}$
$^{115}Cd^{g}$	$(3.19 \pm 0.06) \times 10^{-4}$	$(3.16 \pm 0.19) \times 10^{-4}$	$(6.76 \pm 0.17) \times 10^{-4}$
^{155}Eu	$(4.13 \pm 0.06) \times 10^{-4}$	$(1.15 \pm 0.02) \times 10^{-3}$	$(1.83 \pm 0.03) \times 10^{-3}$
^{156}Eu	$(2.11 \pm 0.02) \times 10^{-4}$	$(6.37 \pm 0.06) \times 10^{-4}$	$(1.38 \pm 0.01) \times 10^{-3}$
^{161}Tb	$(2.40 \pm 0.13) \times 10^{-6}$	$(9.55 \pm 0.47) \times 10^{-6}$	$(6.58 \pm 0.07) \times 10^{-5}$

4. Measurement of ^{238}U (t,X) Cross Sections

(Decman, Estep, Henry, Mann, Meyer, Ussery)

We have bombarded a ^{238}U target with 16-MeV tritons, and have determined the production cross sections for a number of nearby nuclei. The target was a self-supporting uranium foil 1.6 mg/cm^2, irradiated in two stages: 0.4 nA triton beam for 90 h, immediately followed by a 225 nA beam for 2 h. The short-lived ^{237}Pa was counted in-beam during the low current bombardment. The long-lived radioactivities were counted off-line following irradiation. Because of time elapsed between the end of irradiation and the first count, only the sum of the cross sections for ^{239}U and ^{239}Np was determined. Detectors were calibrated using a ^{152}Eu calibration source. In a separate experiment, the fission cross section was estimated by counting both fission products and scattered tritons in a solid state detector at 98° relative to the beam direction. The program DWUCK was used to calculate the cross section for these scattered tritons, and thus by ratio, the fission cross section. The measured cross sections are summarized in Table A-3.

TABLE A-3. Cross section for fission and isotope production for ^{238}U + t.

Residual Nucleus	Cross Section (mb)	Residual Nucleus	Cross Section (mb)
^{237}Pa	12.8 ± 2.1	$^{239}U + ^{239}Np$	~ 210
^{237}U	10.5 ± 1.8(a)	^{240}U	29 ± 3
^{238}Np	196 ± 21	^{240}Np	~ 3
Fission	650		

(a) Virtually all of the ^{237}U comes from ^{237}Pa decay.

5. Neutron Capture Cross Sections for $^{86,87}Sr$ at Stellar Temperatures (Bauer, Becker, Howe, and Mathews)

Neutron capture cross sections for ^{86}Sr and ^{87}Sr have been measured for incident energies from 100 eV to 1 MeV at the Livermore electron linac using the white source of neutrons and time-of-flight techniques. The capture events were recorded by detecting the prompt gamma-ray cascade with two C_6D_6 scintillators, and were normalized to standard gold cross sections (see Fig. A-2). The neutron flux was monitored in a ^6Li-glass scintillator and the reliability of the background subtraction was checked with absorbers in the neutron beam. Corrections to the data were applied for neutron multiple scattering and self-shielding, gamma-ray absorption, and for detector response. The Maxwellian average neutron capture cross sections have been calculated for stellar temperatures ranging from kT = 10 to 100 keV. Capture rates for some representative temperatures are given in Table A-4.

The capture cross sections of the two pure shielded s-process nuclei ^{86}Sr and ^{87}Sr are of importance for stellar nucleosynthesis of nuclei in the mass region near the N = 50 closed shell. Specifically, they are important in the study of the s-process branching through ^{85}Kr as a monitor of the neutron capture time scale, and also in the investigation of the ^{87}Rb-^{87}Sr chronometric pair as an independent measure of the age of the galaxy.

TABLE A-4. Maxwellian averaged cross sections of the measured isotopes as a function of the thermal energy kT (preliminary values).

measured isotope	calculated Maxwellian averaged capture cross sections (mb) at 10 keV	30 keV	100 keV
^{86}Sr	115 ± 20	64 ± 10	35 ± 5
^{87}Sr	185 ± 20	98 ± 10	45 ± 5

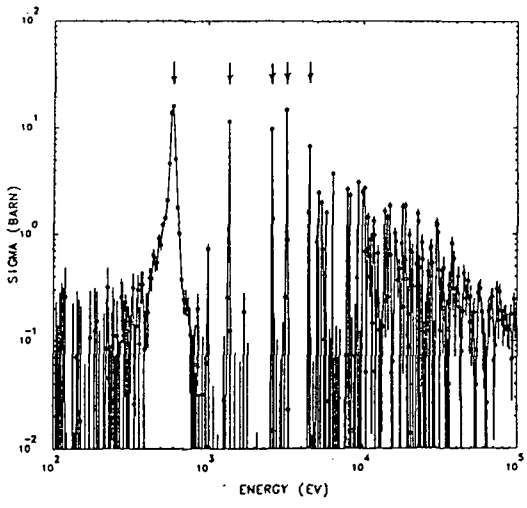

Fig. A-2. Measured capture cross section of ^{86}Sr, displaying strong resonances at 0.588, 1.370, 2.592, 3.247 and 4.496 keV.

6. Influence of Realistic Single Particle Spacings on Precompound Decay Spectra (Blann, Grimes,* Hansen, Komoto, Pohl, Scobel,** Trabandt,** and Wong)

We made (p,n) measurements on 23 targets[7] chosen to enhance the influence of single particle spacings on precompound decay spectra. These data are being interpreted in terms of one proton particle-one neutron hole residual state densities calculated with shell model single particle spacings rather than the more common equidistant spacing model. Nuclei involving the $g_{9/2}$ shell closure have been analyzed.[8] Nuclei involving the $f_{7/2}$ shell closure are presently being analyzed. In Fig. A-3 we show experimental angle integrated (p,n) spectra from $^{50,52,53}Cr$ targets compared with shell model based two-quasiparticle density calculations for spherical (Δ=0.00) and deformed (Δ=0.025) nuclei, using single particle energies due to Seeger-Howard[9] (S-H) and Seeger-Perisho[10] (S-P). The oscillator stiffnesses have been increased by 1/0.70, and BCS pairing strength of 0.75 MeV.

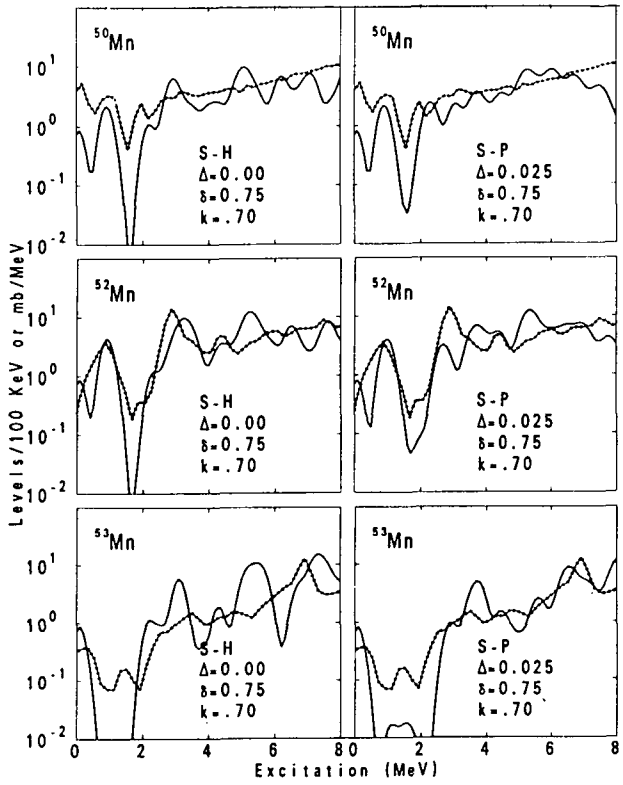

Fig. A-3. Experimental angle integrated (p,n) spectra from $^{50,52,53}Cr$ with 26 MeV incident protons, compared with (p) (n^{-1}) state densities calculated with realistic single particle levels. The connected open points represent the experimental spectra.

---

* Ohio University

** Hamburg University

7 W. Scobel, et al., LLNL Report No. UCID-20101 (1984) unpublished.

8 W. Scobel, et al., Phys. Rev. C30, 1480(1984).

9 P. A. Seeger and W. M. Howard, Nucl. Phys. A238, 491(1975).

10 P. A. Seeger and R. C. Perisho, LANL Report No. LA3751 (1967) unpublished.

7. Spontaneous Fissions from a Source of ^{260}Md
(Lougheed, Hulet, Wild, Dougan, Dupzyk, Henderson, Hahn)

We are measuring provisional mass and total kinetic energy (TKE) distributions of a spontaneous fission (SF) activity produced by bombarding a target of ^{254}Es with ^{18}O and ^{22}Ne ions. We collected recoiled transfer products from these bombardments on tantalum foils and transported them rapidly to an isotope separator. By isotope separation the fraction of mass 260 was collected on a thin aluminum foil and counted. This activity has a half-life of 30 ± 5 d and is believed to arise from previously unknown ^{260}Md, because all other isotopes of mass 260 are either known or are expected to have much shorter half-lives. Four possible sources of SF originate from this sample: direct SF decay of ^{260}Md, beta decay to short-lived ^{260}No, electron capture (EC) decay to very short-lived ^{260}Fm, and alpha decay leading to ^{256}Es and ^{256}Fm. The end products of the last three decay modes are SF emitters. One of our fission detectors also detects beta particles; when a SF event occurs, we record the times of occurrence of the five previous beta events in an effort to observe beta decay to ^{260}No. However, we have been unable to observe any difference between the interval from the last beta particle to the SF event and the intervals between the beta particle events, which are expected to be random. This suggests that beta decay is not a significant mode of decay of ^{260}Md. Figure A-4 shows the TKE and mass distributions we have obtained. The high-energy peak of the TKE distribution, centered at about 235 MeV, is associated with the narrow central peak of the mass distribution. It is possible that these high-energy SF events arise from the decay of ^{260}Fm, the EC-decay daughter, and are similar to those from the SF decay of ^{258}Fm and ^{259}Fm. We are continuing to analyze the decay of ^{260}Md.

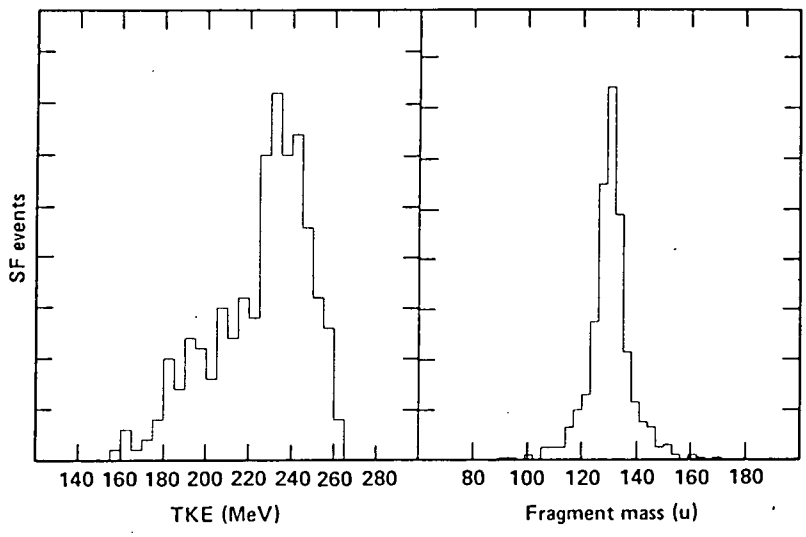

Fig. A-4. TKE and mass distributions. The data were obtained from ∿60 d of coincident fission-fragment counting.

8. Excitation Function Measurements from Proton and Deuteron Bombardment of Natural Ti (West and Lanier)

Excitation functions were measured by the activation method for the production of ^{48}V(∿16d) by protons and deuterons on targets of natural Ti. The measurements were made for a projectile energy range between ∿1.5 and 26 MeV (protons: ∿4.5 to 25 MeV; deuterons: ∿1.5 to 20 MeV). For measurements near threshold, the targets were thin 1 inch diameter evaporated deposits (∿3.6 mg/cm^2) mounted on thick (∿0.5 cm) aluminum disks. At higher energies, where the cross section is slowly varying, a series of foil stacks was irradiated. The stacks contained from 2 to 5, 1 inch diameter circular foils (∿11 mg/cm^2) and each foil was separated by an appropriate thickness of aluminum degrader foil. Yields of ^{48}V were determined from the activated foils by γ-ray counting on well-calibrated (accuracy: ± 2%) Ge (Li) detector systems. To check the accuracy and reproducibility of our charge collection arrangement, we remeasured the well-known $^{65}Cu(p,n)$ cross section at several energies and found excellent agreement between our results and published values.[11] Allowing for unknown systematic errors, we believe that individual cross sections are accurate to ± 5%.

The results of our measurements are summarized in Fig. A-5. Although the targets were natural Ti, approximate individual excitation functions for the production of ^{48}V were obtained by dividing the raw data by the known isotopic abundances. The details are noted in the figure caption.[12] For future studies we plan complimentary measurements with isotopically enriched ^{47}, ^{48}, ^{49}Ti targets.

---

[11] R. Colle, R. Kishore, and J. B. Cumming, Phys. Rev. C, 9, 1819 (1974).

[12] Marshall Blann, private communication, statistical model code ALICE Lawrence Livermore National Laboratory, Livermore, CA, (1984).

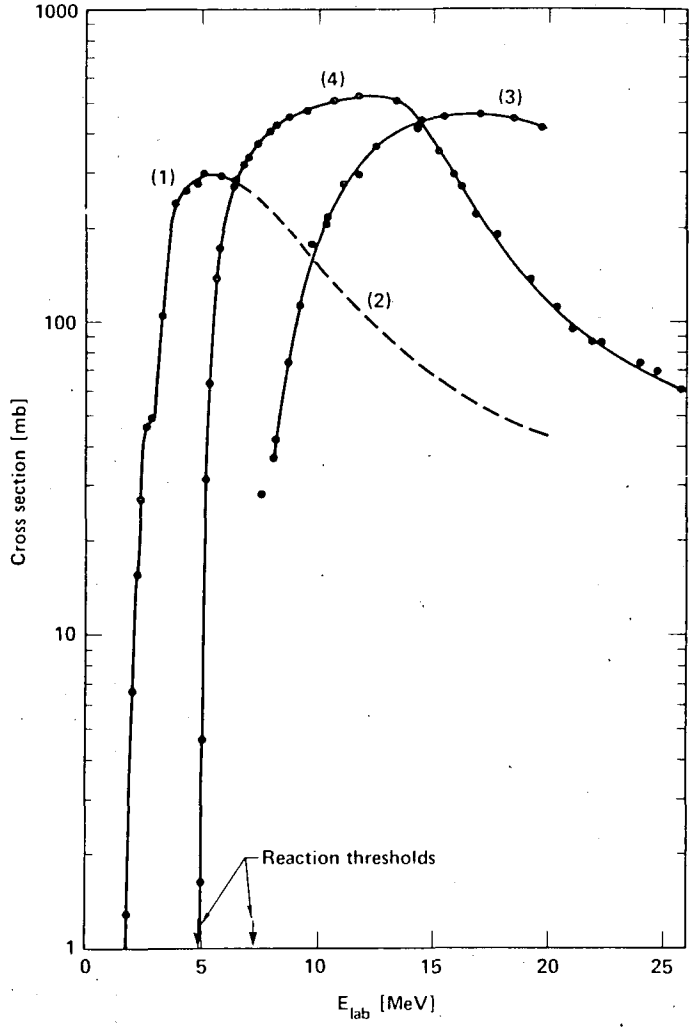

Fig. A-5. Excitation functions from p and d bombardment of natural Ti foils: (1) Ti $(d,xn)^{48}V/0.0728 = {}^{47}Ti(d,n)^{48}V$, (2) extrapolated $^{47}Ti(d,n)^{48}V$ cross sections based on ALICE calculations, (3) Ti $(d,xn)\ ^{48}V/0.7394 = {}^{48}Ti(d,2n)^{48}V$ + contribution from ^{47}Ti, (4) $Ti(p,xn)^{48}V/0.7394 = {}^{48}Ti(p,n)\ ^{48}V$ + contribution from ^{49}Ti beginning at about 15 MeV.

B. NUCLEAR DATA APPLICATIONS - CALCULATIONS

1. Using Modeled Discrete Levels (Gardner, Gardner, and Hoff)

We have continued our study of isomer ratio calculations for the reactions: $^{175}Lu(n,\gamma)^{176m,g}Lu$, $^{175}Lu(n,2n)^{174,g}Lu$, $^{237}Np(n,2n)^{236m,g}Np$, $^{241}Am(n,\gamma)^{242m,g}Am$, and $^{243}Am(n,\gamma)^{244m,g}Am$. All of the cross-section calculations were made with our version of the STAPRE statistical model code,[1] with no fission competition. Below about 1.5 MeV in each deformed, odd-odd product nucleus, we replace the level density expression with a modeled discrete level set consisting of several hundred levels.[2]

The gamma-ray cascades leading to the ground-state and isomeric products are modeled as follows. The continuum bins are depopulated according to our E1 and M2 strength function systematics, where the E1 strength function has an energy-dependent Breit-Wigner line shape and the M2 strength function is a constant.[3] The depopulation of the discrete levels proceeds as described in Ref. 2. We have found that the use, among the discrete levels, of the same E1 and M1 strength functions as described for the continuum led to calculated isomer ratios for the $^{175}Lu(n,\gamma)$ and $^{237}Np(n,2n)$ reactions that were equal to those obtained using a constant E1/M1 ratio of 0.167.

The calculated g/m ratios for the $^{237}Np(n,2n)$ reaction are shown in Fig. B-1a, compared with a 14 MeV measurement.[4] Sensitivity studies of the computed isomer ratio relative to the number of discrete levels describing ^{236}Np also were made. Set A, consisting of 998 levels and 94 rotational bands, was truncated several times just below a new band head to yield Sets B-D. The distribution of the K quantum numbers, P(K), associated with Sets A-D are shown in Fig. B-1b. Although the P(K), of Sets A and B are different, each has a sufficiently representative sampling of K values to yield similar isomer ratios. Sets C and D do not sample all of the K values, leading to isomer ratios that are too high.

In Fig. B-2a we show our calculated m/g ratios for the $^{241}Am(n,\gamma)$ and $^{243}Am(n,\gamma)$ reactions compared with measurements.[5,6] We also computed isomer ratios for s-wave neutrons leading to the 2^- and 3^- resonances for comparison with the thermal and epithermal data. Other calculational results from Refs. 5 and 6 are shown too. For each reaction,

---

1 M. Uhl, Acta Phys. Austriaca 31, 241 (1970).
2 R. W. Hoff, et al., "Level-Structure Modeling of Odd-Odd Deformed Nuclei," UCAR 10062-83/1 (1983), p. 218.
3 D. G. Gardner, ANL-83-4 (1983), p. 67.
4 W. A. Myers, et al., J. Inorg. Nucl. Chem. 37, 637 (1975).
5 K. Wisshak, et al., Nucl. Sci. Eng. 81, 396 (1982).
6 F. M. Mann and R. E. Schenter, Nucl. Sci. Eng. 63, 242 (1977).

our s-wave 3^- resonance result agrees well with data. Fission competition should not have a significant effect at thermal energies for target ^{241}Am and throughout the neutron energy range shown for target ^{243}Am. However, the lack of fission competition in our calculations may be the reason why our ^{241}Am isomer ratio is not in good agreement with the 30-keV data. For the ^{241}Am(n,γ) reaction, our isomer ratio for the 3^- resonance is larger than that for the 2^- resonance, in agreement with the Ref. 5 calculation. In Fig. B-2b we show the spin distributions among the discrete levels that we calculate after the gamma-ray cascade from the continuum for both the 2^- or 3^- resonance cases. These distributions show why the high spin state is favored by the 3^- resonance and why we obtain the relative order of the isomer ratios for each case.

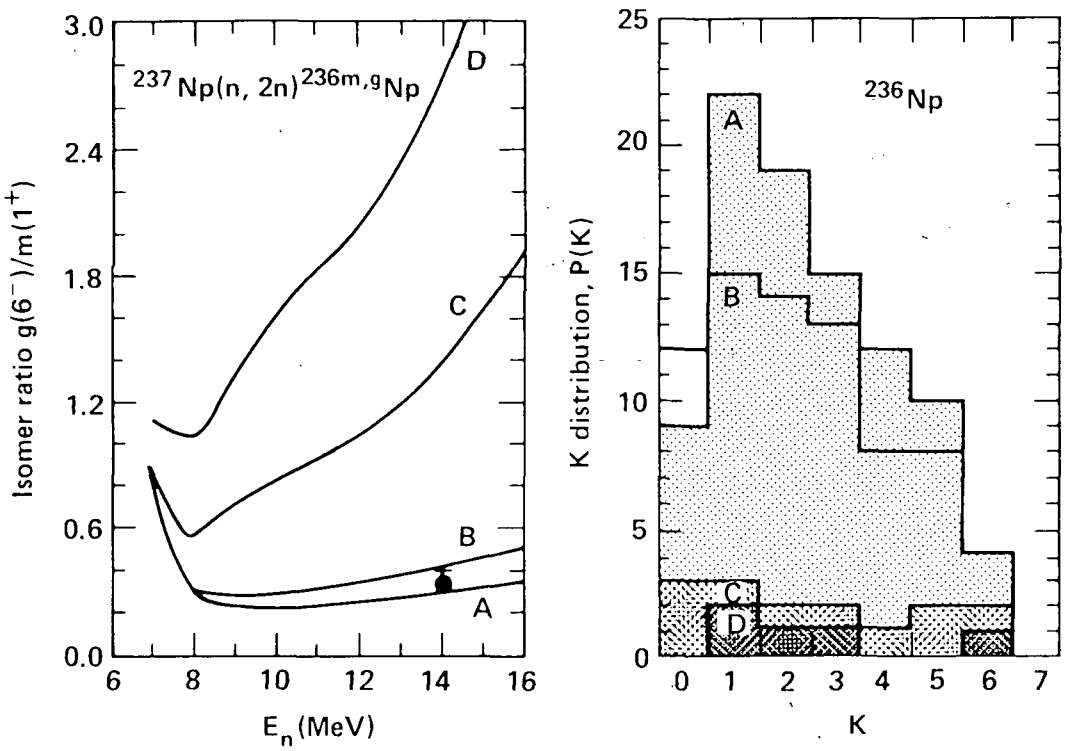

Fig. B-1 a) Calculated ^{237}Np(n,2n) g/m ratios vs E_n using ^{236}Np level Sets A-D, compared with data (●).[4] b) The P(K) for Sets A-D.

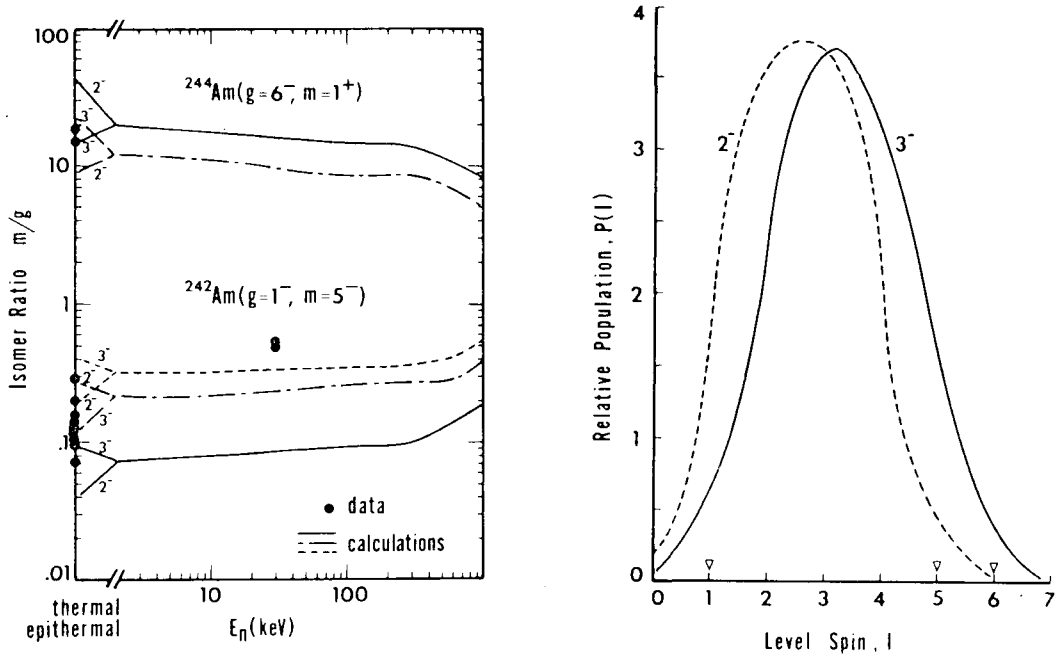

Fig. B-2 a) Calculated ^{241,243}Am (n,γ) m/g ratios vs E_n compared with data [5,6] (——— present work, ----- Ref. 5, - —— Ref. 6) b) Spin distributions among levels calculated after γ-ray cascade from continuum for 2^- and 3^- resonance cases.

2. Modeling Level Structures of Odd-Odd Deformed Nuclei (Hoff, Kern, Piepenbring, and Boisson)

A technique for modeling quasiparticle excitation energies and rotational parameters in odd-odd deformed nuclei has been applied to actinide species where new experimental data have been obtained by use of neutron-capture gamma-ray spectroscopy. The input parameters required for the calculation were derived from empirical data on single-particle excitations in neighboring odd-mass nuclei. Calculated configuration-specific values for the Gallagher-Moszkowski splittings were used. Calculated and experimental level structures for ^{238}Np, ^{244}Am, and ^{250}Bk are compared, as well as those for several nuclei in the rare-earth region. The agreement for the actinide species is excellent, with bandhead energies deviating 22 keV and rotational parameters 5%, on the average. Corresponding average deviations for five rare-earth nuclei are 47 keV and 7%.

TABLE B-1. Odd-odd nuclei in actinide and rare-earth regions: Comparison of experimental and calculated bandhead energies (E), rotational parameters (A), and G-M splittings (E_{GM}).

Nucleus	Number of bands	Energy range (keV)	$\langle E_{exp}-E_{calc}\rangle$ (keV)	$\langle A_{exp}-A_{calc}\rangle$ (keV)	E_{GM} exp/calc
^{238}Np	9	0 - 345	29	0.14 (3.2%)	1.18,0.87
^{244}Am	16	0 - 680	19	0.28 (7.4%)	1.15,0.14,0.96
^{250}Bk	14	0 - 570	17	0.20 (4.7%)	1.11,0.96,2.87, 1.39,1.32
^{160}Tb	8	0 - 380	41	0.61 (8.1%)	1.03,1.07,1.13
^{166}Ho	10	0 - 560	47	0.74 (8.7%)	0.80,1.08,1.31
^{170}Tm	5	0 - 450	63	0.46 (5.2%)	2.04,0.98
^{176}Lu	12	0 - 840	58	1.0 (9.2%)	1.14,0.48,1.01, 0.91,0.39
^{182}Ta	7	0 - 270	24	0.47 (3.9%)	0.94,0.97,1.14

3. Test of a Phenomenological Model of Odd-Odd Deformed Nuclei: An ARC Study of ^{176}Lu (Hoff, Casten,* Bergoffen,* Warner*)

An average resonance capture (ARC) study leading to a complete set of $J^{\pi}=2^{-}-5^{-}$ levels in the odd-odd nucleus ^{176}Lu is reported. A phenomenological model for odd-odd nuclei, which is based on the empirical structure of the neighboring odd mass nuclei and which incorporates the effects of certain neutron-proton interactions, is utilized to interpret the data. Cumulative level-number histograms, obtained from this model, are in generally good agreement with the empirical results up to 1100 keV of excitation. The comparison involves a total of 40 predicted rotational bands (see Fig. B-3). Some specific discrepancies arise for 3^{-}, 4^{-} states in a model energy interval near E_x=700 keV, because of an anomalously large predicted Gallagher-Moszkowski splitting for the $1/2^{+}$[411]p; $7/2^{-}$[514]n two-quasiparticle configuration and because of low predicted energies for states involving the $7/2^{+}$[404] proton orbit.

---

* Brookhaven National Laboratory, Upton, NY 11973

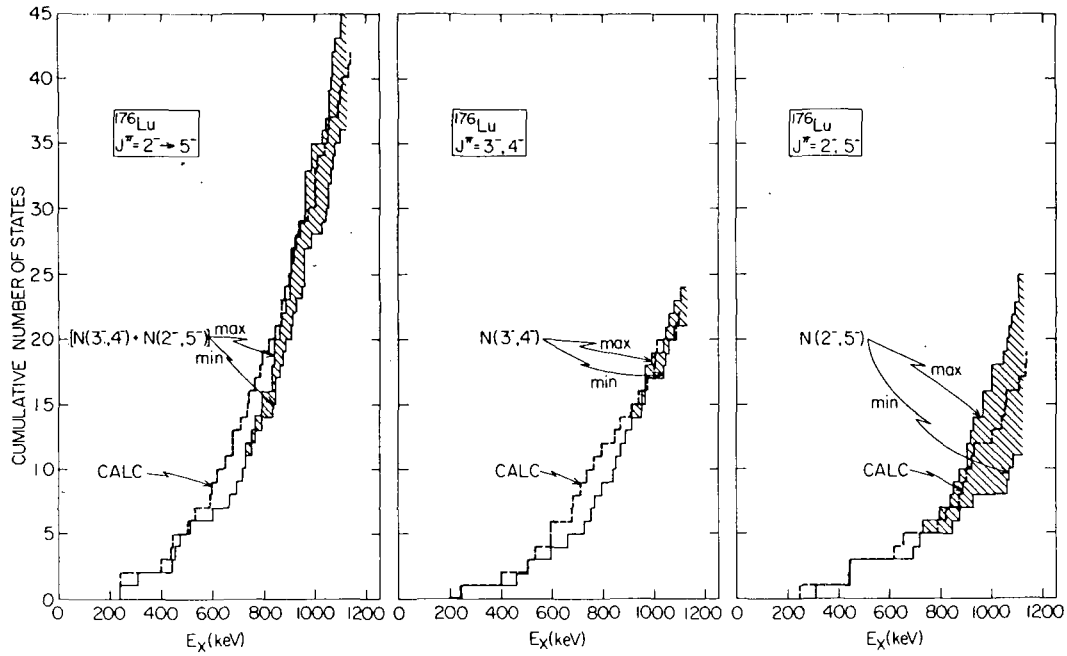

Fig. B-3. Cumulative level number histograms for all states in ^{176}Lu with spins $2^-,3^-,4^-,5^-$ (left), $3^-,4^-$ (middle) and $2^-,5^-$ (right). The cross hatched region shows the range of the maximum and minimum numbers of states allowed by the ARC data. The dashed lines show the results of the model calculations.

4. Absolute Dipole Gamma-ray Strength Functions for ^{176}Lu (Gardner, Gardner, Hoff)

We have derived absolute dipole strength-function information for ^{176}Lu from an average resonance capture study of ^{175}Lu with 2 keV neutrons and from neutron capture cross section measurements with neutrons from 30 keV to about 1 MeV. We found that we needed to increase our previous estimate of the relative M1/E1 strengths near 5 MeV by a factor of 3 and to revise downward the absolute magnitude of our E1 strength function. We accomplished the latter, while still maintaining continuity with the photonuclear data, by adjusting the one free parameter (E_x) in our line shape. The present E1 and M1 strengths now seem correct both near the neutron separation energy and also around 1 MeV.

In Fig. B-4 we show the newly derived E1 and M1 strength functions for ^{176}Lu, as a function of the γ-ray energy (the full curves). For comparison, we also show the results predicted by our original systematics[7] (the dashed curves) and from a Lorentz E1 strength function (the dotted curve). The arrows indicate the E_x value of 11 MeV determined in the present study and the 5 MeV value used previously.

In the E1 case, it is convenient to compare with experiment the function $S_{E1} = f_{E1}(E_\gamma)A^{-8/3} E_\gamma^{-2}$. The McCullagh et al.,[8] compilation of f_{E1} values expressed in this form is plotted in Fig. B-5. For ^{176}Lu at $E_\gamma = 5$ MeV, our new E1 strength function has a value of 5.1×10^{-8} MeV^{-3}, which converts to $S_{E1} = 2.1 \times 10^{15}$. The shaded rectangle in Fig. B-5 shows this value, along with the estimated error limits of ± 40%. The set of curves in the figure were predicted by our original systematics.

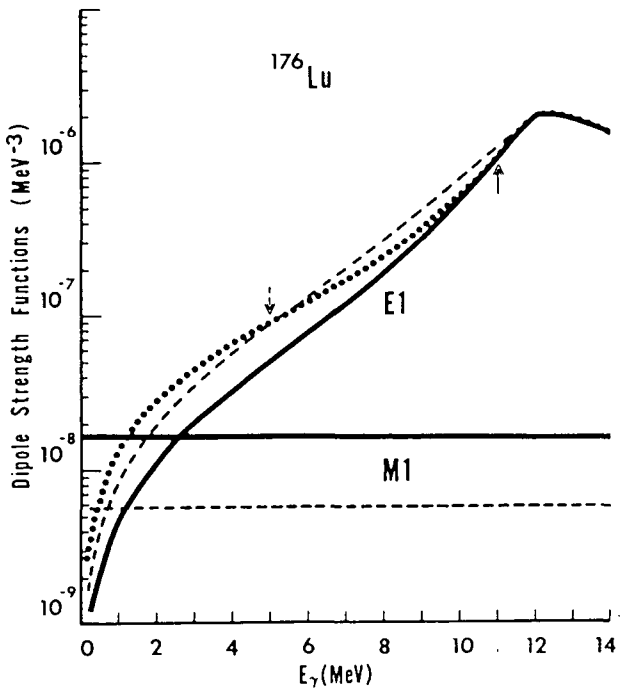

Fig. B-4. Absolute E1 and M1 strength functions for the ^{176}Lu nucleus.

---

7 D. G. Gardner, Proc. NEANDC/NEACRP Specialist's Meeting on Fast-Neutron Capture Cross Sections, Argonne, IL, ANL-83-4 (1983), p.67.

8 C. M. McCullagh, M. L. Stelts and R. E. Chrien, Phys. Rev. C23. 1394 (1981).

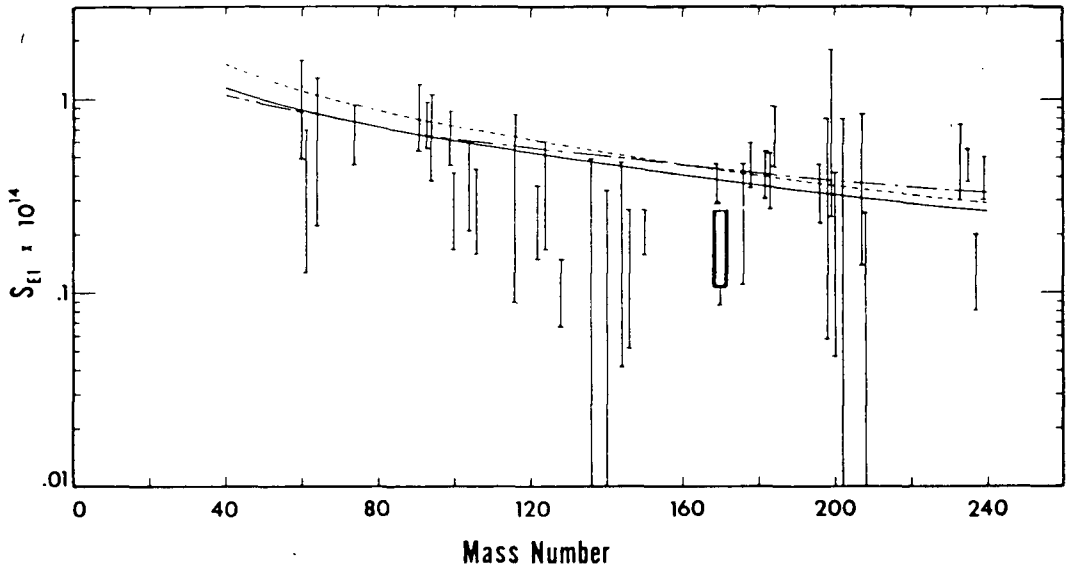

Fig. B-5. Comparison of E1 strength function value derived in this work for ^{176}Lu (shaded rectangle includes error estimate with the data from the compilation of McCullagh et al.[8] The curves are S_{E1} values predicted by our systematics[7] for γ-ray energies of 3, 5 and 7 MeV.

5. Gamow-Teller Matrix Elements from the $^{11}B(p,n)^{11}C$ Reaction at E_p = 26 MeV (Grimes,* Anderson, Davis, Howell, Wong, Carpenter,† Carr,† and Petrovich†)

The $^{11}B(p,n)^{11}C$ reaction has been investigated at 1 MeV intervals for proton bombarding energies in the E_p = 16-26 MeV range. In the experiment, final states in ^{11}C up to $E_x \simeq 10$ MeV were clearly identified and differential cross sections were extracted for the first four levels in ^{11}C. The E_p = 26 MeV data are examined in microscopic DWA calculations using the wave functions of Cohen and Kurath[9] to describe the states in ^{11}B and ^{11}C and using the G matrix interaction of Bertsch et al.[10] for the effective nucleon-nucleon interaction. Gamow-Teller matrix elements for transitions to excited states in ^{11}C are extracted on the basis of these calculations, thus extending the information on GT matrix elements in the mass 11 systems beyond the ground state matrix element known from β-decay. Throughout, the results are contrasted with existing information from electromagnetic studies of ^{11}B.[11-13] It is concluded that the Cohen-Kurath model places too much GT strength in the low lying states of the mass 11 systems and not enough strength at higher excitation energies. In addition this model underestimates the net contribution to M1 matrix elements from the isoscalar spin and current and isovector current parts of the M1 operator. The extracted GT matrix elements for the first four levels in ^{11}C are in excellent agreement with those deduced from (p,n) measurements at E_p = 160 MeV.[14]

---

* Physics Dept., Ohio University, Athens, Ohio 45701
† Physics Dept., Florida State University, Tallahassee, Florida 32306

9 S. Cohen and D. Kurath, Nucl. Phys. 73, 1 (1965); A101, 1 (1967).
10 G. Bertsch et al., Nucl. Phys. A284, 399 (1977).
11 T. Stovall et al., Nucl. Phys. 86, 225 (1966).
12 R. E. Rand et al., Phys. Rev. 144, 859 (1966).
13 P. T. Kan et al., Phys. Rev. C11 323 (1975)
14 T. N. Taddeucci, private communication.

6. K-Distribution for Neutron Fission of ^{232}Th (Becker and Bauer)

The $^{232}Th(n,f)$ fission fragment angular distributions have been measured for incident energies from 0.7 to 10 MeV using the white source of neutrons produced at the 100-MeV LLNL Electron Linear Accelerator Facility. Preliminary angular distribution data were presented in last year's report. In our recent analysis, the fragment angular distributions were binned in intervals of 40 keV, and fit using least-squares techniques to the following expression:

$$W(\Theta) = \sum_{K=\frac{1}{2},\frac{3}{2},\frac{5}{2}} A_K \sum_{J,\Pi} B^{\Pi}_{KJ} W_{KJ}(\Theta),$$

in order to obtain A_K, the distribution of K values among the transition states. The $W_{KJ}(\Theta)$ represent the weighted squared modulus of the wave-functions of the symmetric top, and the B^{Π}_{KJ} are obtained from a Hauser-Feshbach calculation of the partial fission cross-sections as described in Bjørnholm and Lynn.[15] The results for incident neutron energy $0.7 \leq E_n$ (MeV) ≤ 4.5 are presented in Fig. B-6.

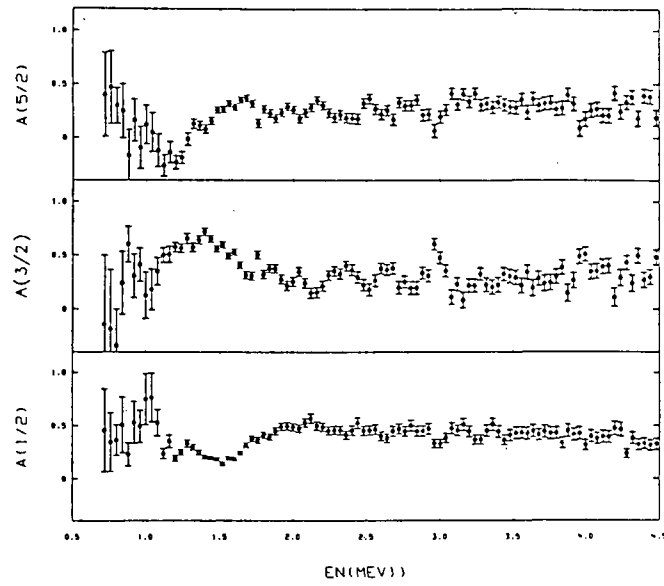

Fig. B-6. K-distribution in the transition nucleus ^{233}Th as a function of E_n. Note that for every E_n, $\sum_K A_K = 1.0$.

---

[15] S. Bjørnholm and J. E. Lynn, Rev. Mod. Phys. 52, 725 (1980).

7. A Shell Model Study of the $^{71}Ga(\nu,e^-)\ ^{71}Ge$ Neutrino Detector (Mathews, Bloom, and Fuller*)

Gamow-Teller allowed neutrino-capture transitions between the ground-state of ^{71}Ga and accessible low-lying states in ^{71}Ge are calculated in a model space of the 2p and 1f shells. The total (p,n) Gamow-Teller strength function is also calculated (see Fig. B-7). The effects of model-space truncation are systematically investigated, and comparisons are made between calculated and experimental energies and spectroscopic factors for states in ^{71}Ga and ^{71}Ge as well as the E2 transition rate from the first excited state in ^{71}Ge. We find that the possible contributions to the count rate in a ^{71}Ga neutrino detector from transitions to excited states in ^{71}Ge are weaker than recent (p,n) measurements at 35 MeV seem to imply. However, these results, together with calculations of similar transitions in neighboring nuclei, indicate that the neutrino capture rate to the first excited state in ^{71}Ge is probably not as small as the value estimated on the basis of the systematics of similar transitions in this region.

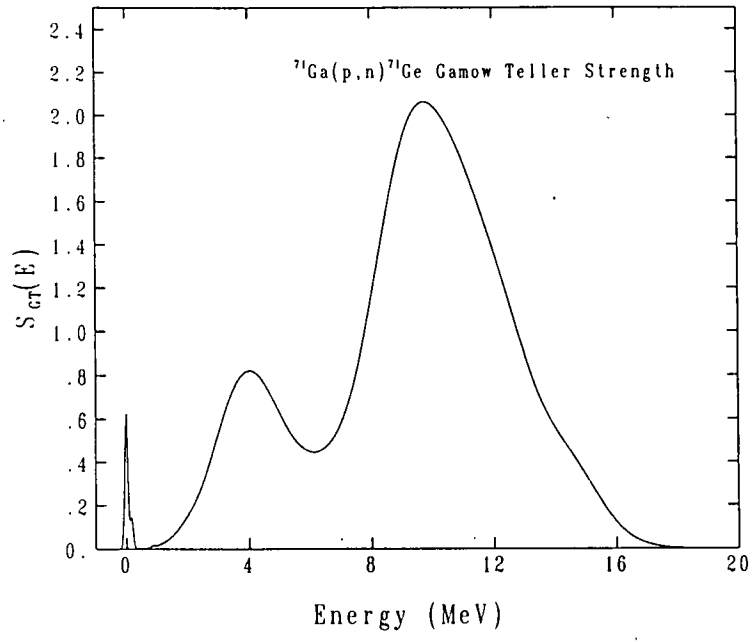

Fig. B-7. Gamow-Teller strength function for $^{71}Ga(p,n)^{71}Ge$.

---

* University of California, Santa Cruz

8. Extension of Microscopic Models for Neutron and Proton Scattering to Inelastic-Scattering and Charge-Exchange Reactions (Dietrich, Petrovich,* Finlay,** and Mellema**)

Results of a systematic study reported over the last two years have shown that a microscopic folding model yields reasonable results for elastic nucleon-scattering differential cross sections and neutron total cross sections in an energy range of roughly 7 to 50 MeV. The physical input to these calculations is the nuclear density and a complex, energy- and density-dependent effective interaction; we have tested three interactions derived from free nucleon-nucleon scattering via many-body theory.[16-18] The transition potentials for a number of other types of reactions, including inelastic scattering, (p,n) reactions to the isobaric-analog state, and radiative nucleon capture through giant multipole resonances, may be calculated in the same framework by replacing the nuclear density by the appropriate transition density. We have begun a study to determine whether a unified treatment of these reactions is successful, in which the same effective interaction is used for both the transition potentials and the distorting potentials for the incoming and outgoing waves.

A detailed summary of results obtained up to the present may be found in Ref. 19. Calculations have been made for the ^{208}Pb(p,n) isobaric-analog reaction, excitation of the first 2+ states in ^{54,56}Fe, and the first 3^- states in ^{208}Pb and ^{16}O. It is found that damping of the scattering wave functions in the nuclear interior due to nonlocality (the Perey effect) is significant and can reduce cross sections by 20 to 30%. When this effect is taken into account, the results for inelastic scattering are reasonably well reproduced. Problems remain with the (p,n) charge exchange reaction, which may reflect a deficiency in the strength of the isovector part of the effective interaction; for example, the interaction based on Ref. 16 underestimates the ^{208}Pb(p,n) cross section by a factor of four, even though the shape of the angular distribution is acceptable.

---

* Florida State University, Tallahassee, FL 32306

** Ohio University, Athens, OH 45701

16 J. P. Jeukenne, A. Lejeune, and C. Mahaux, Phys. Rev. C16, 80 (1977).

17 F. A. Brieva and J. R. Rook, Nucl. Phys. A291, 299, 317 (1977).

18 N. Yamaguchi, S. Nagata, and T. Matsuda, Prog. Theor. Phys. (Japan) 70, 459 (1983).

19 F. S. Dietrich and F. Petrovich, in Neutron-Nucleus Collisions -- A Probe of Nuclear Structure, J. Rapaport et al., ed., AIP Conference Proceedings No. 124, p. 90 (1985).

C. NUCLEAR DATA APPLICATIONS - EVALUATIONS

1. A Reevaluation of the $^{9}Be(n,2n)$ Reaction (Perkins, Plechaty and Howerton)

Using a Monte Carlo technique and recent double-differential measurements, a new evaluation for the $^{9}Be(n,2n)$ reaction has been done. The secondary neutrons are represented as doubly-differential in angle and energy.

The new evaluation is currently being tested by comparison of calculated and experimental leakage spectra from 2.5 and 3.5 MFP ^{9}Be pulsed spheres as discussed elsewhere in this report. It has also been tested by calculating the multiplication constant (k_{eff}) for 16 just-critical assemblies, reflected by ^{9}Be with thicknesses ranging from 1.27 to 20.27 cm. In all cases the calculated k_{eff} value agreed with experiment within the calculational and experimental uncertainties.

A. NUCLEAR DATA MEASUREMENTS

1. Low Energy Fusion Cross Sections (N. Jarmie and R. E. Brown)

The goal of this project is to determine cross sections for interactions among the hydrogen isotopes in the bombarding energy range 10-120 keV. Such cross sections are fundamental to the operation of future controlled fusion reactors. We have constructed a system, the low-energy fusion cross-section (LEFCS) facility, in order to make these measurements.

Our work on the D(t,α)n reaction has been completed and published in Phys. Rev. C29, 2031 (1984). Final analysis of the data for the D+D reactions is in progress. There we are finding reasonably good agreement with other data and small but systematic differences with Hale's unified, mass-4, R-matrix analysis. These data are considerably more accurate (~1.5% absolute) than most previous results and will require some adjustments to be made in the R-matrix fit.

We have now completed our measurements of the cross section for the T(t,α)nn reaction using tritium gas with a 0.5% deuterium impurity. These measurements were significantly more difficult to make than our previous ones, both because of the necessity to flow a radioactive gas through our windowless, cryogenically pumped gas target and because of the three-body nature of the final state. The three-body final state results in the detected α particles being spread over a continuum of energies; consequently, it is more difficult to account for the neutron background in the detectors than for reactions whose yield is confined to a narrow peak.

We have obtained T(t,α)nn data at triton bombarding energies of 115, 105, 90, 75, 60, 45, and 30 keV. A preliminary analysis indicates that the astrophysical S function for this reaction is reasonably constant as a function of bombarding energy, more so than for the D+T and D+D reactions studied earlier. Our data also appear to lie within about 10% of an earlier R matrix analysis by Hale that used data of much lower accuracy than we expect ours to turn out to be. In the low-energy part of our range, we disagree strongly with several previously published data sets that indicate a rather sharply rising S function as the energy decreases (see Fig. A-1).

In extracting the cross section for the T(t,α)nn reaction from the raw data, we need to extrapolate the α-particle spectrum to zero energy through the region of detector noise, and we need to interpolate across the D(t,α)n peak, which occurs near the high-energy limit of the T(t,α)nn α-particle continuum. For our final analysis, we plan to develop a reaction model to aid in these extrapolations and interpolations. Even though there is only a 0.5% deuterium contamination in our present target gas, the D(t,α)n yield is considerable, because its cross section is several hundred times that of the T(t,α)nn reaction. This fact causes the D(t,α)n peak in most instances to obscure the expected structure at the high-energy end of the T(t,α)nn spectrum caused by the nn final-state interaction. We are currently

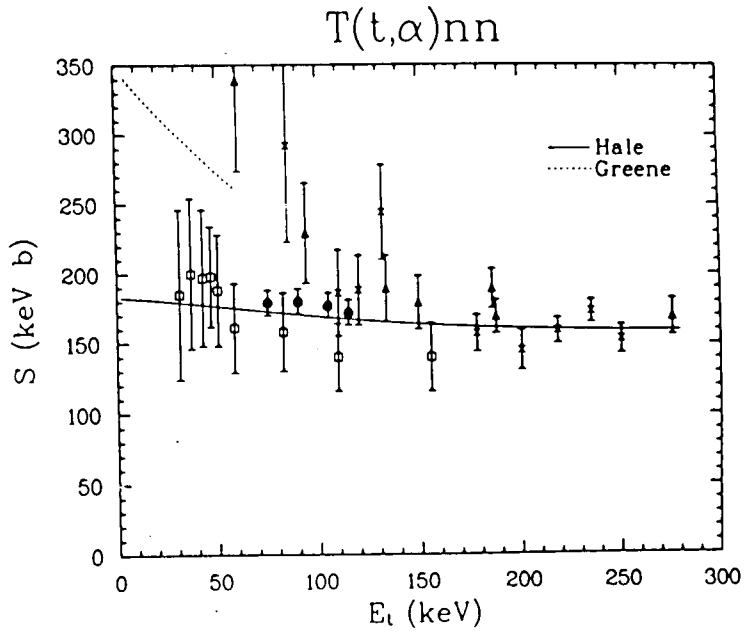

Fig. A-1. Integrated S functions for the T(t,α)nn reaction. Preliminary LEFCS data in the bombarding energy range of 75 to 115 keV are shown as black circles with 5% absolute errors. Various measurements by others are shown for comparison. The solid line is a Los Alamos R-matrix prediction, and the dashed curve is from a widely used compilation by S. L. Greene.

investigating the possibility of obtaining some tritium gas with a significantly lower deuterium contamination in order to study better that spectral region.

Our next experimental work with the LEFCS system will be to investigate several of the possible capture-gamma reactions, such as $D(t,\gamma)^5He$, which may be important as plasma diagnostics. We also plan to make some measurements of the $D(^3He,p)^4He$ reaction.

2. Double Differential Neutron Emission Cross Sections of ^{10}B and ^{11}B at 6, 10 and 14 MeV and of ^6Li, ^7Li and ^{12}C at 14 MeV

(M. Drosg, P. W. Lisowski, R. A. Hardekopf, D. M. Drake, and K. Treitl)

Using the time-of-flight technique about 100 neutron emission spectra were measured at angles between 20 and 145° in the laboratory system with 6 and 10 MeV neutrons from the $^1H(t,n)^3He$ source reaction and with 14.1 MeV neutrons from the $^3H(d,n)^4He$ reaction. When compared with the d-d reaction, which is often used for measurements of the type, the specific neutron yield of the $^1H(t,n)^3He$ source is a factor of 30 larger at 6 MeV and a factor

of 10 larger at 10 MeV. In addition, it is intrinsically monoenergetic up to a neutron energy of 17.6 MeV so that this source is by far the best choice for measuring neutron continua. The measurements at 14.1 MeV were done with the sample (and the detector) at 90° with regard to the beam direction. In this case the scattering angle was changed by rotating the sample around the beam axis rather than moving the detector around the sample. Although the samples were rather small (typically 1 mole of highly enriched material) the uncertainty of the multiple scattering correction, which arises mainly from the data base, generally determines the overall uncertainty. The worst case in this regard is ^{11}B where the input library (based on ENDF/B-IV) appears to be very unrealistic.

3. Fast Neutron Capure with a White Neutron Source (S. A. Wender and G. F. Auchampaugh)

A system has been developed at the Los Alamos National Labotoratory to measure gamma-rays following fast neutron reactions. The netron beam is produced by bombarding a thick tantalum target with the 800 MeV proton beam from the LAMPF accelerator. Incident neutron energies, from 1 to over 200 MeV, are determined by their times of flight over a 7.6-m flight path. The gamma-rays are detected in five 7.6 x 7.6-cm cylindrical bismuth germanate (BGO) detectors which span an angular range from 45 to 145° in the reaction plane. With this system it is possible to simultaneously measure the cross section and angular distribution of gamma-rays as a function of neutron energy. The results for the cross section of the $^{12}C(n,n'\gamma=4.44$ MeV) reaction at 90 and 125° show good agreement with previous measurements, while the complete angular distributions show the need for a large a_4 coefficient which was not previously observed. Preliminary results for the $^{12}C(n,n'\gamma=15.1$ MeV) reaction have also been obtained. The data obtained for the $^{40}Ca(n,\gamma_0)$ reaction in the region of the giant dipole resonance demonstrate the unique capabilities of this system.

4. (p,n) Cross Sections for Nuclear Data Needs (M. M. Meier, G. J. Russell, H. Robinson, R. Whitaker, G. L. Morgan, D. Holtkamp, W. Amian, and N. Paul)

Cross sections for targets of C, Al, Ni, W, Pb and depleted U (p,n) have been measured at bombarding energies of 800 and 318 MeV. Additionally, at 318 MeV, data were obtained for Be and Ta. The data are in the final stages of analysis and will be presented at the International Conference on Nuclear Data for Basic and Applied Science, May 1985. The abstract follows.

Thin Target (p,n) Cross Sections at 318 and 800 MeV.
M. Meier, D. Holtkamp, G. Morgan, H. Robinson, G. Russell and R. Whitaker, Los Alamos National Laboratory and W. Amain and N. Paul, KFA-Jülich.

Neutron yields from proton bombardment of elemental C, Al, Ni, W, Pb and depleted U have been obtained at

bombarding energies of 318 and 800 MeV. Additionally, at 318 MeV, data were obtained for Be and Ta. The data were obtained at angles/flight-paths of 7-deg/30-m, 15-deg/30-m and 30-deg/40m and were collected in two parameter histograms of time-of-flight and pulse-height in order to select detector biases in the analysis and to permit comparison of calculated and experimental pulse height spectra in the calculation of detector efficiency. The data will be presented as absolute double-differential cross sections and will be compared to HETC/MCNP calculations.

5. Gamma-Ray Production by Protons and Neutrons in Thin and Thick Targets (R. C. Reedy, J. R. Arnold*, A. U. Khan*, P. Englert**, J. Brückner***, H. Wänke***, and A. E. Metzger****)

Gamma-ray lines can be used to determine the elemental composition of a planet's surface. An orbital gamma-ray spectrometer is scheduled to fly on the Mars Geoscience Climatology Observer in 1990. To help plan for such missions, a series of irradiations have been or will be done at several facilities. To data, gamma-ray spectra have been measured from various thin targets irradiated with 14-MeV neutrons in Mainz, Be+d neutrons in Jülich, and 650-MeV protons at LAMPF, and from thick targets irradiated with high-energy ($E > 1$ GeV) protons and alpha particles at the Argonne ZGS and the Berkeley Bevatron. The thin-target irradiations provide cross sections for the production of the major gamma-ray lines made by neutrons ($E < 40$ MeV) and protons ($E > 100$ MeV) from important target elements, such as O, Mg, Al, Si, Ca, and Fe. The thick-target bombardments simulate the complete cascade produced in a planetary surface by energetic ($E \sim$ GeV) galactic cosmic rays and will be used to test the effects of chemistry (such as the presence of water) on the transport of particles in a planet's surface. These irradiations also showed that five broad (~ 50 keV), asymmetric peaks were produced in Ge detectors by the inelastic scattering of neutrons with Ge nuclei, but these background peaks usually will not interfere with the mapping of gamma-ray lines from a planet. Additional irradiations will continue to be done at various accelerators.

6. Gamma-Ray Line Intensities for Depleted Uranium (C. E. Moss)

The gamma-ray line intensities from depleted uranium are

* Univ. of Calif., San Diego

** Univ. Cologne, FRG

*** Max-Planck Institute, Mainz, FRG

**** Jet Propulsion Laboratory

necessary for assaying material in nuclear safeguards and for calculating the gamma-ray flux from objects containing depleted uranium. Most of the gamma rays are produced by ^{234m}Pa and ^{234}Pa in equilibrium with ^{238}U. For the strong 1001-keV line from ^{234m}Pa, the Table of Isotopes quotes a branching intensity of 0.59%;[1] Gunnink gives 0.828%.[2] Some difficulties in obtaining agreement between calculated and measured fluxes from objects containing depleted uranium, prompted us to remeasure the intensities of lines from depleted uranium. We measured several samples more than once using three germanium detectors calibrated with NBS sources. For the 1001-keV line we obtained 0.828 ± 0.013%, in excellent agreement with Gunnink.

---

[1] C. M. Lederer and V. S. Shirley (eds.), Table of Isotopes, 7th ed. (Wiley, New York, 1978).

[2] R. Gunnink and J. F. Tinney, "Analysis of Fuel Rods by Gamma-Ray Spectroscopy," Lawrence Livermore Laboratory report UCRL-50186 (1971).

B. NUCLEAR DATA EVALUATION

1. Neutron Spectra from the t + ^{6}Li Reaction (G. Hale, D. George, P. Lisowski)

The interaction of tritons with lithium in the blanket of a fusion reactor could have an important effect on the total neutron spectrum, but the cross sections and spectra for these reactions have not been well determined. Recently, new measurements[1,2] were made at Los Alamos and at Bruyères-le-Châtel, France, to improve the knowledge of spectra for the t + ^{6}Li reaction.

We are using a resonance model,[3] implemented in the SPECTRA code, to interpret the Los Alamos measurements,[1] and to aid with making background corrections. The calculations are illustrated by the zero-degree neutron spectrum at E_t=1.64 MeV shown in Fig. B-1; they contain "direct" contributions from the first 5 levels in ^{8}Be, in addition to a broad, underlying "exchange" contribution from the ground state of ^{5}He. The parameters of this calculation also give a good representation of low-energy ^{6}Li(^{3}He, p) spectra, and a surprisingly reasonable description of the ^{6}Li(t,n) spectra over the range of energies ($1.6 \leq E_t \leq 4.5$ MeV) and angles ($0° \leq \theta_n \leq 150°$) measured at Los Alamos.

At incident triton energies above 2 MeV, there is evidence for structure at low neutron emission energies coming from p + ^{7}Li resonances in ^{8}Be at excitation energies above 17 MeV. We have modified the code to accommodate both the α-α and p-^{7}Li channels in ^{8}Be, and have made some progress accounting for the observed low-energy structure.

---

[1] P. W. Lisowski, R. E. Brown, J. C. Gursky, S. D. Howe, N. Jarmie, and G. L. Morgan, "Cross Sections for the ^{6}Li(t,n)2α Reaction," Bull. Am. Phys. Soc. 29, 748 (1984).

[2] G. Haouat et al., Centre d'Étude de Bruyères-le-Châtel, unpublished.

[3] G. M. Hale, "Resonance Model for Three-Body Spectra," unpublished.

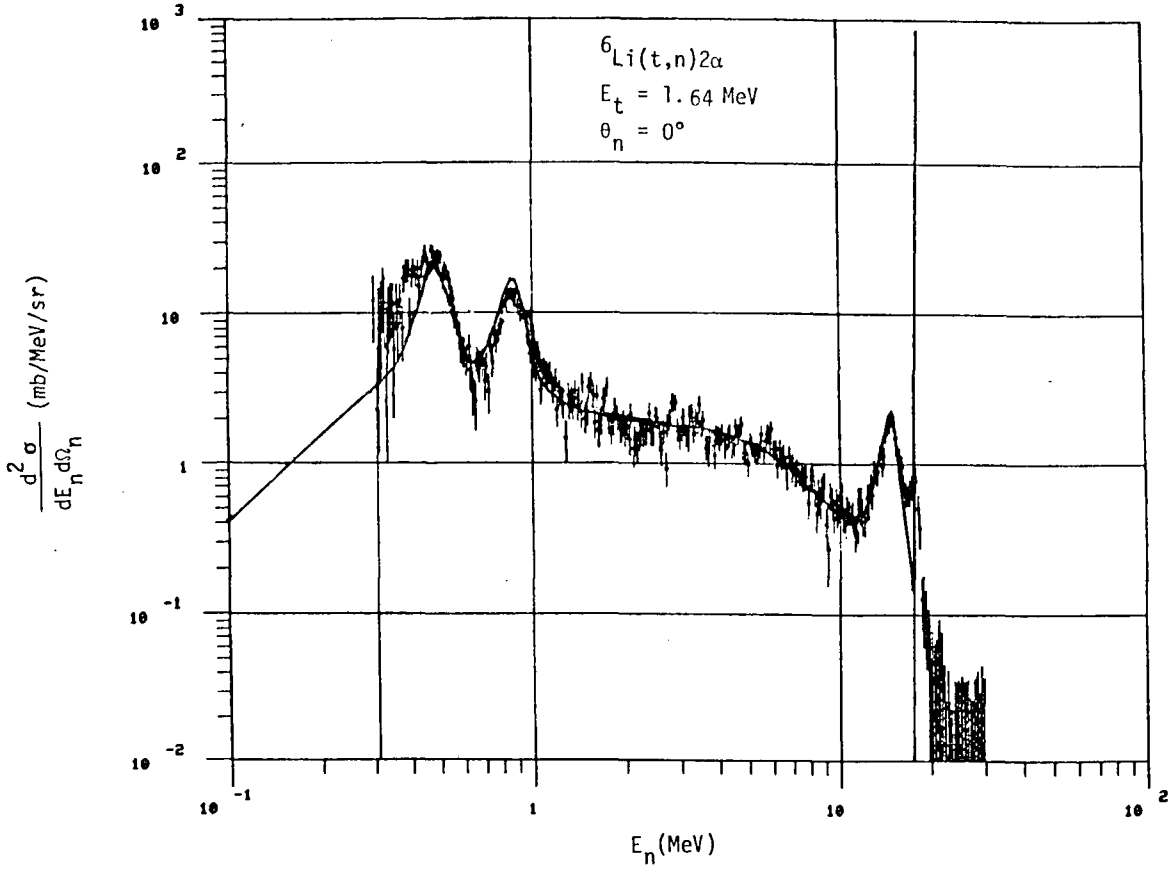

Fig. B-1. Calculated neutron spectrum at $\theta_n = 0°$ for $E_t = 1.64$ MeV, compared with uncorrected measurements by Lisowski et al.[1]

2. Calculation of (n,n') Excitation Functions for Higher-Lying Levels in ^{238}U (E. D. Arthur)

Calculations have been made of cross sections for neutron inelastic scattering from 20 higher-lying levels in ^{238}U that are vibrational band members. Since the ^{238}U nucleus is deformed, neutron inelastic cross sections should exhibit both compound nucleus and direct-reaction contributions, with direct-reaction components being largest for higher incident neutron energies. For the calculations discussed here, compound nucleus contributions were determined through use of the COMNUC[1] Hauser-Feshbach statistical code, which includes a realistic description of fission competition. The description of direct-reaction contributions for scattering from such vibrational states is more complex. If one pursues a coupled-channel approach, then one must couple explictly states occupying higher vibrational bands with ground state band members. This approach is costly in computer time and still requires the use (generally) of an adjustable

parameter to describe interband coupling. In our case, we used an alternative procedure based on distorted-wave Born approximation (DWBA) calculations that employed the spherical iteration of the Madland-Young[2] neutron optical parameters for actinides. Then $B(E\ell)$ values determined from charged-particle reactions[3] (Coulomb excitation and inelastic scattering) were used to produce deformation parameters, β_ℓ, which are necessary for proper normalization of DWBA results.

Figure B-2 compares the calculated results for the excitation function for scattering from the 3^- 0.73 MeV level of ^{238}U with the recent data of Shao.[4] The solid curve represents the incoherent sum of compound nucleus (CN) and direct interactions (DI) while the dashed curve represents only the DI contributions computed as described above. Also shown on the figure are data from $(n,n'\gamma)$ measurements of Olsen.[5] At energies above 2 MeV these data are in substantial disagreement with the directly measured (n,n') data of Shao and with the present calculations. Such $(n,n'\gamma)$ based data had been used in other theoretical calculations[6] to deduce unusually large DI components for scattering from this (and other vibrational) states. In contrast, the present calculations and the Shao data indicate small DI contributions, generally less than 10 mb.

We also calculated cross section excitation functions for several other levels measured in the Shao experiment as well as angular distributions at incident energies of 1.5 and 2 MeV. In all cases, the data agree well with our theoretical approach, which ensures a consistency between neutron inelastic scattering data and charged-particle based reduced transition probabilities. Additionally, our calculations indicate that, at neutron energies around 2-2.5 MeV, direct-reaction contributions are relatively small for scattering from higher-lying ^{238}U vibrational states.

---

1 C. L. Dunford, "A Unified Model for Analysis of Compound Nucleus Reactions," Atomics International report AI-AEC-12931 (1970).

2 D. G. Madland and P. G. Young, "Neutron-Nucleus Optical Potential for the Actinide Region," Proc. Int. Conf. on Neutron Phys. and Nucl. Data for Reactor and Other Applied Purposes, Harwell, U.K., Sept. 25-29, 1978 (published by the Organization for Economic Cooperation and Development, Paris, France), p. 349.

3 E. N. Shurshikov, M. F. Filchenkov, Yu. F. Jaboray, A. I. Khovanovich, "Nuclear Data Sheets for A-238," Nuclear Data Sheets 38, 277 (1983).

4 Ti-Qun Shao, "Fast Neutron Inelastic Scattering Cross Sections of ^{238}U," Ph.D. Thesis, Univ. of Lowell, Lowell, Mass., 1983 (unpublished).

5 D. K. Olsen, G. L. Morgan, J. W. McConnell, "Measurement of $^{238}U(n,n'\gamma)$ Cross Sections," Proc. Int. Conf. Nucl. Cross Sections for Technol., Oct. 22-26, 1979, Knoxville, Tenn. (NBS Special Publication 594, 1980), p. 677.

[6] D. W. S. Chan, J. J. Egan, A. Mittler, E. Sheldon, "Analyses of Fast Neutron Inelastic Scattering Cross Sections to Higher (Vibrational) States of ^{232}Th and ^{238}U. 1 Standard Formalism," Phys. Rev. C 26, 841 (1982).

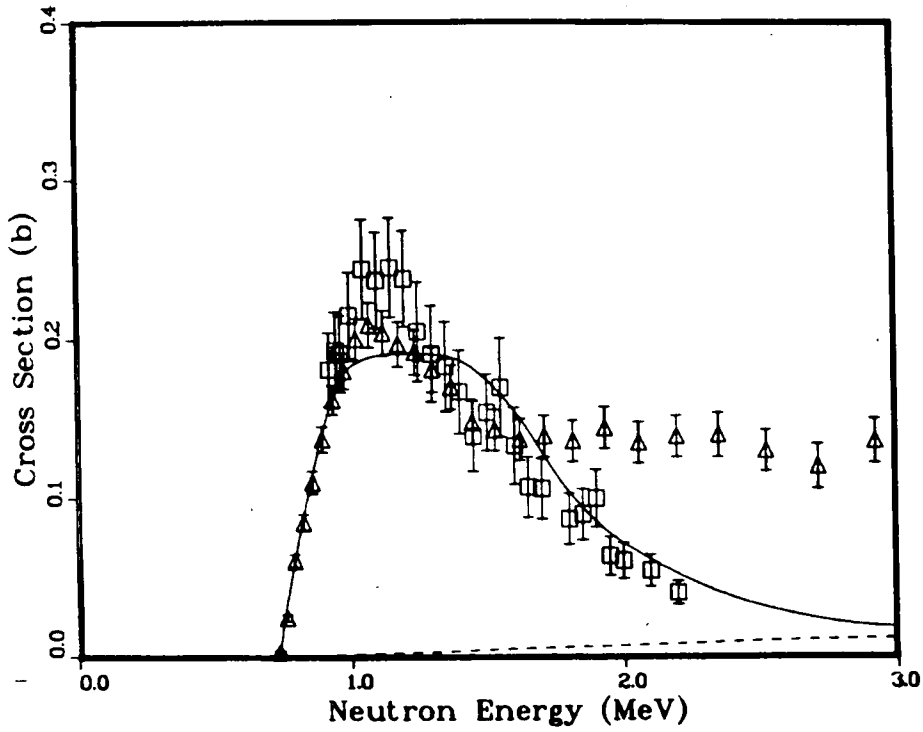

Fig. B-2. The present calculations (solid curve) for excitation of the 3^- 0.73 MeV state in ^{238}U are compared with new measurements of Shao.[4] Shown by triangles are cross sections deduced from the (n,n'γ) values of Olsen[5] The dashed curve represents the DI contribution calculated as described in the text.

3. Neutron-Induced Reactions on ^{11}B (P. G. Young)

The present ENDF/B-V evaluation for n + ^{11}B reactions is based on a 1966 U.K. Atomic Energy Agency analysis and does not incorporate any modern experimental or theoretical results. As pointed out in a recent review,[1] discrepancies of up to 40% exist between new measurements and the evaluated total and elastic cross sections, and even larger inconsistencies occur for elastic angular distributions. Additionally, the ENDF/B-V evaluation does not include gamma-ray production data.

A new evaluation of n + ^{11}B data for neutron energies up to 20 MeV is in progress at Los Alamos. To complement the available experimental data and to facilitate interpolation and extrapolation in the evaluation, an optical model/reaction theory analysis of the experimental data is being performed.

Figure B-3 compares an early scoping calculation of the gamma-ray emission spectrum from 14.5-MeV neutrons on ^{11}B with preliminary experimental data from a recent measurement[2] at Los Alamos. The final analysis will be further optimized for consistency with this experiment as well as modern measurements of neutron total cross sections and scattering angular distributions.

---

[1] P. G. Young and L. Stewart, Prog. Nucl. En. 13, 193 (1984).

[2] G. Auchampaugh and S. Wender, Los Alamos National Laboratory personal communication (1984).

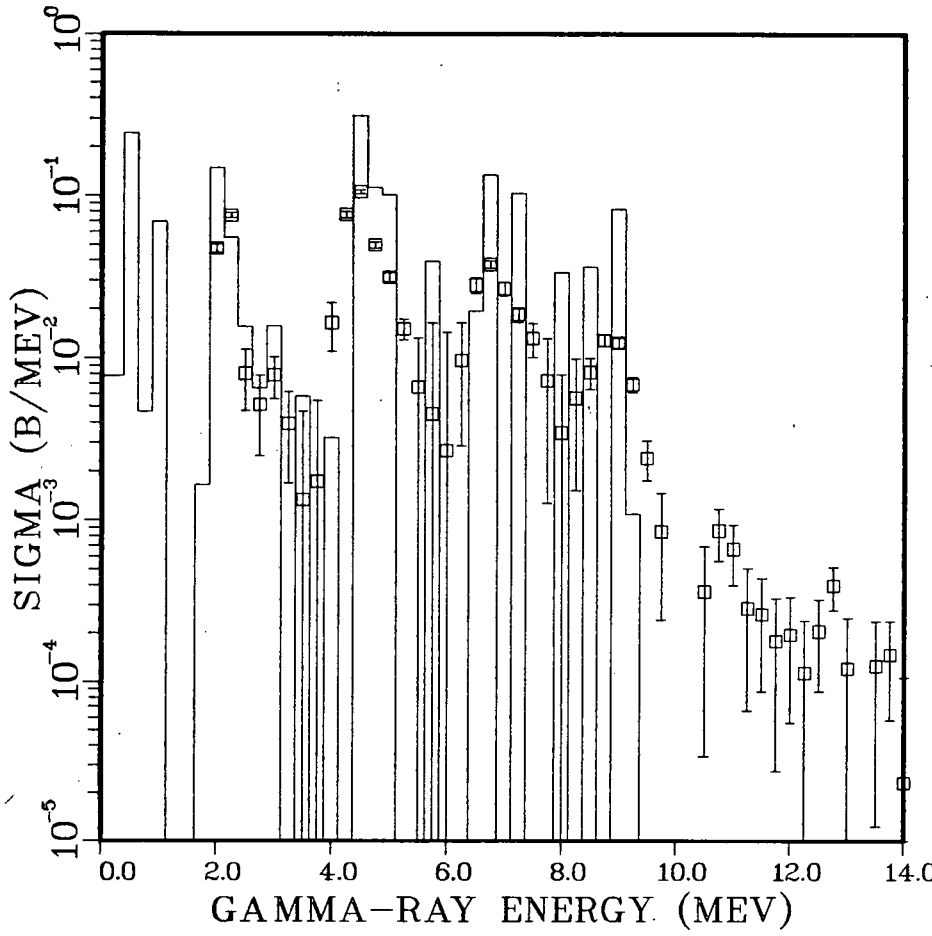

Fig. B-3. Comparison of a calculated gamma-ray emission spectrum from 14.5 MeV neutrons on ^{11}B with preliminary experimental data (squares) from Ref. 2. Note that the calculated histogram has not been broadened for experimental resolution.

4. Delayed Neutrons (T. R. England, W. B. Wilson, R. T. Perry*, and M. C. Brady**

In a cooperative effort with HEDL (see their contributions), we have continued with the evaluations of precursor data and spectra[1 2] and also the effects of using more than six delayed groups. The bromine and rubidium spectra measured by K. Kratz have now been added to the spectra measured by G. Rudstam and the model code spectra generated using the BETA code. New evaluations of the emission probabilities (Pn) for 77 precursors[2] and model estimates for an additional 33 precursors are being used with new evaluations of fission product yields to calculate aggregate equilibrium spectra as well as the six delayed group spectra. These results are essentially an update of all parameters used to calculate the aggregate spectra from 110 precursors, as described in Ref. 1.

In addition we are using all 110 precursors and their parents in kinetics calculations and comparing this detailed treatment with the conventional approximation using six delayed groups.

The spectra and kinetics comparisons will be presented in two papers accepted for the International Conference on Nuclear Data for Basic and Applied Science in May 1985.[3,4]

---

* Texas A & M University

** Los Alamos Collaborator, on leave from Texas A & M University

[1] T. R. England, W. B. Wilson, R. E. Schenter, and F. M. Mann, "Aggregate Delayed Neutron Intensities and Spectra Using Augmented ENDF/B-V Precursor Data," Nucl. Sci. Eng. 62, pp. 139-155 (October 1983).

[2] F. M. Mann, M. Schreiber, R. E. Schenter, and T. R. England, "Evaluation of Delayed Neutron Emission Probabilities," Nucl. Sci. Eng. 87, pp. 418-431 (August 1984).

[3] T. R. England, M. C. Brady, W. B. Wilson, "Delayed Neutron Spectra and Intensities from Evaluated Precursor Data," abstract accepted for presentation at Conf. Nucl. Data for Basic and Applied Sci., Santa Fe, N.M., May 1985.

[4] R. T. Perry, W. B. Wilson, T. R. England, and M. C. Brady, "Application of Evaluated Fission-Product Delayed-Neutron Precursor Data in Reactor Kinetics Calculations," abstract accepted for Conf. Nucl. Data for Basic and Applied Sci., Santa Fe, N.M., May 1985.

5. Fission Product Yield Evaluations (T. R. England, B. F. Rider*, and G. K. Schenter**)

The evaluation of fission product yields for 34 fissioning nuclides, as described in Ref. 1, has continued with an emphasis on model parameters and the method of evaluation.

We have found that the even-odd Z pairing parameter used for ^{238}U was too large by a factor of two. Recent use of a value of 15% (suggested by Grenoble measurements of independent yields) appears to be an excellent value. Delayed neutron yields calculated from the individual short-lived precursors now agree with aggregate measurements.

We have also used a modified version of the least squares adjustment code FERRET[2] in evaluations for use in comparison with the method described in Ref. 1. We found very little difference in yields or uncertainties. This is due apparently to the lack of complete measurements of yield distributions along each mass chain and the need to use values from model systematics.[1]

---

* Retired, G. E. Co., Los Alamos consultant.

**Cornell University, Los Alamos summer graduate research assistant

[1] T. R. England and B. F. Rider, "Status of Fission Yield Evaluations," in Proceed. of "NEANDC Specialists Meeting on Yields and Decay Data for Fission Product Nuclides," Brookhaven National Laboratory, Oct. 24-27, 1983 (jointly sponsored by the NEANDC and Divis. of High Energy Physics, U.S. Dept. of Energy, R. E. Chrien and T. W. Burrows, Eds.), Brookhaven National Laboratory report BNL-51778.

[2] F. Schmittroth and R. E. Schenter, "Finite Element Basis in Beta Adjustment," Nucl. Sci. Eng. 74, 168 (1980).

6. Neutron Sources in Reactor Fuel (W. B. Wilson, R. T. Perry,* J. E. Stewart, and T. R. England)

The SOURCES code and library, under development for the past five years, calculates β,n delayed, spontaneous-fission, and (α,n) neutron sources and spectra from the decay of radionuclides in homogeneous media. Delayed neutron spectra are calculated with evaluated halflife and Pn data using pre-processed spectra for the 105 individual precursors. Spontaneous-fission spectra are calculated with evaluated halflife, SF branching, and $\bar{\nu}$ data using Watt spectrum parameters for 43 actinides. The (α,n) spectra are calculated with a library of nuclide decay alpha spectra, evaluated (α,n) cross sections and produce-nuclide level branching fractions, and functional α stopping cross sections using an assumed isotropic neutron angular distribution in the center-of-mass system.

---

* Texas A & M University

These neutron spectra are now supplemented by photoneutron spectra calculated with PHONX84, an evolved version of PHONEX. PHONX84 uses an input γ energy-binned fluence and deuterium atom density, and evaluated $^2H(\gamma,n)$ photoelectric and photomagnetic cross sections using isotropic photomagnetic and $\sin^2\theta$ photoelectric neutron angular distributions in the center-of-mass system. Individual γ spectra for 86 fission-product nuclides have been processed from ENDF/B-V. Monte Carlo photon transport calculations have been made with MCNP for γ sources homogeneously distributed in the fuel of a ZR-4 clad fuel rod centered in a repeating cubic cell with reflecting boundaries and outside dimensions equal to the rod pitch; these calculations yielded water-volume integrated γ energy-binned fluences for unit γ sources at each energy boundary of the ¼-MeV bin structure extending to 7 MeV. PHONX84 calculations of photoneutron spectra were performed for unit fluences in each γ energy bin. The unit-source fluences were then combined with the unit-fluence photoneutron spectra and the processed ENDF/B-V fission-product γ spectra to produce unit-decay PWR photoneutron spectra for each fission-product nuclide.

The combined SOURCES/PHONX84 capability has been demonstrated in the calculation of the neutron source in discharged 31.5-GWd/tU PWR fuel for cooling times extending to 100 years. The inventory of fission products and actinides at shutdown and at cooling times of interest were calculated with versions of CINDER. These calculated inventories were input to SOURCES for the β,n delayed, spontaneous-fission and (α,n) source and spectra contributions; photoneutron contributions were obtained by combining the inventories with the unit-decay photoneutron spectra described above. The total neutron source rates associated with each source are available upon request, as are the neutron source spectra calculated in a 50-keV bin structure.

7. Prompt Fission Neutron Spectrum for the $^{252}Cf(sf)$ Standard Reaction (D. G. Madland, R. J. LaBauve, and J. R. Nix)

Our most recent calculation[1] of the prompt fission neutron spectrum for the spontaneous fission of ^{252}Cf has been submitted[2] to the IAEA as a candidate for the theoretical representation of this standard spectrum. The spectrum has been accepted[3] as one of three interim representations to be used until an evaluated experimental spectrum is determined for further tests of various theoretical representations. Our calculated spectrum (χ^2 = 0.552) is shown in Fig. B-4 compared with a recent experiment,[4] with the NBS spectrum,[5] (χ^2 = 1.922) and with the best-fit Maxwellian spectrum (χ^2 = 1.201).

---

[1] D. G. Madland and J. R. Nix, in Proc. Specialists' Meeting on Yields and Decay Data of Fission Product Nuclides, Brookhaven National Laboratory, Upton, New York, October 24-27, 1983, p. 423 (Brookhaven National Laboratory report BNL-51778, 1984).

[2] D. G. Madland, R. J. LaBauve, and J. R. Nix, in Proc. IAEA Advisory Group Meeting on Nuclear Standard Reference Data, Geel, Belgium, November 12-16, 1984 (proceedings to be published).

[3] J. W. Boldeman, Chairman's report of the Working Group on the ^{252}Cf Spontaneous Fission Prompt Neutron Spectrum, Proc. IAEA Advisory Group Meeting on Nuclear Standard Reference Data, Geel, Belgium, November 12-16, 1984 (proceedings to be published).

[4] W. P. Poenitz and T. Tamura, in Proc. Int. Conf. on Nucl. Data for Sci. and Technology, Antwerp, Belgium, 1982, p. 465 (Reidel, Dordrecht, 1983).

[5] J. Grundl and C. Eisenhauser, in Proc. First ASTM-EURATOM Symp. on Reactor Dosimetry, Petten, Holland, September 22-26, 1975, Part I, p. 425 (Commission of the European Communities, EUR5667 e/f, 1977).

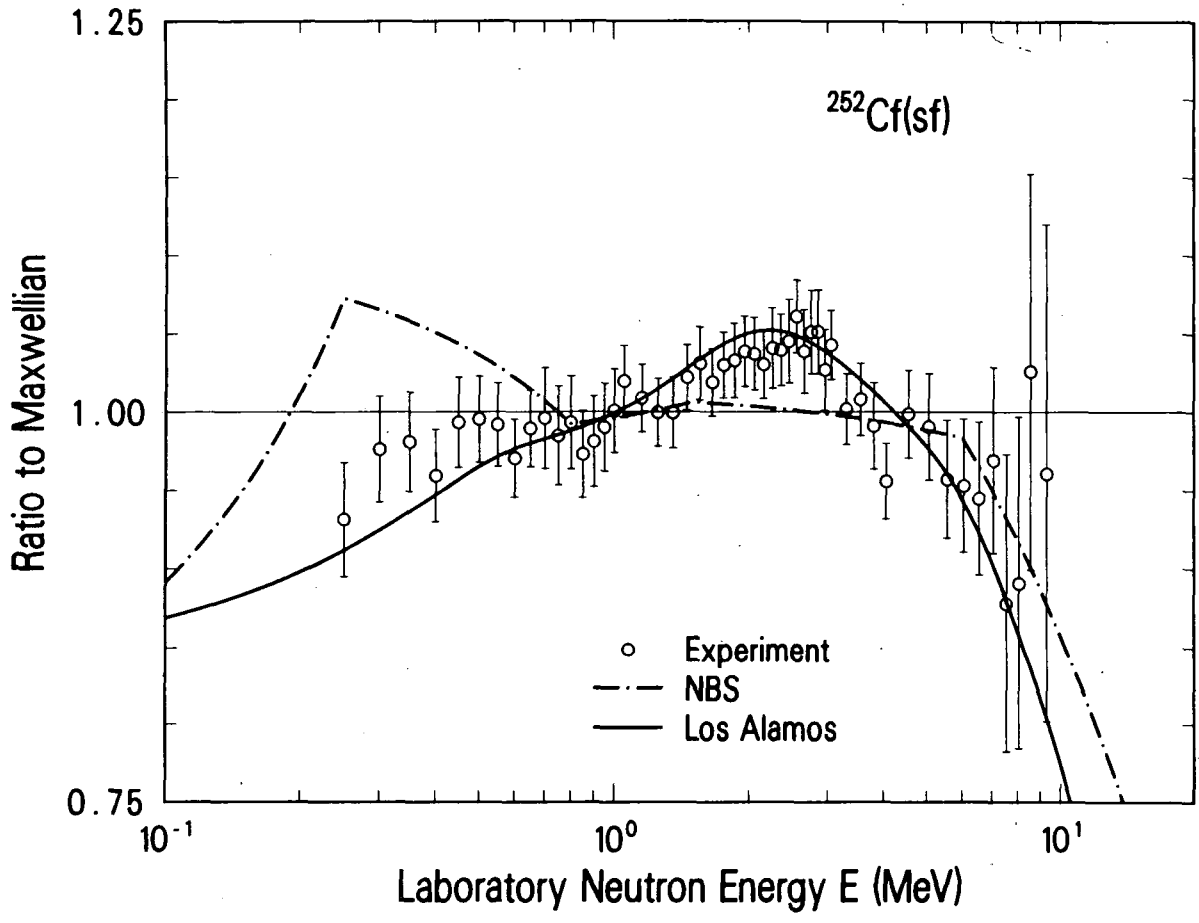

Fig. B-4. Ratio of the NBS spectrum,[5] the least-squares adjusted Los Alamos spectrum,[1,2] and the experimental spectrum[4] to the least-squares adjusted Maxwellian spectrum.[1,2]

A. NEUTRON SCATTERING CROSS SECTIONS IN THE ACTINIDES

(L.E. Beghian, G.H.R.Kegel, J.J. Egan, A. Mittler, J.Q. Shao, G.C. Goswami, G.D. Brady, A. Aliyar, and C.A. Horton)

1. ^{235}U Excitation Function Measurements

We have initiated (n,n') and (n,n'γ) excitation function measurements on ^{235}U for incident neutron energies in the 100- to 500-keV range. Preliminary results of the (n,n') measurements on the ground state and on levels at 13 keV, 46 keV, 51 keV and 82 keV are in tolerable agreement with ENDF/B-V with the exception of the results for the 13-keV state which seem to be larger than the ENDF estimate. The (n,n'γ) measurements are in progress at this writing; this second series covers levels at 129 keV and higher where the conversion coefficients are sufficiently small to assure a reasonable gamma yield.

2. Angular Distribution Measurements at 550-keV

We have measured (n,n') angular distributions at 550-keV incident neutron energy for the ground and first two excited states of ^{232}Th and ^{238}U. These data supplant the 520-keV measurements[1] mentioned in the 1984 Report to the DOE Nuclear Data Committee which contained non-reproducible fluctuations with angle. The new data[2] at 550-keV are more consistent with previous work. We have also included ^{235}U in this new set of measurements obtaining cross sections for the combination of the ground and 13-keV state and for the 46-, 51-keV doublet. Figures A-1, A-2 and A-3 show representative preliminary results for each of the three nuclides compared to previous work as compiled in the supplement to the report of the 1982 Paris Specialists Meeting on Fast Neutron Scattering on Actinide Nuclei.[3]

---

[1]G.C. Goswami, C.A. Ciarcia, G.P. Couchell, J.J. Egan, C.A. Horton, G.H.R. Kegel, S.Q. Li, A. Mittler and J.Q. Shao, Bull. Am. Phys. Soc. 28, 984 (1983).

[2]J.J. Egan, A. Mittler, G.C. Goswami, A. Aliyar and R.L. Schueller, Bull. Am. Phys. Soc. 29, 1038 (1984).

[3]G. Haouat, C. Nordborg, P. Nagel and T. Nakagawa, Compilation of Actinide Fast Neutron Scattering Data, Supplement to the Proceedings of the Specialists' Meeting on Fast Neutron Scattering on Actinide Nuclei, NEANDC-158U, OECD Paris, 1982.

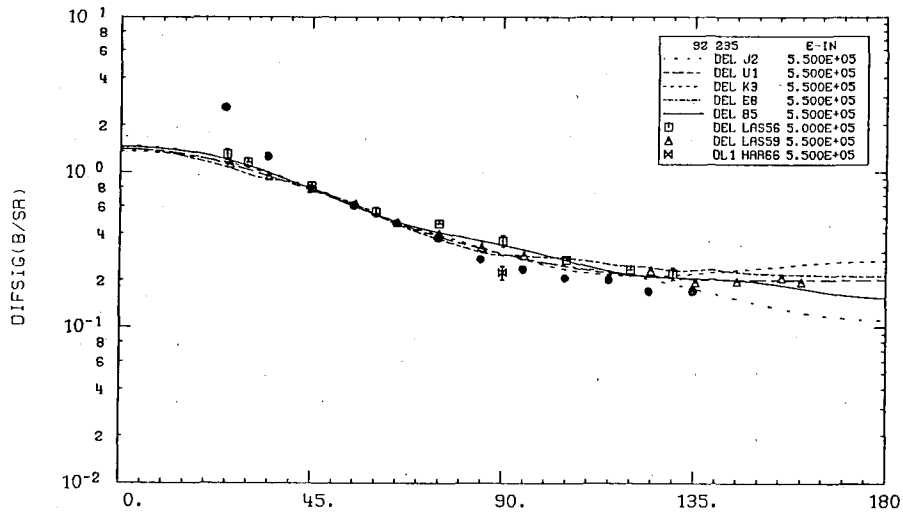

Fig. A-1. Neutron elastic scattering angular distribution at 550-keV for ^{235}U (including an inelastic contribution for the 13-keV state). The present measurements are indicated by solid dots.

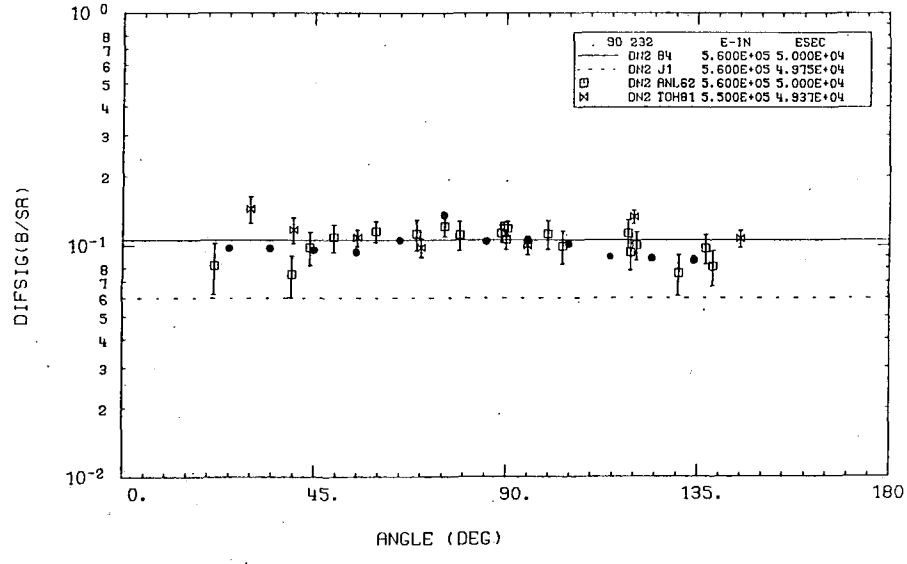

Fig. A-2. Inelastic scattering angular distribution at 550-keV for the 49-keV first excited state in ^{232}Th. The present measurements are indicated by solid dots.

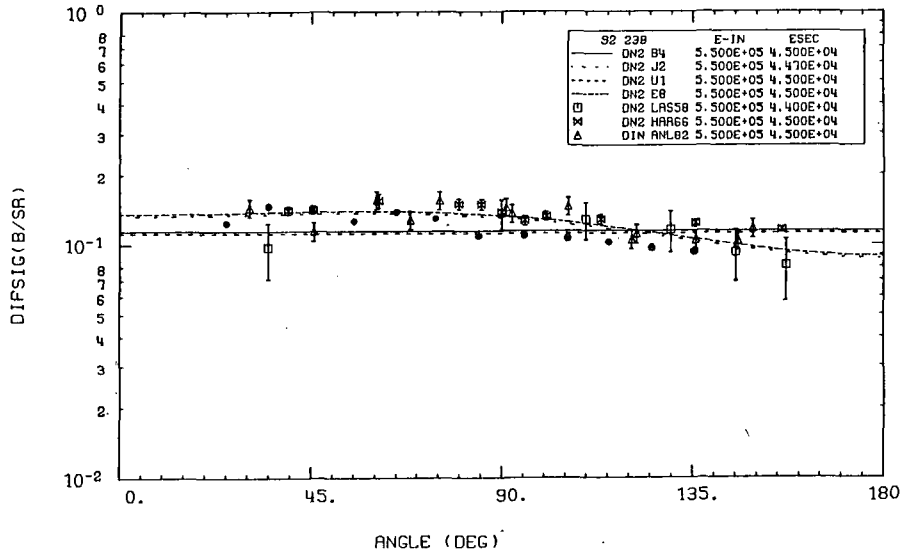

Fig. A-3. Inelastic scattering angular distributions at 550-keV for the 45-keV first excited state in ^{238}U. The present measurements are indicated by solid dots.

3. Use of an Iron Filter in Neutron Cross Section Measurements

There are several nuclei in the actinide region where the separation between the ground state and an excited state is about 10 keV. Good energy resolution is required in time-of-flight cross section measurements to separate inelastic neutrons from the much stronger elastic group. It appears that a substantial resolution enhancement can be obtained by using an iron filter and by utilizing the neutron absorption minimum near 82 keV (see, e.g. Winters *et al.*[4] and Macklin *et al.*[5]).

We have investigated the feasibility of using the iron filter technique. Figure A-4 shows a time-of-flight spectrum of 60-100-keV neutrons from the U. of L. Van-de-Graaff accelerator. Filtered through 40.7 cm of iron. The peak has a full width at half height of 3.9 ns, far more than expected from accelerator and electronics resolution (∿1.3 ns) and from scintillator transit times (∿1.6 ns). The difference is attributed to an unfavorable filter geometry used in these preliminary studies which introduced flight-path dispersion. On the other hand the energy resolution of this peak is good, ΔE = 1.3 keV, in spite of its larger time width. We are preparing a filter of improved geometry which will be used to measure cross sections of low lying levels in the actinides.

---

[4]R.R. Winters, N.W. Hill, R. L. Macklin, J. A. Harvey,, D.K. Olsen and G.L. Morgan, Nucl. Sci. Eng. 78, 147 (1981).

[5]R.L. Macklin, R. R. Winters, N.W. Hill and J.A. Harvey, Astro. J. 274, 408 (1983).

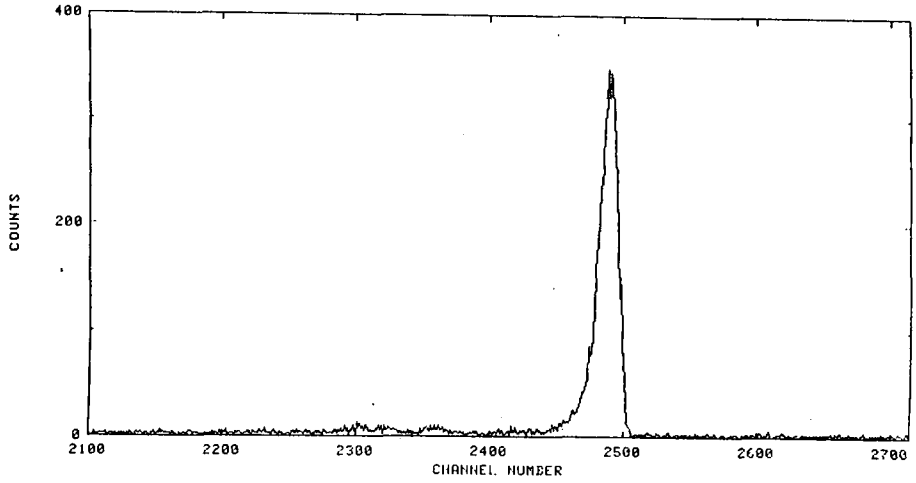

Fig. A-4. A time-of-flight spectrum for neutrons from a thick target filtered through 40.7 cm of iron.

B. LEVEL CROSS-SECTION CALCULATIONS FOR NEUTRON INELASTIC SCATTERING ON THE PRINCIPAL STABLE EVEN-MASS ACTINIDES (Th-232, U-238, Pu-240, 242, 244)

1. Rotational and Vibrational Bands in Th-232

The calculations of total (angle-integrated) and differential cross sections for level excitation functions and angular distributions populating rotational and vibrational states in Th-232 up to an excitation energy $E^* = 1218$ keV via inelastic neutron scattering from threshold up to $E = 3.4$ MeV (lab), described in previous (1983, 1984) Reports to the DOE Nuclear Data Committee have now been completed. As a test of the Bruyeres optical potential employed throughout the computations, analyses of $(n,n'\gamma)$ gamma-ray angular distributions[1] and inferred (n,n') excitation functions[2] were performed in the framework of the compound-nucleus (CN) formalism. Thereafter, with the incoherent addition of a direct-interaction (DI) contribution, the "standard" (CN + DI) approach was utilized for the analysis of (n,n') excitation and distribution data,

---

[1]W.R. McMurray, E. Barnard, I. J. van Heerden and D.T.L. Jones, Southern Universities (RSA) Nuclear Institute Annual Research Report SUNI-45 (1976).

[2]J.H. Dave, Egan, Couchell, Kegel, Mittler, Pullen, Schier and Sheldon Nucl. Sci. Eng., 1985 (submitted for publication).

including principally the latest measurements by the Lowell group.[3,4] The findings were contrasted with the ENDF/B-V evaluation and with the results provided by the "HRTW" (Hofmann, Richert, Tepel and Weidenmuller[5]) approach based on statistical S-matrix theory with intricate coupling of channels (designed for the evaluation of "fluctuation" [CN] cross sections in the presence of DI). Also, where possible, the comparison was made with recent results presented by the Oxford group,[6] who employed a modified "standard" (CN + DI) treatment in their analyses. The substantial body of detailed theoretical and experimental data thus assembled has been communicated to nuclear data banks.

2. Rotational and Vibrational Bands in U-238

A similar batch of calculations has now been completed for individual states in the collective bands of U-238 up to E* = 1269 keV for incident neutron energies ranging from threshold to E = 3.1 MeV, employing the "standard" (CN + DI) and statistical S-matrix (HRTW) formalisms. Likewise, the results were contrasted against ENDF/B-V evaluation data and compared with measured data, primarily from the Lowell and Geel[7] experimental groups.[3,8] A comparison was also undertaken with recent calculations by the Oxford group,[9,10] based upon a modified "standard"

---

[3]E. Sheldon, in Proceedings of the 16th Polish Summer School in Nuclear Physics, Mikolajki, Aug. 27 - Sep. 8, 1984 (Harwood Publ., 1985, in press).

[4]E. Sheldon, Beghian, Chan, Ciarcia, Couchell, Egan, Goswami, Kegel, Li, Mittler, Pullen, Schier and Shao, J. Phys. G - Nucl. Phys. 1985 (in publication).

[5]H.M. Hofmann, Richert, Tepel and Weidenmuller, Ann. Phys. (NY) 90, 391 & 403 (1975).

[6]A.M. Street and P.E. Hodgson, Nucl. Sci. Eng. 1985 (submitted for publication).

[7]H.H. Knitter, Coppola, Ahmed and Jay, Z. Phys. 244, 358 (1971).

[8]E. Sheldon, Beghian, Chan, Ciarcia, Couchell, Egan, Goswami, Kegel, Li, Mittler, Pullen, Schier and Shao, J. Phys. G - Nucl. Phys. 1985 (in publication).

[9]P.E.Hodgson, Oxford University Nuclear Physics Laboratory Report 65/82 (1982).

[10]P.E. Hodgson and A.M. Kobos, Nucl. Sci. Eng. 1984 (submitted for publication).

(CN + DI) approach. The ensuing data have been transmitted to nuclear data-bank archives.

3. Rotational and Vibrational Bands in Pu-240, Pu-242 and Pu-244

To remedy the dearth of calculated cross-section data for these stable members of the plutonium family ($T_{1/2}$ = 6.57x10^3 yr, 3.76x10^5 yr, and 8.1x10^7 yr, respectively), computations of total (angle-integrated) cross sections were undertaken for individual levels of known spin and parity up to an excitation energy of E* = 1138, 1204 and 1210 keV, respectively for Pu-240, Pu-242 and Pu-244, from threshold to E = 2.5 MeV incident neutron energy, in the "standard" (CN + DI) and statistical S-matrix (HRTW) formalism, using estimated values for the relative band coupling strength as the sole variable parameter in the calculations. Level schemes featuring plausible quadrupole and octupole vibrational band assignments were established and comparisons with the available measured excitation-function data were made. Generally good agreement ensued; the results have been prepared for publication[3,11] and archiving in nuclear data banks.

C. DELAYED-NEUTRON MEASUREMENTS

(W.A. Schier, G.P. Couchell, D.J. Pullen, L. Fisteag, M.N. Haghighi, Q. Sharfuddin and R. S. Tanczyn)

We have now completed our measurements of delayed-neutron energy spectra following thermal neutron-induced fission of U-235. The study spans delay times ranging from 0.17-85.5 s after fisson. Table 1 summarizes the effective delay times studied and the estimated six group[1,2] contribution to each spectrum.

Table 1. Six-group composition (%)* of measured spectra

Group	1	2	3	4	5	6
$T_{1/2}$ (s)	55.5	20.2	4.99	2.11	0.64	0.27
Delay Interval (s)						
0.17 - 0.37	0.1	2.1	7.3	33.9	25.7	30.9
0.41 - 0.85	0.2	2.9	10.0	43.1	25.7	18.1
0.79 - 1.25	0.2	4.0	13.2	52.1	21.6	8.9
1.2 - 1.9	0.3	5.3	15.3	58.4	17.2	3.5
2.1 - 3.9	0.8	8.4	22.4	61.5	6.7	0.2
4.7 - 10.2	1.9	19.8	33.8	44.1	0.4	0.0
12.5 - 29.0	6.6	58.0	29.2	6.2	0.0	0.0
35.8 - 85.5	14.7	83.1	2.2	0.0	0.0	0.0

*Based on six-group parameters recommended by Rudstam[2].

[11] E. Sheldon and D.W.S. Chan, J. Phys. G - Nucl. Phys. 1985 (in pub.).

[1] G.R. Keepin, Physics of Nuclear Kinetics Addison-Wesley Publ. Co., Inc., Reading, Mass. (1965).

[2] G. Rudstam, Nucl. Sci., Eng. 80, 238 (1982).

The present work is the first to measure composite delayed-neutron spectra for delay times less than 1 s. Of particualr interest is the shortest delay interval, 0.17-0.37 s, which has a significant contribution (>30%) from the shortest lived group having $T_{1/2}$ = 0.27s. Because the data set of spectra from individual isotopes[2] is incomplete for Group-6, we are now reporting the first complete delayed neutron spectrum for this short a delay time.

Neutron time-of-flight (TOF) measurements were conducted in two stages to span the widest possible neutron energy range:

1) A set of four Pilot U scintillators was used to obtain spectra for the region, E_n = 0.1-2.0 MeV.

2) Spectra were measured for the same delay intervals* (see Table 1) using three Li-6 glass scintillators (NE912) for the region, E_n = 0.01-0.40 MeV. This low-energy region is particularly important for reactor kinetics since low-energy neutrons generally have higher probabilities for interacting with reactor core materials.

In an independent parallel study we used a fourth NE 912 Li-6 glass detector to investigate the possibility of using pulse-shape discrimination (PSD) to further suppress the gamma-ray backgrounds in neutron TOF measurements. Indeed, we discovered a very useable PSD effect in this scintillator. The improvement in quality resulting from the inclusion of the PSD system in our lithium glass studies warranted a re-measurement of all the spectra we had obtained with Li-6 glass up to that time. A typical delayed-neutron TOF spectrum measured with Li-6 glass using PSD is shown in Fig. C-1. Each spectrum showed only a minor loss of neutron counts but a substantial factor-of-two reduction of both the γ-ray peak and the random background. In the spectrum the valley between the neutron and

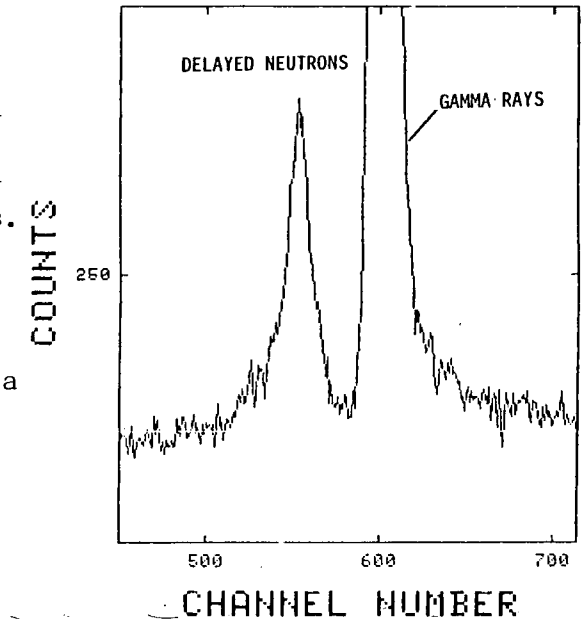

Fig C-1. Typical U-235 delayed-neutron TOF spectrum measured with Li-6 glass (NE-912) using PSD.

*The longest delay time, 35.8-85.5 s, was omitted due to the unfavorable peak-to-background ratio in this spectrum.

γ-ray peaks is observed to approach the random background value, and the neutron peak/random-background ratio is 3.3, in contrast to the poorer ratio of 1.3 when PSD was not used. During the last six months we have re-measured neutron TOF spectra, gated by a neutron-gamma PSD system for all but the two longest delay times of Table 1. The interval 12.5-29.0 s is now being remeasured, while the 35.8-85.5 s delay time is still not amenable to measurement with lithium glass.

Generally, the agreement between our Pilot U and Li-6 glass spectra is excellent in their region of overlap, particularly when account is taken of the better energy resolution of the Pilot U measurements. Each of our delayed-neutron energy spectra has been compared with the corresponding spectrum constructed from the recent Rudstam[2] compilation, based on spectra determined for individual precursors. For each delay time shown in Table 1 there is good agreement in the gross shape of the spectrum. Furthermore, there is a very strong correlation in much of the detailed structure. The most notable systematic differences in the two data sets are: a) for the five shortest delay times of Table 1, our spectra indicate a somewhat larger fraction of high-energy neutrons (E_n>0.8 MeV); b) for the two shortest delay times the Studsvik spectra display more pronounced structure at low neutron energies (E_n<0.3 MeV), although the energy resolution of the experiments is similar in this energy region. The latter discrepancy may perhaps be attributed to the incompleteness of the data base used by Rudstam for the spectra of some of the short-lived precursors.

A sensitive procedure has been developed to search for a dependence of the composite delayed-neutron spectra on the energy of the neutrons inducing fission in ^{235}U. Ideally one should measure delayed neutron spectra in sets of two; one spectrum measured with fission induced by thermal neutrons followed immediately by a second spectrum measured with fission induced by fast neutrons. All other parameters such as detector geometry, transfer tape speed, beta count rate, and background environment should remain basically unchanged. A comparison of the two spectra in a set measured under identical conditions would accentuate differences, namely the dependence of the energy of the neutrons causing fission. Our approach closely approximates the ideal described above.

Fast neutron fission measurements were made on the 5.5-MV Van-de-Graaff with the $^{7}Li(p,n)$ reaction. To make fast neutrons the dominant mode for inducing fission, we simply run in an essentially bare geometry and surround the fission chamber with cadmium to remove any residual thermal neutrons. To make thermal neutrons the dominant mode, the fission chamber and target assembly are imbedded in a paraffin block approximately 3 cubic feet in volume.

A truly bare geometry is undesirable because with the large neutron fluences generated, neutron backgrounds can be observed in all neighboring environments including the control room and the counting room housing the

spectrometer. We, therefore, studied the properties of cavities both mathemetically and experimentally and found that a neutron cave (1 m in diameter and 2.2 m long with the fission chamber and target assembly positioned at is center) could be tolerated. We are now able to create a neutron environment for the fission chamber on the Van-de-Graaff acccelerator where fission is induced approximately 90% of the time by thermal neutrons, or alternatively, approximately 90% of the time by fast neutrons.

The most sensitive approach to analyze a fast-induced/thermal-induced pair of time-of-flight spectra would be to normalize the spectra and subtract one from the other. All but differences in the neutron spectra should remain. The difference spectrum can then be converted to an energy spectrum in the normal manner. When this procedure is applied to our first three sets of delayed-neutron spectra measured with the ^{6}Li-glass detectors the difference spectra generated in Fig. C-2 clearly display a difference structure that evolves from one delay-time interval to the next, as would be expected. Average statistical uncertainties associated with these difference spectra are displayed in the central region at energies of 50, 150, 250 and 350 keV. Much of the structure exceeds these uncertainties.

Final results of all our delayed-neutron energy spectra resulting from thermal fission of U-235 will be presented at the International Conference of Nuclear Data for Basic and Applied Science in Sante Fe, N.M. A more detailed paper to be submitted to Nuclear Science and Engineering is now in preparation.

In addition to the above measurements on U-235 we plan to extend our delayed-neutron studies to include Pu-239 and U-233. The fissionable isotopes Pu-239 and U-233 are considerably more toxic and/or radioactive than U-235. To study their delayed-neutron spectra by our helium jet transfer method, two new fission chambers needed to be lined with metal foils of these enriched isotopes by the Isotopes Division of Oak Ridge National Laboratory. Furthermore, the surfaces of the foils required stabilization to prevent oxidization and to ensure that large clusters of metal atoms would not be released in the natural radioactive decay of these nuclides. A 50-100 $\mu g/cm^2$ gold layer is evaporated onto the fission foil for this purpose. Having just received shipment of our Pu-239 fission chamber from the ORNL Isotopes Division, we shall immediately begin measurements of its delayed-neutron energy spectra. Fabrication of the U-233 fission chamber is scheduled to begin shortly, and studies with this isotope will begin later this year.

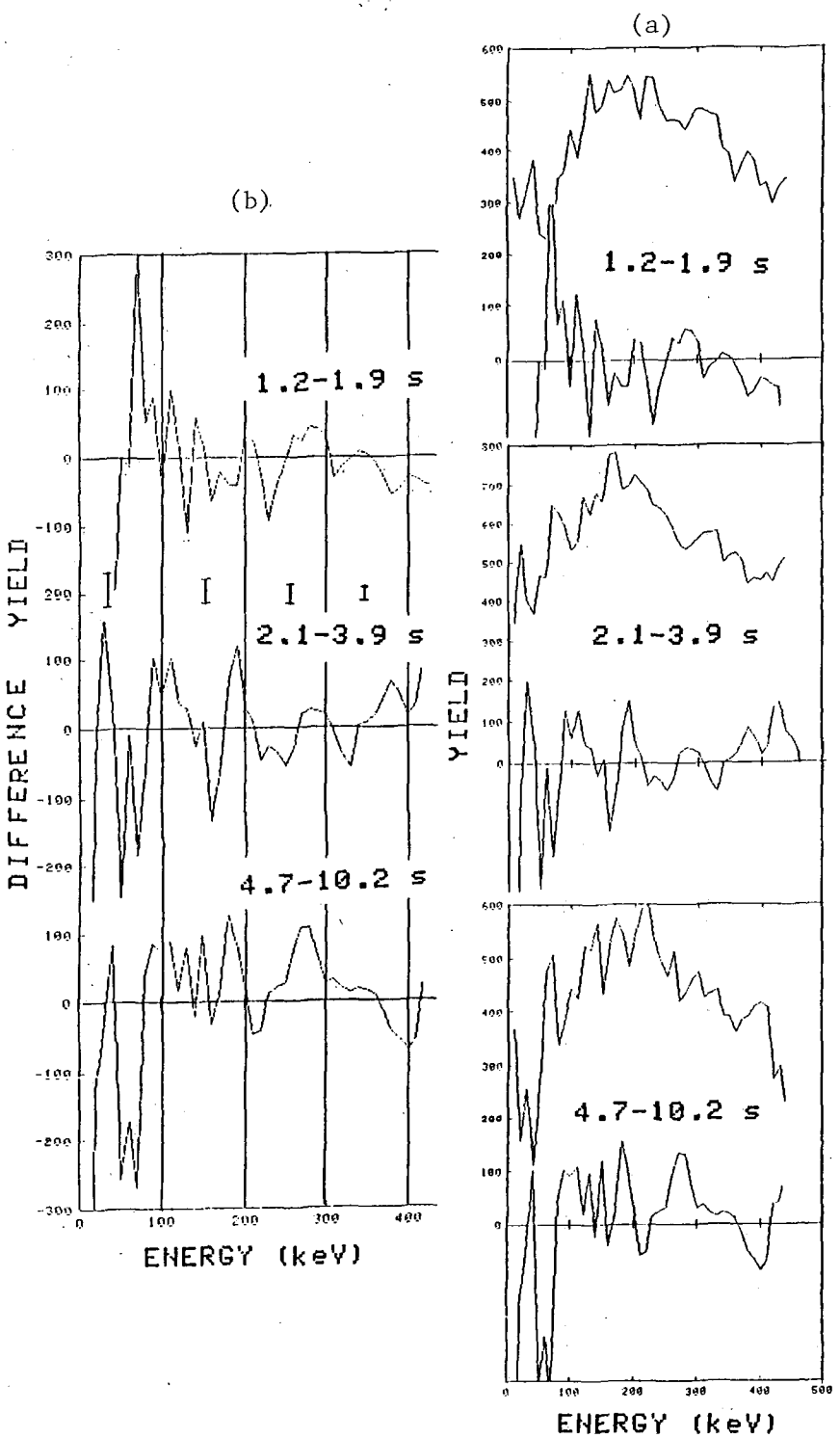

Fig. C-2. (a) Delayed neutron difference spectra of ^{235}U measured with ^{6}Li-glass scintillators. (b) Thermal-induced delayed-neutron spectra with the normalized difference spectra superimposed for the three labeled delay time intervals.

THE UNIVERSITY OF MICHIGAN
DEPARTMENT OF NUCLEAR ENGINEERING

A. INTRODUCTION

We continue to carry out activities in two major experimental areas. The first of these exploits the extensive facilities we have developed for the irradiation, handling, and calibration of highly active photoneutron sources. These facilities are housed adjacent to the 2 MW Ford Nuclear Reactor, and make use of a one meter diameter manganese bath and low-albedo experimental laboratory. The second set of activities make use of a 150 kV Cockroft-Walton accelerator operated as a 14 MeV neutron generator. The accelerator is mounted on a low scatter platform in the center of a large-volume shielded laboratory to minimize corrections due to room scatter neutrons. Extensive beta and gamma counting facilities have been developed in conjunction with both laboratories.

B. CAPTURE CROSS SECTIONS OF Th-232 AND U-238

(S. Wilderman, E. Quang, G. Knoll)

We are carrying out experiments aimed at measuring the Th-232 and U-238 capture cross sections from 140 to 964 keV using our photoneutron facilities. In the case of thorium, techniques are similar to those described earlier[1] for a measurement at 23 keV using an antimony-beryllium source. Other photoneutron sources are now being used to extend the measurement to higher energies. Because of the low neutron yields involved, high efficiency gamma counting techniques have replaced the germanium detector based methods of our previous measurements. We are relying on multistage chemical separation techniques to isolate the induced Pa-233 activity from the large natural activity of the thorium target.

Similar separation techniques have now been demonstrated for the Np-239 activity from irradiated targets of U-238. In order to quantify the separation yield, we have chosen to use Np-237 as a tracer. After investigating alternative techniques such as liquid scintillation counting of the alpha activity, we have decided instead to use the gamma activity of the decay product, Pa-233. Its 27 day half-life is short enough to allow its activity to build into equilibrium from freshly separated neptunium over a period of several months. Because the quantification of the separation yield involves only ratios of activities, true equilibrium need not be reached, and we are able to make useful measurements within several weeks of the separation process.

---

[1] G. T. Baldwin and G. F. Knoll, "Absolute Measurement of the Cross Section for 23-keV Neutron Activation of Thorium," ANL-83-4, Proc. of the NEANDC/NEACRP Specialists' Meeting on Fast-Neutron Cross Sections, April, 1982, at Argonne National Laboratory, pp. 302-311.

C. MEASUREMENT OF THE 14 MeV FISSION CROSS SECTIONS FOR U-233 AND Np-237 (K. Zasadny, H. Agrawal, M. Mahdavi, G. Knoll)

As an extension of previously reported[2] measurements of the 14 MeV fission cross sections for U-235 and Pu-239, we have applied similar experimental techniques to derive fission cross section values for U-233 and Np-237 at a neutron energy of 14.62 MeV. The fission deposits were irradiated with neutrons produced by the $T(d,n)^4He$ reaction at 0° relative to the deuteron beam. Accurate measurement of the mean neutron energy is accomplished by irradiation of a silicon surface barrier detector at 0° and 96° and measuring the alpha-zero peak shift.[3] The mean neutron energy was determined to be 14.62 $\pm$ .02 MeV.

The average neutron flux at the deposit was measured by iron foil activation. The activation products of the $^{56}Fe(n,p)^{56}Mn$ reaction were counted in a 4-pi gas-flow proportional counter whose beta detection efficiency for a particular foil was determined by 4-pi beta-gamma coincidence counting techniques. Corrections for the time variation of the neutron flux were made by monitoring the flux versus time with a long counter. The reference cross section value assumed[4] for the $^{56}Fe(n,p)^{56}Mn$ activation reaction was 110.8$\pm$ 1 mb.

The fission deposits are 2.75 cm diameter x 1 mg/cm^2 evaporations on a platinum backing of thickness 0.0508 cm. Fission targets were fabricated at Oak Ridge National Laboratory and an accurate micro-balance weighing of the targets before and after evaporation serves as an accurate mass determination ($\pm$ .05%).

Fission fragments were recorded in a limited solid angle geometry by a polyester track-etch detector film. The limited solid angle technique minimizes fission fragment energy loss in the deposit surface, but requires knowledge of the angular distribution of emitted fragments to calculate the total fission cross section. The present cross section values depend on previous measurements of the U-233 and Np-237 fission fragment anisotropy evaluated[5] at 14.6 MeV. Anisotropy values used in the present calculations at 14.6 MeV are 1.32 $\pm$ .13 for U-233 and 1.14 $\pm$ .11 for Np-237. The uncertainties quoted in these values arise primarily from the extrapolation of previously published values to a neutron energy of 14.6 MeV. Our cross

---

[2] M. Mahdavi, G. F. Knoll, J. C. Robertson, Proc. of Int. Conference Nuclear Data for Science and Technology, Antwerp, Sept. 6-10, 1982, pp. 58-61.

[3] T. B. Ryves, K. J. Zieba, Nucl. Inst. and Meth., 167, 449 (1979).

[4] T. B. Ryves, E. J. Axton, NBS Pub. 594, 980 (1980).

[5] N. K. Chaudhuri, et al., Nuclear Tracks, 3, 69 (1978).

section values will be recalculated upon completion of our own fission anisotropy measurements. However, a 10% change in the anisotropy parameter, in the worst case, leads to a 1% change in the calculated fission cross section. Fission fragment tracks are counted manually by two independent scanners until less than .25% discrepancy is achieved.

Major corrections to the measured fission cross sections are (sign refers to an increase or decrease in the measured cross section): 1. Correction of the anisotropy of fission fragments from the center of mass to lab coordinate system, with a value determined to be 1.93 ± .48% for Np-237. 2. A correction due to the scattered and (n,2n) neutrons from surrounding materials was calculated by Monte Carlo techniques for the deposit platinium backings and aluminum vacuum chamber components. Scattered neutrons tend to increase the measured cross section so a correction factor from scattering was determined to be -3.1 ± 0.4%. 3. The isotopic composition of the U-233 foil warrants -0.15 ± .04% correction to the measured cross section. The high purity of the Np-237 deposit (>99.99% Np-237) eliminates the need for a similar correction to the Np-237 data. 4. Measurements are made at three different neutron source-to-deposit spacings to measure the room-scattered neutron contributions. It is assumed that the room-scattered flux is constant over the range of source-deposit spacings. Extrapolation to zero spacing eliminates the room-scattered contribution.

The measured values of total fission cross sections at 14.62 ± .02 MeV are 2.43 ± .080 b for U-233 and 2.24±.065 b for Np-237.

Major sources of uncertainty are due to the flux calculation from the iron foil activation (1.2-1.5%), fission track counting statistics (.65-.76%), anisotropy uncertainty (.40-.81%), scattering correction uncertainty (.4%) and geometric uncertainties (.24%).

D. MEASUREMENT OF THE ^{59}Co(n,alpha)^{56}Mn CROSS SECTION AT 14.6 MeV

(H. Agrawal, K. Zasadny and G. Knoll)

An accurate knowledge of the threshold reaction ^{59}Co(n,alpha)^{56}Mn cross section is important in neutron dosimetry and in fusion reactor design. We have carried out a new measurement of this cross section relative to the ^{56}Fe(n,p)^{56}Mn cross section at 14.62 MeV. In this measurement, we have paid particular attention to an accurate determination of the neutron energy and to minimizing errors ascribable to normalization of the neutron flux. Because the ^{56}Fe(n,p) reaction cross section is thought to be known with an accuracy of ±1% as a result of a recent international intercalibration effort to establish it as a primary 14 MeV flux standard,[3] an accurate absolute value for the ^{59}Co(n,alpha) reaction cross section also follows from our work.

Back-to-back irradiations of cobalt and iron foils were carried out using the $T(d,n)^4He$ reaction at 0° relative to the incident 150 keV deuteron beam. The ^{56}Mn beta- activity induced in both the cobalt sample and iron monitor foil was measured absolutely in a 4-pi gas-flow proportional counter. A 4-pi beta-gamma coincidence counting system was used to determine the absolute efficiencies of the 4-pi proportional counter separately for each iron and cobalt foil used in these measurements with an accuracy of $\pm 1.5\%$. Corrections and special care have been taken to deal with the interfering reactions: $^{57}Fe(n,np+pn)^{56}Mn$, $^{57}Fe(n,d)^{56}Mn$, and $^{58}Fe(n,t)^{56}Mn$ from the iron foils, and $^{59}Co(n,gamma)^{60}Co$, and $^{59}Co(n,2n)^{58g,m}Co$ from the cobalt foils.

Since the tritium distribution in the neutron-producing target is not known, the mean neutron energy must be determined from a direct measurement. We used a silicon surface barrier detector as a neutron spectrometer, applying techniques described in the previous section.

Results of these measurements give a value of 0.306 ± 0.0073 for the ratio of the $^{58}Co(n,alpha)^{56}Mn$ to the $^{56}Fe(n,p)^{56}Mn$ reaction cross sections. Assuming a value of 110.8 ± 1.0 mb for the latter cross section,[4] we derive an absolute value of 33.9 ± 1 mb for the $^{59}Co(n,alpha)^{56}Mn$ cross section.

The uncertainties in the present measurement ($\pm 3\%$) arise primarily in determination of the ratio of the induced activities, and include errors in foil masses, geometric efficiencies, and counting statistics. The 1% uncertainty in the $^{56}Fe(n,p)$ reference cross section does not significantly increase the overall uncertainty.

A. NEUTRON DATA MEASUREMENTS AND DETECTORS

1. Absolute Measurements of the $^{235}U(n,f)$ Cross Section for Neutron Energies from 0.3 to 3 MeV (A. D. Carlson, J. W. Behrens, R. G. Johnson, G. F. Cooper)

Measurements of the ^{235}U neutron fission cross section have been made at the NBS neutron time-of-flight facility. The neutron flux was measured at the 200 m end station with a Black Neutron Detector. The ^{235}U fission reaction rate was determined with a fission chamber located on the same beam line at 69 m from the neutron target. A paper[1] on this work was given at the recent IAEA Advisory Group Meeting.

The present data are shown in Fig. A-1. These absolute measurements are grouped to statistical uncertainties of 1% and have total uncertainties of about 2%. In the upper part of Fig. A-1 the present measurements from 0.3 to 1.2 MeV are compared with previous NBS measurements in this energy range. The statistical and total uncertainties are indicated by the small and large error bars, respectively. The Wasson (1976) data[2] are linac measurements made using a hydrogen gas proportional counter for the neutron flux determination and are essentially uncorrelated with the present data. The Wasson et al. (1982) measurements[3] are Van de Graaff data which were obtained with the same fission chamber and Black Neutron Detector as was used for the present measurements. Thus there are appreciable correlations with the present measurements. There is generally good agreement among the measurements throughout the entire energy range; however, the present data are systematically somewhat lower than the previous measurments, particularly in the central part of the energy range. All three data sets are lower than the ENDF/B-V evaluation.

In the lower part of Fig. A-1 the present data are compared with those of Poenitz[4] and Szabo and Marquette[5] for neutron energies from 1.2-3 MeV. The error bars shown are total uncertainties. Also shown are the shape data of Carlson and Patrick[6] which have been normalized to the present absolute data over the interval from 1.5-2.5 MeV. The present measurements agree well with the data sets shown. The shape data, as normalized here, agree well with the Poenitz and Szabo data. The data sets shown here are generally lower than the ENDF/B-V evaluation.

---

[1] Carlson, Behrens, Johnson, Cooper, "Absolute Measurements of the $^{235}U(n,f)$ Cross Section for Neutron Energies from 0.3 to 3 MeV," Proc. of the IAEA Advisory Group Meeting on Nuclear Standard Reference Data, Geel, Belgium, Nov. 12-16, 1984 (to be published).

[2] O.A. Wasson, "The ^{235}U Neutron Fission Cross Section Measurement at the NBS Linac" as reported in Ref. 3.

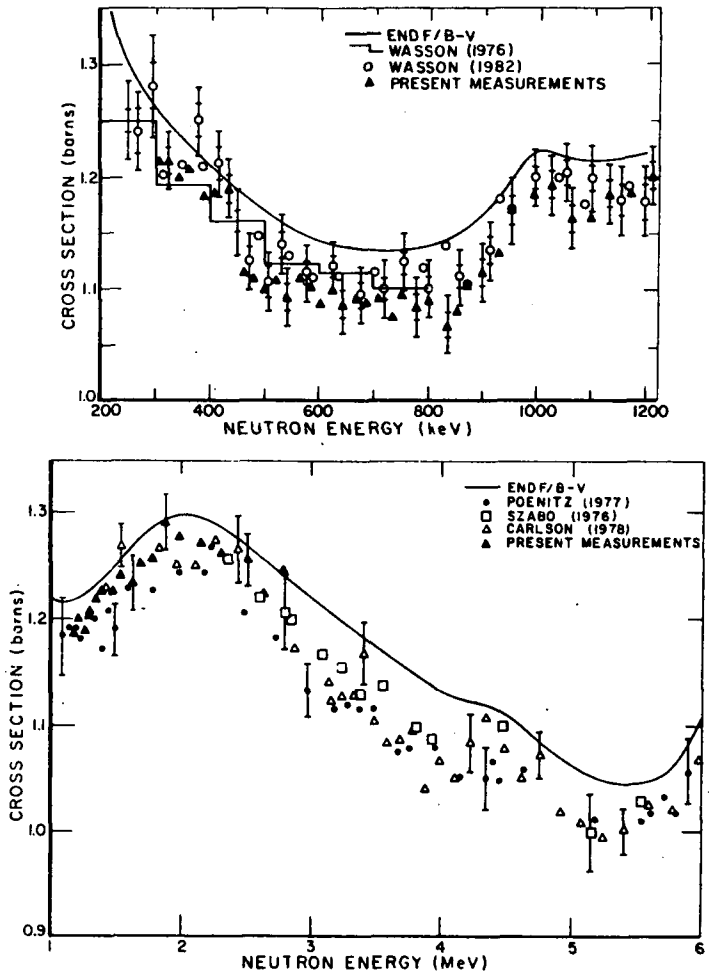

Fig. A-1. Comparison of the present data with some of the previous absolute measurements [2,3,4,5] for neutron energies from 0.3-1.2 MeV (upper part of the figure) and for the higher neutron energies (lower part of the figure). Also shown is the shape data of Carlson and Patrick[6] normalized to the present measurements over the interval from 1.5-2.5 MeV.

[3] Wasson, Meier, and Duvall, Nucl. Sci. Engng. 81, 196 (1982).

[4] W.P. Poenitz, Nucl. Sci. Engng. 64, 894 (1977).

[5] I. Szabo and J.P. Marquette, "Measurement of the Neutron Induced Fission Cross Sections of Uranium-235 and Plutonium-239 in the MeV Energy Range" in Proc. of the NEANDC/NEACRP Specialists Meeting on Fast Neutron Cross Sections of U-233, U-235, U-238, and Pu-239, Argonne National Laboratory (Eds. W.P. Poenitz and A.B. Smith) ANL-76-90, p. 208 (1976).

[6] A.D. Carlson and B.H. Patrick, "Measurement of the ^{235}U Fission Cross Section in the MeV Energy Region," in Proc. of an Int. Conf. on Neutron Physics and Nuclear Data for Reactors and Other Applied Purposes, Harwell, p. 880 (1978).

2. An Absolute Measurement of the ^{235}U Fission Cross Section for Neutron Energies from 2 to 6 MeV (M. S. Dias,* R. G. Johnson, A. D. Carlson, O. A. Wasson)

The dual thin scintillator (DTS) neutron detector[7] was used as the neutron flux monitor for a measurement of the ^{235}U fission cross section over the 2 to 6 MeV range. The neutron flux was measured at the 200-m station of the NBS Neutron Time-of-Flight facility while the fission chamber was placed at 69 m on the same flight line. Preliminary results of the measurement have been recently reported.[8] The final report on this measurement is in preparation.

3. Uranium-235 Fission Cross Section Measurement from Thermal to 1. keV (R. A. Schrack)

A measurement of the fission cross section relative to the shape of the $^{10}B(n,\alpha)$ cross section is planned using a parallel plate ionization chamber with boron-10 coated plates as the neutron flux monitor. Computer model studies of chamber performance have been carried out with estimations of expected uncertainties. The experiment is being designed to reduce as much as possible or cancel systematic errors. A special fission chamber and integrated neutron flux monitor has been designed and is under construction. The parameters of the design are optimized for the measurement of the U-235 fission cross section from .025 to 1000 eV.

4. Absolute $^{235}U(n,f)$ Cross Section Measurement at 2.5 MeV (K. C. Duvall, O. A. Wasson, A. D. Carlson)

A measurement of the $^{235}U(n,f)$ cross section at 2.5 MeV using the time-correlated associated particle technique is being reconsidered in view of the recent purchase of a 100 kV, 0.5 mA ion generator. The high current, low energy deuteron beam will be used in conjunction with the $D(d,n)^3He$ reaction to provide the necessary 2.5 MeV neutron yield while employing foil absorption methods for discrimination against the scattered incident beam. A fission chamber containing several thin, large diameter, and highly uniform U-235 foils will be used to minimize important corrections associated with fission fragment detection and the experimental geometry. This cross section measurement is expected to achieve the ±1.5% (1σ) accuracy required.

---

* Present address: Instituto de Pesquisas Energêticas e Nucleares - São Paulo - Brazil.

[7] Dias, Johnson, Wasson, Nucl. Instr. and Meth. 224 (1984) 532.

[8] Dias, Carlson, Johnson, Wasson, Proceedings of the IAEA Advisory Group Meeting on Nuclear Standard Reference Data, 12-16 November 1984, Geel, Belgium.

5. Analysis of the Effect of Random Events on the 14 MeV $^{235}U(n,f)$ Cross Section Standard Measurement (O. A. Wasson, A. D. Carlson, K. C. Duvall)

The most accurate measurements of the $^{235}U(n,f)$ cross section at 14 MeV neutron energy have used the Time-Correlated Associated-Particle Technique (TCAP) with the $T(d,n)^4He$ reaction. These measurements, using three independent ^{235}U mass standards, are in excellent agreement (1%). However, it has recently been suggested[9] that some of these published measurements should be changed because of the effect of random events on the coincidence timing. Since the NBS conditions differed from those encountered in many other similar experiments, a detailed analysis of the NBS experiment and the electronic suppression of coincidence losses due to random events was performed. The unique combination of electronic components incorporated in the experiment eliminated the effect of losses due to random events in the timing analyzer. There is, thus, no correction to apply and no change in the published value[10] of the NBS measurement is warranted.

6. Detector Development for eV Neutron Scattering Spectrometers (R. G. Johnson)

Detector development for resonance detector spectrometers (RDS) to extend neutron scattering studies to the eV region has continued. In this technique the energy of the scattered neutron is defined by a low energy nuclear resonance. Previously the use of a large area planar HPGe detector which detects the x rays from internal conversion of γ rays following neutron capture was shown to provide good efficiency and good background rejection. Since in the internal conversion process both an electron and an x ray are emitted, detecting both signals in coincidence can improve the background rejection. To test this method two thin gold foils (3-μm thick) were placed between three 1.0-mm thick plastic scintillators. Electrons detected by the plastic scintillator provided a coincidence gate for the HPGe detector. Even with this less than optimum foil and scintillator thicknesses an improvement of ~ 2.5 in the signal to background ratio was observed when operating in the coincidence mode as opposed to the non-coincidence mode. The concept appears to work well and will be developed further.

[9] W.P. Poenitz, (private communication), June 18, 1984.

[10] Wasson, Carlson, Duvall, Nucl. Sci. Eng. 80, 282-303 (1982).

7. New Measurement of the Ratio of the $^{10}B(n,\alpha)$ to $^{6}Li(n,t)$ Cross Sections in the eV Energy Region (A. D. Carlson)

A previous measurement[11] has indicated a deviation of ~ 2% near 10 eV compared with ENDF/B-V for the ratio of the $^{10}B(n,\alpha)$ and $^{6}Li(n,t)$ cross sections. It was surmised that the effect was probably not due to the nuclear cross sections but instead to difficulties in implementing them such as molecular effects in the ^{6}Li glass response. A new measurement is now underway with some improvements compared with the previous experiment. An important change is an increase in the number of black resonance background determinations. Thus possible errors in interpolation of the background will be reduced. Two different Li glass detectors will be investigated, one containing natural abundance lithium and the other containing lithium enriched in ^{6}Li.

8. Development of the Dual Thin Scintillator (DTS) in the 1 + 2 Coincidence Configuration as a Neutron Spectrometer (K. C. Duvall, R. G. Johnson)

The Dual Thin Scintillator (DTS) has been designed and built at the National Bureau of Standards (NBS) for use as an absolute neutron flux monitor in the energy range of 1-20 MeV. The DTS detector consists of two thin, back to back plastic scintillators optically separated from each other and independently coupled to photomultiplier tubes. The detector may be operated in the 1 + 2 coincidence configuration where only simultaneous events in both first and second scintillator are recorded. The events recorded in the 1 + 2 coincidence configuration are due primarily to proton recoils that are produced in the first scintillator and pass into the second scintillator. The energy distribution of the proton recoils recorded is affected by the range of the recoil particles and is determined by the angles allowed for path lengths reaching into the second scintillator. The detector pulse height distribution consists, therefore, of contributions from the more forward scattered, higher energy proton recoil events and exhibits a more peaked response, centered at the incident neutron energy. This is a more favorable response function to be used with spectrum unfolding techniques and should provide improvement over spectral determinations with conventional proton recoil response functions. The usefulness of the DTS detector in the 1 + 2 coincidence configuration for determining neutron energy distribution will be demonstrated.

[11] J.B. Czirr and A.D. Carlson, "Measurement of the $^{10}B/^{6}Li$ Cross Section Ratio Below 1 keV," in Proc. of the Int. Conf. on Nuclear Cross Sections for Technology, NBS Spec. Publ. 594, p. 84 (1980).

9. Development of Rutherford Backscattering Facility for Analysis of UO_2 Samples (O. A. Wasson, W. E. Slater, H. Frederikse)

A Rutherford Backscattering (RBS) facility was established on a new beam line at the 3-MV positive ion Van de Graaff laboratory. This facility, in collaboration with scientists from the Center for Materials Science, is being utilized for studies of the areal density distribution of uranium deposits used in neutron cross section measurements. A versatile scattering chamber with numerous ports, 5 axis goniometer, target ladder, and solid state detector is in operation. In addition to the hydrogen and deuterium beam used for neutron production, the accelerator was modified to produce 1.3 MeV He^+ beams with currents as large as 10 microamperes and 5-MeV He^{2+} beams with currents as large as 100 nanoamperes. The variation in areal density of a 75 cm diameter UO_2 deposit was measured using a 1 MeV He^+ beam. The results are in excellent agreement with those obtained from α-activity measurements.

10. Profile of UO_2 Deposits by α-Particle Counting (R. A. Schrack)

Deposits of U-235 in the form of UO_2 on aluminum backing were obtained from Oak Ridge National Laboratory. The deposits are three inches in diameter and vary in uniformity. Use of the foils in a fission chamber being built to measure the U-235 fission cross section requires a knowledge of the deposit uniformity. Fortunately, the material used to produce the uranium deposit had a 0.99% contribution of U-234. This isotope has a relatively high probability of decay by α-particle emission. Assuming that there is no isotopic separation during deposition, the U-234 distribution can be measured by α-particle detection to determine the U-235 distribution. A collimator system for the α-particle detector was designed and its efficiency and response function determined by a Monte Carlo program. The results from the measurements are in good agreement with those from Rutherford Backscattering and show that the density of the deposit drops by at least 10% from the center to the edge. This variation is acceptable if the fission chamber is to be used for relative measurements but will necessitate careful measurement and corrections for absolute cross section measurements.

11. Neutron Resonance Transmission Analysis of Reactor Fuel Samples (J. Behrens, R. Johnson, R. Schrack)

Neutron resonance transmission analysis has been used to measure the isotopic content of fresh and spent nuclear reactor fuel samples. Our final results have been published.[12]

[12] Behrens, Johnson, Schrack, Nucl. Technol. 67, pp. 162-168 (Oct. 1984).

12. Neutron Resonance Transmission Analysis for NDS of Proximity Fuzes (R. G. Johnson, R. A. Schrack)

In collaboration with Harry Diamond Laboratories we have recently applied the technique of neutron resonance transmission analysis (NRTA) to nondestructively assay (NDA) the power supplies of M732 proximity fuzes. Some of these power supplies, which are simple lead-acid batteries, were failing when the acid leaked from its ampule into the normally separate volume containing the lead plates. In addition to the acid, a buffering agent, methylene bromide, is contained in the ampule. The NRTA technique was used to detect the presence of bromine (using the 35.8-eV resonance) in part of the battery containing the lead plates. Measurements were performed at the NBS Neutron Time-of-Flight facility where the fuze was placed at ~ 6 m from the source and the neutron beam was collimated to a 3.2 cm by 0.64 cm area. Transmitted neutrons were detected at 6.73 m by a ^{6}Li-glass scintillator (4.4-cm diameter by 2.5 cm thick). Originally it was expected that the observation of bromine would be difficult because only the presence of methylene bromide vapor was anticipated. However, experimentally a strong bromine resonance was observed in known bad batteries. We found that the methylene bromide was being concentrated because it attacked the plastic case of the battery. The NRTA technique appears to be a useful method to screen M732 proximity fuzes.

13. Measurement of the NBS Black Neutron Detector Efficiency at 2.3 MeV (K. C. Duvall, A. D. Carlson, O. A. Wasson)

The absolute efficiency of the National Bureau of Standards (NBS) Black Neutron Detector at 2.3 MeV has been measured using the time-correlated associated particle method. Until recently, the NBS Black Neutron Detector had been utilized only in the limited energy range of 0.2 to 1.2 MeV, where the efficiency determination from Monte Carlo calculations has been verified by experiment. A result of 0.760 has been obtained for the Black Neutron Detector efficiency at 2.3 MeV with an experimental uncertainty of ±1.2% and agrees well with the Monte Carlo calculated value. The measurement extends the usefulness of the Black Neutron Detector as an absolute neutron flux monitor to the higher energy region and in fact has been used to measure the ^{235}U(n,f) cross section from 0.3 to 3.0 MeV.

14. The Development of a 6 to 7 MeV Photon Field for Detector Calibrations (K. C. Duvall)

A photon source has been developed at the National Bureau of Standards to measure the response of radiation detection instruments to high-energy photons. The ^{19}F(p,$\alpha\gamma$)^{16}O reaction has been used to produce a 6 to 7 MeV photon field with a fairly uniform photon flux density of approximately 3×10^{3} cm^{-2}s^{-1} at one meter from the source. The photon flux density is obtained from measurements with a 3x3 inch NaI detector whose absolute response has been determined by a Monte Carlo calculation. The spectral

characteristics of the photon field have been determined from measurements with a large volume high purity Germanium detector and the NaI detector with the use of unfolding techniques. The measurement of detector responses is carried out with at least 2.5 cm of plastic in front of the instruments to discriminate against the high-energy electron component in the field.

15. ^{235}U+n "Cold Fragmentation" Experiment at Institut Max Von Laue-Paul Langevin, Grenoble, France (F. Gönnewein,**, A. Oed,† P. Geltenbort,† J. Trochon,†† G. Simon,†† J. Behrens)

Cold fragmentation refers to neutron-induced fission where the fission fragments have such high kinetic energy that prompt neutron emission is not energetically possible. The mass distribution of these fragments as a function of the total kinetic energy was measured at the ILL/Grenoble High Flux Reactor thermal neutron source and the "Cosi Fan Tutte" facility which determines fragment masses by measuring velocities and kinetic energies. For this application, specially adapted time-of-flight detectors and ionization chambers were developed. The energy resolution for fragments from U-235 near mass 100 is typically 400 keV. The data analysis of this experiment is in progress.

16. ^{233}U+n and ^{235}U+n "Cold Fragmentation" Experiments at C.E.N. de Saclay, France (J. Trochon,†† G. Simon,†† F. Brisard,†† J. Behrens)

Another type of cold fragmentation experiment was conducted during June and July 1984 at the Orphée Reactor (C.E.N. de Saclay). The aim was to determine probabilities for specific mass splitting at high total kinetic energy where prompt neutron emission is again not possible. Both ^{233}U+n and ^{235}U+n were measured. The experiment utilized a dual parallel-plate ionization chamber with uranium target positioned on the central cathode. Frisch grids were used so that the fragment energies were measured on the anodes. In preparation for this experiment an entire data acquisition software package was written for a LeCroy 3500 system. Data analysis is in progress.

17. Fission Cross Section Systematics in the MeV Range (J. Behrens, J. Jary,††, J. Trochon,††)

There are at least 66 isotopes among the actinides which are of importance to present-day applications and for which nuclear data have been requested. A significant number of these requests ask for neutron-induced fission cross sections in the MeV range. Unfortunately, only 22 of these isotopes have half-lives greater than 100 years, which is needed for direct

** Institut Max Von Laue-Paul Langevin, Grenoble, France.

† Physikalisches Institut der Universitä Tübingen, Fed. Rep. Germany.

†† Centre d'Etudes de Bruyères-le-Chatel, France.

cross section measurement using standard detector systems and neutron sources. The present approach attempts to infer the fission cross section for long-lived isotopes which have been accurately measured. The present program is to complete the data sets of the uranium, neptunium, and plutonium isotopes and to compare the inferences with statistical model calculations.

B. DATA COMPILATION

1. Electron-Bremsstrahlung Cross Sections (S. M. Seltzer and M. J. Berger)

Through the synthesis of various theoretical results, a comprehensive set of bremsstrahlung cross sections (differential in the energy of the emitted photons) has been prepared. The set includes results for electrons with energies from 1 keV to 10 GeV incident on neutral atoms with atomic numbers Z = 1 to 100.

Numerous comparisons between the calculated and measured bremsstrahlung indicate generally good agreement. Of particular interest is a recent experimental test[13] of the cross sections performed by measuring photodisintegration yields in ^{63}Cu from bremsstrahlung produced in thin radiators of Cu, Mo, Ta, and Th, for electron beam energies from 20 to 60 MeV. An analysis performed using the newly synthesized bremsstrahlung cross sections, those from the unmodified Davies-Bethe-Maximon-Olsen theory, and those given by the Schiff formula, indicates that significantly better fits are obtained with the new cross section set. The authors point out the important implications for photodisintegration measurements.

A full description of the bremsstrahlung cross section set has been completed.[14] Publication of extensive tables is planned, and magnetic-tape data files are being prepared for distribution through the Photon and Charged Particle Data Center of the Center for Radiation Research.

2. Photonuclear Data-Abstract Sheets (H. Gerstenberg, E. G. Fuller)

The first seven volumes of the Photonuclear Data-Abstract Sheets,[15] including nuclei up through calcium, have been published. These abstract sheets cover most classes of experimental photonuclear data leading to information of the electromagnetic matrix element between the ground and excited states of a given nucleus. This fifteen volume work contains nearly 7200 abstract sheets and covers 89 chemical elements from hydrogen through americium. It represents a twenty-seven year history of the study of electromagnetic interactions.

[13] M.H. Martins *et al.*, Phys. Rev. C 30, 1855 (1984).

[14] S.M. Seltzer, and M.J. Berger, to appear in Nucl. Instr. Methods, Sec. B.

[15] E.G. Fuller and H. Gerstenberg, Photonuclear Data-Abstract Sheets, 1955-1984, NBSIR 83-2742 (1985).

A. CROSS SECTION MEASUREMENTS

1. Capture and Total Cross Sections

a. Parity Dependence of the Level Densities of Cr-53 and Cr-55 at High Excitations,[1] (H. M. Agrawal,[2] J. B. Garg,[3] and J. A. Harvey)

b. Neutron Capture cross sections and solar abundances of $^{160,161}Dy$, $^{170,171}Yb$, $^{175,176}Lu$, and $^{176,177}Hf$ for the s-process analysis of the radionuclide ^{176}Lu,[4] (Hermann Beer,[5] Gerold Walter,[5] R. L. Macklin, and P. J. Patchett[6])

The neutron capture cross sections and solar abundances of $^{160,161}Dy$, $^{170,171}Yb$, $^{175,176}Lu$, and $^{176,177}Hf$ have been measured. With this data base s-process studies have been carried out to determine the s-process neutron density and temperature and to investigate the s-process nucleosynthesis of the ^{176}Lu clock. From various branchings the neutron density was found to be $(0.8\text{-}1.8)\times10^8$ neutrons per cm^3 and the temperature kT to be 18-28 keV. On the basis of the present data, ^{176}Lu proved not to be applicable as a cosmic clock because of the temperature sensitivity of the ^{176}Lu half-life but can be used instead as a stellar thermometer. Constraints for the s-process temperature (kT=20-28 keV) were found to be in good agreement with the investigated branchings.

c. $^{198,199,200,201,202,204}Hg(n,\gamma)$ Cross Sections and the Termination of s-process Nucleosynthesis,[7] (H. Beer[5] and R. L. Macklin).

The neutron capture cross sections of $^{198,199,200,201,202,204}Hg$ (n,γ) were measured in the energy range 2.6 keV to 500 keV. The average capture cross sections were calculated and fitted in terms of strength functions. Resonance parameters for the observed resonances were determined by a shape analysis. Maxwellian averaged capture cross sections were computed for thermal energies kT between 5 and 100 keV. The solar mercury abundance was determined to be 0.34 ± 0.04 relative to $Si=10^6$. The termination of s-process nucleosynthesis at lead and bismuth was investigated. The abundances of $^{206,207,208}Pb$ were reproduced introducing a strong fluence

[1]Phys. Rev. C, 30, 1880 (1984).
[2]Present address: University of Michigan, Ann Arbor, MI 48109.
[3]State University of New York, Albany, NY 12222.
[4]Phys. Rev. C, 30, 464 (1984).
[5]Kernforschungszentrum Karlsruhe, Institut fur Kernphysik III, D-7500 Karlsruhe, Federal Republic of Germany.
[6]Max Planck-Institut fur Chemie, D-6500 Mainz, Federal Republic of Germany.
[7]Submitted to Physical Review C.

component of the s-process in addition to normal s- and r-process nucleosynthesis. The radiogenic ^{207}Pb abundance was determined and the r-process age was calculated via ^{235}U. Using Fowler's exponential model an age T = 4.6 Gyr + Δ = 17.2 ± 2.6 Gyr was obtained.

d. Determination of Unbound States in 35-S from Neutron Total and Capture Cross-Section Measurements on 34-S,[1] (R. F. Carlton,[2] W. M. Good, J. A. Harvey, R. L. Macklin, and B. Castel[3])

e. Optical Model Scattering Functions for Low Energy Neutrons on ^{86}Kr,[4] (R. F. Carlton,[2] J. A. Harvey and C. H. Johnson)

Using the ORELA 200-m time-of-flight facility we measured the neutron total cross section with good resolution for a 96%-enriched ^{86}Kr target and made a multilevel R-matrix analysis up to 800 keV. By averaging we deduced optical scattering functions for each partial wave and fit them by adjusting well depths in a spherical model with our standard geometry. Our preliminary best fit for the real wells has V_o = 48 MeV for ℓ=0, V_o = 52 MeV for ℓ=1 and V_{so} = 6 MeV. The resulting predicted spin-orbit enhancement of the $p_{3/2}$ strength relative to $p_{1/2}$ is a ratio of 1.7 whereas the observed ratio is 3.5. Thus, there appear to be structure effects which can be described in the optical model by W_D = 2 MeV for $p_{1/2}$ and W_D = 4 MeV for $p_{3/2}$.

f. Neutron Capture and Total Cross Sections for ^{48}Ca: Astrophysical Implications,[5] (R. F. Carlton,[2] J. A. Harvey, N. W. Hill, and R. L. Macklin)

Attempts to understand abundance anomalies of the Ca isotopes in the Allende meteorite via the nβ-process require 30-keV Maxwellian averaged capture cross sections. Experimental data on ^{48}Ca in this energy region of astrophysical significance is important since a single resonance in this vicinity could dominate the capture cross section. Neutron capture and total cross section measurements have been performed at ORELA on a 9.97-g sample of $CaCO_3$, enriched to 96% ^{48}Ca, over the energy ranges 10 eV-500 keV (σ_γ) and 10 keV-4 MeV (σ_T). Only two small resonances were found for ^{48}Ca in the 30-keV energy region (at 19.3 and 106.9 keV) and those only in capture. Their contribution to the 30-keV-averaged cross section is only 50 μb compared to 1.0 mb calculated from direct capture. The p-wave strength and large $d_{5/2}$ strength observed above 150 keV do not contribute significantly to the 30-keV capture.

[1]Phys. Rev. C. 29, 1980 (1984).
[2]Middle Tennessee State University, Murfreesboro, Tenn.
[3]Department of Physics, Queen's University, Kingston, Ontario, Canada K7L3N6.
[4]Presented at the Neutron Nucleus Collisions--A Probe of Nuclear Structure Conference, Glouster, Ohio, Sept. 5-8, 1984.
[5]Proc. of Int. Conf. on Capture Gamma-Ray Spectroscopy and Related Topics, S. Raman, Ed., Knoxville, Tenn., Sept. 10-14, 1984.

g. Neutron, Radiation and Alpha Widths of Resonances in $^{33}S+n$ from 10-400 keV,[1] (G. Coddens,[2] M. Salah,[3] J. A. Harvey, and N. W. Hill)

High resolution transmission measurements on a 0.97-g sample enriched to 88.29% ^{33}S ($I=3/2^+$) were made at ORELA using an NE-110 scintillation detector. Transmission data on this nuclide are of special interest since some of the resonances can have large alpha widths and the (n,α) cross section has been measured recently at GEEL. The multilevel R-matrix formalism (including an external R-function) was used in analyzing the data by the computer code SAMMY based on Bayes' theorem. Three exit channels (Γ_n, Γ_γ and Γ_α) were taken into account in the analysis. The 2^+ states produced by s-wave neutrons and 1^- and 3^- states produced by p-wave neutrons can decay by alpha emission, whereas 1^+, 0^-, and 2^- states do not. Neutron strength functions and level spacings for s- and p-wave neutrons were obtained.

h. Observation of Extremely Low s-wave Strength in the Reaction $^{136}Xe + n$,[4] (B. Fogelberg,[5] J. A. Harvey, M. Mizumoto,[6] and S. Raman)

The neutron cross section of ^{136}Xe has been investigated at the Oak Ridge Electron Linear Accelerator (ORELA). A sample of xenon gas, enriched to 93.6% in ^{136}Xe, was used as target. Measurements were made with an energy resolution of $\sim$ 0.1%. The transmission data, which were analyzed for neutron energies below 500 keV, show 35 resonances in this region. Only four very weak resonances were found to be possibly due to s-wave neutron interactions, giving an extremely low value for the s-wave strength function in the analyzed region.

i. $d_{5/2}$-Single Particle Strength in $^{48}Ca + n$,[1] (J. A. Harvey, C. H. Johnson, R. F. Carlton,[7] and Boris Castel[8])

The neutron total cross section of ^{48}Ca was measured up to 4 MeV and the data analyzed using an R-matrix code to obtain resonance parameters and potential scattering phase shifts. No s-wave resonances were observed and the small cross section ($\sim$ 0.5 b) at low energy requires a real well depth of 48 MeV. Three strong d-wave resonances (amounting to 45% of the single particle limit) were found in the 0.8 to 2.0 MeV energy region. Shell-model-in-the-continuum calculations agree with these observations.

---

[1]Neutron Nucleus Collisions -- A Probe of Nuclear Structure Conference, Sept. 5-8, 1984, Glouster, Ohio.
[2]Commisariat a L'Energie Atomique, Laboratoire Leon Brillouin, France.
[3]Graduate student from Minia University, Egypt.
[4]Proc. of Int. Conf. on Capture Gamma-Ray Spectroscopy and Related Topics, S. Raman, Ed., Knoxville, Tenn., Sept. 10-14, 1984.
[5]The Studsvik Science Research Laboratory, S-611 82 Nykoping, Sweden.
[6]JAERI, Tokai-Mura, Naka-gun, Ibaraki-Ken, Japan.
[7]Middle Tennessee State University, Murfreesboro, TN 37132
[8]Queen's University, Kingston, Canada K7L 3N 6

j. Measurements of the Neutron Transmission and Capture Cross Sections in 204-Pb,[1] (D. J. Horen, R. L. Macklin, J. A. Harvey, and N. W. Hill)

k. Cesium-133 Neutron Capture Cross Section,[2] (R. L. Macklin)

l. Technetium-99 Neutron Capture Cross Section,[3] (R. L. Macklin)

m. Resonance Neutron Capture by 35,37-Cl,[4] (R. L. Macklin)

n. Neutron Capture Cross Sections of Tantalum from 2.6 to 1900 keV,[5] (R. L. Macklin)

o. Resonance Neutron Capture by $^{39,41}K$,[6] (R. L. Macklin)

Neutron capture by a sample enriched in ^{41}K and by a natural potassium sample (93.26% ^{39}K) was measured at the Oak Ridge Electron Linear Accelerator as a function of neutron time of flight over a 40-m flight path. Resonance peaks were fitted by a least-squares fitting program to obtain Breit-Wigner resonance parameters. The energy range extended to all resonances below 153 keV. Corresponding average capture at a temperature typical of stars, kT = 30 keV, is calculated as (11.8 ± 0.4) mb for ^{39}K and (22.0 ± 0.7) mb for ^{41}K.

p. Neutron Capture Measurements on Fission Product ^{107}Pd,[7] (R. L. Macklin)

Neutron capture measurements were made on a sample of fission product palladium at the Oak Ridge Electron Linear Accelerator time-of-flight facility. One hundred thirty resonance peaks were parameterized up to 3.5 keV and the average cross section from 3 to 600 keV was derived. The data exceed the ENDF/B-V evaluation by ∿25% in the 3- to 300-keV range but drop steeply below it at higher energies where neutron inelastic-scattering competition becomes important. The Maxwellian average cross section for kT = 30 keV is calculated as 1.34 ± 0.06 b, and the dilute resonance capture integral as 108.1 ± 4.3 b.

[1]Phys. Rev. C, 29, 2126 (1984).
[2]Nucl. Sci. Eng. 81, 418 (1982).
[3]Nucl. Sci. Eng. 81, 520 (1982).
[4]Phys. Rev. C, 29, 1996 (1984).
[5]Nucl. Sci. Eng. 86, 362 (1984).
[6]Nucl. Sci. Eng. 88, 129-142 (1984).
[7]Nucl. Sci. Eng. 89, 79-86 (1985).

q. Resonance Neutron Capture by Manganese Below 2.5 keV,[1] (R. L. Macklin)

Radiation widths Γ_γ of (310 ± 20), (312 ± 12), and (340 ± 130) meV were found for $^{55}Mn(n,\gamma)$ resonances at 337, 1099, and 2327 eV, respectively. A fourth resonance was found at 1658 eV, with $g\Gamma_n\Gamma_\gamma/\Gamma$ = (7.6 ± 0.3) meV.

r. Neutron Capture Measurements on Radioactive ^{93}Zr,[2] (R. L. Macklin)

Neutron capture measurements made on a sample of fission-product zirconium containing 20% ^{93}Zr ($t_{1/2} = 1.5 \times 10^6$ a) at the Oak Ridge Electron Linear Accelerator time-of-flight facility resulted in the identification of 138 resonance peaks for the ^{93}Zr isotope at neutron energies up to 21.5 keV. Average capture cross sections from 20 keV to 300 keV were derived by subtracting neutron capture yields of the stable zirconium isotopes $^{90,91,92,94,96}Zr$ and additional backgrounds. The average cross sections found were significantly less than those of JENDL-1. While generally 30% higher than those of ENDF/B-V below 60 keV, the binned data overlapped the smooth ENDF/B-V curve. The average for a Maxwellian neutron spectrum with kT = 30 keV is (95 ± 10) mb and the resonance contribution to the capture resonance integral is (15.0 ± 0.5) b.

s. Accurate Determination of the Parameters of the 292.4-eV Resonance of ^{91}Zr and the 301.3-eV Resonance of ^{96}Zr.[3] (M. M. Salah,[4] J. A. Harvey, N. W. Hill, A. Z. Hussein,[4] and F. G. Perey)

High-resolution transmission measurements of zirconium metal samples have been carried out at ORELA using the 80-m flight path and an improved ^6Li-glass scintillation neutron detector. Zirconium is used for reactor fuel cladding and some structural components. Neutron capture by the low energy resonances is important and resonance parameters from earlier measurements were in disagreement. Four different thicknesses of the pure zirconium metal and one sample of zircalloy were used in four separate experiments. The transmission data for these samples were measured at room temperature, and one sample was cooled to liquid nitrogen temperature. These data were analyzed using the multilevel R-matrix computer code SAMMY. The resonance parameters obtained for this s-wave resonance of ^{91}Zr (not including systematic uncertainties) are: $J^\pi = 3^+$, E_o = 292.40 ± 0.10 eV, Γ_n = 665 ± 3 meV, Γ_γ = 131 ± 7 meV, and $cc(\Gamma_n,\Gamma_\gamma)$ = 0.27. The p-wave resonance of ^{96}Zr at 301.3 eV with J=1/2 has been also analyzed and the parameters obtained are: E_o = 301.14 ± 0.10 eV, Γ_n + 223 ± 7 meV, Γ_γ = 235 ± 38 meV, and $cc(\Gamma_n,\Gamma_\gamma)$ = 0.80.

[1]Accepted by Nucl. Sci. Eng. (December 1984).
[2]Submitted to Astrophysics and Space Science (January 1985).
[3]Int. Conf. on Nucl. Data for Basic and Applied Science, May 13-17, 1985, Santa Fe, N.M.
[4]Visiting scientists from Egypt.

t. Capture in the 1.15-keV Iron Resonance.[1] (L. W. Weston and J. H. Todd)

The 1.15-keV resonance in iron is important to reactors in that a major part of the iron capture integral is due to this one resonance. This resonance is also a good test case for capture gamma-ray detectors, which are meant to have an efficiency independent of gamma-ray energy spectra, because this resonance has an unusually hard spectrum and other iron resonances do not. There have been severe discrepancies among different groups who have measured the capture area and transmission of this resonance. A new measurement, employing C_6F_6 liquid scintillators and pulse-height weighting to effect total energy detectors, has been made of the ratio of the capture area of the 22.8-keV resonance relative to that of the 1.15-keV resonance. The 22.8-keV resonance has a relatively soft gamma-ray spectrum and there is agreement on the capture area. The results (2.91 ± 0.17) agree well with transmission measurements and confirm the applicability of total energy detectors for use on capture resonances with very hard capture gamma-ray spectra.

u. Neutron Capture in s-Wave Resonances of Nickel-64,[2] (K. Wisshak,[3] F. Kappeler,[3] R. L. Macklin, G. Reffo,[4] and F. Fabbri[4])

2. Scattering and Reactions

a. High-Resolution Structural Material (n,xγ) Production Cross Sections for E_n from 0.2 to 40 MeV,[1] (D. C. Larson)

A program has been initiated at the Oak Ridge Electron Linear Accelerator (ORELA) to measure yields of individual gamma rays resulting from interactions of 0.2- to 40-MeV neutrons with structural materials of interest both for applied needs and basic research. A high-resolution gamma-ray detector and two-parameter (neutron time-of-flight vs gamma-ray pulse height) techniques are used to record approximately 40 pulse-height 4K-channel spectra for $0.2 \leqslant E_\gamma \leqslant 10$ MeV corresponding to approximately 40 incident neutron-energy bins covering the 0.2- to 40-MeV range. The neutron flight-path length is 22 m, and the well-shielded Ge(Li) detector is located at an angle of 125° with respect to the incident beam direction and positioned 40 cm from the center of the sample under study. The neutron flux required for reduction of the data to absolute cross sections was carefully measured using NE110 detectors and Monte Carlo calculations were employed to establish the absolute efficiencies of these flux detectors. A small NE110

[1]Int. Conf. on Nuclear Data for Basic and Applied Sciences, May 13-17, 1985, Santa Fe, N. M.
[2]Nucl. Sci. Eng. 87, 48-58 (1984).
[3]Kernforschungszentrum Karlsruhe, Institut fur Kernphysik III, P. O. Box 3640, D-7500 Karlsruhe, Federal Republic of Germany.
[4]Laboratorio Dati Nucleari Ente Nazionale per l'Energie Alternative, Via G. Mazzini 2, 40138 Bologna, Italy.

detector was used as a monitor detector to determine the number of neutrons striking the sample. The efficiency and resolution of the gamma-ray detector as a function of gamma-ray energy was measured using sources for $0.06 \leqslant E_\gamma \leqslant 6.1$ MeV. The electronic setup for the experiment is straightforward with the gamma flash from the accelerator being analyzed and stored to provide a constant neutron-energy calibration, and digitization of the pulse height near the detector being done to eliminate noise pickup over the ∿40 m of cable to the analysis area. Data are accumulated and stored in a SEL-810 computer. Data have been acquired for samples of ^{7}Li, $^{56,57}Fe$, $^{nat,58}Ni$ and $^{nat,53}Cr$. Gamma rays from residual nuclei of the (n,n'γ), (n,p'γ) and (n,α'γ) binary reactions are observed. For the even-even nuclei studied, most (∿90%) of the excited states decay through the first 2^+ level, so the cross section for the gamma ray corresponding to the decay of this level gives a good estimate of the total inelastic scattering cross section for these nuclei. The excellent resolution of the Ge(Li) detector allows us to observe other ground-state transitions and further improve the estimate for this cross section. Of particular interest are the gamma rays which we observe from the residual nuclei following tertiary reactions such as (n,2n'γ), (n,n'αγ) and (n,n'pγ). The gamma-ray measurements provide a unique way of obtaining information on cross sections for these reactions, since the gamma-ray energies are unique signatures of particular tertiary reactions. With ORELA, we are able to obtain information about cross sections for many of these reactions over a wide incident neutron energy range. Information on tertiary reaction cross sections are important, for example, in fusion reactor design applications for heating, radiation damage, and transport calculations. Our data provide cross sections necessary in the development of nuclear models to calculate cross sections for all tertiary reactions, many of which are difficult, if not impossible, to measure experimentally.

b. Improving Neutron Reaction Data Through Linac-Based Flight-Time Spectrometry,[1] (R. W. Peelle)

Pulsed neutron facilities based on electron linear accelerators (linacs) allow measurements of neutron cross sections from $E_n \sim 0.01$ eV to $E_n > 20$ MeV. This paper outlines the capabilities of such facilities and their role in upgrading the neutron cross-section data base.

3. Actinides

a. Measurement of the ^{249}Cf Neutron Fission Cross Section,[2] (J. W. T. Dabbs and C. E. Bemis, Jr.)

The fission cross section of ^{249}Cf has been measured from 0.005 eV to 20 MeV using time-of-flight techniques at the Oak Ridge Electron

[1] 1985 Annual Meeting of the American Nuclear Society, Isotopes and Radiation Division, June 9-14, 1985, Boston, Mass.
[2] Submitted to Nucl. Sci. Eng. (January 1985).

Linear Accelerator (ORELA). The detector was a hemispherical-plate fission-ionization chamber containing three pairs of plates with deposits of 131 μg of ^{249}Cf and 168 μg of ^{235}U plus a "weightless" deposit of ^{252}Cf that served as a monitor of chamber performance. The fission of ^{235}U served as a cross-section standard for energies above 101 keV, while the $^{6}Li(n,\alpha)$ reaction, normalized to ^{235}U fission in the 7.8- to 11.0-eV interval, served as a shape standard below 101 keV. Approximately 360 hours of data were obtained at a flight-path distance of 9.1 m, primarily with 40-ns bursts. Particular attention was paid to corrections for backgrounds, especially inscattered neutron-induced events. The ^{249}Cf fission resonance integral was found to be 2380 ± 85 b and the thermal fission cross section was found to be 1555 ± 55 b.

b. Microscopic Beta and Gamma Data for Decay Heat Needs,[1] (J. K. Dickens)

Microscopic beta and gamma data for decay heat needs are defined as absolute intensity spectral distributions of beta and gamma rays following radioactive decay of radionuclides created by, or following, the fission process. Four well-known evaluated data files, namely the U.S. ENDF/B-V, the U.K. UKFPDD-2, the French BDN (for fission products), and the Japanese JNDC Nuclear Data Library, are reviewed. Comments regarding the analyses of experimental data (particularly gamma-ray data) are given; the need for complete beta-ray spectral measurements is emphasized. Suggestions on goals for near-term future experimental measurements are presented.

c. Measurements of the Neutron Fission Cross Sections of 235-U (En = 0.01 eV to 30 keV) and 239-Pu (En = 0.01 to 60 eV),[2] (R. Gwin, R. R. Spencer, R. W. Ingle, J. H. Todd, and S. W. Scoles)

d. Measurements of the Energy Dependence of Prompt Neutron Emission from ^{233}U, ^{235}U, ^{239}Pu, and ^{241}Pu for E_n = 0.005 to 10 eV Relative to Emission from Spontaneous Fission of ^{252}Cf,[3] (R. Gwin, R. R. Spencer, and R. W. Ingle)

A series of experiments has been performed to measure the dependence on the incident neutron energy of the average number of prompt neutrons emitted per fission from ^{233}U, ^{235}U, ^{239}Pu, and ^{241}Pu relative to the average number of prompt neutrons emitted in spontaneous fission of ^{252}Cf. The incident neutron energy range was 0.005 to 10 eV. A white neutron source was generated by the Oak Ridge Electron Linear Accelerator and the energies of the neutrons incident on the fissile samples were determined by time-of-flight techniques. In each experiment, the samples,

[1]NEANDC specialists Meeting on Yields and Decay Data of Fission Product Nuclides, R. E. Chrien and T. W. Burrows, eds., BNL-51778 (p. 247) (1984).
[2]Nucl. Sci. Eng. 88, 37 (1984).
[3]Nucl. Sci. Eng. 87, 381-404 (1984) and Int. Conf. on Nucl. Data for Basic and Applied Science, Santa Fe, NM, May 13-17, 1985.

including the ^{252}Cf standard, were contained in different sections of a fission chamber that was surrounded by a large volume (0.91 m^3) of liquid scintillator loaded with gadolinium. The fission chamber detected fission events, and the scintillator detected the accompanying prompt neutrons. The resulting data were analyzed to yield: $\bar{R}_p(E) = \bar{\nu}_p(E)$ (fissile)/$\bar{\nu}_p(^{252}Cf)$. Only for ^{239}Pu was any neutron energy dependence definitely confirmed, with $\bar{R}_p(E)$ for ^{239}Pu being lower by 0.7% in the resonance at 0.3 eV than it was near 0.025 eV. For incident energies of 0.02 to 0.05 eV, values of $\bar{R}_p(E)$ were 0.6597 ± 0.0018 for ^{233}U, 0.6443 ± 0.0014 for ^{235}U, 0.7655 ± 0.0014 for ^{239}Pu, and 0.7820 ± 0.0018 for ^{241}Pu.

e. Fission-Product for Thermal-Neutron Fission of 243-Cm Determined from Measurements with a High-Resolution Low-Energy Germanium Gamma-Ray Detector,[1] (L. D. Merriman)

f. Comparison of Measured and Calculated U-238 Capture Self-Indication Ratios Above 4 KeV,[2] (R. B. Perez)

g. Neutron Total Cross Section of Pu-240 Below 6 eV and the Parameters of the 1.0-eV Resonance,[3] (R. R. Spencer, J. A. Harvey, N. W. Hill, and L. W. Weston)

Measurements of the transmission of neutrons through Pu metal samples have been made at the Oak Ridge Electron Linear Accelerator (ORELA) to obtain consistency between the parameters of the 1.056-eV resonance and the measured total cross section at 2200 m/s. Three different thicknesses of Pu metal foils containing 0.727 at. % of Pu-240 were measured at room temperature to obtain the resonance parameters. Assuming the usual Lamb limits for Doppler broadening are satisfied, preliminary analysis of these data resulted in Γ_n = 0.00244 ± 0.00002 eV and Γ_γ = 0.0300 ± 0.0002 eV. In addition, the transmissions of two sample thicknesses of extremely pure Pu-240 metal (99.97 at. %) were measured from 0.003 to 6 eV. Analysis of these data gave a 2200-m/s total cross section of 284 ± 2 barns, which is 2.5% lower than that calculated from the absorption cross section reported by Lounsbury et al. from mass spectrometer analyses of Pu samples after irradiation in a thermal column.

h. Subthreshold Fission Cross Section of 240-Pu and the Fission Cross Sections of 235-U and 239-Pu,[4] (L. W. Weston and J. H. Todd)

---

[1] ORNL/TM-9049 (April 1984)
[2] Second Jackson Hole Colloquium on Fast Reactor Physics: The Doppler Effect in LMFBRs, Teton Village, Wyoming, June 27-29, 1983, Proc. Session III, No. 4 (1983).
[3] International Conference on Nuclear Data for Basic and Applied Science, Santa Fe, NM, May 13-17, 1985.
[4] Nucl. Sci. Eng. 88, 567 (1984).

4. Experimental Techniques

a. Calculations Pertaining to the Design of a Prebuncher for a 150-MeV Electron Linear Accelerator. III. Comparisons with Experimental Data,[1] (R. G. Alsmiller, Jr., F. S. Alsmiller, and T. A. Lewis)

In a previous paper a ballistic model that included space-charge effects was described and calculated results were presented of the extent to which a current pulse of electrons (∿150 keV kinetic energy, ∿1 μC of charge, and ∿15 nsec full width at half maximum) could be bunched, i.e., reduced in width without loss of charge, by passing it through a series of gaps on which time-dependent voltages are applied. A prebuncher system similar to the one considered previously has now been constructed, and experimental data on the current at the end of the prebuncher as a function of time have been obtained. Here the calculated current as a function of time, obtained using the model developed previously, is compared with the experimental data. The calculated and experimental data are in substantial agreement for a variety of electron beam and voltage gap conditions.

b. ORELA Flight Path 1: Determinations of Its Effective Length vs Energy, Experimental Energies, and Energy Resolution Function and Their Uncertainties,[2] (D. C. Larson, N. M. Larson, and J. A. Harvey)

c. Laser Measurements of Distances from the ORELA Neutron Target to Experiment Stations Along Flight Paths 1 and 6,[3] (D. C. Larson, N. M. Larson, J. A. Harvey, F. G. Perey, D. E. Pierce, and R. H. Seals)

Flight-path lengths have been measured by laser techniques for the 200-, 80-, and 18-m stations along flight path 1, and for the 5-, 20-, 40-, and 150-m stations along flight path 6 at the Oak Ridge Electron Linear Accelerator (ORELA). In each case the distance evaluated from the measurements is the slope distance from the center of the neutron-producing target to a position along the beam path, directly above a suitable benchmark at the experiment station. A total of 25 laser measurements were performed between the various stations. These data, along with appropriate uncertainties, were combined using Bayes' method. From this analysis we obtained the desired flight-path lengths, which typically have uncertainties less than 1.5 mm. The measurement technique, uncertainties, analysis method, and results are documented in detail in this report.

---

[1]Abstract of ORNL/TM-9375 (November 1984) and submitted to Particle Accelerators, October 1984.
[2]ORNL/TM-8880 (June 1984).
[3]Abstract of ORNL/TM-9097 (March 1985).

d. Uncertainty Propagation from Raw Data to Final Results,[1] (N. M. Larson)

Reduction of data from raw numbers (counts per channel) to physically meaningful quantities (such as cross sections) is in itself a complicated procedure. Propagation of experimental uncertainties through that reduction process has sometimes been perceived as even more difficult, if not impossible. At the Oak Ridge Electron Linear Accelerator, a computer code ALEX has been developed to assist in the propagation process. The purpose of ALEX is to carefully and correctly propagate all experimental uncertainties through the entire reduction procedure, yielding the complete covariance matrix for the reduced data, while requiring little additional input from the experimentalist beyond that which is needed for the data reduction itself. The theoretical method used in ALEX is described, with emphasis on transmission measurements. Application to the natural iron and natural nickel measurements of D. C. Larson is shown.

e. Shielding Considerations for Multi-GeV/Nucleon Heavy Ion Accelerators: The Introduction of a New Heavy Ion Transport Code, HIT,[2] (T. A. Gabriel, B. L. Bishop, and R. A. Lillie)

A preliminary heavy ion transport code, HIT, has been developed and used to generate basic shielding information for multi-GeV/nucleon heavy ion accelerators. The data presented are the number of neutrons emitted with energies >100 MeV and the amount of energy carried off by these particles external to a central shielding block composed of iron. These data are compared to similar data generated by the high-energy hadronic transport code, HETC. These data will allow preliminary estimates for shielding of heavy ion accelerators based on current shielding requirements around proton accelerator facilities.

f. Majority-Logic NE-110 Detector for keV Neutrons,[3] (N. W. Hill, J. A. Harvey, D. J. Horen, G. L. Morgan,[4] and R. R. Winters[5])

An NE-110 proton-recoil scintillation counter whose efficiency is reproducible and stable has been developed for neutrons in the energy range from 5 keV to 1 MeV. Majority-of-two logic at below the single photoelectron level is used between two or more phototubes viewing the same scintillator. Pulse height distributions as a function of neutron energy have been measured between 5 and 350 keV with two different detector configurations: a thin square slab of NE-110 and a cylinder of NE-110. The

---

[1]International Conference on Nuclear Data for Basic and Applied Science, Sante Fe, NM, May 13-17, 1985.
[2]Abstract of ORNL/TM-8952 (January 1984).
[3]IEEE 1984 Nuclear Science Symposium, October 31 - November 2, 1984, Orlando, Florida.
[4]Los Alamos National Laboratory, Los Alamos, New Mexico 87545.
[5]Denison University, Granville, Ohio 43023.

absolute efficiency of the slab detector has also been determined. The measured results are in good agreement with results from Monte Carlo calculations.

g. A Preliminary Study of Possible ORELA Replacement Options,[1] (D. K. Olsen, J. A. Martin, and D. J. Horen)

Based on two conceptual design studies performed by the LANL Accelerator Technology Division, the possibilities in terms of accelerator systems for replacing ORELA with a more intense Maxwellian-type continuous-energy neutron source are summarized and discussed. The neutron intensities from ORELA are compared with those from existing or potential accelerator systems used for cross-section and condensed-matter studies. The best replacement options seem to involve a spallation source from 200- to 400-MeV protons on an ORELA-like target. Pulsing and intensity desiderata with such a source are discussed which correspond to a spectrum-averaged 100-fold improved figure of merit over ORELA for TOF measurements with only a tenfold increased source strength. Existing accelerator designs seem to be inadequate for such a source. Consequently, two conceptual designs were developed for this study by the LANL Accelerator Technology Division. The first conceptual design is for a 200-MeV large linac capable of accelerating 1.3 A during a macropulse; this linac standing alone could serve as an ORELA replacement source. The second conceptual design is for a much smaller 250-MeV PIGMI linac with a 28-mA macropulse current which feeds a proton accumulator ring and bunch-compressor transport line. This linac-ring-compressor (LIRIC) option would give a more cost-effective neutron source for cross-section measurements, whereas the large linac, or a modified version of it, would give a much simpler system more suitable for expansion. In particular, both conceptual designs would incorporate the present ORELA building and would provide approximately 100-fold improved neutron sources over ORELA for cross-section measurements. The total estimated cost of the LIRIC system would be $43M (1984), whereas the cost of the large linac would be about a factor of two more.

h. A Parallel Plate ^{10}B Neutron Detector,[2] (J. H. Todd, L. W. Weston, and G. J. Dixon)

5. Integral Measurements

a. Fusion Reactor Shielding Benchmark. II. Duct Streaming Experiments and Analyses,[3] (G. T. Chapman,[4] R. T. Santoro, R. G. Alsmiller, Jr., J. M. Barnes, J. S. Tang, P. D. Soran[5])

---

[1]Abstract of ORNL/TM-8669 (July 1984).
[2]Nucl. Inst. Meth. 219, 575 (1984).
[3]Cross Section Evaluation Working Group Benchmark Specifications, BNL-19302, Vol. 11, ENDF-202 (1984). Philip F. Rose (BNL) and R. W. Roussin (ORNL) editors.
[4]Present address: Roane State Community College, Harriman, TN.
[5]Schlumberger Well Services, Houston, TX.

Neutron and photon flux spectra have been measured and calculated for the case of neutrons produced by D-T reactions streaming through a cylindrical iron duct surrounded by concrete. Measurements and calculations have also been obtained when the iron duct is partially filled by a laminated stainless steel and borated polyethylene shadow bar.

b. Combining Integral and Differential Dosimetry Data in an Unfolding Procedure with Application to the Arkansas Nuclear One-Unit 1 Reactor,[1] (R. E. Maerker, B. L. Broadhead, C. Y. Fu, J. J. Wagschal,[2] J. G. Williams,[3] and M. L. Williams[4])

The LEPRICON adjustment procedure involves combining both differential and integral data, including covariances and sensitivities, in such a way that calculated spectral fluences at important locations within a pressure vessel of an operating PWR can be adjusted with significantly reduced uncertainties. The procedure allows simultaneous combination of integral dosimetry measurements performed at a reactor surveillance location with measurements performed in geometrically simpler benchmark facilities. An application of this technique is given to an existing PWR, and the results consistently indicate a need for significant (∿8%) adjustments in the total inelastic cross section of iron in the region between 3 and 8 MeV using cross sections and covariances from ENDF/B-V. Dosimetry cross sections were taken mainly from a revised version of ENDF/B-V and were found to require relatively small adjustments. Covariances of the spectral fluences are reduced by factors lying between two and four.

c. Monte Carlo and Discrete Ordinates Calculations of 14-MeV Neutrons Streaming Through a Stainless-Steel Duct (L/D = 4.6): Comparison with Experiment,[5] (R. T. Santoro, J. M. Barnes, R. G. Alsmiller, Jr., J. D. Drischler)

Integral experiments are being carried out at the Oak Ridge National Laboratory to measure neutron and gamma-ray energy spectra from ∿14 MeV neutrons streaming through cylindrical ducts imbedded in concrete. These data are being used to validate radiation transport code and nuclear data libraries that are being used to calculate nuclear streaming through the penetrations that are found in fusion reactor blanket and shield assemblies. In this paper, measured and calculated neutron and gamma-ray energy spectra from ∿14 MeV neutrons streaming through a stainless-steel duct having a length-to-diameter ratio of 4.6 are compared as a function of detector location relative to the mouth of the duct. The length of the duct is 1.45 m.

---

[1]International Conference on Nuclear Data for Basic and Applied Science, Santa Fe, NM, May 13-17, 1985.
[2]Hebrew University, Jerusalem.
[3]University of Arkansas, Fayetteville, Ark.
[4]Louisiana State University, Baton Rouge, La.
[5]ANS 6th Topical Meeting on the Technology of Fusion Energy, San Francisco, Calif., March 3-7, 1985.

B.. DATA ANALYSES

1. Theoretical Calculations

a. The Dy163-Ho163 Branching: An s-Process Barometer,[1] (H. Beer,[2] G. Walter,[2] and R. L. Macklin)

The neutron capture cross sections of Dy163 and Er164 have been measured to analyse the s-process branching at Dy163 - Ho163. The reproduction of the s-process abundance of Er164 via this branching is sensitive to temperature kT, neutron density, and electron density n_e. The calculations using information from other branchings on kT and the neutron density n_n give constraints for n_e at the site of the s-process.

b. s- and p-Wave Neutrons on 30-Si and 34-S: Spherical Optical Model Analysis,[3] (R. F. Carlton,[4] J. A. Harvey, and C. H. Johnson)

c. Multilevel Analysis of the Low Energy 239-Pu Cross Sections,[5] (G. Desaussure, R. B. Perez, and R. L. Macklin)

It is well known that the ENDF/B-V representation of the ^{239}Pu resonance region is no longer considered satisfactory. Below 1 eV, the cross sections are given by "smooth files" (file 3) rather than by resonance parameters. Above 1 eV, the single-level formalism used in ENDF/B-V necessitates a structured file 3 contribution. This paper presents the results of an R matrix multilevel analysis of several recent data sets as well as of older data. The analysis is concerned with the region up to 30 eV, an energy region that is important for thermal reactors and for which no recent multilevel analyses had previously been available.

d. R-Matrix Analysis of the ^{239}Pu Neutron Cross Sections.[6] (G. Desaussure, R. B. Perez, and R. L. Macklin)

The ^{239}Pu neutron cross section data in the resolved resonance region were analyzed with the R-Matrix Bayesian Fit Program SAMMY. Below 30 eV the cross sections computed with the multilevel parameters are consistent with recent fission and transmission measurements as well as with older capture and alpha measurements. The thermal values are also consistent with the latest evaluation of the thermal parameters. Above 30 eV no suitable transmission data were available and only fission cross-section measurements were analyzed. However, since the analysis conserves the

[1] Int. Meeting on Capture Gamma-Ray Spectroscopy and Related Topics, Knoxville, Tenn., Sept. 10-14, 1984.
[2] Kernforschungszentrum Karlsruhe, IK III, P.O.B. 3640, D-7500 Karlsruhe 1, FRG.
[3] Phys. Rev. C. 29, 1988 (1984).
[4] Middle Tennessee State University, Murfreesboro, Tenn.
[5] ANS/ENS 1984 International Conference, Washington, DC, Nov. 11-16, 1984.
[6] International Conference on Nuclear Data for Basic and Applied Science, Santa Fe, NM, May 13-17, 1985.

complete covariance matrix, the analysis can be updated by the Bayes method, as transmission measurements become available. To date, the analysis of the fission measurements has been completed up to 300 eV and an extension to 600 eV is in progress.

e. Implementation of an Advanced Pairing Correction for Particle-Hole State Densities in Precompound Nuclear Reaction Theory,[1] (C. Y. Fu)

f. Pairing Correction of Particle-Hole State Densities for Two Kinds of Fermions,[2] (C. Y. Fu)

Pairing corrections in particle-hole (exciton) state-density formulas used in precompound nuclear reaction theories are, strictly speaking, dependent on the nuclear excitation energy U and the exciton number n. A general formula for (U,n)-dependent pairing corrections, based on the BCS theory, has been derived for exciton state-density formulas for one kind of Fermion. In the present paper, a similar derivation is made for the case of two kinds of Fermions. It is shown that the constant-pairing-energy correction used in standard level-density formulas, such as U_o in Gilbert and Cameron, is a limiting case of the present general (U,n)-dependent results.

g. Calculated Neutron-Induced Cross Sections for $^{63,65}Cu$ from 1 to 20 MeV and Comparisons with Experiments,[3] (D. M. Hetrick, C. Y. Fu, and D. C. Larson)

Nuclear model codes were used to compute cross sections for neutron-induced reactions on both ^{63}Cu and ^{65}Cu for incident energies from 1 to 20 MeV. The input parameters for the model codes were determined through analysis of experimental data in this energy region. Discussion of the models used, the input data, the resulting calculations, extensive comparisons to measured data, and comparisons to the Evaluated Nuclear Data File (ENDF/B-V) for Cu (MAT 1329) are included in this report.

h. Updated Users' Guide for SAMMY: Multilevel R-Matrix Fits to Neutron Data Using Bayes' Equations,[4] (Nancy M. Larson)

In 1980 the multilevel multichannel R-matrix code SAMMY was released for use in analysis of neutron data at the Oak Ridge Electron Linear Accelerator. Since that time, SAMMY has undergone significant modifications: (1) User-friendly options have been incorporated to streamline

[1]Nucl. Sci. Eng. 86, 344 (1984).
[2]International Conference on Nuclear Data for Basic and Applied Science, Santa Fe, NM, May 13-17, 1985.
[3]Abstract of ORNL/TM-9083, ENDF-337 (August 1984).
[4]Abstract of ORNL/TM-9179 (August 1984).

common operations and to protect a run from common user errors. (2) The Reich-Moore formalism has been extended to include an optional logarithmic parameterization of the external R-matrix, for which any or all parameters may be varied. (3) The ability to vary sample thickness, effective temperature, matching radius, and/or resolution-broadening parameters has been incorporated. (4) To avoid loss of information (i.e., computer round-off errors) between runs, the "covariance file" now includes precise values for all variables. (5) Unused but correlated variables may be included in the analysis. Because of these and earlier changes, the 1980 SAMMY manual is now hopelessly obsolete. This report is intended to be complete documentation for the current version of SAMMY. Its publication in looseleaf form will permit updates to the manual to be made concurrently with updates to the code itself, thus eliminating most of the time lag between update and documentation.

i. Analysis of Neutron Data in the Resonance Region Via the Computer Code SAMMY,[1] (N. M. Larson)

Analysis and evaluation of resonance neutron cross-section data require sophisticated computational procedures. Such procedures have been implemented in a state-of-the-art computer code SAMMY, developed at the Oak Ridge Electron Linear Accelerator at Oak Ridge National Laboratory. Notable features of SAMMY include: (1) Use of Bayes' equations to determine "best" values of parameters. This permits sequential analysis of data sets (or subsets) while giving the same results that a simultaneous analysis would give; examples will be shown. (2) Choice of multilevel Breit Wigner formulation or Reich-Moore approximation to R-matrix. (3) Logarithmic parameterization of the external R-matrix. (4) Choice of transmission, total cross section, scattering, fission, capture, or absorption cross section data types; examples of several will be shown. (5) Several options for Doppler and/or resolution broadening. (6) Inclusion of off-diagonal data correlations if desired. (7) Analysis of different data types simultaneously. (8) Inclusion of channel radius, broadening parameters, sample thickness, and/or parameters of external R-matrix in the fitting procedure, (9) Dynamic allocation of array storage space. Thus, there are no rigid limits on any of the "numbers" - number of resonances, number of varied parameters, number of data points, etc. The only rigid limit is the size of the computer. (10) Frequent I/O to and from temporary files to maximize the size of a job which can be run. (11) Thorough documentation in the form of a complete user's guide. (12) Versions currently available on Decsystem-10 (PDP-10), IBM-360, and VAX computers.

j. Report to the ^{238}U Discrepancy Task Force on SIOB Fits to the ORNL, CBNM, and JAERI Transmission Data,[2] (D. K. Olsen)

---

[1] International Conference on Nuclear Data for Basic and Applied Science, Santa Fe, NM, May 13-17, 1985.
[2] ORNL/TM-9023 (May 1984).

k. Resolved-Resonance Neutron Widths from a Consistent Reanalysis of the Most Recent ^{238}U Transmission Data,[1] (D. K. Olsen)

This paper reports results of a detailed reanalysis of portions of three recent transmission measurements on ^{238}U to determine whether the systematic resolved-resonance neutron-width discrepancies are caused by systematic differences between the reduced transmission data or whether the discrepancies are introduced in the data analysis procedure.

2. ENDF/B Related Evaluations

a. The Neutron Cross Section Standards Evaluations for ENDF/B-VI,[2] (A. D. Carlson,[3] W. P. Poenitz,[4] G. M. Hale,[5] and R. W. Peelle)

As a first step in the development of the new ENDF/B-VI file, the neutron cross section standards are being evaluated. These standards evaluations are following a different process compared with that used for earlier versions of ENDF. The primary effort is concentrated on a simultaneous evaluation using a generalized least squares program, R-matrix evaluations, and a procedure for combining the results of the evaluations. The ENDF/B-VI standards evaluation procedure is outlined, and preliminary simultaneous evaluation and R-matrix results are presented.

b. Office of Basic Energy Sciences Program to Meet High Priority Nuclear Data Needs of the Office of Fusion Energy 1983 Review,[6] (R. C. Haight,[7] and D. C. Larson)

This review was prepared during a coordination meeting held at Oak Ridge National Laboratory on Sept. 28-29, 1983. Participants included research scientists working for this program, a representative from the OFE's "Coordination of Magnetic Fusion Energy (MFE) Nuclear Data Needs Activities," and invited specialists.

c. Calculated Neutron-Induced Cross Sections for $^{63,65}Cu$, $^{58,60}Ni$, and ^{52}Cr from 1 to 20 MeV and Comparisons with Experiments,[8] (D. M. Hetrick, C. Y. Fu, and D. C. Larson)

Nuclear model codes were used to compute cross sections for neutron-induced reactions for $^{63,65}Cu$, $^{58,60}Ni$, and ^{52}Cr for incident energies from 1 to 20 MeV. The optical-model code GENOA and the Distorted Wave Born

[1] ANS Topical Meeting on Reactor Physics and Shielding, Chicago, Ill. Sept. 17-19, 1984.
[2] Advisory Group Meeting on Nuclear Standard Reference Data, Central Bureau for Nuclear Measurements, Geel, Belgium, Nov. 12-18, 1984.
[3] National Bureau of Standards, Gaithersburg, MD 20899.
[4] Argonne National Laboratory, Argonne-West, Idaho Falls, ID 83403-2528.
[5] Los Alamos National Laboratory, Los Alamos, NM 87545.
[6] Abstract of UCID-19930.
[7] Lawrence Livermore National Laboratory, Livermore, CA 94550.
[8] International Conference on Nuclear Data for Basic and Applied Science, Santa Fe, NM, May 13-17, 1985.

Approximation program DWUCK were used to determine optical-model parameters and direct-interaction cross sections needed as input for the Hauser-Feshbach code TNG. The TNG code simultaneously computes the compound and precompound cross sections for all energetically possible binary reactions and tertiary reactions, and computes the resulting gamma-ray production cross sections. Angular momentum is conserved in both compound and precompound reactions. Results from TNG, including energy and angular distributions for particles emitted, are compared with experimental data and are found to agree reasonably well.

d. Office of Basic Energy Sciences Program to Meet High Priority Nuclear Data Needs of the Office of Fusion Energy: Summary of Results 1976-1983,[1] (D. C. Larson and R. C. Haight[2])

Experimental data acquired under the BES program to meet Fusion Data Needs from its inception (1975) to 1983 are summarized by element, reaction, energy, and contributing laboratory. Cases where the data have been incorporated in ENDF evaluations are noted. Work in nuclear model code development under this program is summarized.

e. Status of the Parameters of the 1.15-keV Resonance of 56-Fe,[3] (F. G. Perey)

At the conference in Antwerp, concerns were expressed about large discrepancies in the parameters of the 1.15-keV resonance of ^{56}Fe since they are needed to high accuracies in some reactor calculations. The Nuclear Energy Agency Nuclear Data Committee organized a task force under the chairmanship of F. G. Perey to coordinate work at CBNM, Harwell, JAERI, and ORNL in order to try to resolve the discrepancies and make recommendations. The 1.15-keV resonance has a value of Γ_n about 10 times smaller than the value of Γ_γ. Therefore, information about these parameters, in particular the capture area of the resonance, can be obtained independently from transmission and capture experiments. At the time of the Antwerp meeting, these two types of experiments appeared to give systematically different values. New transmission and capture experiments were planned at most laboratories using new or well-established techniques. Although the work of the task force is not finished (in particular, what may have gone wrong in some of the older experiments is not established and may never be), all transmission experiments completed yield the same value of the resonance parameters, within small uncertainties, independent of experimental techniques and methods of analysis used. Most capture experiments have not been completed. However,

---

[1]Abstract of ORNL/TM-9335 (September 1984).

[2]Lawrence Livermore National Laboratory, University of California, Livermore, CA 94550.

[3]International Conference on Nuclear Data for Basic and Applied Science, Santa Fe, NM, May 13-17, 1985.

at ORNL a new capture experiment using the same type of detector used in an older experiment yields results that are consistent with the transmission results and disagrees with the older capture results. The results of the Task Force, as of the time of the meeting, will be discussed.

f. ^{58}Ni + n Transmission, Capture and Differential Elastic Scattering Data Analysis in the Resonance Region,[1] (C. M. Perey, F. G. Perey, J. A. Harvey, N. W. Hill, and R. L. Macklin)

High-resolution neutron transmission, capture and differential elastic scattering measurements have been made for ^{58}Ni-enriched targets at the Oak Ridge Electron Linear Accelerator from the eV to the MeV region. The three sets of data have been analyzed simultaneously from 10 to 450 keV. The analysis of the transmission and differential elastic scattering data was carried up to 650 keV. Averaged parameters were deduced for the 52 s-wave resonances observed between 10 and 650 keV. The average level spacing, D_o, and the strength function, S_o, were found to be equal to 12.2 ± 1.0 keV and $(3.1 \pm 0.6) \times 10^{-4}$, respectively. The differential elastic scattering data allow us to assign both spin and parity to most of the large non-s-wave resonances which have been observed in the transmission data.

[1] International Conference on Nuclear Data for Basic and Applied Science, Santa Fe, NM, May 13-17, 1985.

OHIO UNIVERSITY

A. MEASUREMENTS

1. Neutron Elastic and Inelastic Differential Cross Sections for ^{10}B*. (E. Sadowski, P. Koehler**, D. Resler, H. Knox and R. Lane)

Differential cross sections for $^{10}B(n,n)^{10}B$ and $^{10}B(n,n')^{10}B^*$ (0.718, 1.740, 2.154) were obtained at incident neutron energies of E_n = 3.0, 3.5, 4.0, 4.5 and 5.0 MeV. The angular distributions were from 20° to 160° in 17.5° steps. The data have been corrected for sample attentuation, air scattering, and dead time. They are presently being corrected for multiple scattering effects.

2. Nucleon-Induced Excitation of Collective Bands in ^{12}C.*** (Ali S. Meigooni†, R.W. Finlay, J.S. Petler and J.P. Delaroche††)

Detailed differential elastic and inelastic neutron scattering data for ^{12}C at E_n = 20-26 MeV have been analyzed in terms of a deformed optical potential and a rotation-vibration interaction in a coupled-channel formalism. All well-established states in ^{12}C up to 15 MeV excitation energy were observed in the experiment. Additional neutron scattering, total and reaction cross section data for $20 < E_n < 100$ MeV were incorporated into the analysis to determine more precisely the energy dependence of the deformed potential well parameters. A newly developed formalism for the treatment of radius, diffuseness and potential depth oscillations of a nucleus with a deformed equilibrium shape was compared with both (p,p') and (n,n') data.

3. Partial Kerma Factors for Neutron Interactions with ^{12}C at $20 < E_n < 65$ MeV.††† (R.W. Finlay)

New measurements of neutron interactions with ^{12}C at incident energies between 20 and 26 MeV were obtained and analyzed in terms of a deformed optical model potential. Results of these analyses were compared

---

* Work supported by U.S. Department of Energy.

** Present address: Los Alamos National Laboratory, Los Alamos, NM.

*** Work supported by PHS grant number 5-R01-CA25193 awarded by the National Cancer Institute and by National Science Foundation grant number PHY-8108456.

† Present address: University of Minnesota, Department of Therapeutic Radiology, Minneapolis, MN.

†† Present address: Centre d'Etudes de Bruyeres-le-Chatel, France.

††† This investigation was supported by PHS Grant Number 5-R01-CA 25193 awarded by the National Cancer Institute, DHHS.

with other recent differential and total neutron cross section measurements and with proton scattering data in order to develop a consistent representation of the energy dependence of neutron scattering over a broad energy range. Heavy ion recoil kerma factors were calculated and compared with earlier estimates of these quantities. That fraction of the $^{12}C(n,n')3\alpha$ that proceeds via inelastic scattering through the 3^- state at 9.63 MeV was measured with very good precision in the present work thus providing a firm benchmark for recent experimental and theoretical efforts (1,2) to obtain this quantity. Theoretical description of inelastic scattering in terms of the rotations and vibrations of a deformed ^{12}C nucleus was compared with the data and with the predictions of the intra-nuclear cascade model. Status of the measurements and analysis of neutron scattering on oxygen, nitrogen and calcium was reviewed.

4. Coupled-Channel Analysis of Neutron Scattering from ^{16}O.* (M.S. Islam, J.S. Petler and R.W. Finlay)

Differential elastic and inelastic neutron scattering cross sections from ^{16}O have been measured at five energies between 18 and 26 MeV. An energy-dependent optical model has been developed to describe these data and the total n-^{16}O cross section up to 70 MeV. Coupled-channel calculations have been performed that well fit the 3^- (6.13 MeV) state and the 2^+ (6.92 MeV)/1^- (7.11 MeV) doublet. The contribution of two-step processes leading to the 2^- (8.87 MeV) state has been evaluated and the effect of coupling additional states in the calculation investigated.

5. Levels in ^{26}Al.** (H. Satyanarayana, M. Ahmad, C.E. Brient, P.M. Egun, S.M. Grimes and S.K. Saraf)

Angular distributions for a large number of final states in the $^{25}Mg(d,n)^{26}Al$ reaction have been measured in the bombarding energy range 3.0 MeV to 8.25 MeV. The time-of-flight spectrometer with a 28 m flight path yielded an overall energy resolution of 10 keV for 1.5-2.0 MeV neutrons. Our spectra show the population of virtually all the levels listed in Endt and van der Leun (3). More than 20 new levels have been observed.

---

* Supported by PHS Grant 5-R01-CA25193 awarded by the National Cancer Institute, DHHS.

** Supported in part by U.S. Department of Energy.

(1) B. Antolković, I. Slaus, D. Plenkovic, P. Macq and J. Meulders, Nucl. Phys. A394, 87 (1983).

(2) D.E. Brenner and R.E. Prael, Nucl. Sci. Eng. 88, 97 (1984).

(3) P.M. Endt and C. van der Leun, Nucl. Phys. A310 (1978), No. 1,2.

6. Spectroscopic Studies of ^{28}Si and ^{27}Al.* (H. Satyanarayana, M. Ahmad, C.E. Brient, P.M. Egun, S.L. Graham, S.M. Grimes and S.K. Saraf)

The angular distributions of the $^{27}Al(d,n)^{28}Si$ and $^{26}Mg(d,n)^{27}Al$ reactions have been measured at bombarding energies between 2.5 and 7.5 MeV. A time-of-flight spectrometer with a 28 m flight path yielded an overall energy resolution as good as 15 keV for some neutron energies. Our spectra show population of virtually all levels listed in Endt and van der Leun (1). Several new levels have been observed.

7. Scattering of 21.7 MeV Neutrons from ^{34}S and ^{40}Ca.** (R. Alarcon, D. Wang, J.R.M. Annand*** and J. Rapaport)

Using the Ohio University time-of-flight facility, elastic and inelastic neutron data at 21.7 MeV from ^{34}S and ^{40}Ca have been obtained. An enriched (93.6%) cylindrical scattering sample of 18.02 grs of ^{34}S (powder) and a metal cylinder of 22.9 grs of natural calcium for ^{40}Ca were used. An energy resolution of about 400 keV was achieved. The scattering neutrons were observed at 39 angles between 13° and 160°.

Data analysis in ^{34}S, using the coupled-channels formalism, for the elastic transition, 2_1^+ (E_x = 2.13 MeV), 2_2^+ (E_x = 3.30 MeV), 2_3^+ (E_x = 4.11 MeV), 3_1^- (E_x = 4.69 MeV) and 5_1^- (E_x = 5.69 MeV) has been completed. In ^{40}Ca, microscopic optical model potential analysis for the elastic transition and collective model analysis for the states 3_1^- (E_x = 3.73 MeV) and 5_1^- (E_x = 4.49 MeV) has been carried out.

8. Analysis of Nucleon Scattering from ^{40}Ca.** (R. Alarcon, J. Rapaport, D. Wang and Y. Wang)

Neutron elastic scattering at 19.0, 21.7 and 25.5 MeV measured at Ohio University and proton elastic scattering with available analyzing power data between 21.0 and 48.0 MeV have been analyzed using a Fourier-Bessel series description of the real central optical potential (2). This method has the advantage of describing the elastic scattering in a potential well not confined to be of a Woods-Saxon geometry and in providing realistic

---

* Supported in part by the U.S. Department of Energy.

** Supported in part by National Science Foundation Grant PHY-8108456.

*** Present address: Kelvin Laboratory, N.E.L., East Kilbride, Glasgow, Scotland.

(1) P.M. Endt and C. van der Leun, Nucl. Phys. A310 (1978), No. 1,2.

(2) E. Friedman and C. Batty, Phys. Rev. C17, 34 (1978).

uncertainties in the calculated values based on the experimental uncertainties and correlations. Values for the volume integral and rms radius were obtained. A comparison of the neutron and proton analysis in terms of Coulomb corrections has been made.

9. Total Charged-Particle Emission Cross Sections for 9.4 and 11 MeV Neutron Bombardment of Type 316 Stainless Steel.* (M. Ahmad, S.L. Graham, S.M. Grimes, H. Satyanarayana, S.K. Saraf and S. Stricklin**)

Total cross sections for the emission of protons and alpha particles have been measured for 9.4 and 11 MeV neutrons incident on a 4.11 mg/cm^2 thick Type 316 stainless steel target. A newly-developed charged-particle time-of-flight spectrometer was used to obtain (n,xp) and (n,xα) cross section data. The measured gas production cross sections have been compared with the values predicted on the basis of measured or calculated cross sections of the constituent materials.

10. Measurement of (n,p) and (n,α) Cross Sections of ^{58}Ni and ^{60}Ni at 8.0 and 9.4 MeV.* (S.L. Graham, M. Ahmad, S.M. Grimes, H. Satyanarayana and G. Randers-Pehrson***)

Cross sections and differential energy spectra for the $^{58}Ni(n,xp)^{58}Ni(n,x\alpha)$, $^{60}Ni(n,xp)$ and $^{60}Ni(n,x\alpha)$ reactions have been measured at the Ohio University Tandem Accelerator Laboratory. Time-of-flight and energies of the particles were used to separate particle types. Measured spectra have been compared with the results of Hauser-Feshbach calculations.

11. Study of Proton and Alpha Emission from Isotopes of Copper Bombarded with 9 MeV Neutrons.* (M. Ahmad, C.E. Brient, P.M. Egun, S.L. Graham, S.M. Grimes, S.K. Saraf, H. Satyanarayana and N.T. Nasser)

We have measured cross sections for $^{63,65}Cu\{(n,p)$ and $(n,\alpha)\}$ reactions induced by 9 MeV neutrons. The measurements were performed at the Ohio University Accelerator Facility with a new large-acceptance charged-particle time-of-flight spectrometer. Preliminary results have been compared with Hauser-Feshbach calculations.

---

* Supported in part by the U.S. Department of Energy

** Present address: Mansfield State University, Mansfield, PA.

*** Present address: Radiological Research Accelerator Facility, Columbia University, Nevis Laboratory, Irvington, NY.

12. Direct Neutron Scattering from ^{182}W and ^{184}W.* (J.R.M. Annand** and R.W. Finlay)

Differential elastic and inelastic neutron scattering cross sections for ^{182}W and ^{184}W have been measured at incident energies 4.87 and 6.00 MeV. Cross sections for the 1st 0^+, 2^+, 4^+, 6^+, 2nd 0^+, 2^+ and some higher excitations were obtained. Angular distributions exhibit direct reaction characteristics, suggesting that compound cross sections for these states are small. This is supported by statistical model calculations. Coupled channel calculations of cross sections have been made using a phenomenological deformed optical potential. Quadrupole and hexadecapole deformation have been searched to optimize fits. The necessity of introducing a β_6 deformation was investigated. Electric multipole transition matrix elements, used in the coupled-channels analysis, were obtained from the rotation vibration model and the dynamic deformation theory.

13. A Low Energy Optical Model Analysis of ^{208}Pb and ^{209}Bi.*** (J.R.M. Annand**, R.W. Finlay and F.S. Dietrich†)

New measurements of differential elastic and inelastic neutron scattering cross sections for ^{208}Pb and ^{209}Bi at energies 4-7 MeV have been completed. Elastic scattering data have sufficient accuracy to exhibit clearly differences between cross sections in these neighboring nuclei. Phenomenological and microscopic, spherical, optical model analyses were performed with compound elastic scattering accounted for using the statistical model. Methods of Moldauer, Tepel et al. and Hofmann et al. for calculating the latter were compared. Improvement to the low energy phenomenological description resulting from inclusion of a surface peaked real component to the potential was examined. A possible connection between the observed energy dependence of the real potential and anomalous behavior of the nucleon reduced mass near the Fermi energy was investigated. Microscopic calculations of the optical potential were made using the methods of Brieva and Rook and Jeukenne et al. Inelastic scattering cross sections for the $7/2^-$ and $13/2^+$ single particle states of ^{209}Bi and the first two excited states of ^{208}Pb, the 3^- and 5^- collective states, were obtained. Direct inelastic scattering from these states was calculated using the DWBA and coupled-channels formalism. Compound inelastic scattering was calculated using the statistical model.

---

* Supported in part by the National Science Foundation Grant Number PHY-8108456.

** Present address: Kelvin Laboratory, N.E.L., East Kilbride, Glasgow, Scotland.

*** Supported by the National Science Foundation Grant Number PHY-8108456 and by U.S. Department of Energy Contract Number W-7405-ENG-48.

† Present address: Lawrence Livermore National Laboratory, Livermore, CA.

14. An Optical Model Analysis of n+^{208}Pb Elastic Scattering at Energies 7-50 MeV.* (R.W. Finlay, J.R.M. Annand**, T.S. Cheema***, J. Rapaport and F.S. Dietrich†)

A phenomenological optical model analysis of neutron elastic scattering from ^{208}Pb at incident energies 7-50 MeV has been carried out. The analysis is based on differential cross sections, analyzing powers and total cross sections. Using a conventional parameterization of the scattering potential, with a combination of volume and surface absorption above 11 MeV and surface only below 11 MeV, a good overall description of the data is achieved. Apart from the spin-orbit component, which is assumed real and energy independent, potential well depths are taken to be linear with energy and a geometry independent of energy is assumed. Possible improvement resulting from inclusion of a real surface peaked component or an imaginary spin-orbit component in the potential was examined.

B. MODEL CALCULATIONS AND ANALYSES

1. Shell Model Calculations for the ^{6}Li+n and ^{7}Li+n Reactions.†† (D.A. Resler, H.D. Knox, R.O. Lane and S.M. Grimes)

Shell model calculations for both normal and non-normal parity states of ^{6}Li, ^{7}Li and ^{8}Li, reported on earlier (1), have been completed. The calculations were made in the m-scheme using the Lanczos process. No explicit core was used; however, the calculations were restricted to 0 and 1hω excitations. Spurious Center-of-Mass states have been removed. Spectroscopic amplitudes have been calculated for the ^{6}Li+n and ^{7}Li+n elastic and inelastic scattering processes. The present results have been compared to other theory calculations. Comparison with experiment were made by using the present results as input to ^{6}Li+n and ^{7}Li+n R-matrix studies reported below.

---

* Funded by National Science Foundation Grant PHY-8108456 and Department of Energy Contract W-7405-ENG-48.

** Present address: Kelvin Laboratory, N.E.L., East Kilbride, Glasgow, Scotland.

*** Present address: Punjab University, Physics Department, Chandiagarh, India.

† Present address: Lawrence Livermore National Laboratory, Livermore, CA.

†† Work supported by the U.S. Department of Energy.

(1) D.A. Resler, H.D. Knox, R.O. Lane and S.M. Grimes, Bull. Amer. Phys. Soc. 29, 629 (1984).

2. R-Matrix Studies of ^{6}Li+n and ^{7}Li+n Reactions.* (H.D. Knox, D.A. Resler and R.O. Lane)

Results of the shell model calculations for ^{7}Li and ^{8}Li described above have been tested in R-matrix analyses of ^{6}Li+n and ^{7}Li+n scattering and reactions. Excitation energies and spectroscopic amplitudes for states in ^{7}Li and ^{8}Li predicted by the model calculations were used to provide the R-matrix parameters E_λ and $\gamma_{\lambda c}$. Cross sections for the open neutron induced reactions below $E_n \sim 4$ MeV have been calculated. Effects of the shell model predictions for the excitation energies and configurations of non-normal parity states on the low energy ^{6}Li+n and ^{7}Li+n reactions have been investigated.

3. Microscopic Optical Model Analyses of Nucleon Elastic Scattering from ^{12,13}C.** (J.S. Petler, R.W. Finlay, A.S. Meigooni***, S.H. Mellema† and F.S. Dietrich††)

Differential neutron and proton elastic scattering from ^{12,13}C in the energy region 20-60 MeV has been analyzed using two different microscopic optical models (1,2). The nuclear matter approach of Jeukenne et al. provides a consistent representation of the differential, total and reaction cross sections if the imaginary potential is reduced by $\sim$ 15%. The Brieva-Rook folding model systematically overpredicts the elastic scattering cross section. RMS radii and volume integrals per nucleon were compared with the results of phenomenological S.O.M. and coupled-channels calculations.

---

* Supported by the U.S. Department of Energy.

** Supported by PHS Grant Number 5-R01-CA25193 awarded by National Cancer Institute, DHHS and National Science Foundation Grant Number PHY-8108456.

*** Present address: University of Minnesota, Department of Therapeutic Radiology, Minneapolis, MN.

† Present address: University of Wisconsin, Department of Physics, Madison, WI.

†† Present address: Lawrence Livermore National Laboratory, Livermore, CA.

(1) J.-P. Jeukenne, A. Lejeune and C. Mahaux, Phys. Rev. C16, 80 (1977).

(2) F.A. Brieva and J.R. Rook, Nucl. Phys. A291, 299 (1977).

4. Further Extensions of the Collective Optical Model for Inelastic Scattering from Deformed Nuclei*. (J.P. Delaroche** and A.S. Meigooni***)

It is suggested that the collective optical potential may undergo radius, diffuseness, and potential depth oscillations around an equilibrium shape with permanent axial deformation. Potential form factors were derived for transitions between the ground state band and $K^{\pi} = 0^{+}$, 0^{-} and 1^{-} vibrational bands, as well as for transitions between $K^{\pi} = 3^{-}$ and $K^{\pi} = 1^{-}$ octupole bands in nuclei. The impact of diffuseness and potential depth-oscillations on coupled-channel predictions was illustrated for the first 0^{+} and 1^{-} excited states of ^{12}C.

5. Nucleon Scattering from ^{34}S and the Relative Sign of Neutron and Proton Transition Matrix Elements for the $(0 \rightarrow 2_2^{+})$ Transition†.

(R. Alarcon, J. Rapaport, R.T. Kouzes††, W.H. Moore†† and B.A. Brown†††)

Data obtained by scattering 29.8 MeV protons and 21.7 MeV neutrons from ^{34}S were used in a consistent analysis to obtain values and relative signs for proton (M_p) and neutron (M_n) multipole matrix elements for E2 transitions to the first three 2^{+} states in ^{34}S. The data for the 0^{+} (gs) $\rightarrow$ 2_2^{+} (3.30 MeV) transition are consistent only with the assumption of the same relative sign of M_p and M_n.

---

* Supported by PHS Grant Number 5-R01-CA25193 awarded by the National Cancer Institute.

** Present address: Centre d'Etudes de Bruyeres-le-Chatel, France.

*** Present address: University of Minnesota, Department of Therapeutic Radiology, Minneapolis, MN.

† Supported in part by the National Science Foundation.

†† Present address: Princeton University, Department of Physics, Princeton, NJ.

††† Present address: Michigan State University, Cyclotron Laboratory, East Lansing, MI.

6. Anomalous Behavior of the n+^{208}Pb Potential Near the Fermi Energy*.
(R.W. Finlay, J.R.M. Annand**, J.S. Petler and F.S. Dietrich***)

New measurements of elastic neutron scattering from ^{208}Pb and ^{209}Bi at $E_n < 7$ MeV have revealed the detailed shape of the Fermi surface anomaly in the nucleon-nucleus potential in an energy region inaccessible by proton scattering. The resulting energy dependence of the real potential strongly supports recent dispersion-theory corrections to the Hartree-Fock mean field.

---

* Supported by National Science Foundation Grant PHY-8108456 and by the U.S. Department of Energy under Contract Number W-7405-ENG-48.

** Present address: Kelvin Laboratory, N.E.L., East Kilbride, Glasgow, Scotland.

*** Present address: Lawrence Livermore National Laboratory, Livermore, CA.

PACIFIC NORTHWEST LABORATORY

A. DELAYED NEUTRON STUDIES

1. New Delayed Neutron Precursor ^{75}Cu (Reeder, Warner, Liebsch, Gill, and Pietrowski)

A new delayed neutron precursor with a half-life of 1.3 ± 0.1 s has been observed at mass 75. Mass formula and fission yield predictions indicate that ^{75}Cu is the most likely precursor. The delayed neutron emission probability (P_n) was measured relative to that of ^{144}Cs (observed at mass/charge = 72). The P_n of the new precursor is (3.5 ± 0.6)%. These experiments were performed using a FEBIAD ion source at the TRISTAN mass separator facility. This work has been accepted for publication.[1]

2. Explanation of Long-Lived Neutron Activity at Mass 128 (Reeder, Warner, and Edmiston)

In a previous Report to DOE/NDC,[2] we reported a 19.6 ± 2.8 s delayed neutron activity at mass 128 and assigned it to an isomer of ^{128}In. A similar long-lived component was reported earlier from Studsvik[3], but it was not confirmed in later work.[4] With the new High Temperature Plasma ion source at TRISTAN, this long-lived component at mass 128 was greatly enhanced and its half-life was accurately measured to be 16.3 ± 0.2 s. This half-life agrees closely to that of ^{88}Br (16.4 s). In fact, the half-life for ^{87}Br (56.1 s) was found at mass 127 and the half-life for ^{89}Br (4.4 s) was found at mass 129. We are convinced that the long-lived components at masses 127-129 are due to molecular ions of Br - possibly $^{40}CaBr^+$. The long-lived impurity is particularly noticeable at mass 128 because the ^{128}In delayed neutron yield is much less than the ^{127}In or ^{129}In yield.

3. Delayed Neutrons at Mass 84 (Reeder, Warner, and Edmiston)

We have measured neutron growth and decay curves at mass 84 with the hope of detecting delayed neutrons from the new precursor ^{84}Ga. This nuclide is of special interest because it has a large energy window ($\sim$6MeV) for beta-delayed two-neutron emission. The P_{2n} is estimated to be about 5%.

---

1 Reeder, Warner, Liebsch, Gill and Piotrowski, Phys. Rev. C (to be published - March 1985)

2 Reeder, Warner, and Gill, BNL-NCS-32614, p. 160 (1983).

3 E. Lund and G. Rudstam, Phys. Rev. C 13, 1544 (1976)

4 Lund, Hoff, Aleklett, Glomset, and Rudstam, Z. Phys. A 294, 233 (1980).

Analysis of the neutron growth and decay curve showed at least two components. One component has the 5.5 s half-life of the previously known precursor ^{84}As. The other component had a half-life of 0.8 ± 0.1 s. This may be due to ^{84}Ge (t 1/2 = 1.2 ± 0.3 s), an isomer of ^{84}As (t 1/2 ≈ 0.65 s), Ga (t 1/2 = ?) or some mixture of these components. Further work is needed to clarify this mass chain.

B. HALF-LIVES OF CD ISOTOPES BY BETA DECAY MEASUREMENTS
(P. L. Reeder and R. A. Warner)

In a previous publication,[5] we reported the measurement of $^{122,\ 123,\ 124}$Cd half-lives by beta counting. Additional measurements have now been done at masses 123, 125, and 127. The beta growth and decay curves are very complex, but at each of these masses there is a strong component with a new half-life. We have assigned these components to the previously unknown Cd isotopes. The assignment is somewhat uncertain because this mass region has numerous isomers. The observed half-lives are as follows:

Nuclide	Half-life(s)
^{123}Cd	1.8 ± 0.1
^{125}Cd	0.66 ± 0.02
^{127}Cd	0.44 ± 0.06

C. INDEPENDENT ISOMER YIELD RATIO FOR ^{90}RB AND ^{138}CS
(Reeder, Warner, Willmes, and Ford)

At the SOLAR on-line mass spectrometer facility which we operate at Washington State University, we are measuring isomer yield ratios for fission of ^{235}U with thermal neutrons. The mass spectrometer is tuned to the desired mass number. Fissions are induced by a burst of neutrons from the TRIGA reactor. Fission product ions are collected for a time interval very short compared to the decay half-life of the parent nuclide. For ^{90}Rb and ^{138}Cs, the half-lives of the isomers are long enough so that beta counting can be performed off-line in a low-background environment. Recently, the facility has been modified so that beta counting can be done on-line at the ion beam deposition point.

The isomeric components are resolved from the beta decay curves and the ratio of saturation activities is plotted versus the ion collection time. This procedure allows the yield ratio to be extrapolated to zero ion collection time in order to eliminate the contribution from the parent decay. An analytical function was derived based on standard equations of radioactive growth and decay but allowing for diffusion of fission products out of the target.

[5] Reeder, Warner, and Gill, Phys. Rev. C 27, 3002 (1983).

The parameters of this function are the initial abundances of the parent and the two isomers. The analytical function is fit by least squares to the experimental yield ratio versus collection time data. The parameters of the best fit curve give us the independent isomer yield ratio and the ratio of parent cumulative yield to the sum of the independent yield of the isomers. For $^{90}Rb^{m}(3^{-})/^{90}Rb^{g}(0^{-})$ we find the isomer yield ratio to be 8.7 ± 0.3. This is in excellent agreement with Madland and England's prediction[6] of 9.0 for this spin combination $(3^{-}/0^{-})$.

The Madland and England prescription does not allow for possible variations among nuclides with the same isomer spin combinations. A more detailed calculation has been done by G. Ford of LANL for the specific case of ^{90}Rb. The Ford calculation is based on a statistical model with the level density calculated by a combinatorial method for single particle states in a spherical potential.[7] The average angular momentum of the independently formed fission products is derived from the measured isomer yield ratio. For ^{90}Rb, the experimental isomer yield ratio leads to the average angular momentum J value of 4.5. This is consistent with average J values determined for other fission products.

We have also obtained beta decay curves for ^{138}Cs isomers by off-line and on-line counting. In this case, the branching fraction for the isomeric transition is quite large ($\approx$0.75). The analysis of the beta decay curves is heavily dependent on the branching fraction. The isomer yield ratio goes to infinity if the branching fraction exceeds 0.81. We plan to remeasure the branching fraction before continuing the isomer yield ratio experiments.

---

[6] D. Madland and T. England, Nucl. Sci. Eng. 64, 859 (1977)

[7] Ford, Wolfsberg, and Erdal, Phys. Rev. C 30, 195 (1984)

A = 11 - 12

This review has been published as Nuclear Physics A433 (1985) pp. 1-158.

A = 13, A = 14, A = 15

Preprints of A = 13 and A = 14 have been sent out to 120 colleagues as PPP 3-84 (October 1984) and PPP 1-85 (January 1985). A = 15 will be sent out as PPP 2-85 in March 1985. We plan to submit A = 13-15 to Nuclear Physics in July 1985 and to begin at that time the review of A = 16-17.

F. Ajzenberg-Selove and G. C. Marshall

GAERTTNER LINAC LABORATORY
RENSSELAER POLYTECHNIC INSTITUTE

A. NUCLEAR DATA MEASUREMENTS

1. Intermediate Structure in the Fission Cross Sections of the Even Curium Isotopes*, [R. C. Block, D. R. Harris (RPI), H. T. Maguire, Jr. (West.), C. R. S. Stopa (CTAIEA), R. E. Slovacek (KAPL), J. W. T. Dabbs (ORNL), R. J. Dougan, R. W. Hoff, and R. W. Lougheed (LLNL)].

The neutron-induced fission cross sections of ^{244}Cm, ^{246}Cm, and ^{248}Cm which were measured(1) with the RINS lead spectrometer at RPI have been analyzed for intermediate structure. Gross structure is observed in ^{244}Cm near 200, 400, 800, and 1700 eV and in ^{246}Cm near 350, 800, and 3200 eV. For ^{248}Cm a very broad type of structure is observed near 10 keV. Assuming double-barrier fission, the structure observed in ^{244}Cm and ^{246}Cm fission is consistent with the second potential well lying ~2 MeV higher than the first potential well. The broad structure observed in ^{248}Cm fission implies significantly different barrier parameters than for ^{244}Cm and ^{246}Cm fission.

2. Fission Cross Section Measurements of Cm-242 and Pu-238, [B. Alam, D. R. Harris, R. C. Block (RPI), R. E. Slovacek (KAPL), J. W. T. Dabbs (ORNL), R. J. Dougan, R. W. Hoff, and R. W. Lougheed (LLNL)].

Fission cross section measurements will be carried out at the RINS facility (lead-slowing-down-time spectrometer and the RPI LINAC), and it is expected that the energy range from about 0.1 eV to 80 keV will be covered. This is the technique and energy range used for the previously reported measurements on Cm-244, Cm-246, and Cm-248. A new fission chamber which can contain six pairs of hemispherical electrodes has been fabricated and sent to Livermore for deposit of the Cm-242 and Pu-238 samples. Since the Cm-242 has a half life of only 163 days, which is almost 40 times less than Cm-244, the problem will be in the alpha-pileup suppression. It is planned to first deposit the order of one microgram of Cm-242 on a single electrode to evaluate the alpha-suppression capabilities of the ORNL-design fast preamplifiers. A RINS run is scheduled for late spring.

---

*Supported by Basic Energy Sciences, USDOE

(1) Maguire, Stopa, Block, Harris, Slovacek, Dabbs, Dougan, Hoff, and Lougheed, "Neutron-Induced Fission Cross Section Measurement of ^{244}Cm, ^{246}Cm, and ^{248}Cm," Nucl. Sci, & Eng. (in press).

A. NEUTRON PHYSICS

1. Helium Generation Cross Sections for 14.8-MeV Neutrons

(D. W. Kneff, B. M. Oliver, R. P. Skowronski, and Harry Farrar IV)

Neutron-induced helium generation is a major consideration in the development of materials for reactor environments. Rockwell International is engaged in two programs to measure total helium generation cross sections for fusion reactor applications. The measurement of the cross sections of a large range of separated isotopes and their associated pure elements for fast (8-15 MeV) monoenergetic neutrons is sponsored by the Department of Energy's Office of Basic Energy Sciences (OBES). Cross section measurements for other fusion-related materials in fast-neutron environments, and for all fusion-related materials in other neutron fields used for fusion reactor materials testing, are sponsored by the Office of Fusion Energy.

The OBES cross section measurements are made by irradiating small (~10-50 mg) samples of selected pure elements and separated isotopes in the neutron spectrum of interest. The amount of helium generated in each sample is subsequently measured by high-sensitivity gas mass spectrometry, with typical measurement uncertainties of ~1-3%. The neutron fluence distribution for the irradiation volume is mapped using a comprehensive set of radiometric plus helium accumulation neutron dosimeters, and then combined with the helium generation measurements for multiple samples of each material to deduce cross sections. Absolute fluence normalization is based on the $^{93}Nb(n,2n)^{92m}Nb$ cross section. The fluence mapping is the dominant source of uncertainty (~5-8%) in the cross section measurements.

Measurements made to date for the OBES program have been for materials irradiated by ~14.8-MeV neutrons from the T(d,n) Rotating Target Neutron Sources-I and -II at the Lawrence Livermore National Laboratory. Previously reported measurements include 26 elements and 22 isotopes; a paper describing these measurements has been submitted for publication in Nuclear Science and Engineering.

Cross section measurements have now been completed at 14.8 MeV for eleven additional isotopes. These measurements, for isotopes of tin and lead, are summarized in Table A-1. Each cross section was derived from the analysis of samples irradiated in RTNS-II. The tabulated results have been corrected for small concentrations of other isotopes in each irradiated material. The effect of small impurity concentrations of the unmeasured isotopes ^{112}Sn, ^{114}Sn, and ^{115}Sn was found to be negligible, based on calculations using estimated values for the unknown cross sections.

The lead and tin helium analyses were performed using a newly developed constant-temperature sample furnace. Since the last report, this

furnace underwent several modifications as part of its development, and was tested extensively using low melting point materials. These tests showed that the furnace performs optimally for low melting point samples without the use of a liquid metal bath. This allows the analysis of a greater number of samples before furnace disassembly for servicing. High melting point samples will require the liquid metal bath for helium release by sample dissolution, and work is in progress to find an alternative metal to nickel for improved furnace performance.

Future work will extend the testing and application of the constant-temperature furnace to materials with high melting points and small (~1 mb) helium production cross sections, and to large (≳200 mg) metallic samples to be irradiated in new neutron energy spectra.

TABLE A-1

Total Helium Generation Cross Sections for ~14.8-MeV Neutrons

Material	Cross Section (mb)	Material	Cross Section (mb)
Sn-116	3.0 ± 0.2	Pb-204	1.02 ± 0.08
Sn-117	3.0 ± 0.2	Pb-206	0.66 ± 0.06
Sn-118	1.4 ± 0.1	Pb-207	0.52 ± 0.04
Sn-119	1.2 ± 0.1	Pb-208	0.42 ± 0.04
Sn-120	0.62 ± 0.05		
Sn-122	0.34 + 0.03		
Sn-124	0.12 ± 0.02		

TRIANGLE UNIVERSITIES NUCLEAR LABORATORY

A. NEUTRON CROSS SECTIONS

1. Overview (J. Dave, C. R. Gould, G. Honore, C. Howell, K. Murphy, H. Pfutzner, R. Pedroni, L. W. Seagondollar, R. L. Walter, R. C. Byrd,* P. P. Guss,** J. Templon,+ S. Whisnant,++ J. P. Delaroche+++)

The neutron cross section program at TUNL has been involved in differential cross section $\sigma(\Theta)$ measurements for elastic and inelastic scattering from many nuclei in the 8 to 17 MeV region, the upper end being a region accessible at only a few neutron time-of-flight facilities. Complementing the $\sigma(\Theta)$ data is a program to provide analyzing power $A_y(\Theta)$ data for neutron scattering in the same energy range. The data sets are utilized in a variety of combinations to develop spherical optical models (SOM), deformed optical potentials through coupled channels (CC) calculations, and isospin-based Lane potentials. Most of the individual projects involve energy-dependent studies on only one or two isotopes, but a few are broader in scope, being global in both energy and atomic number. The analyzing power data are useful for showing that SOM and CC calculations represent data well only when an imaginary part W_{so} of a complex spin-orbit term is included.

The global spherical optical model used for describing the p-shell (n,n) and (p,p) cross-section data has been extended using new ^{14}N data. A Lane model for $^{11}B(N,N)$ has been developed and a phase shift analysis for $^{12}C(n,n)$ in the 9 to 12 MeV range has been completed. The $\sigma(\Theta)$ data for $^{27}Al(n,n)$ have been described with an SOM and a simplified CC model. These ^{27}Al

* Present address: Indiana University Cyclotron Facility, Bloomington, IN
** Present address: Dept. of Physics, The College of William and Mary, Williamsburg, VA
+ Present address: Dept. of Physics, Univ. of Indiana, Bloomington, IN
++ Present address: Dept. of Physics, Univ. of South Carolina, Columbia, SC
+++ Present address: Centre d'Etudes de Bruyeres-le-Chatel, France

models will serve as a foundation for interpreting the data to be obtained in the TUNL experiments of bombarding a polarized ^{27}Al target with a polarized neutron beam. The ^{28}Si and ^{32}S measurements from 8 to 17 MeV have been analyzed in SOM and CC studies which included data from other labs from 20 to 40 MeV. CC and SOM interpretations of ^{40}Ca data from 8 to 80 MeV are in progress and analyses of $^{58,60}Ni$ data from 8 to 80 MeV have been submitted for publication.

2. Cross Section Studies in the 1p Shell Between 7 and 17 MeV

Differential cross sections have been measured for the elastic scattering of neutrons of incident energies 11, 14, and 17 MeV from ^{14}N. Beryllium nitride was used as a scattering sample. Pure beryllium scattering was measured and subtracted from the beryllium nitride data to obtain the nitrogen scattering data. The data have been corrected for finite geometry and multiple scattering effects. Legendre polynomial fits to the measured cross section values are shown in Fig. A2-1 as solid lines. Normalization errors are approximately 3, 5, 7 % at 11, 14 and 17 MeV respectively. The cross section values reported by Bauer *et al.*[1] at 11 and 14 MeV are shown as crosses and are in good agreement with the present data.

Spherical Optical Model calculations have been carried out for the measured data using the computer code GENOA. The fits obtained using the parameters given below are shown in Fig. A2-2 as solid lines.

$V_0 = 50.08 - 0.012E$	$r_0 = 1.22$	$a_0 = 0.66$
$W_d = 8.91 + 0.618E$	$r_i = 1.45$	$a_i = 0.13$
$V_{so} = 5.5$	$r_{so} = 1.15$	$a_{so} = 0.5$

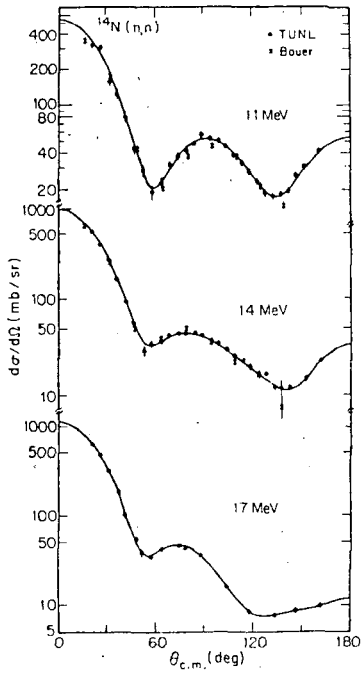

Fig. A2-1. Legendre polynomial fits to 14N data at 11,14,17 MeV. Crosses are the values obtained by Bauer et al. (ref-1).

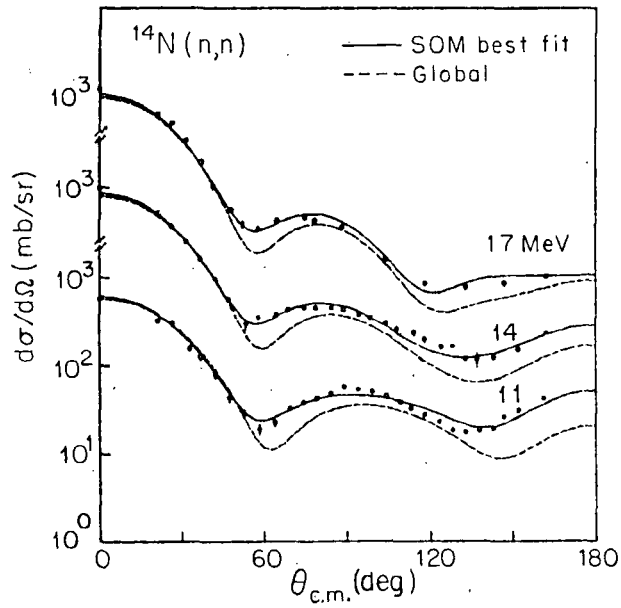

Fig. A2-2. Spherical Optical Model fits to 14N data using "best fit" (Solid lines) and "Global" (dashed lines) parameter sets.

The optical model reproduces the measured data very well. The dashed lines are the predictions of the A-dependent global parameter set published by J. H. Dave' et al.[2] The results are currently being prepared for publication.

In conjunction with the nitrogen scattering experiments, fast neutron scattering cross sections have been remeasured for pure ^{9}Be. Angular distribution data for elastic scattering and inelastic scattering to the 2.429 MeV state were obtained between 20° and 160° at incident neutron energies of 11, 14 and 17 MeV. The data were corrected for finite sample and source effects using a Monte Carlo simulation. The extracted angular distribution data at 11 and 14 MeV agreed well with the previous values obtained at TUNL by Hogue et al.[3] There were no previous data at 17 MeV.

3. Cross Section and Analyzing Power Studies in the 1p Shell

TUNL measurements of $\sigma(\Theta)$ and $A_y(\Theta)$ for the $^{11}B(n,n)^{11}B$ and $^{11}B(p,n)^{11}C$ and measurements of $\sigma(\Theta)$ for $^{11}B(p,p)^{11}B$ conducted elsewhere have been incorporated in a Lane model analysis. The new $\sigma(\Theta)$ measurements were made at 15 and 17 MeV for $^{11}B(n,n_0)$ in order to complement older TUNL data from 10 to 15 MeV. In addition, $\sigma(\Theta)$ for $^{11}B(n,n_1)$ was also obtained. For the three $^{11}B(N,N)$ data sets, the $\sigma(\Theta)$ results have been fairly well reproduced, particularly at the higher end of the energy range. Likewise, $A_y(\Theta)$ for $^{11}B(n,n)$ was successfully reproduced, but $A_y(\Theta)$ for $^{11}B(p,n)$ at back angles was overestimated in magnitude. The form of the potential was:

$$U_{nn} = U_0 - 2(T/A)U_1$$

$$U_{pn} = 2(\sqrt{2}T/A)U_1$$

$$U_{pp} = U_0 + 2(T/A)U_1$$

where U_0 and U_1 are of the form $U = V + iW + V^{so}$. The graphs of V_{nn} and $W_{nn} = (W_d)_{nn}$ are shown in Fig. A3-1. The data points for

---

1. R. W. Bauer et al., Nucl. Phys. A93 (1967) 673
2. J. H. Dave' and C. R. Gould, Phys. Rev. C28 (1983) 2212
3. H. H. Hogue et al., Nucl. Sci. Eng. 68 (1978) 38.

V_{nn} and W_{nn} correspond to values obtained in the single-energy searches on $^{11}B(N,N)$, except for 15 MeV for which the W_{nn} was forced to lie on a smooth curve for $W_{nn}(E)$. The value for V_{nn}^{so} was held fixed at 5.9 MeV following initial searches on the (n,n) and (p,n) data sets. For describing the $^{11}B(p,p)$ data, it was important to introduce a Coulomb correction of the form $\Delta U_c = \Delta V_c + i\Delta W_c$ with a negative ΔV_c of about 0.1 MeV below 14 MeV and about +1.5 MeV at 17 MeV. The ΔW_c was about -2 MeV below 14 MeV and +2 MeV at 17 MeV.

Cross sections $\sigma(\theta)$ and analyzing power $A_y(\theta)$ for $^{12}C(n,n_0)$ from 9 to 12 MeV have been parametrized through a phase shift analysis based on an extension of phase shift analyses of data at lower energies. Good descriptions were obtained and several states in ^{13}C were identified. A paper was submitted to Jour. Phys. G. on this work.

4. Elastic and Inelastic Neutron Scattering from ^{27}Al at 11

This work has been published in Phys. Rev. C30 (1984) 1435. The abstract follows:

> "Fast neutron scattering cross sections have been measured for ^{27}Al using the TUNL neutron time-of-flight facility. Angular distributions were measured at angles from 20° to 160° in 5° increments, at incident neutron energies of 11, 14 and 17 MeV. Data are presented for elastic scattering and for inelastic scattering to the sum of the 0.84 and 1.01 MeV states, the 2.21 MeV state and the sum of the 2.73, 2.98 and 3.00 MeV states. After correcting for compound nucleus effects, the elastic scattering cross sections are well reproduced by the spherical optical model using a linear energy dependence in the real well depth. The inelastic data are interpreted with a coupled channels calculation and the excited core model."

The spherical optical model fits are shown in Fig. A4-1 and the coupled channels fits are shown in Fig. A4-2. The compound nuclear calculations indicate that serious efforts to study the direct interaction processes must be confined to energies above 14 MeV to minimize the uncertainties inherent in these corrections.

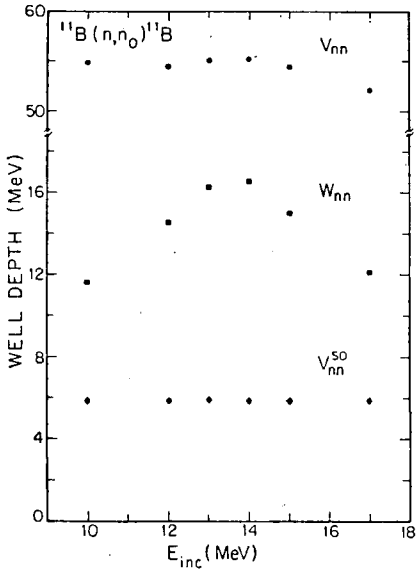

Fig. A3-1. Lane potentials for neutron scattering from ^{11}B.

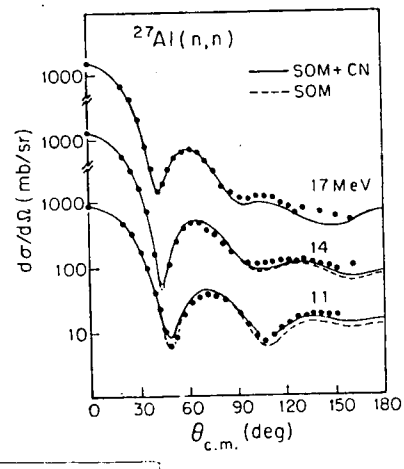

Fig. A4-1. Spherical optical model (SOM) fits to the ^{27}Al neutron elastic scattering data. Compound nuclear corrections are important at 11 MeV and are indicated by the difference between the solid and dashed lines.

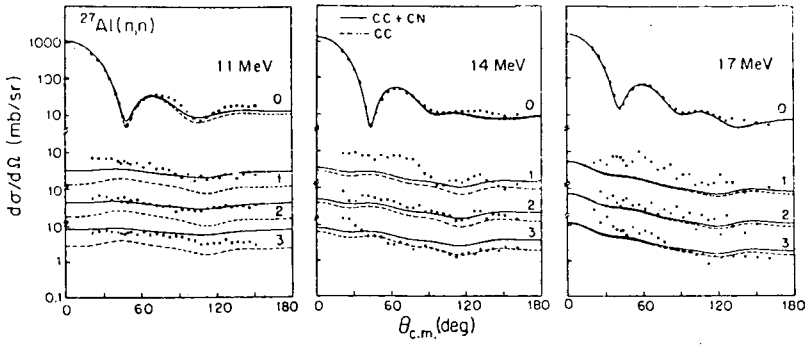

Fig. A4-2. Coupled channels (CC) calculations for neutron elastic and inelastic scattering from ^{27}Al. The CC parameters are derived from a ^{28}Si neutron inelastic scattering analysis. Calculations including compound nuclear corrections (CN) are shown as the solid lines, and calculations without CN corrections are shown as the dashed lines. The ground state is denoted by 0, the unresolved 0.84 MeV (1/2+) amd 1.01 MeV (3/2+) states are denoted by 1, the 2.21 MeV (7/2+) state is denoted by 2 and the 2.73 (5/2+), 2.98 (3/2+) and 3.00 (9/2+) unresolved triplet is denoted by 3.

The elastic and inelastic distributions are reasonably well described by coupled channels calculations based on a ^{28}Si parameter set and the weak coupling model. The shapes of the ^{27}Al inelastic scattering distributions match that of the ^{28}Si 2^+ core state. At 11 MeV the magnitudes of the inelastic scattering cross sections are in qualitative agreement with the model predictions once CN contributions are included. The large CN contributions and the fact that the $5/2^+$ excited state is part of an unresolved doublet preclude extraction of a definite value for the phonon mixing parameter. A higher resolution experiment at an energy above 14 MeV would be of interest in determining whether the mixing parameter deduced from neutron inelastic scattering is the same as that found in other inelastic scattering experiments.

5. Cross Sections and Analyzing Powers for ^{28}Si and ^{32}S

The measurements of $\sigma(\Theta)$ and $A_y(\Theta)$ and their analyses comprised part of the thesis of C. Howell. The thesis abstract follows:

> "Analyzing powers $A_y(\Theta)$ for neutron scattering to the ground and first excited states of natural silicon and sulfur from 20° to 155° c.m. have been measured at incident neutron energies of 10, 14, and 17 MeV. To obtain these data, the 0° neutrons from the $^2H(\vec{d},\vec{n}_0)^3He$ polarization transfer reaction were scattered from cylindrical samples into two symmetrically positioned side detectors. Pulsing the polarized deuteron beam permitted the use of time-of-flight detection techniques. The corresponding differential cross sections $\sigma(\Theta)$ at 8, 10, 12, 14, and 17 MeV were measured with the same detector system but using an unpolarized beam. Both $A_y(\Theta)$ and $\sigma(\Theta)$ data were corrected for flux attenuation, angular resolution, and multiple scattering. These data have been described with spherical optical models and with phenomenological coupled-channels calculations. To minimize the ambiguities in the optical-model parameters, $\sigma(\Theta)$ data for incident neutron energies ranging from 10 to 40 MeV, which were previously reported, were included in this analysis. For both nuclei, a logarithmic energy dependence on the strength of the real potential was necessary to describe the published neutron total cross sections at energies below 3.0 MeV.
>
> In the CC calculations, ^{28}Si was modeled as a symmetric rotor with coupling between the 0^+, 2^+, and 4^+ states, and ^{32}S was modeled as a vibrator in which

one-phonon and two-phonon states were mixed. Sensitivities of the data and of the calculations to the magnitude and sign of the quadrupole and hexadecapole deformation parameters, β_2 and β_4, were demonstrated for the case of ^{28}Si. Special emphasis was put on the determination of the spin-orbit potential parameters for each nucleus. The inelastic $A_y(\theta)$ data were used to determine the relative deformation of the spin-orbit potential to that of the central potential. In addition, these CC calculations were used to extract the Coulomb corrections to the real and absorptive parts of the optical model potentials for nucleon scattering from ^{28}Si and ^{32}S."

The cross section results for $^{32}S(n,n_0)$ from 8 to 40 MeV are shown in Fig. A5-1 where they are compared to CC calculations based on smooth-energy-dependent potentials.

6. ^{40}Ca Cross Sections

The double-closed-shell nucleus ^{40}Ca has been widely studied in neutron and proton experiments and in theoretical explorations. Working with W. Tornow of Tübingen, we have been interested in nucleon scattering from ^{40}Ca for a few years. These studies led us during the past year to extend our experimental work for $\sigma(\theta)$ and $A_y(\theta)$ up to 17 MeV. That is, measurements of $\sigma(\theta)$ for $^{40}Ca(n,n_0)$ and $^{40}Ca(n,n_1)$ at 14 and 17 MeV have been made and corrected for multiple scattering. The data have been combined with earlier TUNL $\sigma(\theta)$ data for (n,n_0), with Ohio U. data and with M.S.U. data to obtain a fairly complete $\sigma(\theta)$ data set from 10 to 40 MeV. The total cross section from 4 to 80 MeV from ORELA along with TUNL $A_y(\theta)$ measurements at 10, 14 and 17 MeV for (n,n_0) and at 11 and 14 MeV for (n,n') complete the data base for our energy dependent optical model analyses. A reasonable description of the data has been achieved with a simple CC vibrational model, but some of the detailed features of the data are not properly calculated, especially for $A_y(\theta)$ at 14 MeV for angles in the region of 110°. Attempts to extend the CC calculations to include coupling to additional states using the anharmonic vibrational model are underway. In addition, $^{40}Ca(p,p)$ data are being analyzed in conjunction with the (n,n) data.

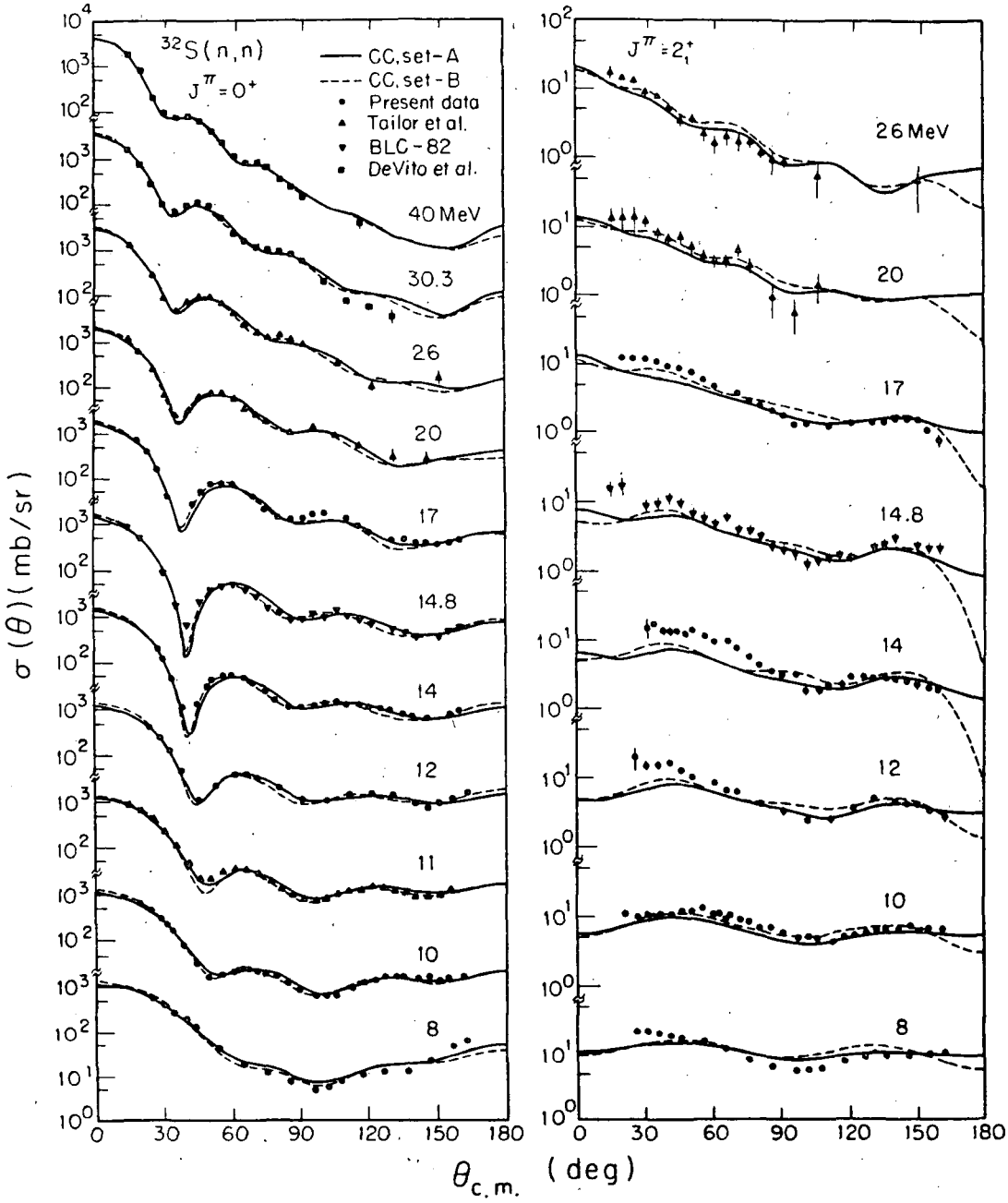

Fig. A5-1. The σ(θ) for elastic and inelastic scattering of neutrons from ^{32}S. The solid curves through the data are the results of CC calculations which model ^{32}S as a vibrator with admixing of one-phonon and two-phonon states. The dashed curves result from an axially symmetric rotational model.

7. Scattering from $^{58,60}Ni$

A paper on the $\sigma(\theta)$ and $A_y(\theta)$ measurements and analyses has been submitted to Nuclear Physics. The abstract follows:

> "Differential cross sections for neutron scattering from ^{58}Ni and ^{60}Ni to the ground state and first excited state have been measured at 8, 10, 12 and 14 MeV. In addition, analyzing powers were measured for scattering to the same states for ^{58}Ni at 10 and 14 MeV, and for ^{60}Ni at 10 MeV. The data were analyzed in the framework of a coupled channels formalism in which the vibrational model was assumed with deformed central and spin-orbit potentials. A spherical optical model analysis of the elastic scattering data was also performed following the coupled channels analysis. Predictions for (p,p) and (p,p') scattering observables have been made and compared with measurements previously published. This approach permits neutron and proton deformation parameters to be deduced similarly from (n,n') and (p,p') scattering measurements for $^{58,60}Ni$. These deformation parameters are compared in the framework of the core-polarization model of Madsen, Brown and Anderson."

In addition, new $\sigma(\theta)$ and $A_y(\theta)$ measurements at 17 MeV have been completed and will be used to test the energy dependence and deformation parameters derived in the above models.